



CENTRO INTERNACIONAL DE ESTUDOS  
DE DOUTORAMENTO E AVANZADOS  
DA USC (CIEDUS)

TESIS DE DOCTORADO

**OPTIMIZATION OF  
THROMBOLYTIC THERAPY IN  
BRAIN PATHOLOGY**

Clara Correa Paz

**ESCUELA DE DOCTORADO INTERNACIONAL  
PROGRAMA DE DOCTORADO EN MEDICINA MOLECULAR**

SANTIAGO DE COMPOSTELA

2019



## DECLARACIÓN DEL AUTOR DE LA TESIS

**Optimization of thrombolytic therapy in brain pathology**

Dña Clara Correa Paz

*Presento mi tesis, siguiendo el procedimiento adecuado al Reglamento, y declaro que:*

- 1) La Tesis abarca los resultados de la elaboración de mi trabajo.*
- 2) En su caso, en la Tesis se hace referencia a las colaboraciones que tuvo este trabajo.*
- 3) La Tesis es la versión definitiva presentada para su defensa y coincide con la versión enviada en formato electrónico.*
- 4) Confirmando que la Tesis no incurre en ningún tipo de plagio de otros autores ni de trabajos presentados por mí para la obtención de otros títulos.*



Asdo. Clara Correa Paz

En Santiago de Compostela, 18 de julio de 2019



**AUTORIZACIÓN DEL  
DIRECTOR/TUTOR DE LA TESIS**  
**Optimization of thrombolytic therapy in brain  
pathology**

D. Francisco Campos Pérez  
D. Tomás Sobrino Moreiras  
D. José Castillo Sánchez

INFORMAN:

*Que la presente tesis, corresponde con el trabajo realizado por D/Dña.  
**Clara Correa Paz** bajo mi dirección, y autorizo su presentación,  
considerando que reúne los requisitos exigidos en el Reglamento de  
Estudios de Doctorado de la USC, y que como director de ésta no  
incurre en las causas de abstención establecidas en Ley 40/2015.*

*En Santiago de Compostela, 18 de julio de 2019.*

Directores

Francisco Campos Pérez



Tomás Sobrino Moreiras



José Castillo Sánchez





## Conflict of interest

The author and the directors of the work agreed to present the results in this Thesis and declare no conflict of interest.







## Research stay

During the development of the Thesis the PhD student performed a **stay in an international laboratory, in the “Physiopathology and imaging of neurological disorders” (INSERM U1237, Cyceron)** in Caen, France, with the Professor Denis Vivien during the period between February-May 2018.





## Publications

During the development of this Thesis the PhD student took part in the following publications:

- Iglesias-Deus A, Campos F, Correa-Paz C, Sobrino T, Fraga JM, Castillo J, Couce ML. Hepatic damage and glutamate oxaloacetate transaminase elevations during fetal asphyxia. *Dev Med Child Neurol.* 2017 Feb;59(2):233-234.
- Iglesias-Rey R, Rodríguez-Yáñez M, Rodríguez-Castro E, Pumar JM, Arias S, Santamaría M, López-Dequidt I, Hervella P, Correa-Paz C, Sobrino T, Vivien D, Campos F, Castellanos M, Castillo J. Worse Outcome in Stroke Patients Treated with rt-PA Without Early Reperfusion: Associated Factors. *Transl Stroke Res.* 2018 Aug;9(4):347-355.
- da Silva-Candal A, Pérez-Díaz A, Santamaría M, Correa-Paz C, Rodríguez-Yáñez M, Ardá A, Pérez-Mato M, Iglesias-Rey R, Brea J, Azuaje J, Sotelo E, Sobrino T, Loza MI, Castillo J, Campos F. Clinical validation of blood/brain glutamate grabbing in acute ischemic stroke. *Ann Neurol.* 2018 Aug;84(2):260-273.
- Pérez-Mato M, Iglesias-Rey R, Vieites-Prado A, Dopico-López A, Argibay B, Fernández-Susavila H, da Silva-Candal A, Pérez-Díaz A, Correa-Paz C, Günther A, Ávila-Gómez P, Isabel Loza M, Baumann A, Castillo J, Sobrino T, Campos F. Blood glutamate EAAT2-cell grabbing therapy in cerebral ischemia. *EBioMedicine.* 2019 Jan;39:118-131.
- da Silva-Candal A, Brown T, Krishnan V, López-Loureiro I, Ávila-Gómez P, Pusuluri A, Pérez-Díaz A, Correa-Paz C, Hervella P, Castillo J, Mitragotri S, Campos F. *J Control Release.* 2019 Jul 19 (DOI: 10.1016/j.jconrel.2019.07.026)

From the development of this Thesis the following article has been published:

- Correa-Paz C, Navarro Poupard M, Polo E, Rodríguez-Pérez M, Taboada P, Iglesias-Rey R, Hervella P, Sobrino T, Vivien D, Castillo J, del Pino P, Campos F, Pelaz B. In Vivo Ultrasound-Activated Delivery of Recombinant Tissue Plasminogen Activator from the Cavity of Sub-Micrometric Capsules. *J Control Release.* 2019 Jul 13 (DOI: 10.1016/j.jconrel.2019.07.017).



## Funding

This study was supported by the Ministry of Science, Innovation and Universities and the Ministry of Economy and Competitiveness of the Government of Spain (SAF2014-56336-R y SAF2017-84267-R); by the Instituto de Salud Carlos III (CP14/00154, PI17/00540; RD16/0019/0001; PI15/01578; PI13/00292; RD12/0014/0001), the Cerebral Vascular Diseases Network (INVICTUS); by the Axencia Galega de Innovación (GAIN), the Consellería de Cultura, Educación e Ordenación Universitaria de la Xunta de Galicia (IN607A 2018/03 y GRC2014/027) and European Union program FEDER.

During the development of the work, the doctoral candidate benefited from a predoctoral contract for the training of doctors (FPI), from the Ministry of Economy and Competitiveness. (BES-2015-073933). During this period, Dr. Francisco Campos, Director of the Thesis, has been the beneficiary of the Miguel Servet contract, of the Instituto de Salud Carlos III (CP14/00154). Dr. Tomás Sobrino, Director of the Thesis, has been the beneficiary of the Miguel Servet contract, of the Instituto de Salud Carlos III (CP12/03121).



## Agradecimientos

Suena muy poco científico decir que esta es la parte que más ganas tenía de escribir. Durante estos cinco años ha habido muchos experimentos fallidos y días muy largos en los que he estado acompañada de gente que me ha llenado de risas, de fuerza y de cariño. *Enciendo música nostálgica*. Allá voy.

A mis directores de Tesis: Prof. José Castillo, Dr. Tomás Sobrino y Dr. Francisco Campos. Antes de nada gracias por todo vuestro esfuerzo por hacernos fácil la investigación, porque sabemos que vosotros también tenéis días mucho más largos para conseguir que todos podamos trabajar en ciencia dignamente, que podamos realizar estancias, cursos e ir a congresos. A nivel personal gracias por haberme dado la oportunidad de hacer este trabajo y por la confianza que habéis depositado en mí. A Pepe por enseñarnos la importancia de la investigación traslacional. Gracias por los tirones de oreja para intentar que seamos más competitivos, que **salgamos de nuestra "zona de confort"**. A Tomás por enseñarme los primeros pasos con aquel Trabajo de Fin de Máster, por confiar en mí desde el principio, por haberme enviado los correos de que podía hacer aquí el TFM y la Tesis, que tan felices me hicieron. A Fran, *"oye Fran, mira, no te voy a contar mi vida, pero ¿tienes un momento?"*, **¿cuántas** veces te lo habré repetido? En general gracias por tener siempre ese momento para hacerme caso, por enseñarme la cirugía, por haber dirigido y corregido esta Tesis. Gracias por hacer amenas las horas en el laboratorio desde tu garita del DJ (menos mal, por cierto, que te hiciste *indie*), con cualquier chorrada para reírnos un rato. Por estar no solo como director, sino también como apoyo cuando las cosas no iban todo lo bien que queríamos.

Gracias también a los médicos que tanto nos han enseñado en los seminarios, y que siempre son tan atentos con algún que otro mareo o migraña: Manuel, Rogelio, Susana, Isabel, María, Juan, Emilio, Iria... Me gustaría recordar con mucho cariño a Miguel, que cuando nos prestó el Doppler me animó un montón con este proyecto.

Al Servicio de Anatomía Patológica por haber realizado las tinciones de los cerebros. Al Dr. Máximo Fraga por su amabilidad y disponibilidad.

Al Dr. Eugenio Vázquez del CIQUS, que nos hizo las imágenes de las nanocápsulas que no pueden ser más bonitas! Muchísimas gracias.

Mención aparte merecen todos mis compañeros del laboratorio, que se han llegado a convertir en parte de mi familia. María, la imagen del esfuerzo y la experiencia, gracias por tener siempre palabras amables. A Bárbara, que tanto me enseñó del laboratorio. A Ramón y a Juan por llenar de risas las horas de resonancia. A Juan por haber hecho tantísimas **resos y hacerme tantas "imágenes bonitas"**. A Ramón por toda la paciencia con aquellos montajes para hacer las primeras resonancias de ratones y por cada vez que he ido a contarle mis problemas científico-físicos. A Pablo, que siempre sabe como animarme, gracias por haberme ayudado en la corrección de la Tesis, a organizar la introducción, en la discusión, etc. A Sonia, que ha corregido el inglés terrible de esta Tesis, eres un sol! A las últimas incorporaciones Marta, Elena, Ana, Antía y Adrián, por traer aire nuevo al laboratorio. En especial a Elena (*esto está fatal*) que ha sido un gran apoyo durante los meses de escritura, y a Adri. Gracias a los dos por venir a hacerme visitas, por los cafés, las excursiones y las cañas que se lían, *bueno chicos... hay que trabajar*. Pero sobre todo a esos que hicieron (y espero que sigan haciendo) que la ciencia sea amor. A Joserra, por toda la paciencia cuando voy a contarte mi vida, por los consejos con las perfusiones, por ser un fiel compañero ~~de~~ **fiesta**, eres el mejor Jota. A Alba (Albi), gracias por enseñarme a ser una



buena científica-cirujana, por las conversaciones sobre cualquier cosa que tanto echo de menos. A Andrés, *ay dios mío...*, gracias por hacer estos años tan divertidos, por enseñarme a reírme un poco más de mi misma, por el apoyo científico y personal. A mi *tutor*, a Esteban, en general por todo, por compartir cinco años pegaditos, por ser más que el mejor compañero del mundo, siempre dispuesto a ayudar, a hacerme reír e incluso a hacer de jefe de protocolo. A mis hermanos patitos: Nacho y Héctor. Qué verdes empezamos y como hemos conseguido volar chicos (aunque a veces nos estrellamos). Me quedo con todos los momentos y ~~horas~~ cafés que hemos compartido, con todo eso que no se puede contar en una Tesis, gracias por haber tenido tanta paciencia con mi carácter mandón. A Vanesa, que desde el CIMUS siempre me ha dado tanto cariño, que siempre ha tenido palabras para hacerme seguir con fuerza. A Tania, *miña Tetis*, qué escribir que no sepas, qué duro fue dejar de compartir días de secretos y experimentos, pero qué emoción tan grande ver en qué te has convertido. Gracias por dejarme formar parte de los momentos más importantes y por todo el apoyo, siempre, sin fallos. A Manu (Manolito), por toda la síntesis de millones de nanopartículas que han hecho que me odies tantísimo, por tener siempre algún comentario para no saber si reír o llorar. A Dopi, por estar tan pendiente de mí especialmente cuando estaba en Francia, por ayudar siempre que hace falta. A Paulo, por esos piques terribles, que han hecho que, por lo menos, intente ser mejor compañera. A Uxia, por tener siempre una sonrisa.

Gracias al grupo Bionanotools del CIQUS. Gracias a Pablo y a Bea por toda la ayuda e implicación en esta Tesis, por haberme tratado como una más del grupo, por todo lo que me habéis enseñado, por toda la paciencia desde los inicios haciendo pompones de gelatina, hasta mis "*odio hacer mega-síntesis*". A Ester, gracias por toda la parte de citometría, por corregirme las cuentas y ayudarme a hacer diluciones. A María, por toda

la cantidad de síntesis que has hecho, por la caracterización, sin ti habría perdido la cabeza en la primera *mega-síntesis*, gracias por ser tan buena compañera y ayudarme cuando llegaba la desesperación. Raquí, gracias por los audios, gifs e imágenes para animarme cuando la ciencia hacía de las suyas. A Aitor, Enrica, Carolina, Javi, Suman, Martina, Victoria, Alessandro, Mozghan, Vida,... Gracias por quitarme el miedo a hablar en inglés, por ayudarme con las muestras de ICP, por enseñarme que con risas, vídeos, maicitos, chocolates y cafés, las horas eternas en el laboratorio saben mejor, por hacerme toda una *runner* (y casi una *surfer*), por los bailes absurdos. Sois geniales.

En febrero de 2018 llegó la estancia. Merci beaucoup Professor Denis Vivien for accepting me in your laboratory, it was an incredible experience to work in your centre and to meet such important researchers in the tPA field. Thanks to the entire lab for their kindness during those three months. Gracias a Marina por haberme ayudado tanto, por haberme enseñado a trabajar con el microscopio de doble fotón (qué imágenes más bonitas!) y por esos truquitos para hacer más fácil la cirugía. Y gracias también a Sara y a Maxime, que idearon algunas de las partes de esta Tesis y me dieron otras muchas ideas que al final no pudieron llevarse a cabo. Gracias también por haberme enseñado Normandía y por haber hecho de mi familia durante esos meses.

A los eumeses con los que he compartido momentos de desconexión y que siempre han tenido un momentito para preguntar "*¿cómo va esa Tesis? ¿qué tal los ratoncitos?*". Desde esos que ya llevan unos cuantos años en mi vida, hasta los que me han ido haciendo un hueco en la pandilla. Gracias también a los Salgado-Tenreiro por haberme acogido con tanto cariño, a Elena, Mongo, Enrique, María, Víctor, Ana, Rodrigo, Rodri y Sabela.

A los amigos que resistieron estos cinco años. A Alberto por los cafés neurocientíficos. A las farmacéuticas de mi corazón: Andrea, María y Noe. En especial a Majo, que aunque no nos vemos todo lo que nos gustaría, me ha salvado alguna caída en el abismo científico con viajes, conciertos y tardes de charlas. A Laura, porque hay amistades clavadas que nadie puede arrancar. Y a mis casi hermanos: Andrés y Andrea, vosotros habéis entendido desde el primer momento lo importante que era esto para mí, por compartir lo mejor y lo peor de la Tesis y de todo lo demás. Gracias por haberme enseñado qué es la amistad.

A mis tíos, tías, padrino, madrina, Merce, primos, primas y parches, con los que comparto comidas-merienda-cena que me han enseñado lo importante que es la familia. También a mis casi tíos Maribel y Paco por haber estado siempre. Gracias en especial a mis tíos Sol y Jesús, por mimarme desde que era una bicha pequeña a la que le chiflaban los **chicles de "bofila"**; y a mi tía Nandi, que me ha enseñado lo importante que es esforzarse y perdonar. A mi prima Laura, la hermana pequeña que **no he tenido, el "qué, no se te ve el pelo" creo que puede ser explicado** con este librito. A Monse, por ser más que mi cuñada, por todos los momentos que compartimos, y porque tus abrazos curan todos los males.

Con mucho cariño a mis abuelos. A los que ya no pueden ver esto: a mis *bis* Chelo y Sindo, a mi abuelo Manolo y a la abuela Toñita, que siempre pienso en ellos. Y a los que me sacan una sonrisa los fines de semana, con sus locuras, sus historias y sus abrazos a mi abuelo Román y a mi abuela Lola.

Y ya voy acabando.

A Javi. Imagina que te canto muy fuerte y (des)afinado: *no sé si lo hubiera logrado sin ti*. Enhorabuena por la co-autoría de esta Tesis. Es tuya. Por todo el tiempo que te ha quitado, pero también por el tiempo

que tú le has dedicado. He de decir que podéis preguntarle de qué trata este libro que lo explicará mejor que yo. Gracias por haber aguantado **estoicamente con aquel temprano** "*yo te apoyaré con lo que decidas*". Por ser el mejor compañero de piso, de fiesta, de aventuras, y de vida. Y sobre todo por haber compartido y querer seguir compartiendo cada día conmigo.

Y por último a Carlos, Gerardo y Dolores, mi hermano y mis padres. Mis ejemplos a seguir, los tres siempre me han demostrado lo importante que es tener pasión, ganas y fuerza de voluntad. A Carlos, imposible imaginar un hermano mejor que tú, gracias por tus consejos, por contagiar esas ganas de comerse el mundo que tienes y por enseñarme que *ser valiente no solo es cuestión de suerte*. A papá, el ejemplo de emprender y arriesgarse siempre en nuevos proyectos, gracias por apoyarme con todas las decisiones que he tomado. Siempre he sentido lo orgulloso que estás de mí y de este trabajo. A mamá, de la que he heredado esta tranquilidad que me caracteriza, tú me has enseñado que nunca es tarde para nada, y **que todo sabe mejor con una sonrisa**. Por tus "*tú vales, tú puedes*", por hacer que me rompa y me recomponga. Gracias por haber sido y ser el ejemplo perfecto de cómo quiero ser. Esta Tesis es por y para vosotros. Os quiero.

Clara

“¡Qué gran tónico sería para el novel observador el que su maestro, en vez de asombrarlo y desalentarlo con la sublimidad de las grandes empresas acabadas, le expusiera la génesis de cada invención científica, la serie de errores y titubeos que la precedieron, constitutivos, desde el punto de vista humano, de la verdadera explicación de cada descubrimiento! Tal hábil táctica pedagógica nos traería la convicción de que el descubridor, con ser un ingenio esclarecido y una poderosa **voluntad, fue, al fin y al cabo, un hombre como todos.**”

*Reglas y consejos sobre investigación científica. Los tónicos de la voluntad*

Santiago Ramón y Cajal



# INDEX

RESUMEN .....	1
ABBREVIATIONS.....	13
INTRODUCTION.....	19
1. STROKE.....	21
1.1. Definition .....	21
1.2. Epidemiology.....	21
1.3. Classification of stroke.....	23
1.4. Risk factors .....	26
1.5. Biochemistry of coagulation.....	28
1.6. Biochemistry of cerebral ischemia.....	37
1.7. Therapeutic approaches for the treatment of stroke .....	42
1.8. Animal models of stroke.....	51
2. TISSUE PLASMINOGEN ACTIVATOR .....	56
2.1. rtPA structure .....	56
2.2. rtPA as a treatment in stroke .....	63
2.3. Sonothrombolysis.....	73
2.4. New approaches for rtPA treatment .....	80
3. NANOMEDICINE AND DRUG DELIVERY SYSTEMS.....	87
3.1. Targeting approaches.....	90
3.2. Stimuli-responsive drug delivery.....	92

3.3.	Carriers for rtPA delivery.....	95
4.	LAYER-BY-LAYER NANOCAPSULES.....	106
4.1.	Preparation of layer-by-layer assembly.....	107
4.2.	Encapsulation and release.....	109
4.3.	Ultrasound-responsive layer-by-layer capsules.....	111
	HYPOTHESIS.....	115
	OBJECTIVES.....	119
	MATERIALS AND METHODS.....	123
5.	PRELIMINARY STUDY.....	125
5.1.	Synthesis.....	125
5.2.	<i>In vitro</i> rtPA activity.....	126
5.3.	<i>In vivo</i> release.....	127
6.	SECTION I: <i>IN VITRO</i> OPTIMIZATION OF rtPA NANOCAPSULES.....	130
6.2.	Characterization of the nanocapsules.....	138
6.3.	<b><i>In vitro</i></b> rtPA activity.....	142
6.4.	<i>In vitro</i> release.....	146
6.5.	Inductively coupled plasma mass spectrometry.....	149
6.6.	Magnetic resonance protocol.....	149
6.7.	Statistical analysis.....	150
7.	SECTION II: <i>IN VIVO</i> STUDIES OF rtPA NANOCAPSULES .....	151



7.1.	Animal management and study approval.....	151
7.2.	Ultrasound safety <i>in vivo</i> .....	152
7.3.	Nanocapsules safety <i>in vivo</i> .....	155
7.4.	<i>In vivo</i> release.....	156
7.5.	Therapeutic effect.....	160
7.6.	Hematoxylin and eosin staining.....	161
7.7.	Animal procedures.....	162
7.8.	Inductively coupled plasma mass spectrometry.....	167
7.9.	Magnetic resonance protocols.....	168
7.10.	Statistical analysis.....	172
	RESULTS.....	173
8.	PRELIMINARY STUDY.....	175
8.1.	<i>In vitro</i> rtPA activity.....	175
8.2.	<i>In vivo</i> release.....	177
9.	SECTION I: <i>IN VITRO</i> OPTIMIZATION OF rtPA NANOCAPSULES.....	180
9.1.	Synthesis and characterization.....	180
9.2.	<i>In vitro</i> rtPA activity.....	201
9.3.	<i>In vitro</i> release.....	203
10.	SECTION II: <i>IN VIVO</i> STUDIES OF rtPA NANOCAPSULES .....	210
10.1.	Ultrasound safety in the brain.....	210
10.2.	Nanocapsules safety <i>in vivo</i> .....	212
10.3.	<i>In vivo</i> release.....	214

10.4. Therapeutic effect .....	223
10.5. Biodistribution.....	237
DISCUSSION.....	239
11. SECTION I: <i>IN VITRO</i> OPTIMIZATION OF rtPA NANOCAPSULES.....	241
12.. SECTION II: <i>IN VIVO</i> STUDIES OF rtPA NANOCAPSULES .....	249
CONCLUSIONS.....	257
13. SECTION I: <i>IN VITRO</i> OPTIMIZATION OF rtPA NANOCAPSULES.....	259
14.. SECTION II: <i>IN VIVO</i> STUDIES OF rtPA NANOCAPSULES .....	260
CONCLUSIONES.....	263
15. SECCIÓN I: OPTIMIZACIÓN <i>IN VITRO</i> DE LAS NANOCÁPSULAS CON rtPA .....	265
16. SECCIÓN II: ESTUDIO <i>IN VIVO</i> DE LAS NANOCÁPSULAS CON rtPA .....	266
BIBLIOGRAPHY .....	269
ANNEXES .....	297

### Resumen

El ictus isquémico es una patología neurológica de origen vascular causada por la obstrucción de una arteria cerebral, la cual supone la segunda causa de muerte en países desarrollados afectando a 15 millones de personas en todo el mundo. Esta situación se agrava en Galicia donde el envejecimiento de la población lleva a las enfermedades de origen vascular a ser la primera causa de muerte.

El pronóstico después del ictus isquémico ha mejorado desde la aprobación del tratamiento trombolítico intravenoso con el activador tisular del plasminógeno recombinante (rtPA). El rtPA es una enzima que una vez administrada actúa disolviendo el trombo causante de la oclusión arterial. El mecanismo de acción por el cual se deshace el trombo se debe a la conversión del plasminógeno en plasmina, la cual deshace la red de fibrina, componente principal de los trombos. Sin embargo, el uso de rtPA en la práctica clínica está limitada a una reducida ventana terapéutica, inferior a las 4.5 horas desde el inicio de los síntomas, debido principalmente a los efectos secundarios asociados al tratamiento, principalmente transformación hemorrágica. Además del efecto trombolítico, el tratamiento con rtPA está relacionado con la activación de las metaloproteinasas de la matriz extracelular, que desencadenan un daño en la barrera hematoencefálica (BHE) causante del riesgo de transformación hemorrágica, que ocurre en 7-15 % de los pacientes. Además de

los efectos adversos su eficacia de recanalización es relativamente baja, solo reperfundan el 40-50 %.

Por este motivo, se hace necesaria la búsqueda de nuevas estrategias capaces de aumentar el beneficio y disminuir los riesgos del rtPA.

Han sido múltiples las estrategias que se han probado para mejorar el tratamiento con rtPA. Una de las estrategias que ha alcanzado un gran interés en el ámbito clínico ha sido el uso combinado de ultrasonidos con rtPA, definido como sonotrombolisis. El mecanismo por el cual los ultrasonidos aumentan la eficacia del rtPA se debe a una mayor penetración y distribución del rtPA en el interior del trombo, favoreciendo su disolución y reperusión de la arteria ocluida. El primer estudio clínico diseñado para comprobar la utilidad de la sonotrombolisis fue el CLOTBUST, el cual combinó el uso del rtPA con una frecuencia de 2 MHz y una intensidad de  $0.72 \text{ W/cm}^2$ , parámetros similares a los utilizados en el Doppler transcraneal. En este estudio se observó un aumento de la tasa de recanalización y mejor pronóstico con dicho tratamiento. Sin embargo, y aunque los resultados avalan positivamente esta técnica, los efectos adversos asociados a la administración sistémica del rtPA no son resueltos por esta técnica.

Por otro lado, la encapsulación de fármacos en nanosistemas permite diseñar nuevas formulaciones, surgiendo como una nueva estrategia para desarrollar sistemas de liberación controlada de fármacos que se pueden dirigir a la zona deseada, y liberar mediante la aplicación de estímulos internos o externos (por

ejemplo, los ultrasonidos). En el campo del tratamiento trombolítico, han sido numerosas las tácticas que se han llevado a cabo para encapsular el rtPA en nanosistemas: liposomas, microburbujas, partículas magnéticas, nanopartículas poliméricas, etc. Entre ellas, en el área de la cardiología, destaca la encapsulación en nanopartículas de gelatina que liberan el rtPA de su interior mediante la aplicación de ultrasonidos, y que a su vez favorece propio efecto trombolítico. La ventaja de la gelatina es que es un producto derivado de la descomposición del colágeno, es un producto biocompatible y que además tiene tendencia a unirse al factor de von Willebrand. Este factor forma parte de los trombos y se encuentra unido al colágeno, lo que explica su predisposición a unirse a la gelatina. El uso de la gelatina tiene además otra ventaja, ya que puede ser degradada por las metaloproteinasas, incrementadas en el ictus isquémico y que degradan el colágeno de la pared vascular. Por lo que la gelatina ayudaría en la liberación del fármaco del interior de la nanopartícula.

Teniendo en cuenta todo lo anterior, en esta Tesis hipotetizamos que el efecto terapéutico del rtPA puede ser aumentado mediante su encapsulación en nanocápsulas sonosensibles, que liberen el fármaco en la región isquémica mediante la aplicación de ultrasonidos.

Hemos estructurado el trabajo en dos objetivos principales:

1. La optimización *in vitro* de un nanosistema para encapsular el rtPA.
2. Los estudios *in vivo* para demostrar su eficacia y seguridad.

Como una primera aproximación, tratamos de encapsular el rtPA siguiendo un protocolo previamente publicado. Para ello se sintetizó una formulación con rtPA, gelatina y acetato de zinc. Los resultados *in vitro* fueron comparables con los resultados obtenidos en estudios previos, la actividad del rtPA se veía inhibida hasta la aplicación de los ultrasonidos. Sin embargo, la administración *in vivo* mostró que esta formulación no era lo suficientemente estable, ya que se producía la liberación del rtPA independientemente de la aplicación de los ultrasonidos.

Teniendo en cuenta este estudio previo, decidimos utilizar otro tipo de nanosistemas más complejos. Para crearlos se utilizaron núcleos de carbonato cálcico, un material poroso en cuyo interior se encapsula el fármaco, y se recubrieron utilizando la técnica del **"layer-by-layer"**. Esta técnica se basa en el uso de dos polielectrolitos, uno negativo y otro positivo, que interactúan mediante fuerzas electrostáticas. Una vez se realizan las bicapas deseadas, los nanosistemas se exponen a ácido etilendiaminotetracético (EDTA), que quelata el calcio del núcleo, obteniendo nanocápsulas. Una de las principales ventajas de la **técnica del "layer-by-layer"** es que permite la encapsulación de proteínas sin someterlas a altas temperaturas o pH que pudieran afectar a la actividad del fármaco encapsulado.

Previamente a encapsular el rtPA, se utilizó albúmina de suero bovino (BSA) para realizar la caracterización del sistema y seleccionar el número de bicapas óptimas para obtener una encapsulación estable y un sistema sono-sensible. Para facilitar todo el proceso de caracterización ambas proteínas, BSA y rtPA, se

marcaron con un fluoróforo (FITC). Después se sintetizaron los núcleos de carbonato cálcico en cuyo interior se encapsularon BSA o rtPA. Posteriormente **se realizó la técnica del "layer-by-layer"**, en nuestro caso utilizamos como polímero positivo el poli(cloruro de dialildimetilamonio) (PDACMAC) y como negativo el poli(4-estirenosulfonato de sodio) (PSS). A mayores, entre las 2 bicapas añadimos partículas de óxido de hierro para hacer estas nanocápsulas visibles por resonancia magnética, y gelatina en la última capa para vectorizar hacia la zona isquémica. Finalmente, tras la exposición a ácido etilendiaminotetraacético (EDTA) se eliminó el componente cálcico, obteniendo unas nanocápsulas con la proteína en el interior.

En el caso de la encapsulación de BSA se utilizaron 2, 4 y 6 bicapas de PSS/PDACMAC para estudiar cual era más estable y sensible a ultrasonidos. Los ensayos de estabilidad mostraron que, en todos los casos, la proteína se mantenía encapsulada durante al menos una semana. A la hora de aplicar ultrasonidos, las únicas que mostraron liberación de proteína fueron las que estaban compuestas por 2 bicapas, por lo que fueron las seleccionadas para encapsular el rtPA.

La caracterización de las nanocápsulas con rtPA resultantes se realizó mediante 1) técnicas de dispersión dinámica de la luz (DLS) para estudiar su tamaño y potencial zeta, 2) microscopía electrónica de barrido (SEM) para estudiar su morfología, 3) por fluorescencia y 4) citometría. Los resultados mostraron unas nanocápsulas de alrededor de 800 nm, con un potencial zeta de aproximadamente +15 mV. Además, pudimos calcular la cantidad

de rtPA dentro de cada nanosistema, la cual variaba entre 0.2-0.5 pg/NCs, lo que se traduce en un 13 % del máximo de carga que se podría obtener. Esto se calculó estableciendo la relación entre la fluorescencia emitida por el rtPA, y el número de nanocápsulas. Es importante puntualizar que estos análisis nos permitieron conocer en todo momento la cantidad de rtPA que teníamos en nuestras muestras para poder realizar el resto de experimento *in vitro* e *in vivo*.

Por otro lado, ensayos de estabilidad por citometría demostraron que las partículas no se agregaban en diferentes medios (plasma y PBS) y que al menos durante una semana la encapsulación de la proteína no se veía afectada.

Uno de los aspectos más críticos era confirmar que la actividad de la enzima no se veía afectada tras el proceso de encapsulación. Para ello se utilizó un sustrato comercial que al interactuar con el rtPA activo daba señal de absorbancia. Una de las características de este sustrato es que tenía un peso molecular muy pequeño (658.9 g/mol), lo cual le permitió atravesar la capa polimérica de las nanocápsulas. Esto nos permitió ver que tanto dentro de los núcleos, como dentro de las nanocápsulas, este rtPA continuaba siendo activo. Esto nos permitió garantizar que la síntesis de los núcleos de carbonato cálcico, el recubrimiento de los mismos y la exposición a EDTA no afectaban de ninguna manera a la actividad de la proteína. Por otro lado, este sustrato se utilizó también para estudiar la protección del rtPA frente a su principal inhibidor en la sangre, el inhibidor tisular del plasminógeno (PAI-1). El PAI-1 tenía un peso molecular mucho mayor al sustrato (43 kDa), por lo que



no es capaz de atravesar la capa polimérica, con lo que pudimos estudiar si el rtPA encapsulado estaba protegido frente a este compuesto. Se observó que al contrario que el rtPA libre, el cual era completamente inactivado tras incubarlo con PAI-1, los nanosistemas mantenían el rtPA protegido, aspecto trascendental ya que la vida media del rtPA podría aumentarse en la sangre debido a este efecto protector de las nanocápsulas.

La liberación *in vitro* aplicando ultrasonidos se demostró por imágenes de SEM, citometría y mediante la cuantificación de la fluorescencia. Para llevar a cabo los experimentos, se hicieron las cuantificaciones en el sobrenadante y en el precipitado. De esta forma, tras aplicar ultrasonidos a las nanocapsulas, el rtPA encapsulado debería ser liberado y encontrarse en el sobrenadante. En todos los casos en los que aplicamos ultrasonidos, se utilizaron los parámetros seguros para humanos (2 MHz y  $0.72 \text{ W/cm}^2$ ). Los estudios demostraron que estos parámetros permitían liberar hasta un 50 % del rtPA encapsulado. Manifestando además cambios en los perfiles de citometría tras aplicar ultrasonidos, y la disrupción de los nanosistemas en imágenes de SEM. A pesar de liberar únicamente el 50 %, estudios con coágulos *in vitro* mostraron una actividad similar a la de la misma concentración que el rtPA libre.

Las propiedades como agente de contraste de las cápsulas fueron estudiadas con resonancia magnética, obteniendo una relaxividad mayor que los agentes comerciales, lo que nos facilitaría posteriormente el seguimiento las nanoestructuras en el cerebro de los animales tras su administración.

Previamente a estudiar la liberación *in vivo* y el efecto terapéutico de estos nanosistemas, se realizaron ensayos en animales para comprobar la seguridad las nanocápsulas y de los ultrasonidos. Demostramos que la administración de las nanocápsulas no producía alteraciones de la circulación cerebral ni hemorragias en animales sanos, así como tampoco producen toxicidad renal ni hepática, lo que determinamos analizando marcadores sanguíneos relacionados con estos daños (transaminasa glutámico-oxalacética, transaminasa glutámico-pirúvica y creatinina). El estudio de la seguridad de los ultrasonidos utilizados para inducir la liberación del rtPA *in vivo*, se realizó con el fin descartar cualquier efecto sobre la disrupción de la BHE. Para comprobarlo se utilizó la técnica del evans blue, este compuesto se une a la albúmina de la sangre, esta proteína únicamente cruza la BHE cuando está dañada. Cuantificando la cantidad de evans blue extravasado, confirmamos que utilizando la frecuencia y la intensidad previamente citadas, no se observó un aumento del daño de barrera ni en animales sanos ni en animales isquémicos.

Para estudiar la liberación *in vivo*, se administraron las nanocápsulas en animales sanos. La administración de los tratamientos se llevó a cabo en la vena femoral, se aplicaron ultrasonidos en la región abdominal y se extrajeron muestras de sangre a diferentes tiempos, para analizar la actividad plasmática del rtPA. Cabe destacar que en este trabajo las administraciones de las nanocápsulas se llevaron a cabo en forma de bolus, con una dosis de rtPA 10 veces menor a la que se usa en modelos murinos (10mg/Kg). Uno de los principales problemas del rtPA en la clínica,

es que debe ser administrado un 10 % en forma de bolus y el otro 90 % en forma de infusión, para mantener la dosis terapéutica. En nuestro caso, observamos que el grupo tratado con rtPA, tal y como se esperaba, tuvo un aumento en la actividad plasmática del rtPA en los primeros minutos, disminuyendo a partir del minuto 5, debido a su corta vida media. El grupo tratado con nanocápsulas mostró un perfil de actividad similar al grupo tratado con rtPA a 1 mg/kg. Sin embargo, cuando se aplicaron los ultrasonidos, la actividad de rtPA aumentó con el tiempo, alcanzando aproximadamente 3.5 veces más en comparación con 1 mg/kg, después de 40 minutos. Este resultado fue particularmente importante ya que demostró que la vida media del rtPA podía ser aumentada con la encapsulación sin necesidad de hacer una perfusión continua, como se hace actualmente con el rtPA.

Por otro lado, la administración de las nanocápsulas sin gelatina mostraron un perfil de liberación de rtPA muy diferente, en ambos grupos (con y sin ultrasonidos) la actividad plasmática del rtPA se mantuvo elevada durante los 40 minutos. Esto pudo deberse a diferentes motivos, por ejemplo, a la diferencia en el potencial zeta de las partículas, ya que sin gelatina era de aproximadamente -40 mV y con gelatina +15 mV, que hace que su comportamiento en sangre sea diferente. Además, el hecho de tener gelatina hace que sea menos antigénico, evada el sistema retículo endotelial y se prolongue el tiempo de circulación. Con todo esto se demostró que la gelatina es un factor principal para mantener la estabilidad en sangre de los nanosistemas.

Para estudiar el efecto terapéutico se utilizó un modelo de isquemia tromboembólica, mediante la cual se inyecta trombina en la arterial cerebral media de ratones para crear un trombo *in situ*. Los grupos de estudio utilizados para evaluar la reperfusión, los volúmenes de infarto y las transformaciones hemorrágicas, fueron los siguientes: vehículo, vehículo + ultrasonidos, rtPA (1 mg/kg) administrado en forma de bolus, rtPA (1 mg/kg) administrado en forma de bolus + ultrasonidos, rtPA (10 mg/kg) administrado en forma de bolus e infusión, nanocápsulas con gelatina, nanocápsulas con gelatina + ultrasonidos, nanocápsulas sin gelatina y nanocápsulas sin gelatina + ultrasonidos. Todos los tratamientos fueron administrados 30 minutos después de la oclusión de la arteria, se administraron en forma de bolus y en aquellos grupos tratados con ultrasonidos, se llevó a cabo durante 40 minutos. En nuestro caso todos los grupos tratados con rtPA disminuyeron el volumen de infarto comparado con el control con el vehículo. Sin embargo, entre los grupos tratados con rtPA (1 mg/kg, 10 mg/kg y 1 mg/kg + ultrasonidos) no se observaron diferencias en el volumen de infarto. En los grupos tratados con nanosistemas, únicamente mostró reperfusión el grupo tratado con nanocápsulas con gelatina y ultrasonidos (60 %), sin embargo, el resto de grupos no mostraron ninguna recuperación del flujo cerebral. En el análisis del volumen isquémico determinado por la resonancia magnética, se observó que únicamente el grupo tratado con nanocápsulas con gelatina y ultrasonidos mostraba una pequeña reducción del volumen de infarto, comparado con el resto de grupos tratados con nanocápsulas. Sin embargo, comparado con el grupo control no existen diferencias. El hecho de

que las nanocápsulas (con gelatina) y ultrasonidos disminuyan el volumen de infarto puede explicarse por lo siguiente: i) la estabilidad de estas en la circulación; ii) pueden alcanzar el trombo; y iii) pueden liberar el rtPA mediante la aplicación de ultrasonidos. Al contrario de lo mencionado anteriormente, las metaloproteinasas mostraron no funcionar como un factor interno para degradar la gelatina y liberar el rtPA, lo cual se habría demostrado si el grupo tratado únicamente con las nanocápsulas (con gelatina) mostraran una reducción del volumen de infarto. Esto demostró que los ultrasonidos son cruciales para liberar el rtPA en la región ocluida.

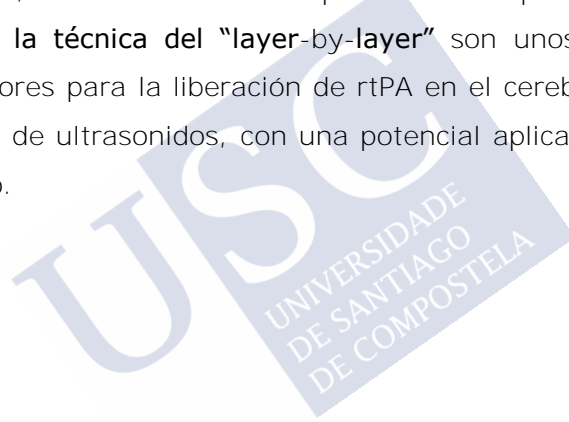
Por otro lado, estudios con resonancia magnética mostraron la aparición de señales en secuencias de T2\*, en las que se puede observar el hierro, en la región isquémica correspondiente a la nanocapsulas administradas.

Todo esto demostró la presencia de las nanocápsulas en el cerebro tras administrarse de forma intravenosa en la vena de la cola. Esto demostró que este sistema puede ser utilizado como sistema de liberación vectorizado al trombo, aunque algunas modificaciones deberían realizarse para aumentar el efecto terapéutico, tales como disminuir el tamaño de partícula y aumentar la tasa de liberación tras aplicar ultrasonidos.

En conclusión, hemos desarrollado unos nanosistemas sonosensibles que permiten encapsular el rtPA sin afectar a su actividad y que mantienen la proteína protegida de su principal inhibidor. Además, únicamente liberan el rtPA mediante la aplicación de ultrasonidos. Todo esto permite prolongar la vida

media del rtPA con una sola administración en forma de bolus. Desde un punto de vista clínico esto supone un avance en el tratamiento con rtPA, puesto que una de sus principales limitaciones es su administración, que debe ser realizada en forma de bolus e infusión debido a su corta vida media. Lo que podría traducirse en una reducción de la complicación de la administración del rtPA y un mayor porcentaje de pacientes beneficiados del tratamiento trombolítico.

En general, hemos demostrado que las nanocápsulas sintetizadas **utilizando la técnica del "layer-by-layer"** son unos nanosistemas prometedores para la liberación de rtPA en el cerebro mediante la aplicación de ultrasonidos, con una potencial aplicación en el ictus isquémico.



## Abbreviations

AMPA:  $\alpha$ -amino-3-hydroxy-5-methyl-4-isoxazol propionic acid

AMPA<sub>r</sub>:  $\alpha$ -amino-3-hydroxy-5-methyl-4-isoxazol propionic acid receptor

ANOVA: analysis of variance

ATP: adenosine tri-phosphate

BBB: blood brain barrier

bL: bilayer

BSA: bovine serum albumin

CBF: cerebral blood flow

CCA: common carotid artery

CLOTBUST: Combined Lysis of Thrombus in Brain Ischemia Using Transcranial US and Systemic tPA trial

C<sub>NP</sub>: nanoparticle concentration

CNS: central nervous system

COX: cyclooxygenase

DEDAS: Dose Escalation of Desmoteplase in Acute Stroke trial

DIAS: Desmoteplase in Acute Ischemic Stroke trial

DLS: dynamic light scattering

d<sub>NP</sub>: nanoparticle diameter

EB: evans blue

ECA: external carotid artery

ECASS: European Cooperative Acute Stroke Study trial

LE: loading efficiency

EDTA: ethylenediaminetetraacetic acid

EGF domain: epidermal growth factor-like domain

EU: European Union

FA: flip angle

F domain: finger domain

FDA: Food and Drug Administration

FITC: fluorescein-5-isothiocyanate

FOV: field of view

FS: forward scattering

GABA: gamma aminobutyric acid

GOT: glutamate oxaloacetate transaminase

GP: glycoprotein

GPT: glutamate pyruvate transaminase

HT: hemorrhagic transformation

i.a.: intraarterial

i.v.: intravenous

ICA: internal carotid artery

ICP-MS: inductively coupled plasma mass spectrometry

I<sub>F</sub>: fluorescence intensity

iNOS

IU: international units



K1 domain: Kringle 1 domain

K2 domain: Kringle 2 domain

kDa: kilodalton

LbL: layer-by-layer

LBS: lysine binding site

LRP: low density lipoprotein receptor-related protein

MB: microbubble

MCA: middle cerebral artery

MGE: multi-gradient-echo sequence

MMP: metalloproteinases

$m_{NP}$ : nanoparticle mass

$m_{organ}$ : organ mass

MRI: magnetic resonance imaging

MSME: multi-slice multi-echo sequence

MW: molecular weight

**NF- $\kappa$ B: nuclear factor  $\kappa$ B**

NINDS: National Institute of Neurological Disorders and Stroke

nm: nanometer

NMDA: N-methyl-D-aspartate glutamatergic

NMDAr: N-methyl-D-aspartate glutamatergic receptor

nNOS: neuronal nitric oxide synthase

NC: nanocapsule

NO: nitric oxide

NP: nanoparticle

PAH: poly(allylamine hydrochloride)

PAI-1: type 1 plasminogen activator inhibitor

PAR: protease-activated receptor

PBS: phosphate-buffered solution

PDACMAC: poly(diallyldimethylammonium chloride)

PDGF-CC: platelet derived growth factor

PI3-Akt: phosphatidylinositol-3-kinase pathway

PDI: polydispersity index

PLGA: poly(lactic-co-glycolic acid)

PMA: Poly(methyl acrylate)

pNA: p-nitroaniline

PSS: sodium poly(styrene sulfonate)

PT: precipitate

PVSA: poly(vinylsulfonic acid)

r: radius

$R_{rtPA}$ : rtPA radius

RES: reticuloendothelial system

RGD: L-arginine-glycine-aspartic acid peptide

RGDS: L-arginine-glycine-aspartic acid-serine peptide

RT: room temperature

## Abbreviations

rtPA: recombinant tissue plasminogen activator

sc-tPA: single chain tissue plasminogen activator

SD: standard deviation

SEM: scanning electron microscopy

sICH: symptomatic intracerebral hemorrhage

SITS-MOST: Safe Implementation of Thrombolysis in Stroke-Monitoring Study

SN: supernatant

SS: side scattering

SW: spectral bandwidth

TAFI: thrombin-activatable fibrinolysis inhibitor

tc-tPA: two chain tissue plasminogen activator

TE: echo time

TEM: transmission electron microscopy

TF: tissue factor

tPA: tissue plasminogen activator

TR: repetition time

TRUMBI: Transcranial Low-Frequency US-Mediated Thrombolysis in Brain Ischemia trial

uPA: urokinase plasminogen activator

US: ultrasound

$V_{NC}$ : nanocapsule volume

$V_{NP}$ : nanoparticle volume

$V_{rtPA}$ : rtPA volume

vWF: von Willebrand factor

WHO: World Health Organization





## Introduction

---



## 1. Stroke

### 1.1. Definition

Stroke, or brain infarct, is the most common type of cerebrovascular disease. Based on clinical features, the **World Health Organization (WHO) defines stroke as "rapidly developing clinical signs of focal (or global) disturbance of cerebral function, lasting more than 24 h or leading to death, with no apparent cause other than of vascular origin"**<sup>1</sup>.

From a physiopathological point of view, stroke can be defined as a cerebrovascular disease in which the central nervous system (CNS) blood flow is interrupted due to a vessel obstruction (ischemic stroke) or vessel rupture (hemorrhagic stroke) causing oxygen and nutrients deprivation to surrounding tissue. This deprivation must be sustained over the time, causing cell damage often resulting in cell death, with the consequent loss of function in the neural tissue. The tissue injury is clinically observable by a rapid loss of motor function and/or neuroimaging evidences<sup>2</sup>.

### 1.2. Epidemiology

Stroke is the major cause of mortality and morbidity worldwide. According to the WHO, the world average incidence of cerebrovascular disease is around 200 new cases per 100.000 inhabitants<sup>3</sup>. In Europe there are differences between northern and

southern populations; the higher figures are found in Nordic countries such as Finland (270 per 100.000 in men), and the lower in others such as Italy and Portugal (100 per 100.000 men)<sup>4</sup>. The incidence in Spain is 167 per 100.000 / year (181 for men and 153 for women), being higher in Galicia due to the aging population<sup>5</sup>.

In developed countries, the prevalence of stroke adjusted by age in people over 64 years is between 4.6 and 7.3 %. It is higher in men (5.9 to 9.3 %) than females (3.2 to 6.1 %) and increases with age. In Spain, the age-specific prevalence rate is 4.9 % for the total of cerebrovascular disease and 3.5 % for ischemic stroke<sup>6</sup>. Due to the progressive aging of European population in general, and the Spanish and Galician in particular, the incidence and prevalence of stroke increase progressively, which will lead to a serious social health.

Therefore, stroke is a health problem that requires the establishment of better guidelines for prevention and treatment to reduce its incidence as well as the degree of disability caused. Taking into consideration that the incidence of stroke increases in people over 65 and that life expectancy in developed countries **doesn't stop growing** due to the improvements in the quality of life, the prevalence of the disease will continue raising and with it the magnitude of this social problem.



### 1.3. Classification of stroke

Focusing on the nature of the lesion, stroke can be classified in two main groups, ischemic and hemorrhagic stroke (Figure 1). However, alternative classifications of this cerebrovascular disease can be used looking at other parameters such as stroke subtype, progression profile, neuroimaging characteristics, lesion size, topography of the lesion, nature, mechanisms of induction and etiology<sup>2, 7</sup>.

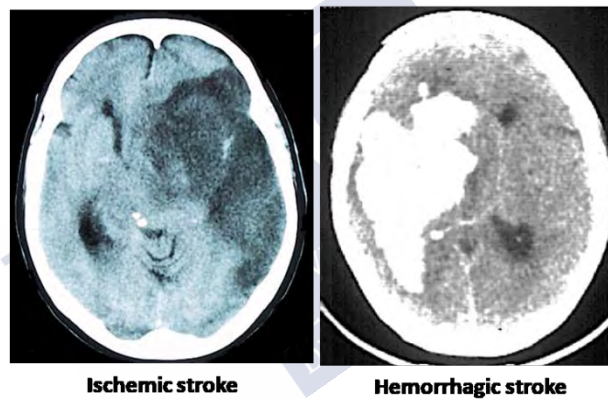


Figure 1. Representation of ischemic and hemorrhagic stroke. Image of the file of Professor José Castillo.

#### 1.3.1. Hemorrhagic stroke

Among all cerebrovascular diseases, the pathologic group of hemorrhages corresponds to approximately 15 % of all the cases of stroke. In spite of its low prevalence, it is associated to high mortality.

Hemorrhagic stroke is caused by a non-traumatic blood vessel rupture with the consequent bleeding into the brain parenchyma or in the ventricular space. Extravasated blood is accumulated and pressures the surrounding tissue, which in combination with the toxicity of some blood components for CNS cells, leads to necrosis of the focal area affected, and to global brain stress. The most common cause of hemorrhage is arterial hypertension or amyloid angiopathy. Less frequently it is due to vascular malformation, drugs, toxics, hematological diseases, brain vasculopathy, primary or metastatic tumors, among others<sup>8</sup>.

### 1.3.2. Ischemic stroke

It is the most frequent type of stroke, constituting around 85 % of all stroke events. In ischemic stroke, blood flow disruption is due to a dysregulation of the coagulation-fibrinolysis cycle and other metabolic cycles causing a physical obstruction in the blood vessel, often due to the presence of a clot. The obstruction occludes the vessel blocking the blood supply to the vascular territory.

There are different alternatives to classify ischemic strokes, attending to etiology, size, or vascular territory affected, among others. In the clinical practice, ischemic strokes are frequently classified in five subgroups: large-artery atherosclerotic stroke, cardioembolic stroke, lacunar stroke, stroke of other etiology, and stroke of undetermined etiology. This classification is not rigorously etiological, but it constitutes a useful tool for clinicians,

allowing taking fast management decisions based on the stroke subtype<sup>9, 10</sup>.

- Atherosclerotic stroke (~20%): they are also called **“large-artery strokes”**. These patients show a significant stenosis (>50 %) or occlusion of a major brain artery (or a cortical branch) due to atherosclerosis. Functional impairment concerns cortical, brain stem or cerebellar symptomatology, and large lesions are observable in neuroimaging studies<sup>9, 10</sup>.
- Cardioembolic stroke (~20%): this type of stroke is caused by an embolus originated and released from the heart. Clinical and neuroimaging findings are similar to those observed in atherosclerotic strokes, but the identification of risk factors of cardiac source of embolism (atrial fibrillation, atrial thrombus, mechanical prosthetic valve, recent myocardial infarction, etc.) determines the diagnostic<sup>9, 10</sup>.
- Lacunar stroke (~25%) they are also called small-artery strokes. They are characterized by small sized infarct (<15mm of diameter), localized in the territory of the penetrating arterioles. The main pathologic substrate in lacunar infarcts are micro-atheromatosis and lipohyalinosis, other less frequent potential causes are cardiac embolism, arterial embolism, infectious arthritis or prothrombotic state<sup>9, 10</sup>.

- Stroke of other etiology (~5%): strokes with infrequent etiologies, for example arterial dissection, non-atherosclerotic vasculopathies or hematologic disorders, among others<sup>9, 10</sup>.
- Stroke of undetermined etiology (~30%): brain infarcts of medium or large size with more than two potential etiologies or unknown origin<sup>9, 10</sup>.

#### 1.4. Risk factors

##### 1.4.1. No modifiable risk factors

- Age: aging is one of the main risk factors in the cerebrovascular disease. The incidence increases exponentially with age, reaching his maximum values over 65 years old<sup>11</sup>.
- Sex: the incidence in men is higher than in women<sup>12</sup>.
- Race: the large-vessels affects more often to Caucasian individuals, while small vessel pathology is more frequent in Africans and Asians<sup>11</sup>.

### 1.4.2. Modifiable risk factors

- Systemic hypertension is the main risk factor in the ischemic and the hemorrhagic stroke. Both systolic and diastolic hypertension increases the risk of stroke from moderate values. Values of 140-160 mm Hg in systolic and 90-94 mm Hg in diastolic hypertension increase the risk of suffering a stroke 1.5-fold<sup>13, 14</sup>.
- Cardiopathy: heart diseases are associated with the stroke, especially atrial fibrillation, valvulopathies, myocardial infarction, left ventricular hypertrophy and cardiomegaly<sup>13, 14</sup>.
- Diabetes mellitus: the risk of stroke increases 1.8-fold in diabetic men and 2.2-fold in diabetic women. Diabetes predisposes to ischemic stroke due to its influence in the development of atherosclerosis<sup>13, 14</sup>.
- Hyperlipidemia: Hyperlipidemia promotes the development of atheromatosis and ischemia, both coronary and carotid<sup>13, 14</sup>.
- Smoking: Cigarette smoking predisposes to the appearance of atherosclerosis in men and women, with an increased risk of 2-3-fold. Tobacco facilitates arterial spasm and endothelial damage. It has been seen that this added risk of smoking disappears after five years of abstention<sup>13, 14</sup>.

- Other factors: sedentarism, obesity, night snoring, sleep apnea syndrome, oral contraceptives and excessive alcohol consumption have also been linked to an increased risk of stroke<sup>13, 14</sup>.

It is important to know the prevalence and the relative risk of each risk factor, because a factor with a high relative risk may have little relevance if it is not very frequent<sup>12, 14</sup>. This is summarized in Table 1.

Table 1. Prevalence and relative risk of modifiable risk factors.

Risk factor	Prevalence (%)	Relative risk
Systemic hypertension	25 - 40	x 3 - 5
Atrial fibrillation	1 - 2	x 5 - 18
Dyslipidemia	6 - 40	x 1 - 2
Smoking	20 - 40	x 1.5 - 2.5
Diabetes mellitus	4 - 20	x 1.5 - 3
Alcoholism	5 - 30	x 1 - 3
Sedentarism	20 - 40	x 2.7

### 1.5. Biochemistry of coagulation

Since the main cause of ischemic stroke is the presence of a thrombus that obstructs the cerebral blood flow (CBF), the

biochemistry of coagulation and alterations related with, are relevant aspects to consider in the etiology of this pathology.

The hemostatic system is a combination of biochemical and cellular events that allow the blood to stay in a fluid state and prevent bleeding when damage to a vessel occurs. When the hemostatic mechanisms do not work properly, the control of the size and stability of the thrombus is lost, and the probability of an occlusion in vessels increases. This is known as thrombosis.

The hemostatic system comprises the platelet activation, the coagulation system and the fibrinolytic system, that are the primary, secondary and tertiary hemostasis respectively<sup>15, 16</sup>.

### 1.5.1. Primary hemostasis: platelet activation

#### 1.5.1.1. Platelet adhesion

Collagen and von Willebrand factor (vWF) are the main responsible of the adhesion of the platelets to the endothelium. After vessel damage, collagen, which is the main component of the subendothelium, is exposed to the blood becoming the main thrombogenic substance. Then, vWF binds to the collagen.

Later, platelets interact with vWF through the glycoprotein (GP) Ib-IX-V which GP binds to thrombin enhancing the thrombosis response. Platelet also express on the membrane other proteins related with the thrombosis, named as integrins. Two main

integrins have been describes,  $\alpha_2\beta_1$  and  $\alpha_{IIb}\beta_3$ . These intregrins proteins participate in coagulation process by interacting with collagen<sup>15</sup> (Figure 2).

#### 1.5.1.2. Platelet activation

Platelets, that are small anucleate cells from megakaryocytes, contain two different secretory granules:  $\alpha$ -granules and  $\delta$ -granules. On one hand,  $\alpha$ -granules are the responsible for the secretion of hemostatic agents as P-selectin and platelet activating factor 4, clotting factor, type 1 plasminogen activator inhibitor (PAI-1), cell modulators, interleukins and chemokines. On the other hand, **inorganic and small organic molecules compose  $\delta$ -granules**<sup>17</sup>.

To carry out the recruitment of more platelets and the stimulation of other neighboring cells, the activation of more platelets is needed. Some agonists could release different compounds of the platelet granules that are involved in the activation; also, collagen, vWF, and thrombin help in this process<sup>15</sup>.

#### 1.5.1.3. Platelet aggregation

Aggregation of platelets is due to the activation of  $\alpha_{IIb}\beta_3$  integrin. In normal conditions,  $\alpha_{IIb}\beta_3$  integrin has low affinity in the platelet-platelet interaction; however, once the platelets are activated their



conformation changes and the aggregation occur. As other integrins,  $\alpha_{IIb}\beta_3$  also interacts with fibrinogen and vWF<sup>15</sup>.

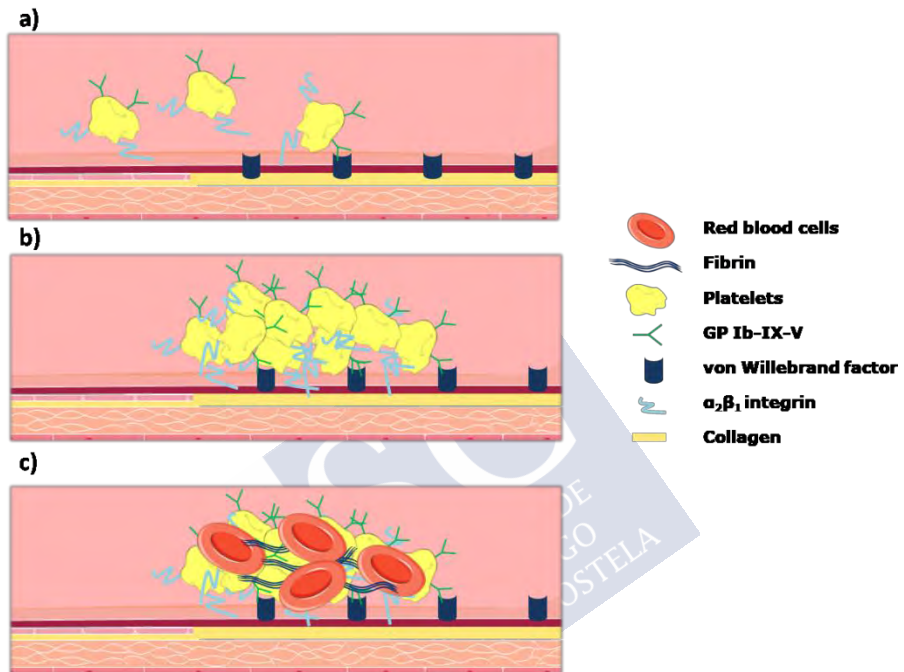


Figure 2. Primary hemostasis scheme. a) Collagen and vWF exposure after vessel damage. b) Platelet adhesion through the interaction of the GP Ib-IX-V with the vWF, and the  $\alpha_2\beta_1$  integrin with the collagen. c) Adhesion of the red blood cells after the platelet activation. Self-created image (using elements with Creative Common license).

### 1.5.2. Secondary hemostasis: coagulation system

When the vessel wall is breached, in addition to the exposure of the collagen, the exhibition of the tissue factor (TF) occurs. TF is a membrane protein of fibroblast and pericytes in the adventitia and medial smooth muscle cells of the vessel wall. TF works in the

hemostasis as a cofactor for the serine proteases that are involved in the coagulation cascade.

Classically, secondary hemostasis is divided into extrinsic, intrinsic and common pathway. The general scheme of the secondary hemostasis can be observed in Figure 3.

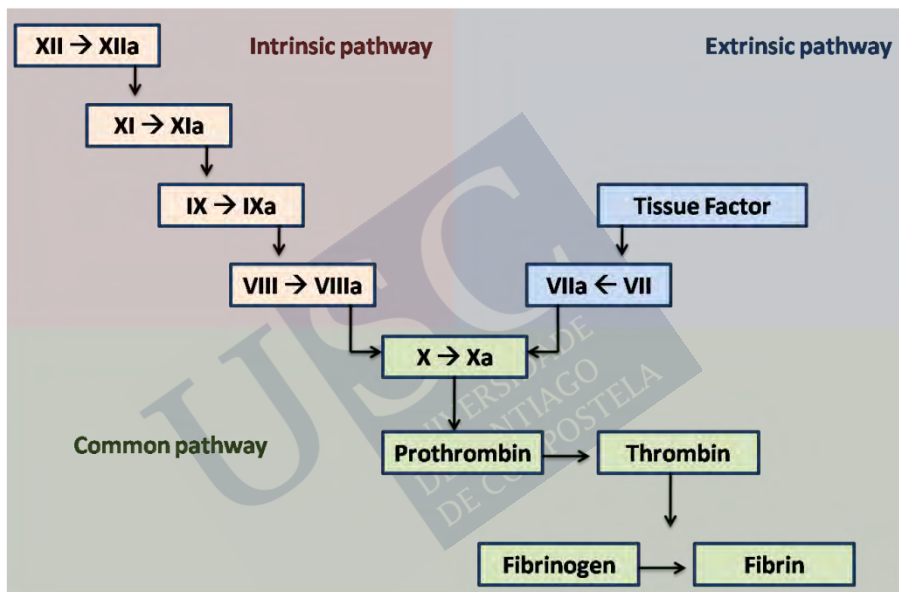


Figure 3. Coagulation cascade. Self-created image.

The active TF forms a complex with the factor VIIa (active form of the factor VII) which activates the factor X and initiates the proteolytic cascade generating the thrombin. This pathway is historically termed as extrinsic pathway of coagulation. The intrinsic pathway is started by XII factor. This cascade involved the

XI, IX and VII factor that, as in the extrinsic pathway, finishes with the activation of the factor X. Finally, the thrombin converts the fibrinogen into the insoluble fibrin mesh<sup>18</sup>.

In addition, thrombin is involved in other coagulation events. For example, in the platelet activation via cleavage of protease-activated receptor 1 and 4 (PAR1 and PAR4) releasing agonists from the platelet to activate other platelets, or in the clot propagation activating factor XI, VII and V as a positive feedback loop<sup>18</sup>.

Some serine protease inhibitors as thrombomodulin, heparin sulfate proteoglycans or antithrombin work as down-regulators of the coagulation cascade.

It is important to note that this fibrin mesh is generated at the same time that the platelets aggregation; primary and secondary hemostasis work in parallel. Therefore, when the platelets are activated via thrombin the interactions between them and the vWF and collagen do not exist. Depending on the injury or the disease, primary or secondary hemostasis is going to predominate, and the composition of the thrombus will vary<sup>19</sup>.

### 1.5.3. Tertiary hemostasis: the fibrinolysis

The role of fibrinolysis is to dissolve and prevent the formation blood clots. Fibrinolytic system is composed by serine proteases that work as zymogens. Plasminogen is the inactive form, which is

converted into plasmin that is the active form and it is involved in the dissolution of the clot, converting the fibrinogen into fibrin (Figure 4).

Plasminogen is converted into plasmin by tissue plasminogen activator (tPA) and urokinase plasminogen activator (uPA). These components differ in the place where they are synthesized; whereas tPA is synthesized in endothelial cells, the uPA is synthesized in monocytes, macrophages and urinary epithelium. Furthermore, tPA has more affinity for the plasminogen, playing a more important role in the fibrinolysis. On the other hand, both of them are inactivated by PAI-1 and are cleared in the liver, what makes them have a short half-life (4-8 min)<sup>20</sup>.

In the fibrinolytic system are involved other players that participates in the maintenance of homeostasis, such as serpin inhibitors (e.g; PAI-1, PAI-2, and  $\alpha$ 2-antiplasmin) which blocks the action of the plasminogen and the plasmin; and the thrombin-activatable fibrinolysis inhibitor (TAFI) which binds to the fibrin avoiding the binding of the plasmin.

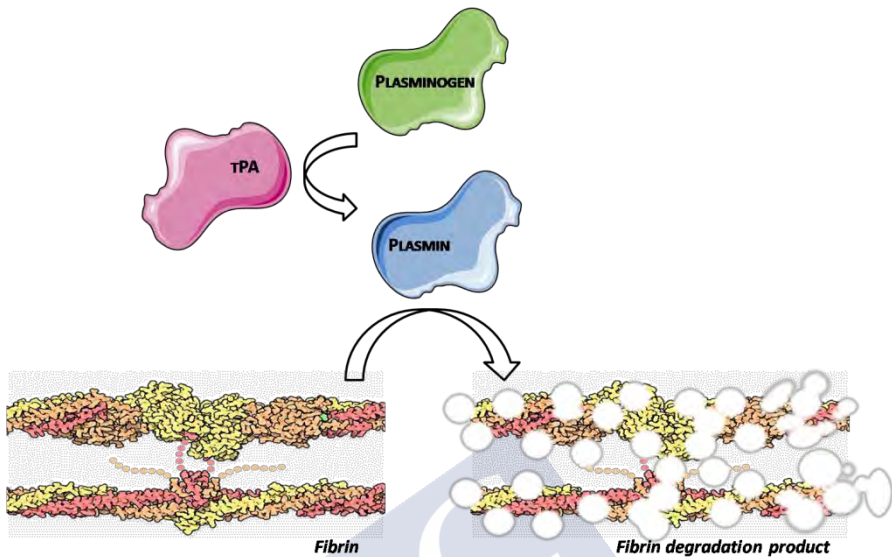


Figure 4. Dissolution of the clot by the conversion of the plasminogen into plasmin by the tPA. Self-created image (using elements with Creative Common license).

#### 1.5.4. Thrombus

The different interactions between platelets and coagulation factors to form a clot lead to different compositions of the thrombus. Knowing the composition of thrombi is crucial to understand their pathogenesis, properties and clinical management<sup>21</sup>.

Platelets and thrombin are the main component of thrombi, but the amount of each one varies depending on the thrombus origin. Thrombi formed on top of disrupted atherosclerotic plaque are usually composed by platelets, and have little fibrin. In contrast, thrombi from patients with atrial fibrillation tend to be composed by large amount of fibrin, and less platelet composition<sup>22</sup>.

The resistance to fibrinolysis depends on the composition of the thrombi. Thrombi rich in platelets are more resistant to fibrinolysis than thrombus rich in fibrin. This is due to the following mechanisms:

- The 90 % of the circulating PAI-1 is contained into the platelets, that prevents the tPA from exerting its thrombolytic effect.
- Platelets are involved in the generation of thrombin, not only during the formation of the clot, but also during the lysis. In addition to PAI-1, TAFI also contributes to thrombolysis resistance.
- Another component that is abundant in the platelets is the Factor XIII. The main functions of this factor are to cross-linking fibrin and play an important role in thrombolysis resistance. When the Factor XIII is activated, it joins the plasmin inhibitor  $\alpha_2$ -antiplasmin to fibrin, inhibiting the clot degradation. Also, it alters the structure of the fibrin network to reduce pore size and increase fiber density. In fact, genetic disorders related with this factor are associated with the increasing of the risk of myocardial infarction.

Another factor that influences the thrombolysis is the structure of the fibrin network. The fibrin fibers in stroke patients are usually thick, which make them more porous and deformable. Although this high porosity facilitates the tPA penetration in the

clot, the elevation in circulating PAI-1,  $\alpha$ 2-antiplasmin or TAFI can also influence the resistance to the fibrinolysis<sup>22</sup>.

### 1.6. Biochemistry of cerebral ischemia

The acute obstruction of one of the brain arteries induces an instantaneous reduction of blood flow in the corresponding irrigation area (focal ischemia). But that reduction of blood supply is not homogeneous in the affected area, and can change within minutes or hours, especially if blood supply is not reinstated<sup>23</sup>.

Two regions can be distinguished: the ischemic core and the penumbra. Ischemic core is the portion of tissue closest to the affected blood vessel and where the ischemia becomes severe. In the penumbra, the reduction of blood flow is less severe due to the blood supply carried out by collateral arteries of the non-ischemic neighbor tissue. The impact of brain ischemia will depend on the level of the artery occlusion and duration of the reduction of blood flow, which is why time is a very important parameter in this disease<sup>24</sup> (Figure 5).

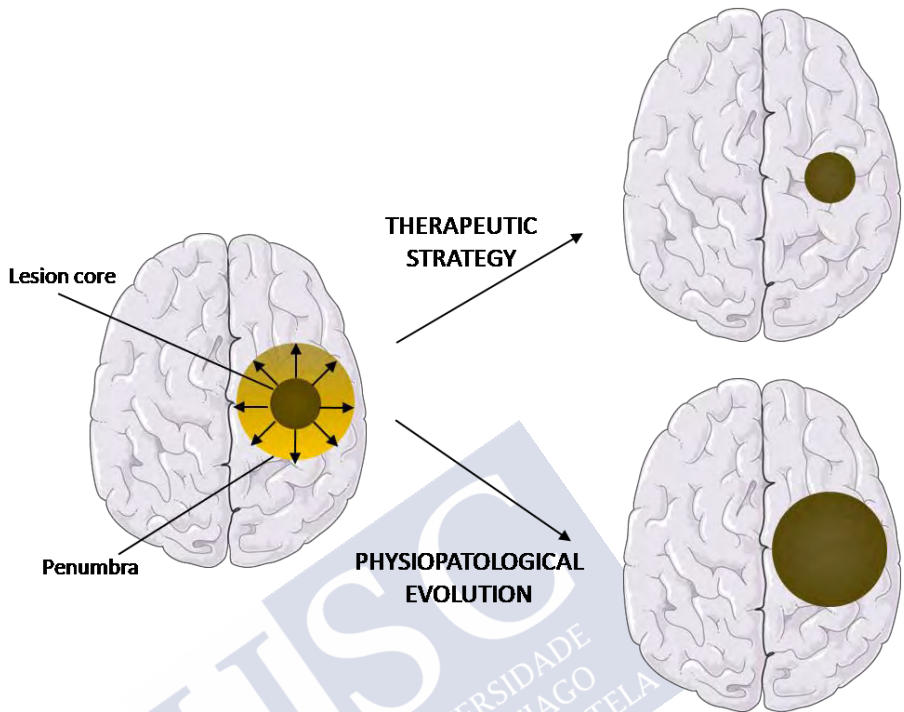


Figure 5. Core lesion generated after ischemic stroke closest to the occluded vessel, and the penumbra area, still salvable, which is the target of neuroprotectants treatments. Self-created image (using elements with Creative Commons license).

After the onset of brain ischemia, a sequence of molecular events is triggered in the short and the long term, initiated with an energetic failure in cells, related to the interruption of oxidative phosphorylation processes and the deficient production of adenosine tri-phosphate (ATP) (Figure 6).



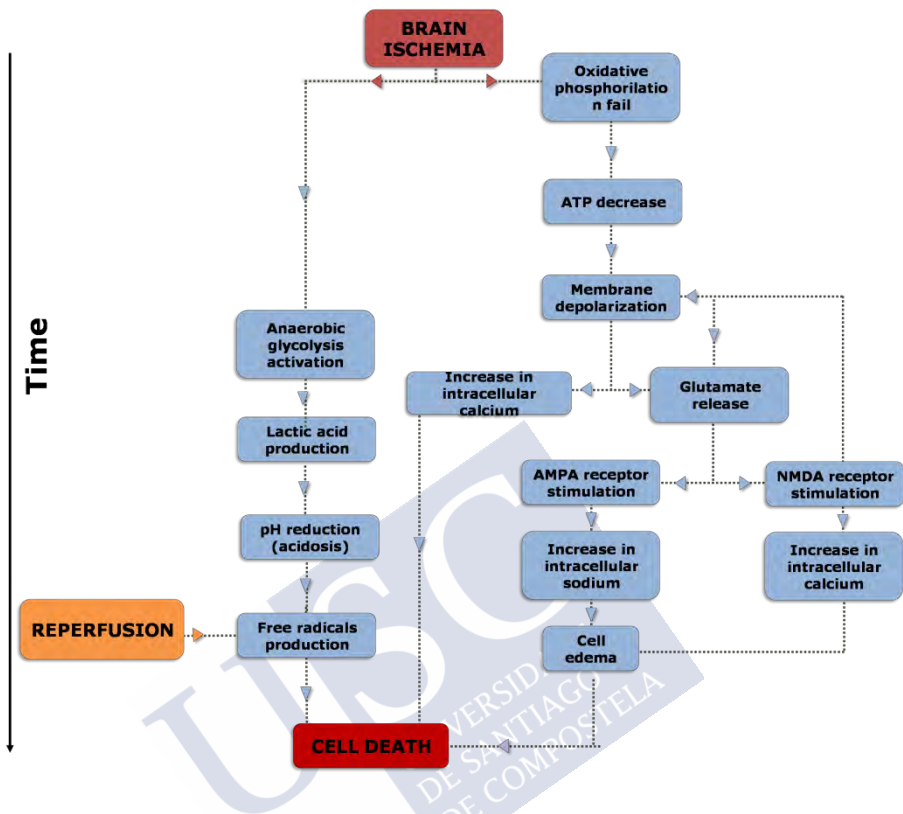


Figure 6. Major events that occurred after cerebral ischemia, leading to neuronal death. Self-created image.

The cessation of transmembrane ionic gradients due to the failure of sodium-potassium-ATPase pumps, and other ATP-dependent ionic pumps, is the key step of the physiopathological mechanisms in stroke, especially of cell death in the ischemic core, when the vascular occlusion lasts for few minutes<sup>25</sup>. Neurons and glial cells suffer an extreme depolarization because of the entrance of sodium, chloride, calcium and water into the cytoplasm<sup>26</sup>, and, in addition, potassium leaves the cell inducing a sudden increment of

its extracellular levels<sup>27</sup>. The energetic failure and the associated ionic changes, originate an increment in glutamate, a hyperexcitability of N-methyl-D-aspartate glutamatergic (NMDA) receptors (NMDAr) and of  $\alpha$ -amino-3-hydroxy-5-methyl-4-isoxazol propionic acid (AMPA) receptors (AMPA), which induces an even higher increase of intracellular calcium (Figure 7)<sup>28-30</sup>.

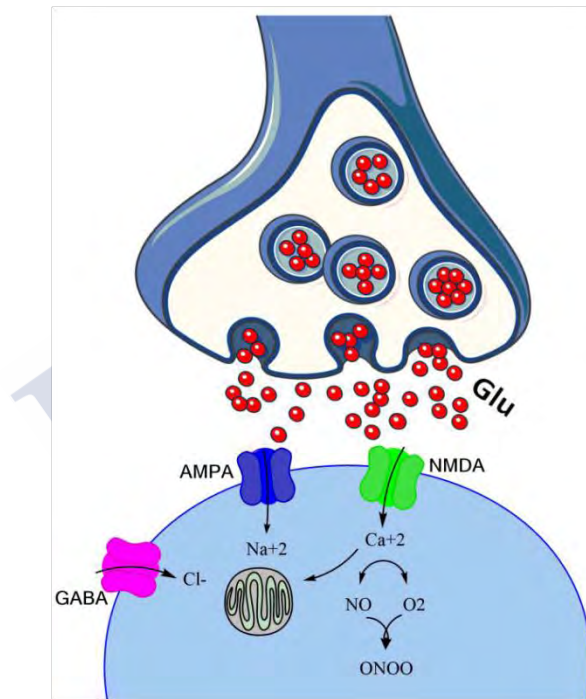


Figure 7. Glutamate release in the neurons under ischemic conditions. Self-created image (using elements with Creative Common license).

Hyperexcitability causes a depolarization phenomenon in the periphery of the infarct, which increases the energetic cost while

the membrane tries to re-polarize itself<sup>24, 31, 32</sup>. Calcium increment, together with acidosis and peri-infarct depolarization, contributes to initiate the damage and, after it, inflammation and activation of apoptotic phenomena contribute to increment the lesion<sup>30, 33</sup>. During ischemia, and particularly during reperfusion, free radicals are generated. These are highly reactive species produced at the initial and late stages of brain ischemia, following different physiopathological mechanisms. In the first place, oxygen reactive species are produced by the metabolism of arachidonic acid and the activity of neuronal nitric oxide (NO) synthase (nNOS). During intermediate stages, free oxygen radicals are provided by the infiltration of neutrophils in the ischemic area. At later stages, they are produced via synthesis and activation of inducible NO synthase enzymes (iNOS) and cyclooxygenase-2 (COX-2)<sup>34, 35</sup>. Ischemic stroke triggers a series of complex molecular events, where the activation and the expression of genes are included.

However, ischemic cellular death can take place in two different ways. The most common one is necrosis<sup>36</sup>, which is the result of the acute energetic failure, mainly located in the core region of the lesion zone, and it is characterized by morphology changes and, at the end, cellular lysis, which also triggers inflammatory processes<sup>37</sup>. The second one, apoptotic or programmed cell death, in the area around the core region, can be observed when energy-dependent intracellular mechanisms are activated, leading to cell degradation<sup>33, 38</sup>.

## 1.7. Therapeutic approaches for the treatment of stroke

The different approaches for the treatment of stroke can be classified into: strategies to restore brain flow, neuroprotection, and neurorepairing treatments (Figure 8).

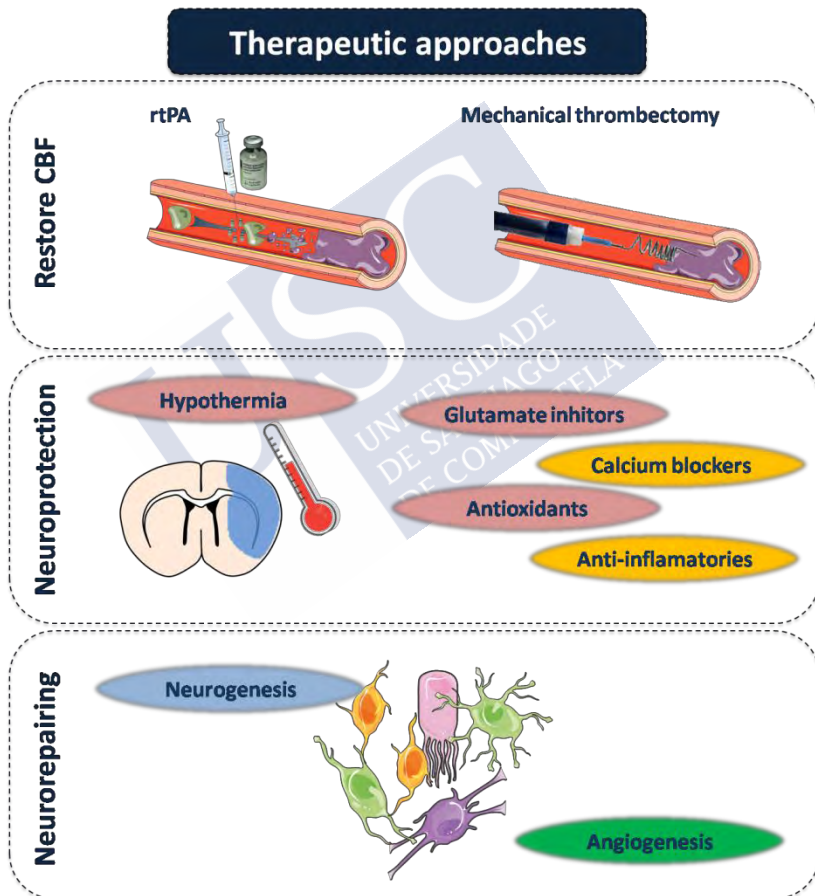


Figure 8. Scheme of the different therapeutic strategies for the ischemic stroke. Self-created image (using elements with Creative Common license).

### 1.7.1. Strategies to restore cerebral blood flow

When an ischemic event takes place, the CBF decreases; but it is not homogeneous in the affected area, and it can change within minutes or hours, especially if blood supply is not reinstated<sup>23</sup>. The immediate blood flow restoration or reperfusion is the main goal in the treatment of the acute ischemic stroke. Reducing the disability and the mortality is the long-term goal.

To perform the reperfusion there are two strategies that report higher benefits for the patient: pharmacological or mechanical (thrombectomy) thrombolysis. Both therapies have pushed for the creation of stroke units in the hospitals, which have improved the management of stroke patients.

#### 1.7.1.1. rtPA administration

The most common thrombolytic agent is the recombinant tissue plasminogen activator (rtPA) or alteplase, an enzyme involved in the clot degradation of the occluded vessel. However, it has a narrow therapeutic window and high risk of hemorrhage transformation. The therapeutic window associated with i.v. thrombolytic treatment is 4.5 h<sup>39</sup>.

Due to the pivotal role of rtPA in this Thesis, it is going to be explained in depth at Section 2.2.

#### 1.7.1.2. Mechanical thrombectomy

Thrombectomy is a technique that allows the extraction of the thrombus by a mechanical device. A semi-invasive intravascular catheter is used to reach the occluded vessels and to remove the thrombus (Figure 9).

Recently, mechanical thrombectomy has demonstrated beneficial effects on ischemic stroke in selected patients and has become the standard of care for patients with large-vessel occlusion up to 24 h of stroke onset.

The main drawback of the mechanical thrombectomy is the technical difficulty, the sedation and the risk of vascular trauma produced by the rupture of the vessel or a vasospasm. In addition, the thrombus can be fragmented and cause an embolism in a healthy tissue<sup>40</sup>.

Nevertheless, the short therapeutic window and the lack of specialized stroke units make that only 3-7 % of stroke patients are currently treated by these procedures in most developed countries.

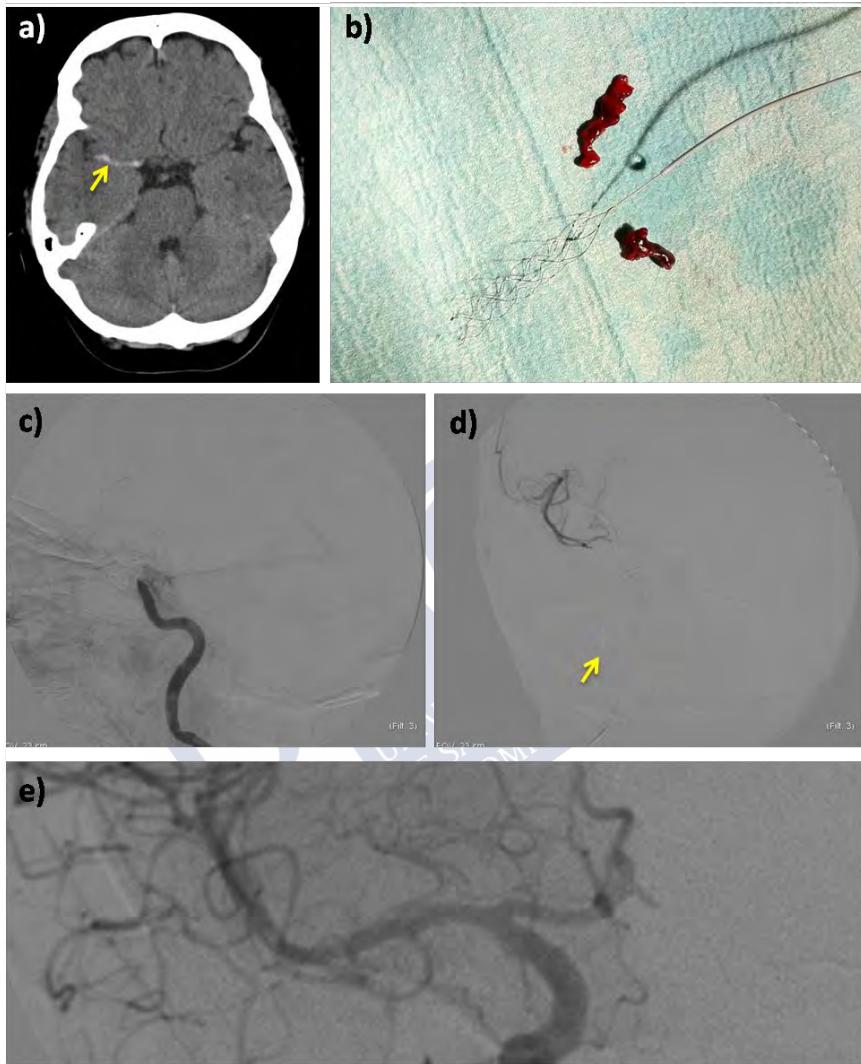


Figure 9. Example of mechanical thrombectomy. a) Computed tomography of an ischemic stroke 35 min after the onset of the symptoms. b) SOLITAIRE stent and thrombus. c) Angiography before treatment. d) Angiography of SOLITAIRE stent (marked with yellow arrow). e) Angiography after mechanical thrombectomy with recanalization. Images of the file of Professor José Castillo.

### 1.7.2. Neuroprotection

Neuroprotection is a term that conglomerates a variety of strategies focused on reducing cell death after an ischemic event without affecting tissue reperfusion. So far, several compounds have been proposed to block the pathway leading to ischemia-induced cell death at different steps of the ischemic cascade. These interventions ranged from physical approaches as hypothermia to the use pharmacological drugs as well as hypothermia<sup>41</sup>.

In case of hypothermia, it is well known that after an ischemic insult the temperature of the infarcted area increases<sup>42</sup>. In this context, hypothermia is one of the most attractive neuroprotective therapies. This therapy has shown to be one of the most effective treatments to protect the brain, but the clinical translation of hypothermia is still hampered due to the associated side effects such as shivering, hypotension, arrhythmia or increased risk of pneumonia, that usually require the use of sedation or anesthesia<sup>43, 44</sup>.

Regarding to the use of pharmacological strategies, different neuroprotective drugs have been studied. According to the mechanism of action, these drugs can be classified mainly into: calcium blockers, antioxidants, phospholipid precursors, inhibitors of glutamate release, gamma aminobutyric acid (GABA) agonists, anti-inflammatory, and glutamate antagonists.



Nimodipine is an example of calcium blocker that has been deeply studied, but it has not demonstrated a clear neuroprotective effect on clinical trials<sup>45</sup>. A similar case is the uric acid, an antioxidant that was quite promising in preclinical studies, that did not show differences between the placebo and the treated group<sup>46</sup>. Citicoline, a phospholipid precursor integrated in the membrane of neurons, restores mitochondrial ATPase activity, reduces excitotoxicity and stimulates brain plasticity<sup>47, 48</sup>. In preclinical studies, its administration led to an improvement on functional deficits 28 days after the ischemia<sup>49</sup>; however, a recent clinical trial has demonstrated the lack of protection<sup>50</sup>.

In the case of glutamate, it is well established that it is the major excitatory CNS neurotransmitter. The disruption of glutamate homeostasis occurs in different CNS injuries, such as stroke<sup>51-54</sup>. Glutamate interacts with NMDA and AMPA receptors<sup>55</sup>. One neuroprotective approach is based on the use of antagonists of these receptors. However, its administration showed numerous side effects in stroke patients<sup>56</sup>. Another strategy related with the glutamate is the use of grabbers to reduce the amount of glutamate on blood, thereby lowering the toxicity of glutamate in the ischemic region<sup>57-59</sup>. Reduction of the glutamate concentration can be carried out interacting in the glutamate oxaloacetate transaminase 1 (GOT1) that catalyzes the glutamate and **oxaloacetate to aspartate and  $\alpha$ -ketoglutarate**. Thus, the administration of recombinant GOT1, oxaloacetate or other molecules that interact with GOT are a great neuroprotective approach. In fact, a recent clinical trial showed the efficacy of a

blood glutamate grabber, the riboflavin (vitamin 12) that interacts with GOT. Patients treated with riboflavin had a significantly greater improvement compared with the placebo group<sup>60</sup>.

Despite these positive results, unfortunately so far, there not yet available any neuroprotective compounds for stroke patient<sup>61</sup>.

There are some mismatches between the preclinical studies and the clinical trials that could explain the lack of success of neuroprotective drugs:

- The chosen animal model. More than 80 % of preclinical studies with neuroprotective drugs used transient ischemic models, instead of permanent occlusions. This aspect does not correspond with what happens in patients, in which the reperfusion only occur in a third of them.
- Evaluation of therapeutic effects. The main criterion evaluated to assess the effectiveness in patients is the 90-day modified Rankin score for long-term neurological function. However, in preclinical studies the infarct volume is usually the single evaluation of the therapeutic effect. Furthermore, this infarct volume is evaluated in postmortem tissue.
- Age and sex. Despite being well established that the age is a risk factor in the ischemic stroke, most of the preclinical studies are made using young adult animals. The capacity of the brain to restore cellular and biochemical functions decreases throughout life, so the age of the animals should

be a very important factor to take into account to study the ischemic stroke. Another important agent to consider is the sex of the animals. Only a 3 % of all the preclinical studies are made with male, but around 55,000 more women are afflicted annually by stroke than men.

- Comorbidities. The risk of stroke is related with other factors, such as hypertension, diabetes, smoking, etc. However, in preclinical studies these morbidities are not usually taken into account<sup>62</sup>.

### 1.7.3. Neurorepairing

Neurorepair strategies involve the restoration of brain function, either by regeneration of damaged cerebral tissue (neuroregeneration) or by the establishment of alternative neural pathways or synapses (brain plasticity). However, therapeutic window for those therapies is wider than for thrombolytic or neuroprotective approaches. The aim of the treatments for neurological function recovery after stroke is not restricted to neurons; it is more focused on the neurovascular unit, including procedures that enhance synaptogenesis and angiogenesis<sup>63</sup>. Thus, neurorepair treatments may use stem cells, pro-neurogenic, pro-angiogenic and/or pro-synaptogenic drug delivery, among others.

- Neurogenesis: In the adult brain, there are niches for the production of neural stem cells. The enhancement of endogenous neurorepair mechanisms is one of the main

goals on new therapies for the treatment of stroke. Several strategies have been used to enhance endogenous neurogenesis. Thus, a great number of newly differentiated neurons would be available, increasing the chance of survival and integration in neuronal networks, therefore improving functional recovery. Both cellular and pharmacological therapies have been used to achieve this goal by activating the phosphatidylinositol-3-kinase (PI3-Akt) pathway. This pathway is involved in cell survival, proliferation, differentiation and migration<sup>64</sup>.

- Angiogenesis: after an ischemic event brain, capillaries surrounding the lesion proliferate, and new vessels are formed between 2 and 28 days after the onset of stroke. The angiogenic process is essential for brain recovery after cerebral ischemia. In experimental studies both cellular and pharmacological therapies have been used to increase angiogenesis, promoting the functional recovery of ischemic animals<sup>65-67</sup>.
- The role of oligodendrocytes, astrocytes and axons in neurorepair: in the brain parenchyma there are not only neurons, but other cellular components as well oligodendrocytes, astrocytes and the development of functional axons are also involved on neurorepair. After an ischemic event, astrocytes proliferate forming a glial scar that surrounds the lesion and release proteoglycans that inhibit axonal growth. Hence, there should be mechanisms

for reducing glial scar formation, and also to stimulate axonal growth, leading to an efficient neurorepair<sup>68</sup>.

### 1.8. Animal models of stroke

Animal models are fundamental tools in the preclinical study of diseases and injuries, allowing to explore the physiopathology and to design and test new therapeutic approaches for a posterior translation to the clinic. When the original disease is not present endogenously in the animal model, it has to be artificially induced, as is the case of cerebral ischemia.

Attending to the injury extension, the animal models of cerebral ischemia can be classified in two main categories: animal models of global ischemia and animal models of focal ischemia. On the first case, the whole brain is deprived from blood flow; therefore, these models are frequently used to study the cerebral consequences of heart attack. In the animal models of focal ischemia are used to mimic brain stroke, since the blood flow interruption is restricted to a focal vascular territory. Moreover, attending to the duration of blood flow interruption, focal ischemia models are classified as permanent or transient, allowing studying the pathophysiological consequences of stroke and reperfusion injury.

Clinical data show that most of the human brain strokes result from occlusions in the territory of the middle cerebral artery (MCA); consequently, many of the focal ischemia models are

based in the temporary or permanent occlusion of this artery, which is achieved by different ways:

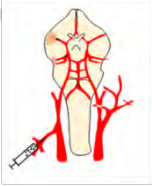
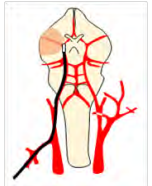
- MCA occlusion with intraluminal filament: is one of the most popular models, it was first described by Longa et al in 1989<sup>69</sup>. It is based in the introduction of a monofilament through the internal carotid artery (ICA) to occlude the blood flow in the origin of the MCA.
- Intraluminal thromboembolism: this model was described by Kudo et al in 1982, and later revised by Kaneko and by Busch et al in 1985 and 1997 respectively<sup>70, 71</sup>. This model was an improvement over the filament model, substituting the intraluminal filament by the injection of autologous blood clots through the ICA.
- MCA electrocoagulation: was firstly published by Tamura et al in 1981<sup>72</sup>. It is based on the direct electrocoagulation of the MCA.
- MCA ligation: van Chen et al published this model in 1986<sup>73</sup>. The procedure is similar to the model of MCA electrocoagulation, requiring also a craniotomy; however in this case the MCA is ligated with a suture, allowing producing both, temporary or permanent occlusions.
- MCA thromboembolism: published in 2007 by Orset et al<sup>74</sup>. This model allows to the in situ microinjection of thrombin in the MCA, triggering the local formation of a blood clot.




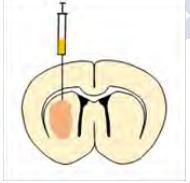
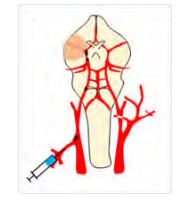
Other models do not affect properly the MCA, or produce multifocal infarcts:

- Endothelin 1 injection: was firstly published by Sharkey et al in 1993<sup>75</sup>. Endothelin 1, a potent vasoconstrictor is stereotaxically injected into the striatum.
- Embolism by microspheres: described by Zivin et al in 1987<sup>76</sup>. In this case, suspensions of calibrated microspheres or other non-clot emboli are injected in the ICA producing diffuse microembolization.

The main advantages and limitations of the different models are summarized in the Table 2.

Table 2. Models of animal ischemia.

Model		Advantages	Limitations
MCA occlusion with intraluminal filament  Longa et al 1989	 A schematic diagram of a coronal brain section showing the cerebral vasculature. A red filament is inserted into the middle cerebral artery (MCA) to occlude it. A syringe is shown injecting the filament into the artery.	Do not need craniotomy.  High reproducibility of lesion size and localization.	Not useful to study thrombolytic therapies.
Intraluminal thromboembolism  Kudo et al 1982	 A schematic diagram of a coronal brain section showing the cerebral vasculature. A black thrombus is shown occluding the middle cerebral artery (MCA).	Do not need craniotomy.  Useful to test thrombolytic therapies.	Low reproducibility of lesion size and localization.  Risk of spontaneous reperfusion.

<p>MCA electrocoagulation Tamura et al 1981</p>		<p>Permanent occlusion, no risk of spontaneous reperfusion.</p>	<p>Needs craniotomy. Electrocoagulation may injury surrounding tissue.  Not useful to study thrombolytic therapies.</p>
<p>MCA ligature Chen et al 1986</p>		<p>Can be permanent or transient.  High reproducibility of lesion size and localization.</p>	<p>Needs craniotomy.  Not useful to study thrombolytic therapies.</p>
<p>MCA thromboembolism Orset et al 2007</p>		<p>Useful to test thrombolytic therapies.  High reproducibility of lesion size and localization.</p>	<p>Needs craniotomy.  Risk of spontaneous reperfusion.</p>
<p>Endothelin-1 injection Sharkey et al 1993</p>		<p>High reproducibility of lesion size and localization.</p>	<p>Not useful to study thrombolytic therapies.  Needs a small craniotomy.</p>
<p>Embolism by microspheres Zivin et al 1987</p>		<p>Do not need craniotomy.</p>	<p>Low reproducibility of lesion size and localization.  Not useful to study thrombolytic therapies.</p>



Most of the preclinical studies use small rodents as models. The use of rats and mice present the advantage that the molecular mechanisms leading to ischemic cell death are well characterized, and the availability of genetically modified strains makes easier the study of specific molecular targets. Moreover, the costs of maintenance and space requirements of rodents are low, allowing to be used in a wider number of research centers. However, despite of these advantages the use of rodents presents important limitations: they are lysencephalic animals, with a small proportion of white matter compared to humans, or the fact that small body size implies metabolic and physiological particularities, which are different from large body animals such as humans. These limitations hamper the direct translation of results from rodents to humans, implicating that once a drug show efficacy in rodents, has to be tested in larger gyrencephalic animals such as cats, dogs, pigs or monkeys, before being tested in humans<sup>77</sup>.

Briefly, there is a wide range of available options to mimic stroke, therefore, the selection of the model must be based on the study objectives, assuming the best balance between the model strengths and technical limitations since there is not a universal model<sup>78</sup>.

## 2. Tissue plasminogen activator

In this section it is explained the different aspects of the tPA molecule, its use as drug, and the new approaches to increase the efficacy and effectiveness of rtPA treatment in ischemic stroke.

### 2.1. rtPA structure

tPA is a glycoprotein that belongs to the superfamily of serine proteases and it is a member of the chymotrypsin family. It is a 70 kilodaltons (kDa). protein composed by 523 amino acids, and 17 disulfide bridges that maintain the structure It has five domains that form the heavy chain (A-chain) and the light chain (B-chain)<sup>39</sup>. Each domain is responsible for the different properties of the tPA. Beginning in the N-terminal ends of the tPA the domains are the following (Figure 10):

- Finger (F) domain is the responsible for the tPA binding to the fibrin, and is necessary for promoting fibrinolytic activity at low plasminogen activator concentrations<sup>79</sup>. Also it is related with interaction with the Low Density Lipoprotein Receptor-related Protein (LRP)<sup>80</sup> and Annexin II receptors<sup>81</sup>.

- Epidermal growth factor (EGF)-like domain activates the EGF receptor related with the antiapoptotic role of the tPA in the oligodendrocytes<sup>82</sup>.
- Kringle 1 (K1) domain has high mannose-type glycosylation which makes it has affinity for the mannose receptor of the liver endothelial cells. K1 domain is involved in the uptake and clearance of the tPA<sup>83</sup>.
- Kringle 2 (K2) domain has an active site having a high affinity for lysine (lysine binding site; LBS). It is demonstrated that K2 domain cleaves to the platelet derived growth factor (PDGF-CC) receptor and the NMDAr<sup>84, 85</sup>.
- Serine protease, which is the B-chain, is located in the C-terminal of the tPA and it is the responsible of its catalytic activity. There are three amino acids involved: His-322, Asp-371 and Ser-478, which enables the activation of plasminogen to plasmin<sup>39</sup>.

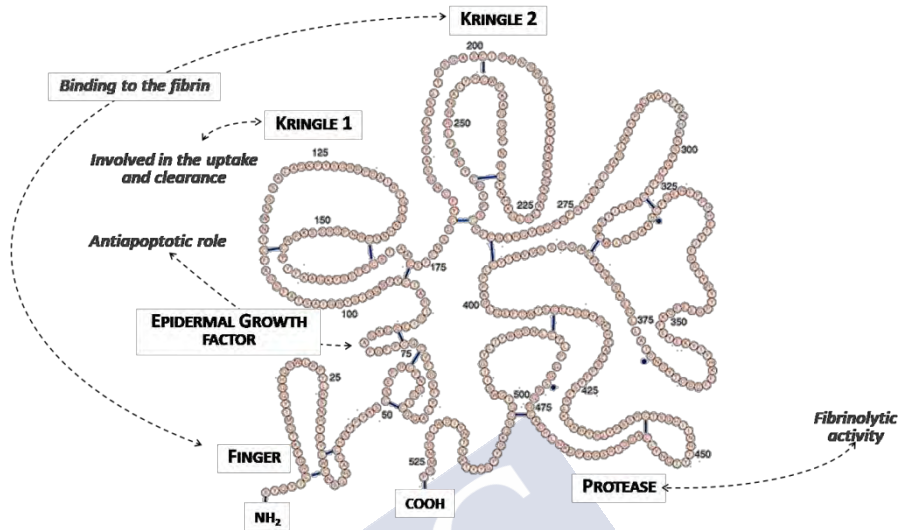


Figure 10. tPA molecule and its domains. Self-created image.

tPA coexists as single chain (sc-tPA) and two-chain (tc-tPA) forms, as all the serine proteases. First, tPA is secreted as sc-tPA and in the presence of plasmin is processed to the tc-tPA. In the presence of fibrin both of the two forms have the same proteolytic activity. Nevertheless, when there is no allosteric regulator, tc-tPA is more active than sc-tPA<sup>86</sup>.

### 2.1.1. Localization and inhibition

tPA is mainly synthesized and released by the endothelial cells to the blood circulation. Nevertheless, in the brain, it is expressed and synthesized by most of the cell types: astrocytes, neurons,

oligodendrocytes and microglia<sup>87</sup>. When thrombosis occurs, tPA is released from the endothelial cells to preserve the patency of the blood vessel<sup>88</sup>.

The primary inhibitor of the tPA is PAI-1, a 52 kDA single-chain glycoprotein with 370 amino acids that belongs to the serpin superfamily and that is synthesized by platelets. It reacts with sc-tPA and tc-tPA forming a 1:1 stoichiometric reversible complex. tPA could be inhibited also by TAFI, that is the most recently discovered tPA inhibitor<sup>22</sup>.

Main process by which tPA activity is restricted, hence the responsible for its short half-life, are: the inhibition by PAI-1 that inhibit 50 % of the tPA in 5 min, and the clearance by the liver. The K1 domain interacts with the liver endothelial cells, and liver parenchymal cells with the EGFdomain<sup>89</sup>.

### 2.1.2. Effects in the central nervous system

Apart from its role in maintaining homeostatic control in the blood coagulation cascade, tPA plays important roles in CNS.

On one hand, it takes part in the remodeling of the extracellular matrix during brain development. It mediates neuronal precursor migration, and the neurite and axonal extension. In adult brain, tPA is involved in long-term potentiation, possibly by micro proteolysis of extracellular space that allows dynamic remodeling at the synaptic and dendritic levels<sup>39, 90</sup>.

Many studies have also suggested that tPA has neurotoxic effects, a fact which may explain its complications associated with its use in clinic<sup>91</sup>.

In general, the effects of the tPA can be divided into plasmin dependent and independent. When the tPA is in the vascular space its thrombolytic effect is related with the plasmin-dependent mechanism. When the BBB is disrupted this plasmin can cross it and carries out other plasmin-dependent mechanisms linked to the neurotoxicity, excitotoxicity and plasticity. On the other hand, the tPA can cross the BBB and activates NMDAr, a mechanisms plasmin-independent (Figure 11).

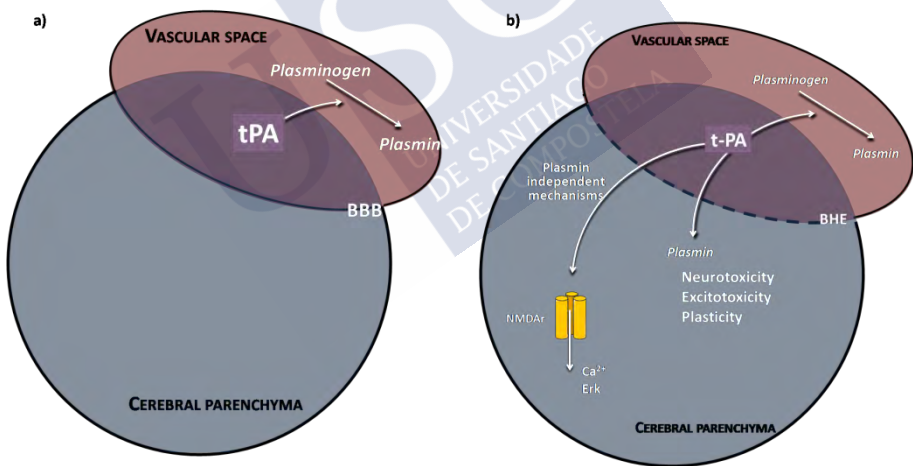


Figure 11. a) Effect of the tPA in the vascular space (plasmin-dependent). b) Mechanism after BBB damage, both plasmin-dependent and independent. Self-created image based on<sup>92</sup>.

## 2.1.2.1. Blood brain barrier permeability

There are strong evidences, both experimental and clinical, that relate the tPA to BBB damage. Besides the deleterious effect of ischemia, on the permeability of the BBB. In endothelial cells, tPA upregulate the synthesis of metalloproteinases (MMP). MMP are a zinc endopeptidases family that is involved in remodeling all matrix substrates in the brain. In particular, MMP-9 and MMP-3 contribute to increase the blood brain barrier (BBB) permeability and intracranial bleeding.

In perivascular astrocytes, tPA interacts with the LRP, which activates nuclear factor (NF)- $\kappa$ B and Akt pathways that ultimately increases the synthesis of MMP-9. In addition, tPA can activate PDGF-CC to PDGF-C. PDGF-CC plasma concentration can be used to predict the HT after rtPA treatment<sup>86</sup> (Figure 12).

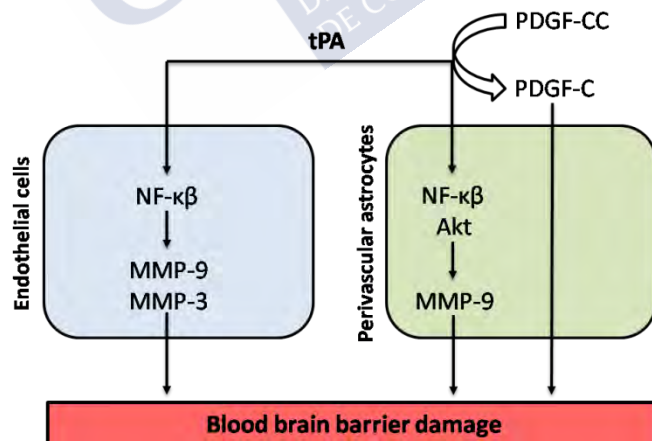


Figure 12. Mechanisms by which BBB is damaged. Self-created image based on<sup>86</sup>.

#### 2.1.2.2. NMDA receptor

tPA increases neuronal cell death mediated by glutamatergic receptors. tPA was associated with an increasing in the influx of calcium due to an interaction with the NR1 subunit of the NMDAr. This takes place by the interaction of tPA with LRP, enhancing calcium downstream NMDAr. Moreover, tPA interacts with the N1 subunit of the NMDA via its K2 domain. Controversially, some studies described a neuroprotective effect related with the NMDAr via the interaction of the tPA with the N2A subunit of NMDAr<sup>86</sup>.

#### 2.1.2.3. Inflammatory process

Via interaction between F domain with microglial LRP and annexin II, tPA can promote the microglial activation. A study revealed a regulatory loop in which neuron-derived tPA activates microglia, which in turn produces more tPA. Furthermore, during the reperfusion, plasmin and tPA have been described to contribute to neutrophil and leukocyte infiltration in the tissue. This could be explained via plasmin-dependent: the MMP-9 upregulation that provokes the BBB damage, which increase the infiltration; and via plasmin-independent due to mast cells activation and lipid mediator release<sup>86</sup>.



### 2.1.2.4. Apoptosis

The effect of the tPA in the apoptosis is quite controversial. There are studies that described a pro-apoptotic and others an anti-apoptotic effect.

The pro-apoptotic effect is related with the capability of tPA in converting the proneurotrophins into their active forms. Additionally, it is related with the activation of PI3K/Akt pathway, by the mediation of annexin II in neurons and EGF receptor in oligodendrocytes<sup>86</sup>.

Related with its pro-apoptotic effect, it was observed that tPA potentiates NMDA effect on apoptotic cell death in human brain endothelial cells<sup>90</sup>.

### 2.2. rtPA as a treatment in stroke

As previously stated, the role of rtPA is the degradation of the clot, converting the plasminogen into plasmin, which breaks up the clot into fibrin degradation products. Its aim is to promote endogenous recanalization rates and tissue reperfusion<sup>93</sup>.

Different aspects related with rtPA treatment should be taken in account: therapeutic window, rtPA dose, risk of intracerebral hemorrhage, recanalization rate and the importance of the anatomy in the trombolytic treatment (Figure 13).

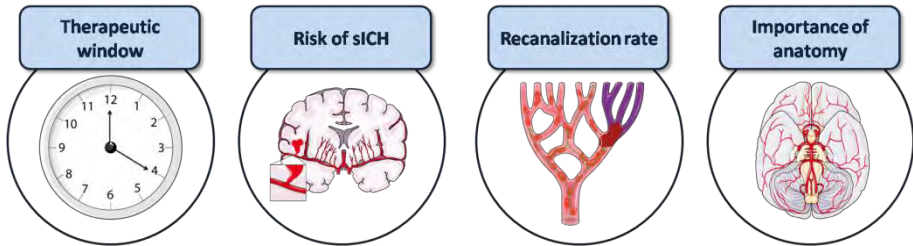


Figure 13. Aspects to be taken into account in thrombolytic treatment. Self-created image (using elements with Creative Common license).

### 2.2.1. Therapeutic window

In 1996 the Food and Drug Administration (FDA) in the United States approved rtPA as a treatment in the acute ischemic stroke. Its safety and efficacy were proven in several clinical trials. The National Institute of Neurological Disorders and Stroke (NINDS) rtPA Study Group published the study, which showed that despite of an augment in the incidence of intracerebral hemorrhages, the use of rtPA in the first 3 h after stroke onset was associated to a clinical improvement after 3 months<sup>94-96</sup>.

However, in the European Union (EU) its use was approved until 2002, under the condition of the realization of two studies to assess the safety profile of rtPA within 3 h of the onset of the stroke symptoms, and to study the extension of the therapeutic window. These studies were the Safe Implementation of Thrombolysis in Stroke-Monitoring Study (SITS-MOST), and the European Cooperative Acute Stroke Study (ECASS) III, respectively. The SITS-MOST showed similar results to the first

studies, and it recommended the thrombolytic therapy as a part of routine care for suitable stroke patients<sup>97</sup>. The ECASS concluded that the greater benefit of rtPA was achieved within the first 90 min; it also suggested the potential benefit beyond 3 h, but with a risk that should be considered<sup>98</sup>.

It was in 2008 when the therapeutic window was extended to 4.5 h. It was demonstrated a moderate but significant clinical outcome. In addition, the risk of hemorrhagic transformations (HT) was not higher than in patients treated in the first 3 h<sup>99</sup>.

Currently, this time window is being questioned, Ma et al published a clinical trial in which the therapeutic window was extended to 4.5 to 9 h. They found that, although with an increase in the number of hemorrhages, the neurological outcome was better in patients treated out of the therapeutic window<sup>100</sup>. Similar results were shown in a meta-analysis on the extension of the therapeutic window, in which it was demonstrated that the administration of rtPA between 4.5 and 9 h after the onset of the symptoms did not show an increase in the symptomatic intracerebral hemorrhage (sICH), and it was correlated with an increase in the neurological outcome<sup>101</sup>.

In recent years improvements in neuroimaging techniques confirmed that stroke is a dynamic process, and the different variables present in different patients (clot size and nature, localization, comorbidities, etc.) may determine differences in the temporal development of ischemic injury. These observations point out that the therapeutic window for rtPA should also be dynamic,

and not restricted to the temporal criteria. Maybe in the coming years candidate patients to be treated with rtPA will be selected in the basis of the presence of salvageable tissue observed by neuroimaging techniques, independently that time could be also considered, but in a second place<sup>102-104</sup>.

### 2.2.2. rtPA dose

The dose used in patients is 0.9 mg/kg (maximum dose, 90 mg) and it is i.v. administered, 10 % as bolus and 90 % as infusion. The administration of rtPA as infusion is due to its short half-life, which is only 5 min, leading to 75 % clearance in 8 min, due to the effect on PAI-1.

Although some studies showed the safety and efficacy of other rtPA doses (0.6 mg/kg<sup>105</sup> or 1.1 mg/kg<sup>106</sup> for instance), the 0.9 mg/kg rtPA continues to be the one used.

### 2.2.3. Risk of intracerebral hemorrhage

The worst complication related to rtPA therapy is the sICH, which occurs in 7-15 % of the patients<sup>107</sup> (Figure 14). In addition, it comprises the 50 % of the deaths associated to rtPA mortality<sup>108</sup>.

The definition of sICH is quite controversial, but it requires the presence of blood on computerized tomography scan of the head

after rtPA treatment. In the ECASS II the different sICH were classified in four types that are briefly explained in Table 3<sup>109</sup>.

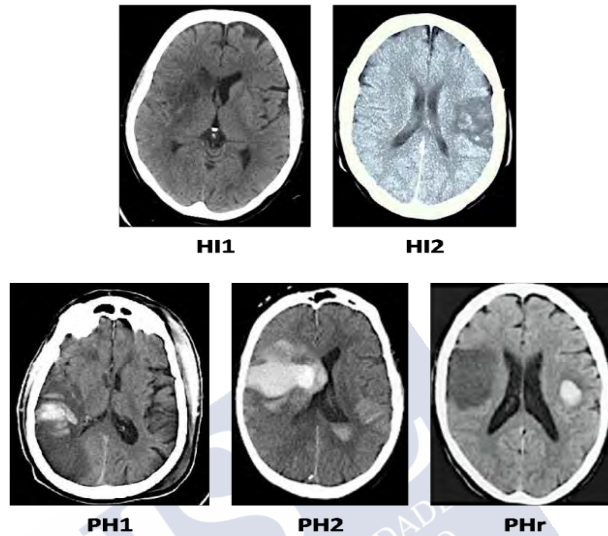


Figure 14. TC of the different HT. Images of the file of Professor José Castillo.

Table 3. sICH classification.

Classification	Definition
Hemorrhagic infarction 1 (HI 1)	Small petechia without mass effect.
Hemorrhagic infarction 2 (HI 2)	Confluent petechia without mass effect.
Parenchymal hematoma 1 (PH1)	Hemorrhage in <30 % of the infarcted area with mild mass effect.
Parenchymal hematoma 2 (PH2)	Hemorrhage in >30 % of the infarcted area with mild mass effect.
Remote parenchymal hematoma (PHr)	Hemorrhage located remote from the actual infarct.

Whiteley et al published a meta-analysis of 55 studies in which they identified some factors associated with the sICH. For example, there is twice the risk when the patient suffers atrial fibrillation, congestive heart failure, renal impairment, previous antiplatelet agents, leukoaraiosis, and acute cerebral ischemic lesion on pretreatment brain imaging<sup>110</sup>. However, based on prediction scores, patients with high risk of sICH still have benefit from thrombolysis<sup>107</sup>.

The mechanisms by which rtPA increases the risk of sICH are related to the previously described effects of the tPA in the CNS, especially the ones related to the increase in the MMP expression, and the interaction with the PDGF and LRP receptors<sup>111</sup>. Furthermore, despite the fact that the half-life of rtPA is short, the effect in the coagulation system persists during more time. The reduction in fibrinogen levels and the prolongation of prothrombin and partial thromboplastin time are related to the sICH risk<sup>107</sup>.

#### 2.2.4. Recanalization rate

The favorable outcome of patients is related to the recanalization during the first 24 hours after the onset of the symptoms<sup>112</sup>. However, the reperfusion rate associated with rtPA therapy is around 35 %<sup>113</sup> and 53 %<sup>114</sup> (Figure 15), depending on the trial. Knowing the thrombi characteristics, it is important to predict the response to rtPA therapy, moreover because it is demonstrated

that there is a worse outcome in stroke patients with an ineffective thrombolytic treatment<sup>115</sup>.

The resistance to the thrombolytic treatment depends on location, size, composition, and source of the thrombus. Distal occlusions in the MCA recanalize more frequent, faster, and complete than proximal occlusion. For example, occlusions in the ICA are more resistant to the thrombolytic treatment than occlusions in the MCA. This is due to the size of the thrombi, which are bigger in the proximal occlusions. Also, the occlusions in large vessels are more likely to have an atherosclerotic origin, in which the response to rtPA is lower<sup>113, 116</sup>.

The size of the thrombus is another important factor that determines thrombolysis. When the volume of thrombus is increased, the probability of reperfusion is lower. Specifically, **patients with thrombi  $\geq 200 \text{ mm}^3$**  are unlikely to reperfuse<sup>117</sup>

Thrombi with cardioembolic origin are uniform fibrin-rich. Due to the high affinity of rtPA for fibrin, these thrombi respond better to the thrombolytic treatment, because rtPA penetrates and distributes leading to the thrombi dissolution. The recanalization is more frequent, faster, and complete<sup>118</sup>.

In contrast, atherosclerotic thrombi, which are rich in platelets, are more resistant to fibrinolysis than cardioembolic thrombi. Besides, due to the small amount of fibrin that these thrombi have, some mechanisms by which it could be less responsive are related to the components and functions of the platelets. For example, the

amount of PAI-1 and Factor XIII in platelets is related to the resistance to thrombolytic treatment<sup>22</sup>.

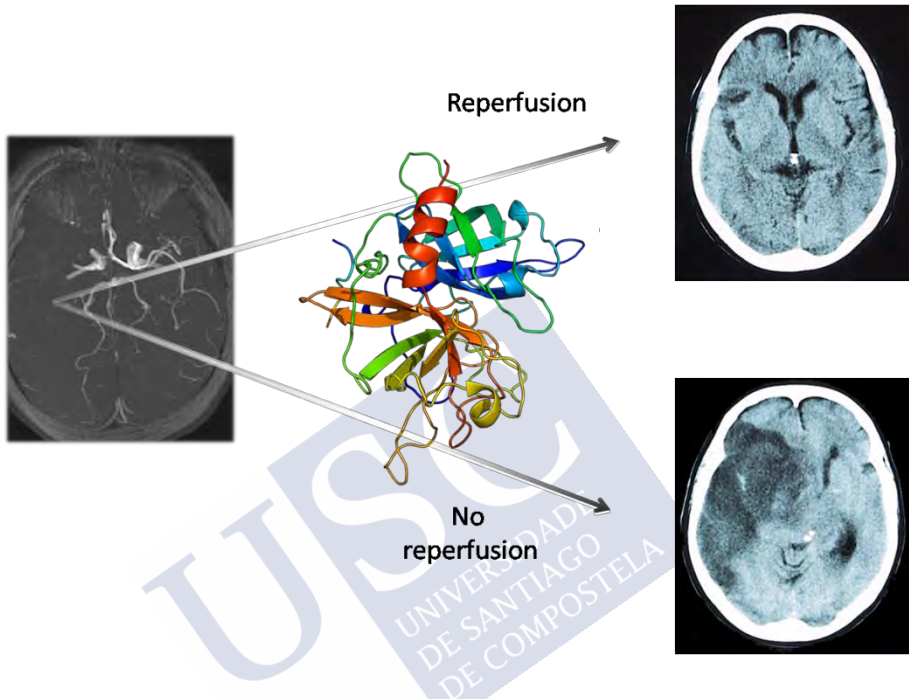


Figure 15. TC after thrombolytic therapy with and without reperfusion. Self-created image. Images of the file of Professor José Castillo.

### 2.2.5. The importance of the anatomy

Three groups of vessels compose collateral circulation: the large-arteries that communicate the extracranial and the intracranial circulation, the four arteries that supply blood to the brain that compound the circle of Willis, and the leptomeningeal anastomoses that provide blood to the cortex of the brain.



Collateral circulation could limit the infarct growth, because it could maintain the flow in the territory irrigated by the occluded artery. It is well studied that there is an improvement of the neurological outcome in patients with a good collateral circulation, relating it especially to reperfusion<sup>119</sup>. Miteff et al described the good outcome associated with the collateral and rtPA administration. Patients without reperfusion and good collateral circulation have an improvement at 90 days. Conversely, when the patients had reperfusion but not good collaterals the good outcome is not remarkable<sup>120</sup>. Besides this, another study found that the collateral circulation was associated with a lower risk of HT after rtPA treatment<sup>121</sup>.

#### 2.2.6. Excluded patients from thrombolytic treatment

Despite all the benefits of treatment with rtPA, this therapy is totally contraindicated in some cases (Table 4)<sup>122</sup>.

Table 4. Absolutely contraindications to rtPA therapy

Contraindication	Reason of contraindication
Advanced age	Benefits are less frequent and mortality higher.
Mild or Improving Stroke Symptoms	Thrombolysis improves symptoms at three months.
Recent major surgery	Increase the risk of hemorrhages.
Arterial puncture of non compressible vessel	Increase the risk of hemorrhages.

Gastrointestinal or genitourinary hemorrhage	Increase the risk of hemorrhages.
Seizure at onset	It could not be a ischemic stroke. Risk of sICH.
Recent myocardial infarction	Potential myocardial hemorrhage.
CNS structural lesions	Increase the risk of sICH.

In addition, the contraindications are relative in other cases. These are summarized in Table 5<sup>122</sup>.

Table 5. Relative contraindications to rtPA therapy.

Contraindication	Reason of contraindication
Advanced age	Benefits are less frequent and mortality higher.
Mild or Improving Stroke Symptoms	Thrombolysis improves symptoms at three months.
Recent major surgery	Increase the risk of hemorrhages.
Arterial puncture of noncompressible vessel	Increase the risk of hemorrhages.
Gastrointestinal or genitourinary hemorrhage	Increase the risk of hemorrhages.
Seizure at onset	It could not be a ischemic stroke. Risk of sICH.
Recent myocardial infarction	Potential myocardial hemorrhage.
CNS structural lesions	Increase the risk of sICH.

## 2.3. Sonothrombolysis

Since 1956, doppler sonography (ultrasounds, US) has been used to detect the blood flow from cerebral vessels and to study the cerebrovascular disorders. The main advantages of this technique are that it is a non-invasive, portable and fast imaging method. Because of these reasons the doppler sonography is an useful tool in emergency department to access acute stroke etiology, predict the response to thrombolytic therapy and manage the recanalization procedure<sup>123</sup>.

### 2.3.1. Ultrasound for diagnosis

Cervical and transcranial ultrasonography are based in the propagation of mechanical sound vibrations at frequencies between 20 kHz and 1 GHz. Doppler sonography comprises different imaging methods explained in Table 6. In each method the advantages of the previous method are added<sup>124</sup>.

Table 6. Doppler sonography methods.

B-mode	Pulse-wave	Color flow imaging	Power Doppler
Anatomical organization			
	Blood flow analysis		
		Differentiation between pathological and normal flow	
			Amount of blood at each point

Transcranial doppler US consists only in applying US through the skull; when imaging techniques are involved it is called transcranial colour-coded sonography. In both methods, the examination is only possible in the regions where the skull is thin enough. These regions, called "acoustic windows", are summarized and marked in Figure 16.

Acoustic window	Artery insonated
Zigomatic arch (1)	MCA ACA (anterior cerebral artery) PCA (posterior cerebral artery)
Sub-occipital (2)	Basilar artery (BA) Vertebral artery (VA)
Submandibular (3)	Retromandibular portion of ICA (internal carotid artery)
Orbital (4)	ICA siphon

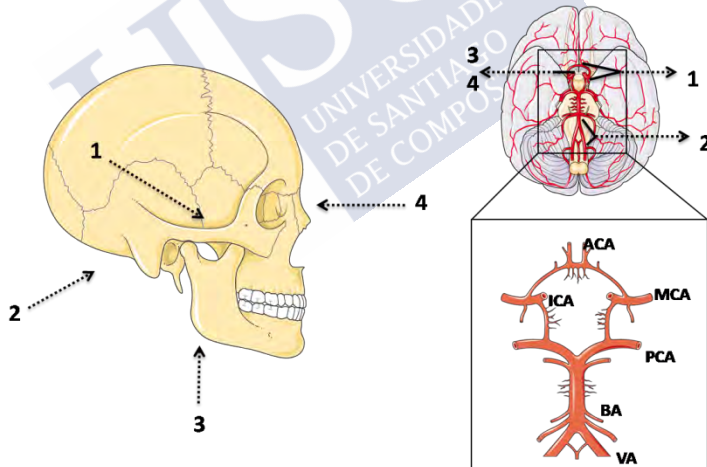


Figure 16. Acoustic windows. Self-created image (using elements with Creative Common license).

The main use of US in the ischemic stroke diagnostic is the study of the intracranial arterial recanalization both in i.v. and endovascular thrombolysis. Another important use of the US in ischemic stroke is the study of the etiology, for example to characterize the atheromatous plaque<sup>123</sup>.

### 2.3.2. US as a thrombolytic tool: sonothrombolysis

The adjunctive treatment of the US with rtPA to the acute ischemic stroke has increased to avoid the disastrous side effects of this thrombolytic treatment. Many *in vitro*, *in vivo* and clinical trials have shown that the tPA efficacy is increased when US is applied. This concept is called sonothrombolysis, which consists of the adjuvant treatment of tPA and US. Using an ultrasound beam may enhance the efficacy and has the potential to improve the safety of the treatment<sup>124</sup>.

#### 2.3.2.1. *In vivo* studies

Since 1974 the first tests with ultrasounds were carried out to recanalized iliofemoral arteries in dogs. In the following years, several studies showed that the US enhanced the fibrinolytic effect of the tPA what led to the first clinical trials in which the adjunct effect of US and the fibrinolytic therapy in ischemic stroke patients was evaluated<sup>125</sup>.

### 2.3.2.2. Clinical trials

In 2004 Alexandrov et al published the Combined Lysis of Thrombus in Brain Ischemia Using Transcranial US and Systemic tPA trial (CLOTBUST), a multi-center, randomized, phase 2 clinical trial on 126 patients. There were two groups of treatment, placebo and the patients that received 2 MHz during 2 h. The results showed that almost 50 % of patients, to which US was applied, reperfused comparing with the placebo group in which only 30 % of the entire patients reperfused. Also, no secondary damages were found<sup>126</sup>.

In 2015 the phase 3 trial was finished demonstrating the security and safety of the additional use of TDU with the tPA to improve the functional outcome of stroke patients<sup>127</sup>.

Another clinical trial was the Transcranial Low-Frequency US-Mediated Thrombolysis in Brain Ischemia (TRUMBI), a phase II, prospective, nonrandomized, multicenter trial of 26 patients divided in two groups of treatment: rtPA and rtPA plus US. In contrast with the CLOTBUST, a 300 kHz US was used in this trial. The use of a different intensity was performed trying to increase the thrombolytic effect of the rtPA, because the penetration of the US through the skull is higher and the isolation of the brain could ensure better targeting occlusion. However, it was prematurely stopped because the patients treated with rtPA plus US showed signs of bleeding in magnetic resonance imaging (MRI)<sup>128, 129</sup>.

### 2.3.3. Mechanisms of thrombolytic enhancement

The mechanism by which the ultrasounds accelerate thrombolysis is not clear and it is a quite controversial. However, the most studied mechanisms are categorized as thermal, primary mechanical effects or secondary mechanical effects (acoustic cavitation).

- Thermal effects

It is well studied that the lytic effect of the tPA is reduced at lower temperatures. This is because the conversion of plasminogen to plasmin is temperature-dependent. Also, it has been studied in clots, showing that the lysis time increased from 111 min at  $T=37.5\text{ }^{\circ}\text{C}$  to 186 min at  $30\text{ }^{\circ}\text{C}$  and the clot lysis decreased 0.5 % per  $^{\circ}\text{C}$  in clot exposed to tPA<sup>130, 131</sup>.

Some studies showed that the exposure to the US increases the temperature and therefore there is an acceleration of the enzymatic plasma clot lysis. However, it could be a problem to translate it to humans, because heating tissues could be dangerous<sup>132</sup>. In addition, a study published in 2015 demonstrated that the mechanism is not thermal- dependent, but only when low frequency and intensity parameters were used<sup>133</sup>.

- Primary mechanical effects (acoustic radiation)

Acoustic radiation force results from the application of the US through the tissues. It is responsible for the initiation of the fluid motion that can help the tPA to penetrate into the clots<sup>134</sup> (Figure

17). Also *in vitro* studies have demonstrated that US could result in the erosion of 99.2 % of the clot volume<sup>129</sup>.

Also an *in vitro* study suggests that an intermittent application of a 2 MHz, using in clinic to diagnostic, would be the most potent application for lysing blood clots<sup>135</sup>.

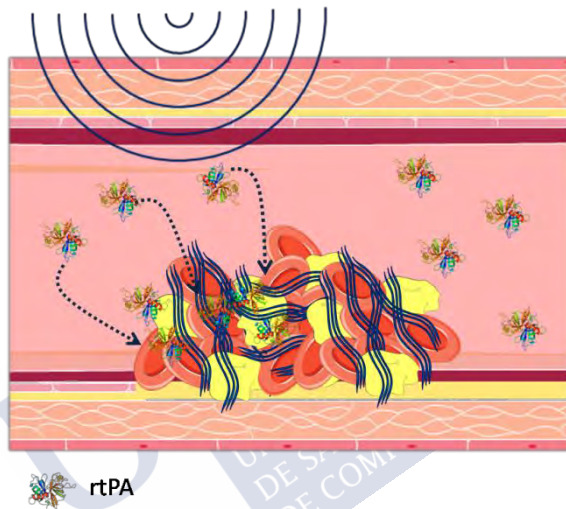


Figure 17. Representation of the acoustic radiation that allow the rtPA penetrate into the clot. Self-created image (using elements with Creative Common license).

- Secondary mechanical effects (acoustic cavitation)

Acoustic cavitation is the formation and oscillation of bubbles due to the acoustic pressure. Cavitation can be enhanced by microbubbles (MB) (Figure 18), which are also used as contrast agent.



The inertial cavitation is the responsible for the MB growing and its collapse. The MB creates microjets and shock waves that can create holes in vessels and cell membranes. This type of cavitation causes damage in tissues.

However, when the US energies do not induce this cavitation, MB have a stable cavitation. This type of cavitation can induce alternating invagination and distention of blood vessel walls, which can increase the permeability of the vessels. In addition, it is a technique that can be used to open the BBB.

In general, thermal and acoustic radiations are the main reason for the use of US to increase thrombolysis<sup>136</sup>.

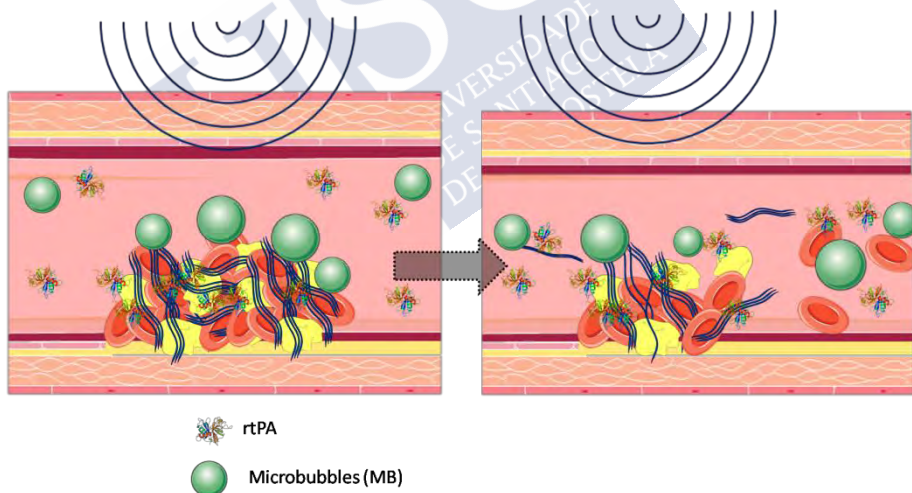


Figure 18. Representation of the acoustic cavitation that with the formation and oscillation of MB enhance thrombolysis. Self-created image (using elements with Creative Common license).

## 2.4. New approaches for rtPA treatment

Despite its low recanalization rate and the risk of sICH, rtPA therapy continues to be the only approved drug treatment for the acute phase of the ischemic stroke. Because of this, the research on new approaches to increase the recanalization effectiveness and decrease the side effects is an important goal in rtPA therapy.

### 2.4.1. Intraarterial administration

Although rtPA is administered usually i.v. there are studies using the intra-arterial administration. The main reason to use rtPA intra-arterial (i.a.) is to provide a more specific way to focally concentrate the therapeutic agent near the thrombus, reducing the amount of pharmacological agent needed to achieve the recanalization, and reducing the amount of circulating fibrinolytic, which potentially reduces systemic adverse effects. Despite all these advantages, i.a. administration is highly invasive, and the high concentration of thrombolytic agent in the occluded region could increase the risk of sICH or neurovascular toxicity<sup>104</sup>. Although a recent meta-analysis have shown that i.a. therapy combined with i.v. administration could improve functional outcome without increasing the risk of sICH<sup>137, 138</sup>.

## 2.4.2. Modification of the rtPA molecule

One of the strategies to increase the proteolytic efficacy, to decrease the clearance of rtPA to prolong its half-life, and/or to decrease its neurotoxic effects, is the bioengineering. Using this technique, rtPA molecule could be modified, some domains eliminated, and new molecules created. The three molecules created from the rtPA that have been tested in patients are: *desmoteplase*, *tenecteplase* and *reteplase*<sup>91</sup>. Their structures are schematized in Figure 19.

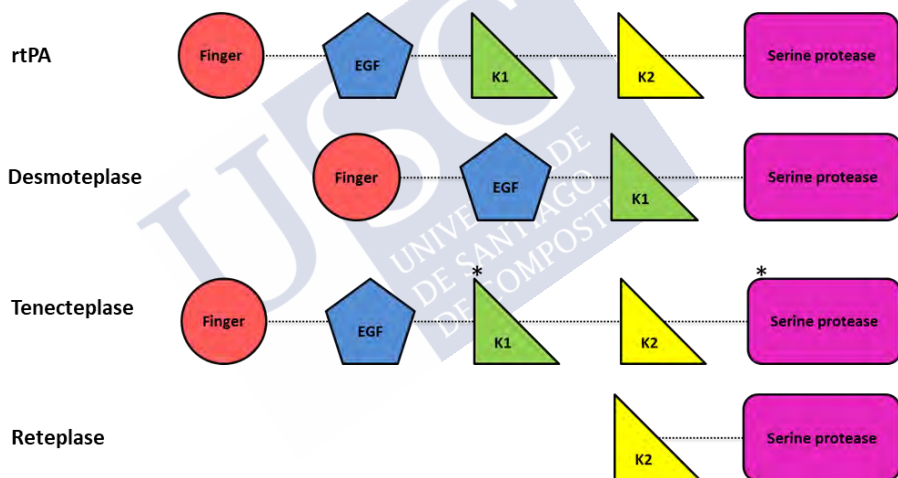


Figure 19. Schematic representation of the different molecules derived from rtPA. Self-created image based on <sup>91</sup>.

The main advantage of *desmoteplase* is the lack of the K2 domain, responsible for the neurotoxicity, that avoid the cleavage to the NMDA receptor<sup>139</sup>. Moreover, *desmoteplase* is high fibrin specific

and it has a longer half-life than rtPA. Two placebo-controlled, double-blind, and randomized clinical trials were performed to study its safety and efficacy: the Desmoteplase in Acute Ischemic Stroke trial (DIAS) and the Dose Escalation of Desmoteplase in Acute Stroke (DEDAS). The DIAS was divided in Part 1 and 2. Part 1, where *desmoteplase* was administered in three doses of 25 mg, 37.5 mg, and 50 mg, was terminated prematurely because of the risk of sICH. However, in Part 2 the administered doses were changed to 62.5 µg/kg, followed by 90 µg/kg and 125 µg/kg. The trial concluded that *desmoteplase* administration between three and nine hours after the ischemic onset were correlated with a favorable clinical outcome<sup>140</sup>. These results were supported by DEDAS, in which *desmoteplase* was administered at different concentrations demonstrating its safety and efficacy at 125 µg/kg<sup>141</sup>.

Other genetically engineered mutant tPA is *tenecteplase*, which have modifications in the K1 and serine protease domain. The amino acid substitutions make this molecule 15-fold higher fibrin specific, 80-fold reduced binding to the PAI-1, and 6-fold prolonged plasma half-life, what allows an administration in a single dose<sup>142, 143</sup>. This molecule was studied until phase 2B trial, showing that the 0.25 mg/kg dose in the first three hours courses with better reperfusion rates and clinical outcome. *Retepase* only has the K2 and the serine protease domain. This feature makes it more specific for the fibrin than rtPA, and has a longer half-life (15-18 min). There are few reports about its use in ischemic stroke, but they concluded that it has the same reperfusion rates

and sICH. The main advantage compared with rtPA administration could be that reteplase could be administered in a single dose<sup>144</sup>.

### 2.4.3. Combination and alternative therapies

rtPA is not the only plasminogen activator used as thrombolytic therapy. *Streptokinase*, a bacterial enzyme derived from *Streptococcus* that is commonly used in myocardial infarction, was tested in ischemic stroke. Its administration 3 h after the onset of the symptoms did not show any improvements in the outcome compared with the saline<sup>145</sup>. Importantly, the administration within 6 h after the onset of stroke resulted in an increase of mortality<sup>146</sup>.

A derivate of rtPA, *uPA*, has been also suggested as alternative. The study concluded that its i.a. administration improved the clinical outcome at 90 days<sup>147</sup>, but also increased the risk of sICH<sup>148</sup>.

Another approach is the administration of *plasmin* which i.a. administration could achieve the thrombus easier. Its main **drawback is that it is rapidly inactivated by  $\alpha 2$ -antiplasmin**. It was administered within 9 h after the stroke symptoms in a clinical trial. It results to be well tolerated and it did not increase adverse outcomes, however, the recanalization was only achieved in a few patients<sup>149</sup>. Trying to increase the half-life, a recombinant of *plasmin* (*microplasmin*) that cannot be inactivated by  $\alpha 2$ -antiplasmin, was tested in a clinical trial to investigate its safety; however, its effectiveness has not yet been tested<sup>150</sup>.

The combination of rtPA with other drugs as anticoagulants or antiplatelets was also tested in clinical trials. In the case of anticoagulants, *heparin* stands out and has been tested in many clinical trials, but it has failed to demonstrate a better outcome so far. Also, antiplatelets such as *aspirin* and GP IIb/IIIa inhibitors have been extensively studied without showing any clinical benefit<sup>151</sup>. Furthermore, a thrombin inhibitor, *argatroban*, was combined with rtPA demonstrating its safety and high recanalization rates<sup>152</sup>.

Moreover, many neuroprotective agents combined with rtPA have been studied in preclinical studies to decrease the excitotoxicity and the ROS generation. For example, *statins* showed an important role in BBB conservation after rtPA administration by attenuating the MMP expression<sup>153</sup>. In addition, antioxidants as *ascorbic acid* or *edavarone* showed less BBB disruption, infarct size and mortality when they were administered combined with rtPA, but they only have been tried in preclinical models and they have not been tried in clinical trials<sup>154</sup>. Furthermore, other treatments were combined with rtPA to decrease the HT. For instance, a preclinical study used  *fingolimod*, a treatment for the multiple sclerosis, that has anti-inflammatory mechanisms and vasculoprotection, confirming its protective effect in a thromboembolic model<sup>155</sup>.

Some studies employed antibodies against the mechanisms involved in proneurotoxic effects. For example, a polyclonal antibody against the interaction site of rtPA on the NR1 subunit of NMDAR, related to the proexcitotoxicity, was administered with

rtPA in mice. This study concluded that the infarct lesion was reduced as well as the BBB damage. Also, the outcome improved compared with the control group<sup>156</sup>.

In addition, to increase the half-life of rtPA, antibodies against those components related to its inhibition were developed. Wyseure et al published the effect of rtPA administration combined with a diabody against TAFI and PAI. They found that the infarct size was two-fold decrease without increasing the HT<sup>157</sup>.

Another antibody against vWF was employed to avoid the platelet aggregation, adhesion, inflammation, and thrombus formation, in which this protein is involucrated. Results showed that this synergic administration improved the behavioral function following embolic stroke due to the suppression of the reduction of inflammatory response and reduced leukocyte adhesion<sup>158</sup>.

It is well known that MMP increase the BBB damage. However, the MMP-10 has a profibrinolytic effect in ischemic stroke model. It could reduce the infarct size via TAFI-dependent mechanisms. Roncal et al administered the MMP-10 with rtPA obtaining a decreasing in reperfusion time and in infarct size compared with rtPA alone<sup>159</sup>.

Finally, the use of CD11b/CD18 antagonist showed an increase of the therapeutic window of rtPA in an embolic rat model. This effect is due to the inhibition of the neutrophil adhesion to the endothelium carried out by this antagonist<sup>160</sup>.

#### 2.4.3.1. Nanoparticles for rtPA delivery

The development of different nanoparticles (NPs) has been carried out to increase the efficacy of the thrombolytic treatment and decrease its side effects. To use these systems to encapsulate rtPA has the advantage of protecting it in bloodstream, increasing its half-life, enhancing its recanalization effectiveness and targeting the treatment to the desired region.

Due to the pivotal role of the NPs containing rtPA in this Thesis, they are going to be explained in depth in Section 3.





### 3. Nanomedicine and drug delivery systems

At the end of 1959 a new area of study emerged, the nanometric scale technology, and new concepts such as nanoscience and nanotechnology appeared. Nanotechnology is a multidisciplinary science that involves the creation of materials or systems in the nanometer (nm) scale. The application of this science in the treatment, diagnosis and monitoring of disease related to human health is coined nanomedicine.

The drug delivery aspects towards the therapy and diagnostic have been revolutionized by the nanomedicine. Nanotechnology allows the design of novel formulations for the greatest benefit of health<sup>161</sup>. With this aim, the primary objectives of NPs include: to target and to deliver the drug at the desired region, to improve the poorly soluble drugs, to decrease the toxicity maintaining its therapeutic effectiveness, and to improve its biocompatibility<sup>162</sup>.

Over the years with the emergence of nanotechnology, the complexity of the nanosystems has increased. The first formulations were focused on increasing the drug solubility and decreasing its inactivation with the consequent increase in the half-life. However, achieving a specific release in the site of action and decrease the toxicity was the next step in the improvement of the drug delivery systems. Two different ways are explored to reach the diseases sites. On one hand, passive targeting takes into advantage the anatomical and pathological abnormalities of the

disease. On the other hand, active targeting based on specific ligand that recognizes ligand in the delivery area.

Moreover, triggered release in the desired region is a modified form of active targeting. This last approach enables the release of the encapsulated payload in a specific area, thus minimizing the risk of the drug in the rest of the body. Different stimuli to carry out the triggered release are explained in the following Section. Stimuli-responsive drug release not only reduces premature drug release but also improves the efficiency of the drug delivery<sup>161</sup>.

Taking into consideration the above, rtPA treatment can be enhanced using nanomedicine. Encapsulate rtPA in nanocarriers have the following advantages<sup>163</sup> (Figure 20):

1. To extend the half-life of the molecule through its protection in the bloodstream.
2. To reduce the secondary effects of rtPA, mainly the risk of sICH.
3. To target the treatment to improve the treatment efficacy.
4. To improve the recanalization effectiveness through the penetration of rtPA into the clot.

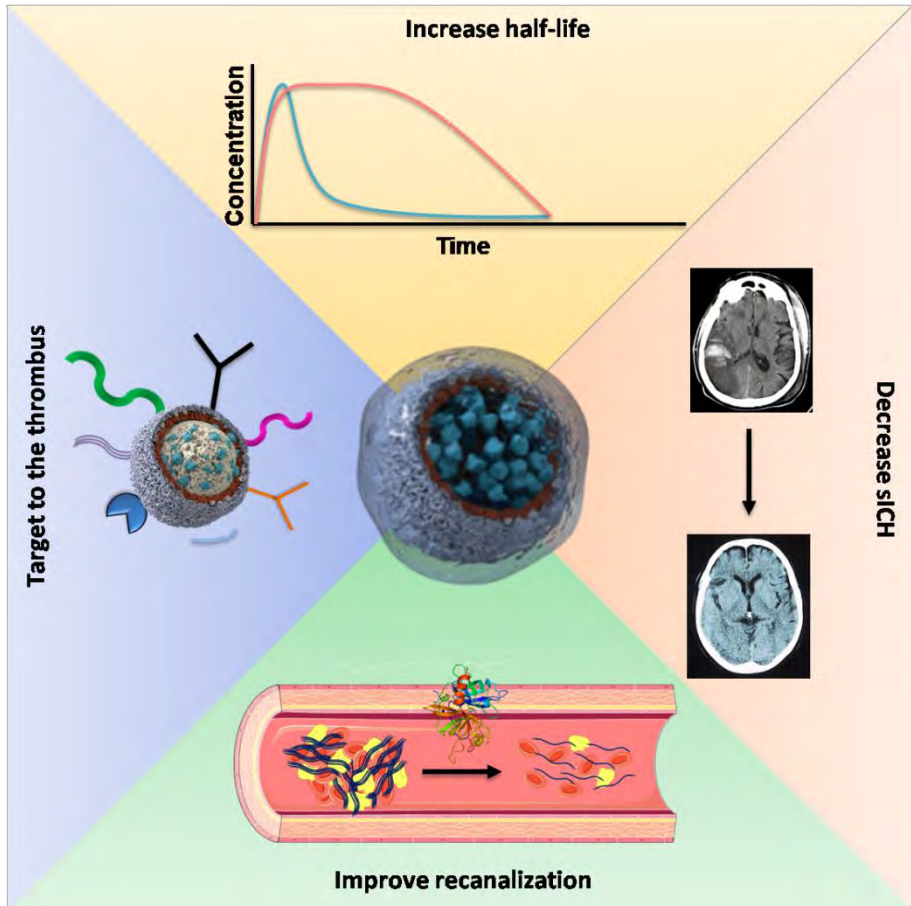


Figure 20. Advantages of using nanocarriers to encapsulate rtPA. Self-created image (using elements with Creative Common license).

As well as using nanocarriers to improve the thrombolytic treatment, target and triggered approaches can be employed to accumulate rtPA in the occluded region by the thrombus. The most common targets and stimuli are explained below.

### 3.1. Targeting approaches

One of the main drawbacks of the nanomedicine is the lack of specificity that nanosystems have. The use of targets to improve the concentration of the drug in the desired area could decrease the side effects related to high-dose and non-specific toxicity.

In case of the thrombolytic therapy, the most used targets are the main components of thrombi such as thrombin, fibrin, activated platelets, endothelial surface and vWF., and antibodies and peptides are commonly used to guide the NPs to thrombi region<sup>164, 165</sup> (Figure 21).

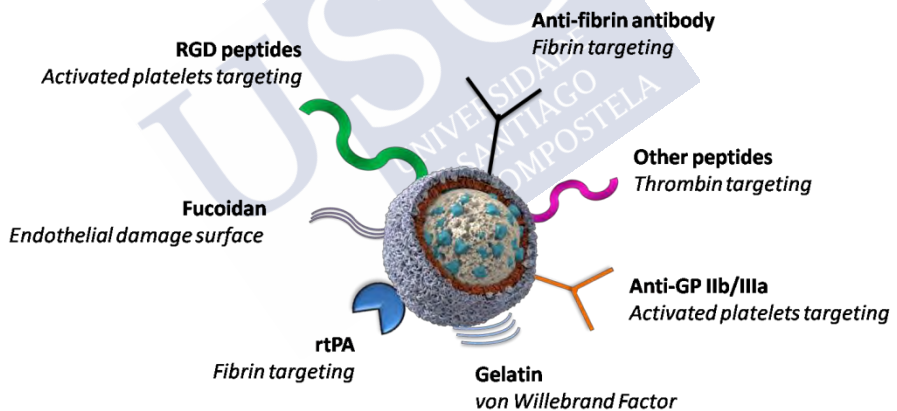


Figure 21. Schematic thrombus targeted drug delivery system. Self-created image.

The main antibodies used for rtPA delivery are against activated platelets and fibrin. In addition to be one of the main components of thrombi, fibrin is absent in blood circulation and in the normal

tissue, what makes them a suitable target to the fibrinolytic nanosystems<sup>166</sup>. Antibodies against B-chain of fibrin and fibrin fragment D-dimer have also been studied, both resulting in an increase in thrombolytic capacity<sup>167</sup>.

In the case of platelets, the main component used to target is the GP IIb/IIIa receptor, which is the final common pathway of platelet aggregation. This receptor in normal conditions, when the platelets are inactive, is stable. However, in presence of thrombin or collagen, which works as agonist, the conformation of the receptor changes, what makes it a suitable target to thrombolytic treatment. L-arginine-glycine-aspartic acid peptide (RGD) and L-arginine-glycine-aspartic acid-serine tetrapeptide (RGDS) has been used as antagonists of GP IIb/IIIa receptor<sup>168, 169</sup>.

Another example of thrombus targeting is the endothelium. In this way, P-selectin, expressed in the vascular damage, has been employed as a target through the incorporation of fucoidan to NPs. Fucoidan refers to a type of polysaccharide that exhibits high affinity for P-selectin, and NPs coated with fucoidan- have showed more interaction with the activated platelet than the NPs control<sup>170</sup>.

Finally, gelatin has been used to target NPs to vWF. vWF is a component of the thrombus that is linked to the collagen of the extracellular matrix. The fact that gelatin is denatured collagen explains why it has tendency to bind to the vWF.. Furthermore, the used of gelatin has the advantage of being used as an internal stimuli-responsive. This feature is explained in the next Section.

### 3.2. Stimuli-responsive drug delivery

Once the nanocarriers reach the site of action, they should release the drug to allow its therapeutic effect. To achieve this, stimuli responsive drug carriers can be used. In general, these stimuli that trigger drug release from the nanocarriers can be differentiated into external or internal and biological, chemical or physical (Figure 22).

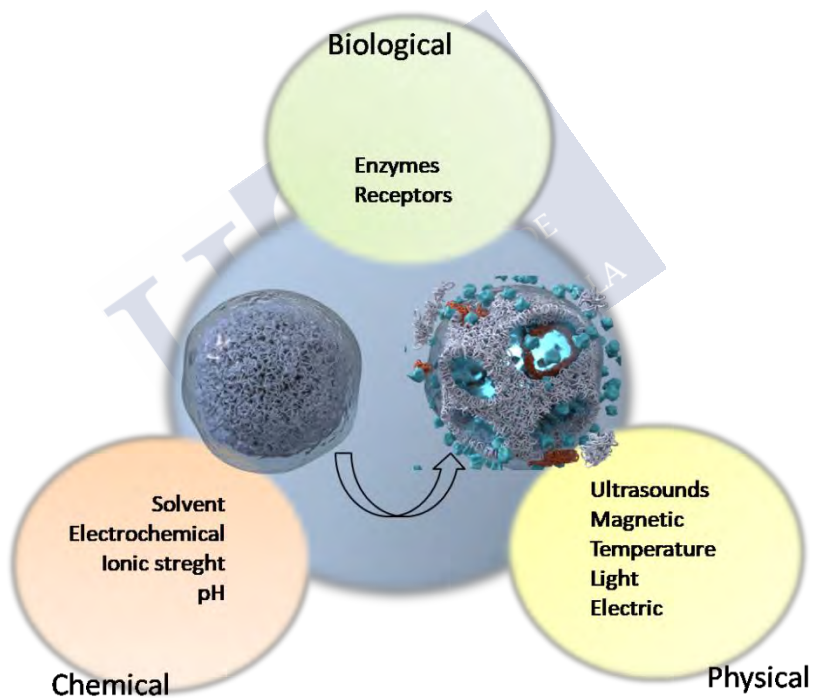


Figure 22. Biological, chemical and physical stimuli to promote drug release. Self-created image.

### 3.2.1. Internal stimuli

Internal stimuli have chemical and biochemical origin, and they could be classified in pH, redox, ionic, and enzyme-responsive. In the case of the thrombolytic therapy, carriers could be developed with the idea of using thrombosis itself as trigger. This is the case of thrombin sensitive capsules<sup>166</sup> and phospholipase A2 degradable liposome<sup>171</sup>. Other characteristics of the thrombosis, such as the elevated oxidative stress<sup>172</sup> and the high shear-stress<sup>173-175</sup> have shown to be great mechanisms to promote the release of the drug in the thrombus.

In addition, it is well known that MMP are increased in the stroke, and they could be used as enzymes to destabilize the NPs. Accordingly, gelatin NPs could be employed as enzyme-responsive carriers. This is because MMP, enzymes that degrade the matrix of the endothelium, can degrade also the gelatin due to its collagenous nature<sup>176-178</sup>. Thus, the effect as trigger for release rtPA is added to the target effect for vWF.

### 3.2.2. External stimuli

Another strategy to control the delivery of the proteins is physical external stimuli, which involve, among others, temperature, light, magnetic fields and US. There are some thermo-sensitive polymers that change its physic-chemical properties depending on the temperature, what could be used to performed temperature-responsive NPs. Use of light as an external stimulus offers some

advantages, such as ease of application, biocompatibility and controllability both spatially and temporally<sup>179</sup>. The application of a magnetic field in coordination with superparamagnetic iron oxide NPs (ioNPs) is other approach as external trigger release<sup>180</sup>. Not only they can be guided by a magnetic field<sup>181</sup>, but also these systems can create a local hyperthermia which accelerates thrombolysis<sup>182</sup>, or they can drill the blood clots by means of a magnetically powered helical movement<sup>183</sup>.

US application to promote the drug release has several advantages, as is the cheapest method and it does not use ionizing radiation. In the case of the stroke, its use as stimuli-response to release rtPA is added to sonothrombolysis (Section 2.3). The mechanisms by which the US causes the release of rtPA are the following:

- Thermal effects

Thermal effects in US-responsive drug delivery systems must be taken into account in the NPs synthesis. This is due to the destabilization that can occur in certain components when the temperature varies. When combined, the thermal and the US-responsive can increase the efficacy of the formulation<sup>184</sup>.

- Acoustic radiation

Acoustic radiation can localize and concentrate particles near a vessel wall, which may assist the delivery of targeted agents, what can enhance the targeting<sup>184</sup>.



- Cavitation

Cavitation is especially important when MBs are used as drug delivery system. Inertial cavitation is the responsible for the MBs rupture, while stable cavitation is the one that can increase the permeability of the vessels and allow the entry of the drug in the tissues<sup>184</sup>.

### 3.3. Carriers for rtPA delivery

There are many structures described in the literature used as carriers for rtPA delivery that could be classified in: camouflaged-rtPA, magnetic NPs, liposomes, MBs, echogenic liposomes (ELIP), polymeric NPs, and biomimetic nanosystems (Figure 23).

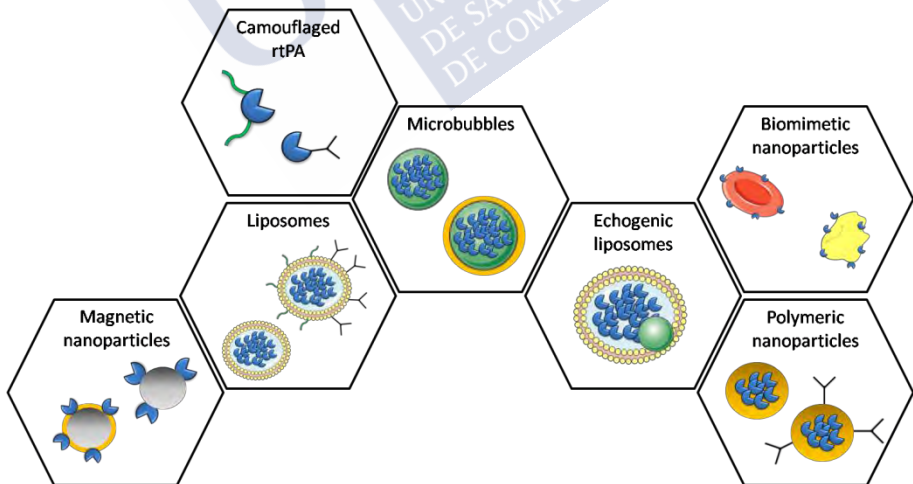


Figure 23. Schematic representation of the different carriers for rtPA delivery. NPs (nanoparticles, MB (microbubbles), ELIP (echogenic liposomes). Self-created image (using elements with Creative Common license).

### 3.3.1. Camouflaged-rtPA

One of the first strategies to improve rtPA treatment through the nanomedicine was published in 1988 by Berger et al. They performed a camouflage of rtPA molecule. For this purpose, they used polyethylene glycol (PEG) to complex rtPA increasing its short half-life. Furthermore, the derivatization of the protein with PEG decreases its antigenicity and immunogenicity. They managed to increase the half-life of rtPA to 16 min. However, the covalent conjugation PEG-rtPA leads to a decrease in the activity because the formulation reduces the interactions between the substrates and rtPA<sup>185</sup>.

Other way to camouflage the molecule was performed by Absar et al, who created two different conjugates. They complexed rtPA with a low molecular-weight heparin (LMWH), which was linked to another complex of albumin-protamine. The fact of using albumin is to camouflage rtPA in the blood. They showed that the complex was stable in plasma during 30 min and that it had more fibrinolytic efficacy than rtPA alone. However, due to the heparin, the risk of hemorrhages was increased<sup>186</sup>. For that reason, they eliminated the heparin and added a homing peptide (CQQHHLGGAKQAGDV), which binds to the GPIIb/IIIa receptor of the platelets. This change allowed the binding to platelets, and demonstrated controlled fibrinolysis of human blood clots<sup>187</sup>. Furthermore, they added another peptide with affinity for the thrombin (GFPRGFPAAGGctPA), what results in a suppression of rtPA activity in the bloodstream and the recovery of the fibrinolytic activity almost 100 % and the reduction of the hemorrhagic risk<sup>188</sup>.

In spite of the good results obtained, none of the new formulations has been tested in clinical trials.

### 3.3.2. Magnetic nanoparticles

Magnetic NPs are other approach to increase the benefits of rtPA treatment. Magnetic NPs have been used as drug delivery system or contrast to the MRI. Due to its biodegradability, ioNPs are the most used NPs. Zhou et al developed theranostic NPs with Fe<sub>3</sub>O<sub>4</sub> NPs that are recovered with rtPA, poly(lactic-co-glycolic acid) (PLGA), chitosan and RGD peptide. These structures showed a dual function as thrombus detectors and as a thrombolytic therapy that allow the monitoring of the thrombolysis using the MRI<sup>189</sup>.

Recently, the use of Fe<sub>3</sub>O<sub>4</sub> microrods was studied by Hu et al. Rods are elongate NPs, which have a higher and stronger contact area with the endothelium. They developed microrods with an average length of **1.3± 0.2 μm, and an average diameter of 0.5±0.1 μm.** *In vitro* experiments showed that rtPA loaded into these systems enhance the thrombolysis efficiency compared with rtPA alone<sup>190</sup>. In addition, these NPs were tested *in vivo*, where a magnetic field was used to guidance the NPs to the occluded vessel, and the clots were dissolved by rotation of the rods and by rtPA. The results showed a significant reduction of the infarct volume, the recanalization time was also decreased, the microrods treatment showed a complete recanalization at 25 min, whereas in the group

treated with rtPA (10 mg/Kg) it occurred a delayed recanalization at 85 min<sup>191</sup>.

### 3.3.3. Liposomes

Liposomes are a vesicular drug-delivery system that comprises a hydrophobic phospholipid bilayer (bL) and a hydrophilic aqueous core. One of the main advantages of the use of liposomes is the opportunity of encapsulating water-soluble and water-insoluble compounds, in the hydrophobic part or in the hydrophilic part, respectively. Other advantages are that these nanostructures are biocompatible, biodegradable, and they have low immunogenicity<sup>163, 192</sup>.

Liposomes have been employed in the encapsulation of rtPA for many years. Heeremans et al, achieved the encapsulation of rtPA in liposomes with high efficiency (90 %) <sup>193</sup>. Testing these nanostructures *in vivo* they found that they could decrease the dose of rtPA by administering the encapsulated forms, without losing the efficacy of the treatment<sup>194</sup>.

However, the main drawback of liposomes is its short circulation time, due to the phagocytosis by the reticuloendothelial system (RES). To overcome this disadvantage, the recovering of the liposomes using PEG was one of the approaches. Besides increasing the circulation time, PEG has low immunogenicity and it increases the solubility in water<sup>195</sup>. The PEGylation of liposomes

was studied by Kim et al, showing up to a 21-fold increase in lifetime compared with free rtPA<sup>196</sup>.

Another advantage of rtPA encapsulation in liposomes is the capability to decorate the surface with peptides to increase the targeting to the thrombus. For example, Absar et al developed liposomes with PEG and a peptide (CQQHHLGGAKQAGDV) with affinity for the GPIIb/IIIa. This formulation increase the adhesion to the platelets and rtPA half-life was extended from 5 to 141 min<sup>197</sup>. Recently, liposomes (**164.6 ± 5.3 nm**) decorated with PEG and the RGD peptide was achieved to increase the fibrinolytic activity and target to the platelets<sup>198</sup>.

### 3.3.4. Microbubbles

MBs are tiny gas or air-filled microspheres, and they were first used as contrast agents for imaging due to their acoustic characteristics. Cavitation due to US, is the main mechanism by which US increase thrombolysis. Cavitation leads to oscillations of MBs, that results in micro-streaming and erosion of clot, that allow to the thrombolytic drugs to penetrate in the clot and facilitate the thrombolysis<sup>163, 192, 199</sup>.

The MBs concentration, size, stability and the surface of the clot are factors of which depends the thrombolytic effect. The first MBs generation had a short half-life, due to the poor stability. To increase these aspects, the second generation was performed with high molecular weight gas and with a layer of phospholipids or

albumin<sup>200</sup>. The MBs use as thrombolytic has been reported in two different ways: by separate administration of MBs and rtPA and as a carrier to encapsulate rtPA.

Hua et al encapsulated rtPA inside MBs, and they decorated the surface with L-arginine-glycine-aspartic acid-serine peptide (RGDS). The new US-responsive formulation showed thrombolytic efficacy and less hemorrhagic risk using a reduced rtPA dose in a rabbit femoral artery thrombus model<sup>168, 169</sup>. Afterwards, a new technique to encapsulate rtPA inside the MBs was developed. The main advantages of this technique are that the aggregation of the bubbles is decreased and the load is increased<sup>201, 202</sup>.

### 3.3.5. Echogenic liposomes

Echogenic liposomes (ELIPs) arise from encapsulate MBs into the hydrophobic part of liposomes. Tiukinhoy-Laing et al and Smith et al developed ELIPs with 50 % encapsulation efficiency. The ELIPs showed similar thrombolytic activity than rtPA, and this activity was increased when the US was applied, proving the echogenicity of these structures<sup>203, 204</sup>.

Several studies have developed ELIPs that encapsulate rtPA and MBs. In general, they have demonstrated that rtPA released from the ELIPs has the same activity, the US applications increase the thrombolysis and it is comparable to rtPA alone, both *in vitro* and *in vivo*<sup>205-207</sup>.

### 3.3.6. Polymeric NPs

With the purpose of developing a drug delivery system to control the release and to target to the thrombus, some polymeric compounds were used. The PLGA, chitosan, and gelatin are some of the polymers used due to their biocompatibility, biodegradability, and their good adhesion properties to tissues.

Park et al developed a semi-interpenetrating polymer network hydrogel using the PLGA and PEG. They achieved rtPA encapsulation in a 10–20  $\mu\text{m}$  drug delivery system without affecting to the activity<sup>208</sup>.

Chung et al and Wang et al employed PLGA and chitosan NPs, adding the RGD tripeptide. In the study, they showed that PLGA-chitosan NPs ( $320.1 \pm 5.7$  nm) digest faster the clots,  $40.9 \pm 1.5$  % of digestion compared with free rtPA<sup>209</sup>. On the other hand,  $265.2 \pm 7.4$  nm PLGA-chitosan-RGD also had high percentages of digested clots compared with rtPA alone<sup>210</sup>.

Other strategy using polymeric structures was developed by Korin et al. They performed micro-aggregates ( $3.8 \pm 1.5$   $\mu\text{m}$ ) of NPs that had rtPA on the surface. These structures break up and release rtPA when they are exposed to high shear stress in the occluded vessels. They achieved a release locally that allowed lowering the used dose of rtPA<sup>175</sup>.

Li et al performed polymeric NPs with a high half-life and targeted to the thrombin. First, acrylamide and ammonium persulfate were used to create a thrombin-degradable hydrogel shell, with rtPA

inside. Furthermore, glutathione was used to prevent the interactions with the blood components. These NPs released rtPA only in the presence of thrombin, and their fibrinolytic activity was similar to rtPA alone. Moreover, with the glutathione addiction they prolong the circulation time<sup>211</sup>.

Juenet et al developed polysaccharide-poly(isobutylcyanoacrylate) NPs functionalized with fucoidan and loaded with rtPA. The selected target was P-selectin, by which fucoidan has affinity. The thrombolysis efficiency was improved in the thrombosis acute phase, revealing for the first time the relevance of the P-selectin targeting in rtPA treatment<sup>170</sup>.

Recently, fibrin-specific poly(N-isopropylacrylamide) nanogels were developed. These nanogels were tested in myocardial infarction and controlled the release of rtPA and an inhibitor of the cell contractibility. It was demonstrated that the NPs degraded fibrin *in vitro*, and decrease the infarct size *in vivo*<sup>212</sup>.

Gelatin nanostructures were also developed to encapsulate rtPA. In this case the gelatin was used because its biocompatibility, and because it tends to bind to the vWF. This can be explained because gelatin is denatured collagen, and the collagen is the main component of the endothelium where the vWF is present. Uesugi et al used this polymer to create US-responsive NPs (Figure 24). rtPA activity was suppressed around 50 % in these gelatin complexes, and when the US was applied (2 MHz, 0.72 W/cm<sup>2</sup>) the activity is completely recovered. To stabilize the junction between the gelatin and rtPA, zinc acetate was used. The result



complexes (100 nm) showed a prolongation of rtPA half-life about three times, a tendency to bind to the clots, and they increased the recanalization effectiveness in a model of thrombosis in swine<sup>213, 214</sup>.

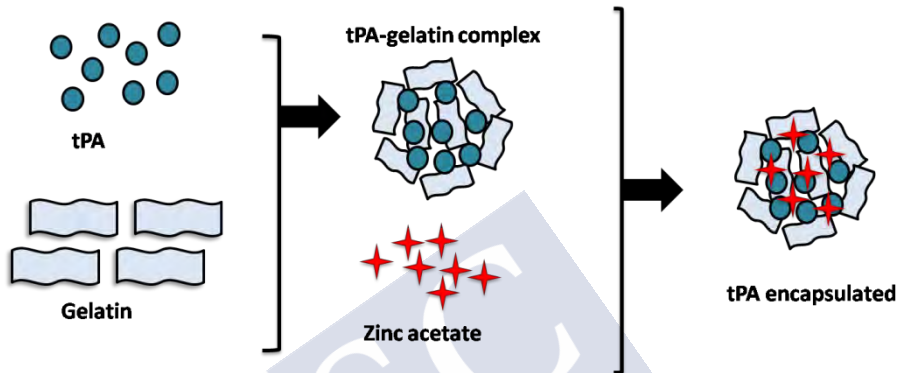


Figure 24. Scheme of the gelatin nanostructures. Self-created image.

### 3.3.7. Biomimetic nanosystems

One of the major limitations of the NPs as medicinal products is that after i.v. administration, they are rapidly sequestered by circulating phagocytes and macrophages cells. For this reason, the synthesis of biomimetic nanocarriers is an approach to remain invisible to the phagocytic system, to increase the half-life of the NPs and to improve the targeting efficiency.

### 3.3.7.1. Red blood cells

Due to their long half-life red blood cells are an approach to improve the delivery and to prolong the circulation time of drugs<sup>215</sup>. The first study with this type of encapsulation was published in 2003 by Murciano et al. The circulation of rtPA in the red blood cells was increased to 2 hours. Furthermore, in a pulmonary thrombosis model and in an arterial thrombosis the dissolution of the clots in the animals treated with red blood cells encapsulating rtPA was greatly increased. However, this formulation was used as prophylaxis, not as a treatment after the thrombosis<sup>216</sup>.

The first use of the red blood cells as a treatment after the thrombosis was in 2018. Vankayala et al conjugated rtPA on the surface of red blood cells membranes. They demonstrated the fibrinolytic activity in clots *in vitro* using this 34 nm NPs<sup>217</sup>.

### 3.3.7.2. Platelets

The use of the membranes of platelets as a biomimetic system is because they are one of the components of thrombi. In this way, besides making the nanosystems invisible, it would be increasing the targeting.

rtPA encapsulation in platelets is not quite developed in the ischemic stroke field. However, Hu et al published in 2016 a biomimetic platelet nanosystem for cancer treatment. In this nanosystem rtPA was linked on the surface of the membrane, in order to degrade thrombi in the multiple myeloma<sup>218</sup>.

Despite the promising results of all the formulations and nanosystems that have been developed and tested *in vitro* and in preclinical studies, none of them have been proven in clinical trials.



#### 4. Layer-by-layer nanocapsules

As it was previously described, polymeric nanocapsules (NCs) can be used to improve the effectiveness of drugs. A simple, versatile process to construct these NCs is multilayered films formed via layer-by-layer (LbL) assembly. This technique is based on the deposition of oppositely charged polyelectrolytes in a sacrificial template<sup>219</sup>.

In the late 1990s, LbL assembled capsules emerged as a promising drug delivery system. LbL assembly of polymers onto porous templates allows the fabrication of ultrathin polymer shell capsules that may be loaded with drugs<sup>220-222</sup>. The main advantages are based in the ability of the LbL method to:

- Encapsulate almost any drug, ranging from small molecules (e.g., dyes) to large macromolecules (proteins, enzymes, oligonucleotides, etc.)<sup>223</sup>.
- Layer self-assembly by charge, hydrogen bonding, host-guest interactions, etc. of a wide variety of polymers (e.g., biodegradable, stimuli-responsive, bearing therapeutic function)<sup>224</sup>.
- Incorporate inorganic NPs into their shell in order to provide, for instance, multimodal imaging and/or stimuli-responsive capabilities<sup>225</sup>.

#### 4.1. Preparation of layer-by-layer assembly

The polyelectrolyte capsules have two main components: the core and the polyelectrolyte pair. These capsules are fabricated by LbL adsorption, by which different polymers are deposited around a preformed a charged spherical core. After the LbL process, the core is removed to obtain hollow and stable capsules (Figure 25). The loading of the proteins can be performed in the core synthesis (pre-loading) or at the end of the LbL (post-loading). Usually, the polymeric wall can vary, from nanometers to several micrometers, depending on the size of the original core.

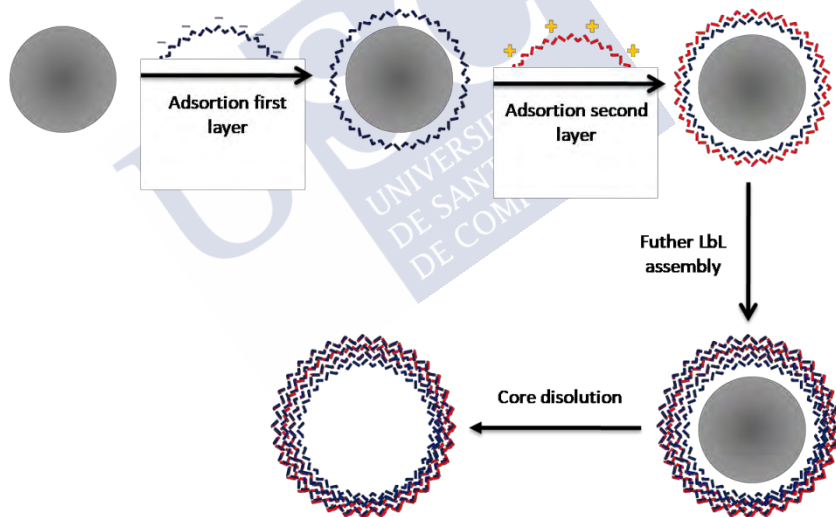


Figure 25. Preparation of LbL capsules. Self-created image.

The core template used depends on the desired drug to encapsulate and the polyelectrolytes. The ideal core has to be

stable during the LbL assembly, soluble in mild conditions, and completely removable from the inside of the capsules without affecting to the polymeric shell.

Different sacrificial templates have been used to prepare micro- and NCs, including silica, polystyrene or  $\text{CaCO}_3$  particles, among others<sup>219, 226</sup>.  $\text{CaCO}_3$  particles are particularly well suited for encapsulation of delicate macromolecules during the formation of microporous particles, which are removed after LbL using, in general, a calcium chelating agent (ethylenediaminetetraacetic acid, EDTA). In contrast, polystyrene and silica-templated particles require stronger conditions than using EDTA, such as organic solvents or buffered hydrofluoric acid. In the case of  $\text{CaCO}_3$  particles, macromolecule encapsulation and LbL polymer deposition do not affect in general the bioactivity of the encapsulated macromolecules<sup>227</sup>.

The self-assembly of the layers occurs through the electrostatic interaction between the oppositely charged polyelectrolytes in solution. The versatility in the procedure depends on the capability of a charged molecule to be adsorbed onto the core or layer. The ideal material to perform the LbL technique are those biodegradable that can be excreted from the body and prevent toxic accumulation<sup>219</sup>.

## 4.2. Encapsulation and release

There are two different strategies to encapsulate the molecules in the LbL capsules: post-loading and pre-loading (Figure 26). In the Post-loading method, the loading is done after the fabrication of the capsules, altering the permeability of the capsule shell. Although this method is very useful to encapsulate many types of molecules, it has a very low encapsulation efficiency (that is the amount of protein encapsulate relative to the amount of protein added at the beginning), and it can provoke loss of bioactivity of the therapeutic molecule due to the methods needed to increase the capsule shell permeability.

On the other hand, pre-loading is especially used for the encapsulation in the  $\text{CaCO}_3$  cores. The pre-loading takes place by the adsorption in the porous or by co-precipitation during cores synthesis. In addition to the innocuous core removal to the majority of biomolecules, this method allows for achieving high-loading capacities, in contrast to silica or polystyrene templates<sup>227</sup>.

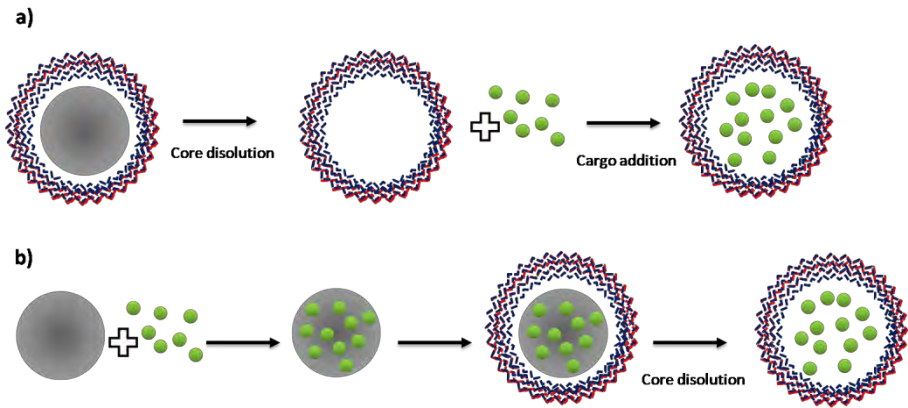


Figure 26. Encapsulation in CaCO<sub>3</sub> LbL capsules. a) Post-loading. b) Pre-loading. Self-created image.

Cargo release from capsules can occur by simple diffusion<sup>219, 226</sup>, or upon the biodegradation of the polymeric shell, typically driven by enzymatic degradation processes<sup>228</sup>, or through active processes mediated by the use of an external trigger<sup>219</sup>.

The use of external stimuli such as light, magnetic fields or US appears particularly appealing to create local macromolecular gradients *in vivo*. Stimulus-controlled drug delivery may be a suitable solution to improve targeted delivery of nanomedicines by choosing when (temporal resolution) and where (spatial resolution). It has been demonstrate that it is possible to control the intracellular release of dyes and different macromolecules by illumination of NPs embedded in the semipermeable wall of LbL microcapsules<sup>223, 229</sup>, as well as by US application (sonosensitive microcapsules)<sup>230, 231</sup>.



### 4.3. Ultrasound-responsive layer-by-layer capsules

In contrast to other NPs, LbL assembled multilayer capsules can encapsulate a large amount of protein and they have easily adjustable composition and properties. The physical properties can be modified by varying the polymeric composition, the number of the layers and incorporating NPs in the shell.

US is an excellent viable stimulus to control the cargo release of polymeric drug delivery system. The main advantage is that US offers precise control over spatiotemporal drug release<sup>232</sup>.

The effect of the US in the LbL capsules has been studied since 2006<sup>233</sup>. It is well established that the response to US depends mainly on the US parameters applied, and the thickness and composition of the shell<sup>234</sup>.

The group of H. Möhwald performed polystyrene templatemicrocapsules composed by a shell of poly-allylamine hydrochloride (PAH) and sodium poly-styrene sulfonate (PSS), in which they incorporated  $\text{Fe}_3\text{O}_4$ . The capsules were treated with 20 kHz and different intensities; it was found that the shell disruption increased as the US intensity augmented<sup>233</sup>.

In addition, the response to US was not affected, since both diagnostic (2.25 MHz, 115 mW/cm<sup>2</sup>, 15 min) and therapeutic US (20 kHz, 14 W/cm<sup>2</sup>, 60 s) showed the release of the encapsulated encapsulated<sup>232, 235</sup>.

When inorganic NPs are embedded the mechanical properties of the shell can be changed (Figure 27). Different types of inorganic NPs like magnetite<sup>232</sup>, gold<sup>236</sup> or zinc oxide (ZnO) were incorporated to the shells to control the mechanical properties of the shell, and, in that way, to control the interaction between US and capsules. Thus, when using magnetite into the capsules, they broke into pieces after 60 s ( $377 \text{ W/cm}^2$ , 500 W), while the capsules without magnetite only got its shell deformed after the application of US<sup>233</sup>. Also gold NPs shown that its incorporation into the shell makes them more suitable to the rupture after the US application<sup>235</sup>. Also gold NPs showed that its incorporation into the shell made them more suitable to the rupture after the US application<sup>235</sup>. However, the incorporation of ZnO NPs into the shells was the one that provoked the fastest shell destruction there was a total rupture after 9 s of US ( $30 \text{ W/cm}^2$ ) when lowering the capsule stiffness and embedding ZnO in PSS/PAH capsule wall<sup>237</sup>.

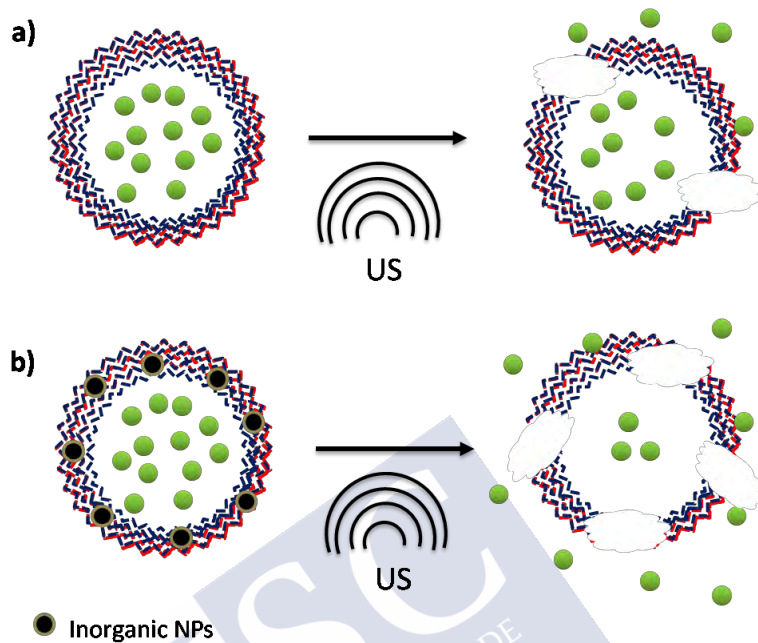


Figure 27. Release with US. The response to US increase when inorganic NPs are embedded in the LbL capsule. Self created image.





Hypothesis



The only approved drug treatment in the acute phase of the ischemic stroke continues to be rtPA. However, this treatment has some limitations such as a short therapeutic window, hemorrhage transformation risk, low reperfusion rates or neurotoxicity side effects. Therefore, the development of new strategies or approaches able to improve the efficacy and reduce the side effects of rtPA is highly demanded for the clinical community.

In the past two decades, extensive efforts have been undertaken to extend its therapeutic time window and reduced the sides effects associated with this drug. Nanotechnology has emerged as a promising strategy to improve the efficacy and safety of rtPA. Using nanocarriers to deliver rtPA in combination with external stimulus (light, US, magnetic fields, etc) offers many advantages to enhance the efficacy and safety of rtPA therapy.

In this study, we proposed to develop rtPA-loaded nanocapsules coated with gelatin, which in combination with US application will trigger the rtPA release from our nanocapsules in *in vitro* clots models and in *in vivo* ischemic models. Gelatin coating is used because this substance is known to bind to von Willebrand factor (vWF), a key component of thrombus, and is degraded by the MMP over expressed in the ischemic area, therefore this design would increase the drug release in the clot region.

Based on the above mentioned observations, we hypothesize that the therapeutic effect of rtPA could be increased by its encapsulation in sonosensitive NC that will

deliver and release the drug in the ischemic region by the application of US. This innovative strategy is expected to improve the outcome of rtPA-treated stroke patients, increase the therapeutic time-window, and thus the number of stroke patients that can benefit from this treatment.







## Objectives

---



The main goal of this project was to design, to synthesize and to test a sono-sensitive NC for the delivery of rtPA. In order to achieve the main goal, two specific aims were proposed in this Thesis:

1. *In vitro* optimization of rtPA nanocapsules:

- To design a suitable sono-sensitive nanocapsules for the delivery of rtPA.
- To synthesize and characterize the rtPA encapsulation in NCs.
- To validate the rtPA activity in NCs.
- To study the *in vitro* release by the application of US.

2. *In vivo* studies of rtPA nanocapsules:

- To validate the *in vivo* safety of US parameters applying through the Doppler.
- To demonstrate the *in vivo* safety of NCs administration.
- To demonstrate the *in vivo* release of rtPA from the NCs by applying US.

- To investigate the therapeutic effect of the NCs in a thromboembolic model in mice.
- To analyze the biodistribution of the NCs in the different organs.





## Materials and methods



## 5. Preliminary study

Following a protocol published by Kawata et al<sup>214</sup>, we initially developed a system to suppress rtPA activity and recovery it with US. In this method, we developed NPs comprising rtPA, basic gelatin, and zinc ions that suppresses tPA activity, but is recovered by US. This method has been tested in heart attack models but not in ischemic stroke model.

### 5.1. Synthesis

Gelatin (100,000 MW, Nitta Gelatin, Inc., Osaka, Japan) and zinc acetate (Sigma-Aldrich, #379786) were used to encapsulate rtPA. The method to prepare the complex is similar to the method described by Uesugi et al<sup>213</sup>. Briefly, a solution of 30 mg gelatin in 1 mL of 10 mM phosphate-buffered solution (PBS, pH 7.4) was mixed with 1 mL of rtPA at a concentration of 3mg/mL. After agitation at 37°C for 30 min, zinc acetate (at a final concentration of 10 mM) was added to stabilize and tighten their connection, and the mixture was agitated at 37°C for 30 min.

## 5.2. *In vitro* rtPA activity

### 5.2.1. Amidolytic activity

We used the fluorogenic-based assay Sensolyte® (Sensolyte® AMC tPA Activity Assay Kit from Anaspec, #AS-72160) to measure rtPA amidolytic activity in samples. Briefly, this kit contains a fluorogenic substrate with high reactivity and low background. tPA cleaves the substrate resulting in the release of AMC (7-amino-4-methylcoumarin) fluorophore. We use this assay following the **manufacturer's instructions**.

### 5.2.2. Fibrinolytic activity

To study the effect of the fibrinolytic activity of encapsulated rtPA on thrombus, an *in vitro* assay was performed by measuring the percentage of clot weight reduction.

Firstly, Eppendorf tubes were weighted. Afterwards, to make clots, Sprague-Dawley rats (300-350 g) were anaesthetized with 6 % sevoflurane and maintained with 4 % in a 70 %/30 % mixture of NO<sub>2</sub>/O<sub>2</sub> and blood samples were extracted and collected into Eppendorf tubes (0.5 mL/tube). The collected blood was incubated at 37°C during 90 min to form the clot, the supernatant (SN) was removed and the clot was weighted (initial weight). Then, 200 µL of treatments were added to clots.

There were 6 groups of treatment (n=14):



- Vehicle.
- Vehicle + US.
- rtPA (1.5 mg/mL).
- rtPA + US (1.5 mg/mL).
- Encapsulated rtPA (1.5 mg/mL).
- Encapsulated rtPA (1.5 mg/mL) + US.

The US was applied using a Doppler (pulse wave, 2.0 MHz, 0.72 W/cm<sup>2</sup>) during 10 min. Once the treatment was added, clots were incubated again at 37°C during 90 min. Then, the samples were centrifuged at 9900 rcf, 4°C during 5 min. The SN was removed and the final clots were weighted (weight after incubation).

The percentage of weight reduction was calculated as follows:

$$\text{Reduction (\%)} = \frac{(100 - \text{final weight})}{\text{Initial weight}} \times 100$$

### 5.3. *In vivo* release

Swiss mice were used as animal model to investigate the *in vivo* performance of the encapsulated rtPA for US-controlled release of rtPA.

0.2 mL of sample was injected as an infusion in the tail vein. Blood extractions (0.2 mL) were done through a cannula inserted in the carotid artery. US was continuously applied (40 min) in the abdominal region. Blood samples were collected in a microtainer BD (Microtainer K2E Tubes. Ref: 365975, Franklin Lakes, NJ) and centrifuged at 3000 rcf, 4°C during 7 min. The plasma obtained was kept at -80°C until the measurement. To measure rtPA plasmatic activity in the extracted samples, we used the SensoLyte® kit following the manufacturer's instructions.

The first study was carried out with four experimental groups (n=4):

- Vehicle (~200 µL).
- rtPA 10 mg/kg: 10 % bolus + 90 % infusion (~200 µL).. This protocol is commonly used in preclinical mouse models and as thrombolytic treatment in the clinic (0.9-1 mg/kg, 10 % bolus + 90 % infusion). In preclinical mouse models, the 10-fold rtPA dose is motivated by the characteristics of the fibrinolytic system in rodents, which is known to be about 10 times less sensitive to rtPA than in humans<sup>238</sup>.
- Encapsulated rtPA (10 mg/kg): 10 % bolus + 90 % infusion (~200 µL).
- Encapsulated rtPA (10 mg/kg): 10 % bolus + 90 % infusion + US (~200 µL).

Blood samples were taken prior to administering the treatments (basal) and 5, 20 and 40 min after the administration.



## 6. Section 1: *In vitro* optimization of rtPA nanocapsules

After evaluate the encapsulation efficacy of rtPA using basic gelatin and Zn ions, a new and more complex encapsulation protocol was developed. In this new protocol, rtPA was encapsulated in CaCO<sub>3</sub> templated NCs by the LbL method. We adapted methods typically used for the fabrication of LbL microcapsules (3-5 microns in diameter) and achieved sub-micrometric macromolecule-loaded NCs (800 nm in diameter).

This Section was performed in collaboration with the group Bionanotools from the Centro Singular de Investigación en Química Biolóxica e Materiais Moleculares (CiQUS) of the Universidade de Santiago de Compostela.

This Section was accepted for publication in Journal of Controlled Release in July 2019.

### 6.1.1. rtPA labeling and quantification

Commercial rtPA (70 kDa, Alteplase, Actilyse®, Boehringer Ingelheim) was diluted to a concentration of 10mg/mL. Due to the low rtPA solubility, Actilyse® is always prepared in the presence of arginine and polysorbate 80, which work as excipients avoiding the precipitation of the drug.

rtPA was mixed with fluorescein-5-isothiocyanate (FITC, #1245460250, Sigma-Aldrich) at pH 8 in phosphate-buffered saline (PBS), and left to react protected from light 4 hours. We used 25 units of FITC by each unit of rtPA. Then a size exclusion column (PD-10, MWCO = 5000 Da; #GE17-0851-01) was used to purify the labeled protein from the excess of free dye and from the **excipients. The column was used according to the manufacture's** instructions. To avoid the precipitation of rtPA-FITC, the column was equilibrated with 3.5 mg/mL arginine in PBS (10mM, pH 7.4). The same buffer was used to collect rtPA-FITC. Without arginine rtPA would precipitate (PT), as we could observe simply by visual inspection.

We use a Bradford assay (Pierce TM Coomassie Plus Assay Kit; ThermoFisher #23263) to determine the protein concentration after dye-labeling. The respective calibration curve was prepared by measuring the fluorescence of different samples of known concentration. The fluorescence was measured using a plate reader, which allowed us to correlate protein concentration and fluorescence. The samples of rtPA-FITC in 3.5 arginine in PBS were protected from the light and stored at -20° at 1 mg/mL.

Bovine serum albumin (BSA, 66 kDa, #A2153, Sigma-Aldrich) was used to perform the characterization assays. It was labeled, quantified and stored as rtPA. The only difference was that the BSA was collected from the column and stored using PBS without arginine.

### 6.1.2. Synthesis, polymer coating and characterization of iron oxide nanoparticles

ioNPs were synthesized by a thermal decomposition method adapted from previous work<sup>239</sup>. Briefly, the inorganic precursors, Fe(acac)<sub>3</sub> (5 mmol), ZnCl<sub>2</sub> (1.1 mmol) and MnCl<sub>2</sub> (1.6 mmol) were placed in a three neck 50 mL round bottom flask. Then the organic surfactants oleic acid (31.5 mmol), oleylamine (60.8 mmol) and the solvent benzylether (34.2 mmol) were added. The mixture was degassed at 90°C for 30 min and then heated to 200°C under N<sub>2</sub> atmosphere. Finally, the temperature was increased to 310°C for 1 h. After the system reached room temperature (RT), methanol was added to the resultant mixture and the ioNPs were cleaned by centrifugation (1500 rcf, 5 min). Finally, after 3 centrifugation steps, the PT (ioNPs) were redispersed in an organic solvent (chloroform) and stored in the refrigerator (4°C).

The resulting colloids (oleic acid/oleylamine stabilized Mn/Zn ioNPs) were analyzed by transmission electron microscopy (TEM).

On the other hand, Inductively Coupled Plasma Mass Spectrometry (ICP-MS) was used to determine the ioNPs composition and the ioNPs mass concentration (m).

In order to make the oleic acid/oleylamine stabilized Mn/Zn ioNPs stable in aqueous solution, NPs were coated with the amphiphilic polymer dodecyl grafted-poly(isobutylene-alt-maleic anhydride), herein after referred to as PMA, following previous reports<sup>240</sup>.

PMA was synthesized by mixing two precursors, that is, poly (isobutylene-alt-maleic anhydride) and dodecylamine. 20 mmol of poly (isobutylene-alt-maleic anhydride) and 15 mmol of dodecylamine were dissolved in 40 mL of tetrahydrofuran and the solution was kept under magnetic stirring and reflux (70 °C) overnight. The solvent was evaporated under vacuum and the obtained film was redispersed with 40 mL of chloroform. The final PMA concentration was 0.5 M (expressed in terms of PMA monomers per nm<sup>2</sup> of NPs).

PMA was synthesized by mixing two precursors, that is, poly (isobutylene-alt-maleic anhydride) and dodecylamine. 20 mmol of poly (isobutylene-alt-maleic anhydride) and 15 mmol of dodecylamine were dissolved in 40 mL of tetrahydrofuran and the solution was kept under magnetic stirring and reflux (70 °C) overnight. The solvent was evaporated under vacuum and the obtained film was redispersed with 40 mL of chloroform. The final PMA concentration was 0.5 M (expressed in terms of PMA monomers per nm<sup>2</sup> of NPs).

NP PMA-coating was made by mixing the PMA solution with the ioNPs dissolved in chloroform. The experimental conditions of this reaction were taken upon consideration based on parameters like diameter and surface area of the IONPs and PMA concentration. The final conformation used for the coating was 2000 PMA monomers per nm<sup>2</sup> of NPs. Briefly, the coating procedure consisted of the evaporation of the organic solvent under vacuum and the transference of the hydrophobic NPs into an aqueous medium, in this case sodium borate buffer (pH 12). The final step consisted of

the cleaning of the PMA excess by centrifugation ( $3 \times 10^4$  rcf) and the consequent redispersion in water. Once the IONPs were soluble in water, further analyses were carried out. Hydrodynamic size and surface zeta potential were measured in a Zetasizer Nano ZSP.

### 6.1.3. Synthesis of $\text{CaCO}_3$ nanocores

$\text{CaCO}_3$  were grown by the coprecipitation of  $\text{CaCl}_2$  and  $\text{Na}_2\text{CO}_3$  in the presence of rtPA or BSA. It was prepared as follow: 1 mL of 20 mM  $\text{CaCl}_2 \cdot 2\text{H}_2\text{O}$  (147.01 g/mol, #223506, Sigma-Aldrich) solution in water and poly(vinylsulfonic acid) (PVSA, 0.1 mM; 30wt. % in  $\text{H}_2\text{O}$ , 5 g/mol, #278424, Sigma-Aldrich) were mixed under continuous stirring (550 rpm) in a covered beaker (protected from the light) with a magnetic stirrer at RT. Then, 20  $\mu\text{L}$  of BSA or rtPA (1 mg/mL) was added. After 5 min, 1 mL of 20 mM  $\text{Na}_2\text{CO}_3$  (105.99 g/mol, #S7795, Sigma-Aldrich) was rapidly injected. The solution was mixed at the same speed during 30 min. The nanocores were obtained by precipitation at  $3 \times 10^3$  rcf (5 min) (Figure 28). After centrifugation the PT was washed with a sodium bicarbonate buffer solution (0.1 M  $\text{NaHCO}_3$ , pH 9) and washed/precipitated one more time at  $3 \times 10^3$  rcf (5 min). Finally, we resuspended the nanocores in 1 mL of the  $\text{NaHCO}_3$  buffer and we immediately used it for LbL.



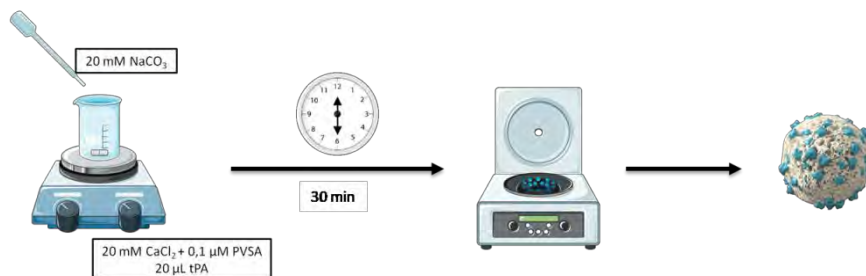


Figure 28. Schematic representation of the nanocores synthesis. Self-created image (using elements with Creative Common license).

#### 6.1.4. Layer-by-layer

LbL assembly was performed by the addition of alternating charged polyelectrolyte layers onto the sacrificial CaCO<sub>3</sub> cores. Solutions of PSS (MW= 70 kDa, #243051, Sigma-Aldrich) and poly(diallyldimethylammonium chloride) (PDACMAC MW=200000-350000, 20wt. % in H<sub>2</sub>O, #409022 Sigma Aldrich) at 20 mg/mL with 0.5 M NaCl were prepared in NaHCO<sub>3</sub> buffer.

Then, 0.5 mL of cores (in buffer) were added to the PSS solution (0.5 mL). The solution was mixed in a vortex mixer for 5 min, and cores@PSS were precipitated at  $3 \times 10^3$  rcf (5 min) and washed/precipitated one more time with the buffer. Next, the PDAMAC solution was used (same conditions as the PSS deposition) to form the next layer (cores@PSS/PDACMAC)

Then, after the first PSS/PDACMAC bL a solution of 2 mg/mL in milliQ water with 0.5 M NaCl of ioNPs was used as the

polyelectrolyte solution to form a layer of ioNPs, which was stabilized by a layer of PSS (cores@PSS/PDACMAC/ioNPs/PSS).

Next, a second PDACMAC/PSS bL was formed as previously described (cores@PSS/PDACMAC/ioNPs/PSS/PDACMAC/PSS).

Alternatively, an outermost layer based on basic gelatin was formed (cores@PSS/PDACMAC/ioNPs/PSS/ PDACMAC/PSS/gelatin) or additional PSS/PDACMAC bL were formed, that is, structures with 4 o 6bL: cores@PSS/PDACMAC/ioNPs/PSS/(PDACMAC/PSS) x 3 or x5, respectively.

To prepare the gelatin solution 0.6 g of basic gelatin (G9391, Sigma-Aldrich) were dissolved in 12 mL of milliQ water at 50°C under stirring. When the gelatin was completely dissolved, 12 mL of acetone were rapidly added to the solution. After 10 s, part of the gelatin precipitated in the form of a dense solid. This purified gelatin was dried, and a solution of 7 mg/mL in water was prepared and used for de LbL.

The CaCO<sub>3</sub>nanocores coated with the different bL, ioNPs and gelatin were exposed to ethylenediaminetetraacetic acid (EDTA, 0.02 M, pH 5.5) for 1 hour to produce the hollow NCs loaded with the selected biomacromolecules.

Finally, NCs were washed/precipitated twice at  $5 \times 10^3$  during 5 min.

The LbL process is represented in Figure 29.

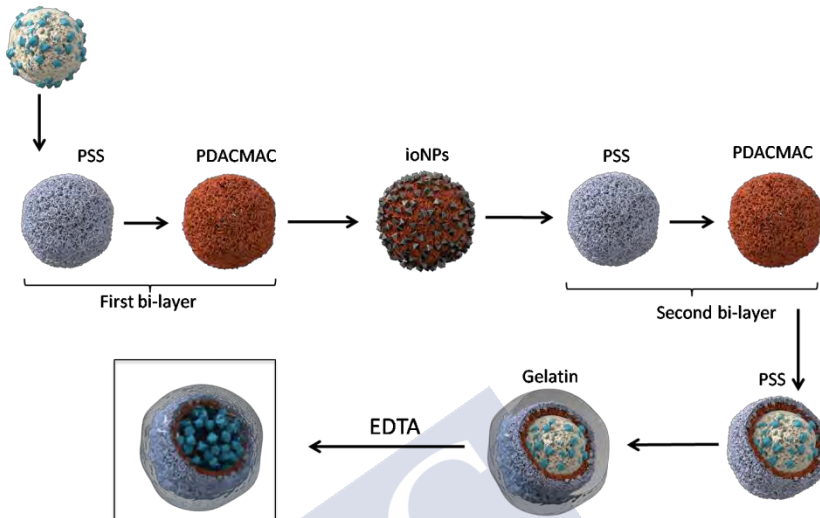


Figure 29. Schematic representation of the LbL process starting with the  $\text{CaCO}_3$  nanocores loaded with the protein, which after coating with 2bL of PSS/PDACMAC, ioNPs and gelatin, they were exposed to EDTA to dissolve de  $\text{CaCO}_3$  matrix. Self-created image.

Henceforth, cores with rtPA and BSA are going to be marked as core@rtPA and core@BSA, respectively. In the case of hollow NC with BSA will be NC@BSA, with rtPA and with gelatin NC@rtPA, and when the NC have not been synthetized with gelatin, it will be remarked as NC@rtPA without gelatin (Table 7).

Table 7. Nomenclature code.

	Core	NC with gelatin	NC without gelatin
BSA	core@BSA	NC@BSA	NC@BSA without gelatin
rtPA	core@rtPA	NC@rtPA	NC@rtPA without gelatin

## 6.2. Characterization of the nanocapsules

### 6.2.1. Scanning Electron Microscopy

A Phillips CM-12 and a FESEM Ultra Plus electronic microscope operating at 3.0 kV were used to study the morphology and mean diameter ( $d_c$ ) of nanocores loaded with the different proteins and NCs was analyzed by Scanning Electron Microscopy (SEM). We prepared the SEM samples by evaporating a drop of the different samples on a silicon wafer.

### 6.2.2. Dynamic Light Scattering

To perform the Dynamic Light Scattering (DLS) we used a Malvern Zetasizer Nano ZSP to determine hydrodynamic size of nanocores and NCs. Also, zeta potential values were measured using the same instrument to track the LbL procedure. The efficiency of the different polyelectrolyte layers was proven by the alternating of the net charge of the particles.

### 6.2.3. Leaking: encapsulation stability

The encapsulation stability was studied with an indirect measurement of the mass of cargo based on fluorescence, using the calibration curve previously described. The experiment was performed at 4°C and 37°C as follows. After NCs synthesis (with

and without cores) we take samples at different time points: basal (after the synthesis), 1, 2, 3 and 7 days. We centrifuged the samples and we compared the fluorescence intensity ( $I_F$ ) in the precipitated systems and in the SN (Figure 30).

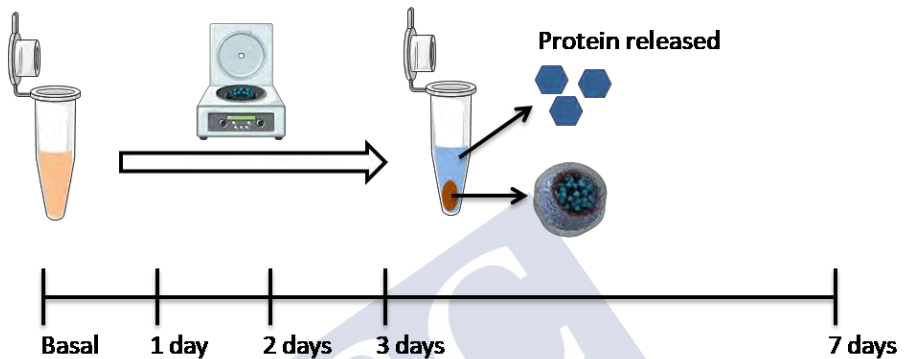


Figure 30. Schematic representation of the leaking assay. Self-created image (using elements with Creative Common license).

### 6.2.1. Nanocapsule stability

The stability and the aggregation of NC@rtPA and NC@rtPA without gelatin were studied by flow cytometry in PBS and in plasma. 0.01 mg/mL of rtPA encapsulated in NCs were diluted in different medium, we used this concentration because it is the one achieved in the blood when 1 mg/kg rtPA is administered in a 30 g mouse (3 mL of blood, approx.).

The assays were performed in a 96-well plate, following the same flow cytometry parameters as those explained in the Section

6.2.2.2, and at 1, 4 and 8 h after the incubation of the NC with PBS and plasma.

#### 6.2.2. Loading: quantification of cargo

Loading efficiency (LE) was evaluated using fluorescence and flow cytometry.

$$\mathbf{LE\ (\%)} = \frac{\mathbf{mass\ of\ cargo\ in\ purified\ cores}}{\mathbf{mass\ of\ cargo\ added}} \times 100$$

##### 6.2.2.1. Fluorescence

Quantification of cargo (BSA-FITC, rtPA-FITC) content was done as an indirect measurement of mass of cargo based on fluorescence, using the calibration curves previously described (Section 6.1.1)

##### 6.2.2.2. Flow cytometry

Flow cytometry measurements were performed to determine NCs concentration (NC/mL). The lower size detection limit for light scattering of conventional flow cytometers is typically of the order of 300-500 nm. We can distinguish the signal of NCs ( $d > 500$  nm) from the background in fluorescence, and forward and side light scattering detector. The forward (FS) and side scattering (SS) and fluorescence intensity of NCs samples were measured with a

Guava® easyCyte BG HT flow cytometer (Millipore®), at a constant flow rate of 0.12 µL/s, using a blue laser emitting at 488 nm and a green laser emitting at 532 nm as excitation sources. Background measurements in PBS buffer were performed before each measurement series. FS and SS signals were recorded to gather information of the NC concentration and dispersion. Fluorescence and SS signals were recorded to gather information of the fluorescently labeled encapsulated cargo (BSA or rtPA).

The number of proteins per NC was estimated using the following expression:

$$\frac{\text{Cargo}}{\text{NC}} = \frac{\text{mass of cargo in purified NC/mL}}{\text{Number of NC/mL}} \times \frac{\text{Avogadro's number}}{\text{MW}}$$

### 6.2.2.3. Quantification of mass of protein

Once the quantification of protein was calculated, the sample was lyophilized and the resulting dust was weighted to calculate the amount of protein (mg) per mg of sample. This procedure was carried out with NC@rtPA and NC@rtPA without gelatin.

### 6.2.3. Minimum information reported in bio-nano experimental literature

Minimum information reported in bio-nano experimental literature (MIRIBEL) consists of the categorization of nanosystems into three

sections: material characterization, biological characterization and details of experimental protocols. We performed this checklist with the aim of enhancing the standardization and adopt a reporting standard to enhance the quality and reuse of published research<sup>241</sup>.

### 6.3. *In vitro* rtPA activity

#### 6.3.1. Amidolytic activity

The enzymatic activity, amidolytic activity, of rtPA encapsulated in cores and NCs were investigated by a chromogenic-based assay: a chromogenic substrate (MW = 658.9 g/mol, #T2943, Sigma-Aldrich). When rtPA reacts with the chromogenic substrate, a proteolytic reaction occurs releasing p-nitroaniline (pNA). The free pNA was determined by absorbance at 405 nm. Due to the low MW of the substrate, it can pass through the pores of both the nanocores and the semipermeable LbL shell, allowing us to know if rtPA inside them remained active (Figure 31).

To perform this assay, the same amount of rtPA (100 IU) in the samples was incubated with 0.12 mg of chromogenic substrate **(following the manufacturer's instructions)**. After 72 h the samples were read at 405 nm.



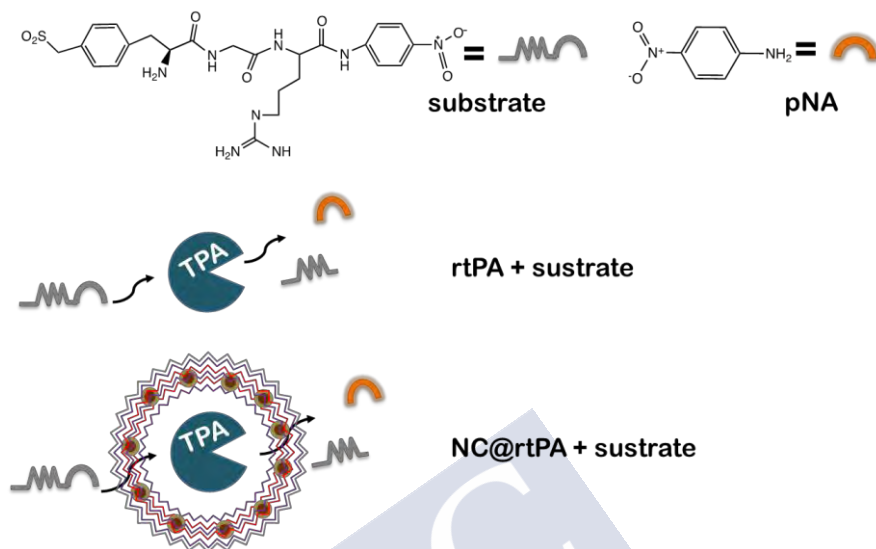


Figure 31. Schematic representation of the experimental setup of the chromogenic substrate with the “free” rtPA and the NC@rtPA. Self-created image.

### 6.3.2. Plasminogen activator inhibitor assay

PAI-1 is the main inhibitor of the rtPA in the blood stream responsible for the short half-life of the rtPA<sup>242</sup>. When encapsulating rtPA in NCs, the half-life should be increased. To confirm it, an assay with the chromogenic substrate and PAI-1 (MW = 43 kDa, #A8111, Sigma-Aldrich) was performed. Conversely, to what happens with the chromogenic substrate, PAI-1 has a high MW that does not allow it to cross the shell of the NCs, enabling the study of the rtPA protection against its main inhibitor (Figure 32).

Samples containing 100 IU of rtPA were incubated with 100 IU of PAI-1. They were allowed to react during 30 min. After, 0.12 mg of substrate was added to the samples. Absorbance at 405 nm was measured at 48 hours.

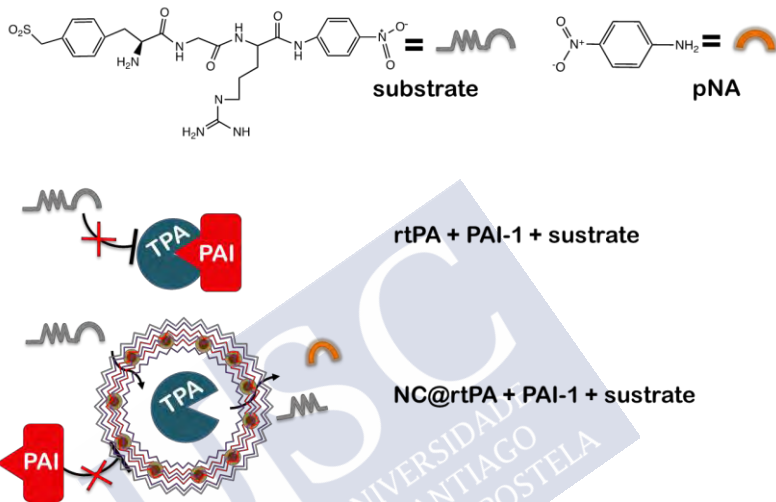


Figure 32. Schematic representation experimental setup of the chromogenic substrate with the "free" rtPA and the NC@rtPA in the presence of PAI-1. Self-created image.

### 6.3.3. Sensolyte®

We used the fluorogenic-based assay Sensolyte® (Sensolyte® AMC tPA Activity Assay Kit from Anaspec, #AS-72160) to measure rtPA amidolytic activity in some samples. We use this assay following the manufacturer's instructions.

## 6.3.4. Fibrinolytic activity: clot assay

The study of the fibrinolytic activity of the rtPA free and encapsulated was carried out in rat clots. Clots were artificially pre-formed in 96-well plates after drawing blood from rats; we added 75  $\mu\text{L}$  of freshly extracted blood to each well. After 1 h to allow clotting, we added the different samples (Figure 33). We performed a calibration curve by adding increasing concentrations of free rtPA (100  $\mu\text{L}$ , 0-100  $\mu\text{g}/\text{mL}$  rtPA) to the clots. After 1 h incubation, the SN was extracted and the absorbance, at 540 nm, was measured.

When we added NCs we used NC@rtPA with 1  $\mu\text{g}/\text{mL}$  rtPA, and the same number of NC@BSA as NC@rtPA.

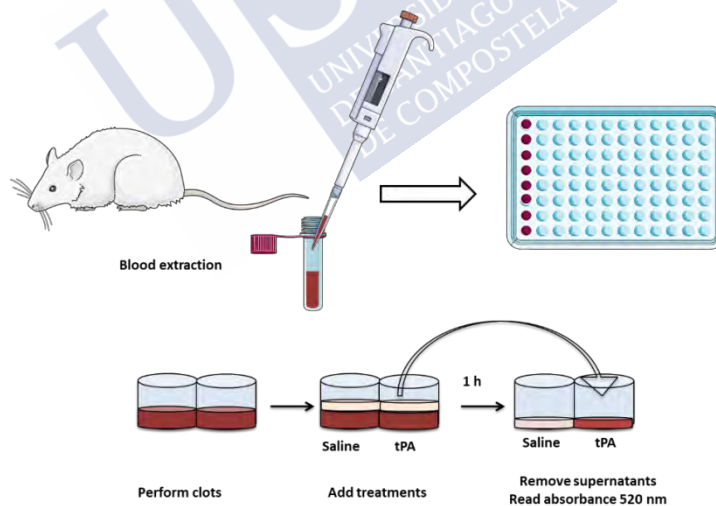


Figure 33. Schematic representation of the experimental setup. Self-created image (using elements with Creative Common license).

#### 6.4. *In vitro* release

US was used to release rtPA from the cavity of NCs. To apply the US, we used a transcranial Doppler and we selected the parameters that have been confirmed safe in rodent models<sup>243</sup> and are in the range of parameters used in clinical transcranial Doppler sonography<sup>244</sup> (0.72 W/cm<sup>2</sup>, 2 MHz, 15- or 120-min). After the application of US, the samples were centrifuged and the SN and the PT were subjected to different assays.

All US experiments were performed in Eppendorf tubes built in polypropylene; this material is transparent to US. An ultrasound gel (Transonic Gel®) was applied to properly transmit the US waves<sup>245</sup> (Figure 34).

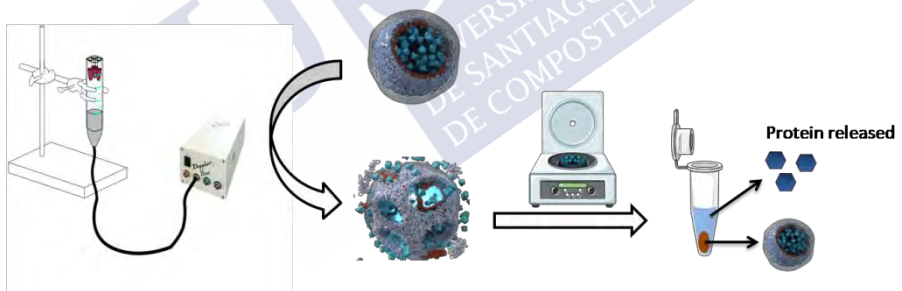


Figure 34. Schematic representation of the US application *in vitro* and the sample processing. Self-created image (using elements with Creative Common license).

### 6.4.1. Scanning Electron Microscopy

A Phillips CM-12 and a FESEM Ultra Plus electronic microscope operating at 3.0 kV were used to study if any change in the morphology of the NCs occurred after applying US. We prepared the SEM samples by evaporating a drop of the different samples on a silicon wafer.

### 6.4.2. Analysis of changes in fluorescence

The quantification of US-triggered release of proteins (BSA and rtPA) from the cavity of NCs was first indirectly estimated from fluorescence measurements: relative fluorescence of the SN (US-release) with respect to the fluorescence of the precipitated product (cargo non-released).

### 6.4.3. Analysis of changes in flow cytometer

Flow cytometry measurements were performed to characterize NCs dispersion and fluorescence after US treatment. The FS and SS and fluorescence intensity of NCs samples and the SN with and without US treatment were measured with a Guava® easyCyte BG HT flow cytometer (Millipore®), at a constant flow rate of 0.12  $\mu\text{L/s}$ , using a blue laser emitting at 488 nm and a green laser emitting at 532 nm as excitation sources. FS and SS signals were recorded to gather information of NCs concentration and

dispersion. Fluorescence and SS signals were recorded to gather information of the fluorescently labeled encapsulated protein.

#### 6.4.4. Analysis of changes in rtPA activity

##### 6.4.4.1. Amidolytic activity

We used the SensoLyte® assay to measure the fluorescence in the SN and in the PT of the samples before and after apply US. We centrifuged the samples because, as it was explained before, the MW of the substrate is so low that it has the capability to cross the LbL wall, what does not allow us to differentiate between the rtPA that is inside NCs@rtPA or outside released from the cavity of NCs@rtPA).

##### 6.4.4.2. Fibrinolytic activity

The clot assay explained at Section 6.3.3 was performed after applying US to the different NC. To perform this assay, we follow the same protocol, also adding the NC@rtPA with and without US, and the SN and PT after the US application.

Please, note that the US application was not done directly on the clots. US was applied to the NCs in Eppendorf tubes and, afterwards transferred to the 96-well plate containing the pre-formed clots.

### 6.5. Inductively coupled plasma mass spectrometry

ICP-MS was performed using an ICP-MS Agilent 7700x. This analysis was used for knowing the different metal concentration in the ioNPs. In this case, prior to the analysis, ioNPs were digested with aqua regia for 2 hours. Then the samples were diluted additionally by a factor of 10 using a low matrix consisting of 2 wt % HCl.

### 6.6. Magnetic resonance protocol

MRI studies were conducted on a 9.4 T horizontal bore magnet (BrukerBioSpin, Ettlingen, Germany) with 12 cm wide actively shielded gradient coils (440 mT/m) (Figure 35).



Figure 35. 9.4 T magnetic resonance.

### 6.6.1. Nanocapsules relaxivity

1.6 % agar phantoms were used as templates to study the ioNPs as a contrast agent with a range from 0.21 to 0.1 mM of Fe. T2-weighted images were acquired using a multi-slice multi-echo sequence (MSME) with 10.44 ms echo time, 3 s repetition time, 16 echoes with 10.4ms echo spacing, 50KHz spectral bandwidth, flip angle (FA) = 110°, 14 slices of 1 mm, 1 average, field of view (FOV) of 75 × 75 mm<sup>2</sup> (with saturation bands to suppress signal outside this FOV), a matrix size of 256×256 (in-plane resolution of **293µm/pixel×293µm/pixel**) and implemented without fat suppression option. T2\*-weighted images were acquired using a MGE sequence with the following echo time; 11.32, 22.64, 33.96, 45.28, 56.6, 67.92, 79.24, 90.56, 101.88, 113.2, 124.52, 135.84, 147.16, 158.48, 169.8 and 181.12 ms.

### 6.7. Statistical analysis

All data are presented as the mean and standard deviation (SD) of the mean (mean ± SD). Data was first examined to assess distribution using the D'Agostino-Pearson omnibus normality test. **Student's** *t*-test was used to test the differences between two groups. Statistical significance was set at  $P < 0.05$ . The statistical analysis was conducted using GraphPad Prism 5.01.



## 7. Section II: *In vivo* studies of rtPA nanocapsules

Once the osnosensitive NCs loaded with rtPA were characterized the drug release determined by *in vitro* assays previously describes, the *in vivo* analysis was performed.

### 7.1. Animal management and study approval

All animals were proceeded from the animalarium of the Universidad de Santiago de Compostela. To perform the studies two different species were used depending on the experiment.

- Rats

Sprague-Dawley rats (250 to 300 g, Harlan Laboratories, Barcelona, Spain) were used to extract blood to perform *in vitro* clots (Section 6.3.4).

- Mice

Swiss male mice (Harlan Laboratories, Barcelona, Spain) with a weight between 25 to 30 g were used.

Both rats and mice were kept in separate rooms both under controlled conditions of temperature ( $22\text{ }^{\circ}\text{C}\pm 1^{\circ}\text{C}$ ) and humidity ( $60\text{ }\%\pm 5\text{ }\%$ ) with a 12/12 h light/dark cycle for a week prior to

surgery and up to 7 days after surgery. They had access to food and water *ad libitum*.

All the procedures were performed under anesthesia. Anesthesia was induced by the inhalation of 5 % sevoflurane in a nitrous oxide/oxygen mixture (70/30). Rectal temperature was monitored and maintained at  $37\text{ }^{\circ}\text{C}\pm 0.5\text{ }^{\circ}\text{C}$  by using a feedback-controlled heating system. At the end of the procedures, mice were sacrificed under deep anesthesia (8 % sevoflurane).

Experimental protocols and animal handling were approved by the chief of the *Servicio provincial de ganadería del departamento territorial da consellería de medio Rural e do Mar de la provincia de A Coruña* being the main responsible Dr. Francisco Campos Pérez. The animal experiments were conducted under the procedure number: 15010/2019/004 according to the Spanish and EU rules (86/609/CEE, 2003/65/CE, 2010/63/EU, RD 1201/2005 AND RD 53/2013).

All the procedures were carried out in the Health Research Institute of Santiago de Compostela (IDIS), with the registration number: ES1507802928[01].

## 7.2. Ultrasound safety *in vivo*

First of all, to evaluate the safety of US on brain, we assessed BBB integrity by the Evans blue (EB) technique. This technique is based on the ability of the EB to bind to the serum albumin immediately.

The extravasations of the albumin to the cerebral parenchyma are correlated with the BBB disruption<sup>246, 247</sup>. The reason of conducting this study is because BBB disruption is related with the US application<sup>248</sup>.

To perform this study, EB was injected at 4 mg/kg in 4 experimental groups (n=4):

- Healthy mice.
- Healthy mice + US.
- Ischemic mice.
- Ischemic mice + US.

In healthy animals, EB was injected previously to the US application. In ischemic groups, EB was injected 30 min after the thrombin injection, and just after US was applied (Figure 36). The ischemia was performed following the protocol explained at Section 7.7.1.

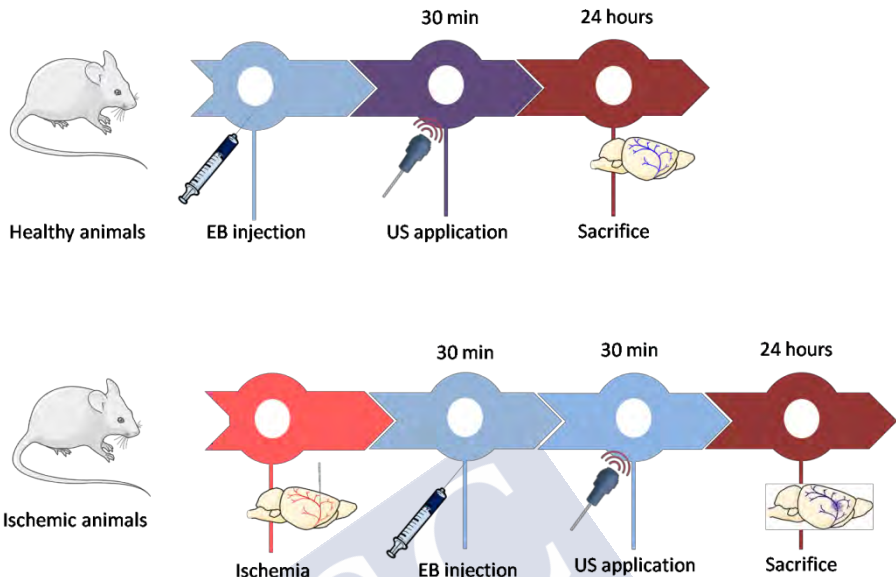


Figure 36. Protocol used for the study of the EB extravasation after the US application. Self-created image (using elements with Creative Common license).

Mice were euthanized 24h after the EB injection. Brains were removed, divided into ipsilateral and contralateral hemispheres, and weighted. Hemispheres were frozen immediately in liquid nitrogen and stored at  $-80^{\circ}\text{C}$  before further analysis.

A calibration curve with different concentrations of EB was performed ( $0-64\ \mu\text{g/mL}$ ). Brain samples were put in the stove at  $55^{\circ}\text{C}$  in 1 ml of N-metilformamide during 48 h. Then, they were centrifuged (9,000 rcf, 20 min) and the absorbance of the SN was measured with a plate reader (630 nm). Extravasated dye content was normalized to the weight of the brain.

### 7.3. Nanocapsules safety *in vivo*

In order to study whether NCs provoke any damage in the brain and hepatic or renal failure, Swiss mice (n=3) were treated with NCs. We performed MRI analysis and blood extractions before the administration and 24 h, 3 days and 7 days after (Figure 37). In the case of MRI study, both T2-weighted sequence and T2\*-weighted sequence were analyzed to search ischemic or hemorrhagic damages respectively.

Furthermore, three standard toxicity markers were evaluated after i.v. administration of NC@rtPA (1 mg/kg rtPA dose, bolus): GOT and glutamate pyruvate transaminase (GPT) levels as hepatotoxicity markers, and creatinine levels as nephrotoxicity marker. These markers are widely used to assess toxicity after administration of nanomaterials in rodent models, being the liver and kidneys the most likely recipients of the NPs after i.v. administration<sup>249</sup>. Briefly, blood extractions (32  $\mu$ L) were carried out from the tail vein before (basal level) and after administration of the NC@rtPA (24 h, 3 days and 7 days). The analysis was **conducted with Reflotron®plus (Roche) by adding 32  $\mu$ L of blood sample to reactive strips for GOT (10745120202, Roche), GPT (10745138202, Roche) and creatinine (10886874202, Roche) following manufacturer's instructions.**

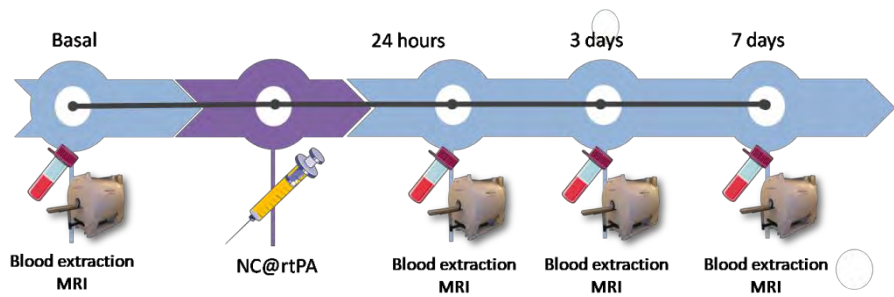


Figure 37. Protocol used for the study of the security of NCs administration. Self-created image (using elements with Creative Common license).

#### 7.4. *In vivo* release

Swiss mice were used as animal model to investigate the *in vivo* performance of the NC@rtPA for US-controlled release of rtPA. The study of the *in vivo* release was carried out using two different protocols as it is indicated below.

In all cases, 0.2 mL of sample was injected (bolus or bolus + infusion) in the femoral vein. Blood extractions (0.2 mL) were done through a cannula inserted in the carotid artery. US was continuously applied (40 min) in the abdominal region, as schematically depicted in Figure 38. Blood samples were collected in a microtainer BD (Microtainer K2E Tubes. Ref: 365975, Franklin Lakes, NJ) and centrifuged at 5,000 rcf, 4°C during 7 min. The plasma obtained was kept at -80°C until the measurement. To measure rtPA plasmatic activity in the extracted samples, we used the SensoLyte® kit following **the manufacturer's instructions**.

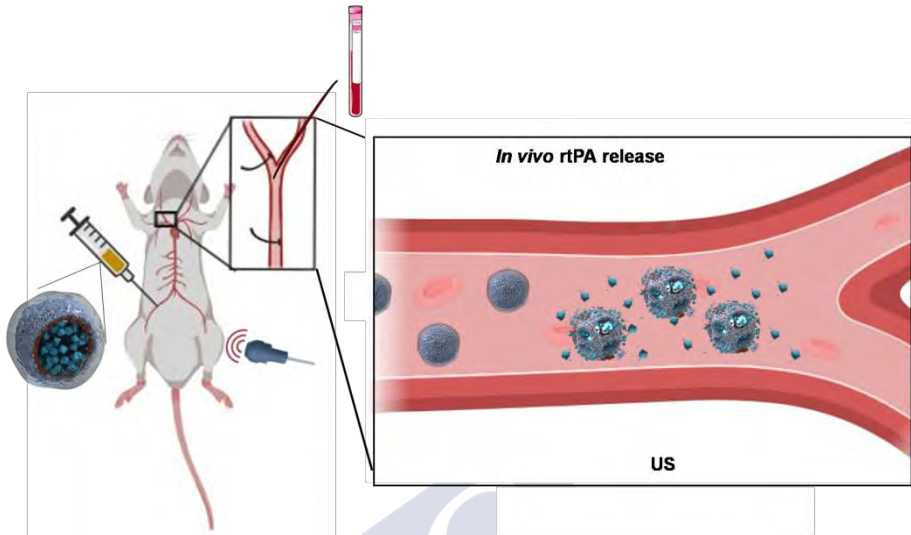


Figure 38. Schematic representation of NC@rtPA in the femoral vein, US application in the abdominal region and extraction from the carotid to study the release *in vivo*. Self-created image (using elements with Creative Common license).

The first study was carried out with five experimental groups (n=3) and all the treatments were administered in ~200  $\mu$ L:

- Vehicle.
- rtPA (1 mg/kg) bolus.
- rtPA 10 mg/kg: 10 % bolus + 90 % infusion. This rtPA dose is commonly used in preclinical mouse models and as thrombolytic treatment in the clinic (0.9-1 mg/kg, 10 % bolus + 90 % infusion). In preclinical mouse models, the 10-fold rtPA dose is motivated by the characteristics of the

fibrinolytic system in rodents, which is known to be about 10 times less sensitive to rtPA than in humans.

- NCs@rtPA (1mg/kg) bolus.
- NCs@rtPA (1mg/kg bolus) + US.

Blood samples were taken prior to administering the treatments (basal) and 5, 20 and 40 min after the administration (Figure 39).

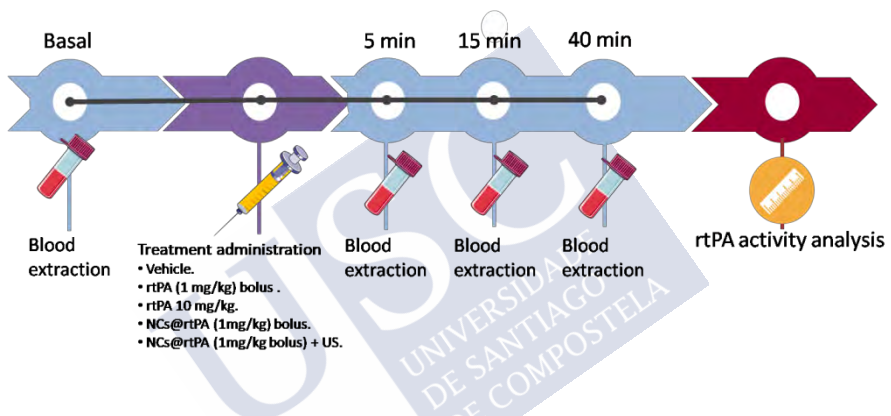


Figure 39. Protocol used for the study of the rtPA release *in vivo*. Blood extractions were taken at basal, 5, 15, and 40 min after the treatment administration. Self-created image (using elements with Creative Common license).

The second study was carried out in eight experimental groups (n=3) and all the treatments were administered in ~200  $\mu$ L of treatment:

- Vehicle.
- Vehicle + US.
- rtPA (1 mg/kg) bolus.



- rtPA (1 mg/kg) bolus + US.
- NCs@rtPA (1 mg/kg) bolus.
- NCs@rtPA (1 mg/kg bolus) + US.
- NCs@rtPA without gelatin (1 mg/kg) bolus.
- NCs@rtPA without gelatin (1 mg/kg bolus) + US.

Blood samples were taken prior to administering the treatments (basal) and 1, 5, 20 and 40 min after the administration (Figure 40).

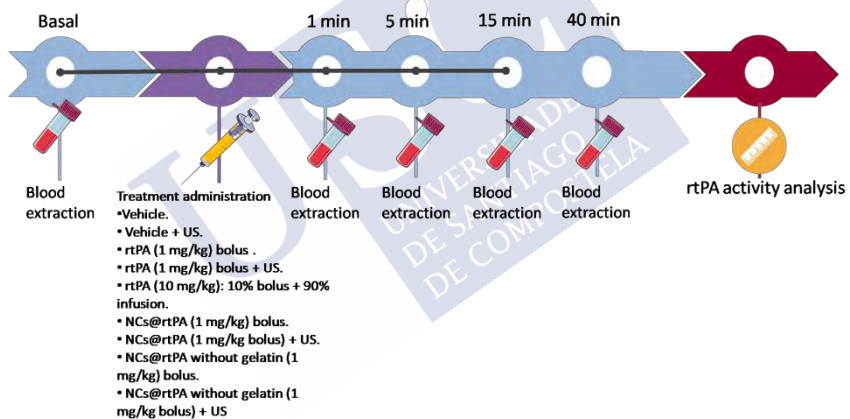


Figure 40. Protocol used for the study of the rtPA release *in vivo*. Blood extractions were taken at basal, 1, 5, 15, and 40 min after the treatment administration. Self-created image (using elements with Creative Common license).

After blood sampling (40 min after treatments administration), the catheters were removed, and the animals were sacrificed and perfused for further ICP-MS organs (brain, heart, liver, lungs, spleen, and kidneys) analysis, described in Section 7.8.

## 7.5. Therapeutic effect

In order to evaluate the therapeutic effect properties of the different NCs treatments in an animal model of ischemic stroke, 8 groups were studied (n=5-9):

- Vehicle.
- Vehicle + US.
- rtPA (1 mg/kg) bolus .
- rtPA (1 mg/kg) bolus + US.
- rtPA (10 mg/kg): 10 % bolus + 90 % infusion
- NCs@rtPA (1 mg/kg) bolus.
- NCs@rtPA (1 mg/kg bolus) + US.
- NCs@rtPA without gelatin (1 mg/kg) bolus.
- NCs@rtPA without gelatin (1 mg/kg bolus) + US.

Treatments were administered 30 min after the thrombin injection in the MCA (30 min after occlusion). The reperfusion was recorded by measuring the CBF using a Doppler during all the ischemia surgery and the treatment administration (90 min in total). Infarct volume and HT was determined 1, 3 and 7 days after ischemia through the T2-weighted and T2\*-weighted sequences respectively. Finally, after the last MRI animals were transcardially perfused, their organs (brain, heart, liver, lungs, spleen, and kidneys) were stored at -80°C for further ICP-MS analysis. Some

animals were sacrificed at 24 h to perform histological analysis of the brain (Figure 41).

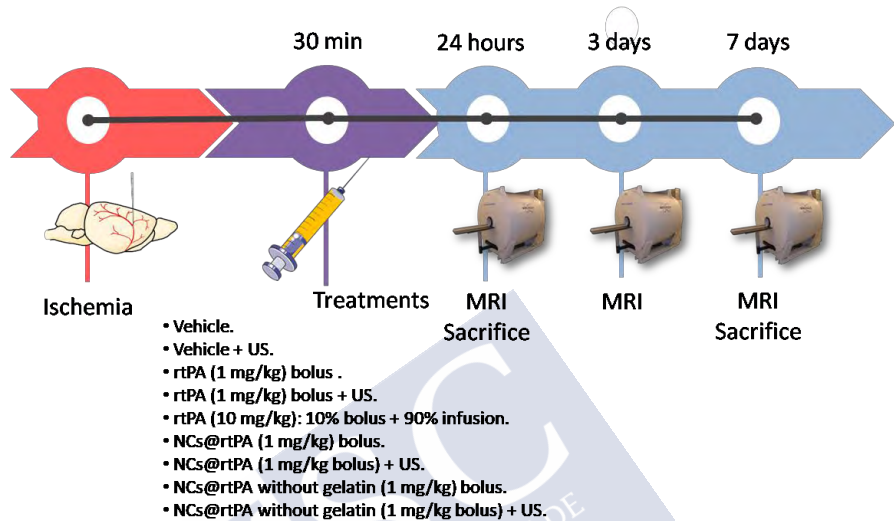


Figure 41. Protocol used for the study of the therapeutic effect of NCs administration. Self-created image (using elements with Creative Common license).

## 7.6. Hematoxylin and eosin staining

The hematoxylin and eosin staining used to evaluate the hemorrhagic lesions was performed by the service of Anatomía Patológica of the Hospital Clínico Universitario de Santiago de Compostela.

## 7.7. Animal procedures

### 7.7.1. Cerebral ischemia animal model

Thromboembolic stroke model was induced by injection in the MCA of mice as originally described Orset et al<sup>74</sup> (Figure 42). Mice were placed in a stereotaxic frame, the skin between the right ear and eye was cut, the temporal muscle retracted and the temporal and parietal bones exposed. A small craniotomy was performed over the artery bifurcation, the meninges were cut using a 25 G needle (BD Microlance, Ref. 300600) and the MCA was exposed.

A micropipette (tip size: 20-40  $\mu\text{m}$ ), made with hematologic glass capillaries (World Precision Instruments, Inc. USA) using a puller (Sutter Instruments), was pneumatically filled with 1.5  $\mu\text{L}$  of 1 U/ $\mu\text{L}$  thrombin (Murine Thrombin 0.05 mg MIIA. Stago-BNL). **The micropipette was placed in a micromanipulator and 1  $\mu\text{L}$  of thrombin solution was injected into the lumen of the artery bifurcation to induce the formation of a clot.** The micropipette was removed 15 min later, when the clot had stabilized.

CBF was monitored with a Periflux 5000 laser Doppler perfusion monitor (Perimed AB, Järfälla, Sweden) by placing the Doppler probe (MT B500-OL240, Straight Microtip, Perimed) in the parietal territory of the MCA. Basal CBF and throughout the experiment was measured.

Artery occlusion was considered successful when the CBF downfall more than 60 % relative to the basal.

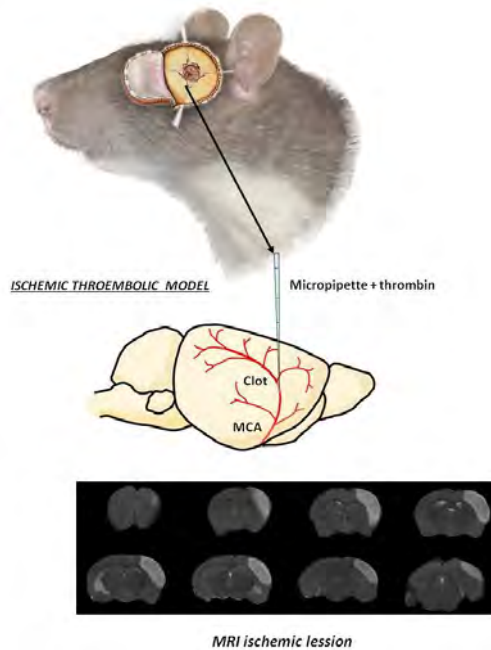


Figure 42. Schematic representation of the cerebral ischemia animal model. Self-created image (using elements with Creative Common license).

## 7.7.2. Treatment administration

### 7.7.2.1. Intravenous administration

Treatments were administered i.v. through the femoral and in the tail vein.

Animals treated with a femoral administration were intravenously injected into the right femoral vein. After anesthetizing the animals, 0.5 cm incision was made on the right paw, subcutaneous fat was cut out, and the femoral vein was exposed. A 30g needle

was used for every treatment administration; the puncture is rapidly closed to preventing bleeding.

In the animals treated with a tail administration a small incision was made in the animal's tail. The skin was cut out, and the tail vein was exposed. A 30 G needle (BD Microlance, Ref. 4656300) was used for every treatment administration; the puncture is rapidly closed to prevent bleeding.

In the animals that the treatment was administered as perfusion, the 30 G needle was put in a catheter (polythene tube, 0.28 mm internal diameter, 0.61 mm outside diameter, Smiths) and we controlled the rate of injection using an injection pump.

#### 7.7.2.2. Intraparenchymal injection

For intraparenchymal injection, mice were placed in a stereotaxic frame (Stoelting Co., Wood Dale, IL, USA) under sevoflurane anesthesia. A 1-cm-long midline incision was made in the scalp. Two small cranial burr holes were drilled through the skull, one on the right hemisphere and other on the left, for the subsequently injection of NCs@rtPA and saline, respectively. A Hamilton syringe (Hamilton, Reno, NV, USA; 10  $\mu\text{L}$ ) was filled with 3.0  $\mu\text{L}$  of NCs@rtPA or vehicle (saline). The syringe was mounted onto the injection pump and the needle was slowly inserted into brain to a depth of 3.25 mm below the surface of the skull. A volume of 2.0  $\mu\text{L}$  of NCs or vehicle was injected at a rate of 0.5  $\mu\text{L}/\text{min}$  over 4 min. The needle was left in place for 5 min and then removed

slowly at a rate of 1 mm/min. The burr hole was filled with bone wax (Ethicon, Somerville, NJ, USA), and the scalp incision was closed and moved to the MRI for brain scan.

### 7.7.3. Ultrasound application

The selected US application parameters (0.72 W/cm<sup>2</sup>, 2 MHz) have been confirmed safe in rodent models<sup>243</sup>, and are in the range of parameters used in clinical transcranial Doppler sonography<sup>244</sup>.

In all the experimental groups, the US was applied during 40 min. In the group of healthy animals to study the US-triggered *in vivo* delivery of rtPA, the US was applied in the abdominal region. To study the US safety in the brain, and the therapeutic effect in an ischemic animal model, the US was applied in the brain.

### 7.7.4. Animal blood extraction

#### 7.7.4.1. Vein extraction

To extract blood from the tail vein animals were anesthetized. A small incision was performed at the apical end, and fresh blood was collected using glass micropipettes (ringcaps with heparin, Ref. 9550532).

#### 7.7.4.2. Carotid extraction

Blood extractions from the carotid were done through a cannula inserted in the common carotid artery (CCA). Briefly, under an operating microscope, the right CCA, external carotid artery (ECA) and ICA were dissected from the connective tissue through a midline neck incision. The ECA and the ICA were separated and tied by 6-0 silk sutures (Mersilk, W529H.). A catheter (polythene tube, 0.28 mm internal diameter, 0.61 mm outside diameter, Smiths) was introduced 0.3 mm (aprox.) in the ECA until the bifurcation of the CCA. The ligature of the ICA and the CCA was removed to allow the blood flow.

#### 7.7.5. Perfusion

Animals were deeply anesthetized and transcardially perfused with 20 mL of PBS 0.1 M pH 7.4 and 50 mL of 4 % formaldehyde. Brains were carefully removed from the skull and they were postfixed by immersion in 4 % formaldehyde overnight. Then, brains were cryoprotected in 30 % sucrose solution in PBS containing a 0.05 % of sodium azide. After 24 h, tissues were frozen with liquid nitrogen and stored at  $-20^{\circ}\text{C}$ . The other organs (heart, liver, lungs, spleen, and kidneys) were removed and stored at  $-20^{\circ}\text{C}$ .



### 7.8. Inductively coupled plasma mass spectrometry

ICP-MS analysis was performed to study the biodistribution after 40 min and 7 days after the administration of the treatments in the animals. In this case Fe was measured in the organs (brain, lungs, heart, spleen, liver and kidneys), because it is the main component of the ioNPs that we incorporated to NCs. We know that the amount of Fe administered was  $\sim 128 \mu\text{g Fe/ animal}$  ( $5.1 \text{ mg/kg}$ ). It is important to note that this dose is much smaller than that used in other investigations, in which  $700 \mu\text{g Fe/animal}$  ( $35 \text{ mg/kg}$ ) could be detected in biodistribution assays<sup>250, 251</sup>.

The organ preparation for ICP-MS and evaluation of the results were done following the methods reported by Talamini et al<sup>252</sup>. Briefly, the samples were weighted ( $m_{\text{organ}}$ ) and entirely digested via the addition of 5 mL of ultra-pure (67 wt %)  $\text{HNO}_3$  (Fisher Chemical) under constant agitation in 50 mL falcon tubes. The digestion took place over 48 h at  $21^\circ\text{C}$  until no organic residuals were left. This liquid solution was then further digested through aqua regia consisting of three parts concentrated ultra pure (35 wt %) HCl (Fisher Chemical) and one part of ultra pure (67 wt %)  $\text{HNO}_3$ . For this final digestion,  $100 \mu\text{L}$  of well mixed sample solution were added to  $300 \mu\text{L}$  of aqua regia and left under agitation for at least 2 h (i.e. the sample was diluted by a factor of 4). In order to introduce these samples in the ICP-MS, they had to be diluted additionally by a factor of 10 using a low matrix consisting of 2 wt % HCl which was adapted to the material. The samples were

measured in the ICP-MS from the University of Santiago de Compostela.

## 7.9. Magnetic resonance protocols

MRI studies were conducted on a 9.4 T horizontal bore magnet (BrukerBioSpin, Ettlingen, Germany) with 12 cm wide actively shielded gradient coils (440 mT/m). Radiofrequency transmission was achieved with a birdcage volume resonator; signal was detected using a two-element arrayed surface coil (RAPID Biomedical, Germany), positioned over the head of the animal, which was fixed with a teeth bar, earplugs and adhesive tape. Respiratory frequency and body temperature were monitored throughout the experiment. Transmission and reception coils were actively decoupled from each other. Gradient-echo pilot scans were performed at the beginning of each imaging session for accurate positioning of the animal inside the magnet bore.

### 7.9.1. T2-weighted sequence

The progression of ischemic lesions and infarct volumes were determined from T2-maps (Figure 43) calculated from T2-weighted images. Ischemic lesion was determined by counting pixels with apparent T2-map values above a threshold in the ipsilateral brain hemisphere.

In healthy mice, the T2-map values of the brain are over 50 ms. In the ipsilateral ischemic hemisphere, hyperintensity on T2-map determined the analysis of the ischemic damage (T2 map values > 60 ms).

T2-weighted images were acquired using a multi-slice multi-echo (MSME) sequence with a 11 ms echo time (TE), 2.8 s repetition time (TR), 12 echoes with 11 ms echo spacing, FA of 180°, 2 averages, 50 KHz spectral bandwidth (SW), 16 slices of 0.5 mm, 19.2 × 19.2 mm<sup>2</sup> FOV with saturation bands to suppress signal outside this FOV, a matrix size of 256 × 256 (isotropic in-plane resolution of 75 μm/pixel × 75 μm/pixel) and implemented without fat suppression option. The acquisition time was 23 min.

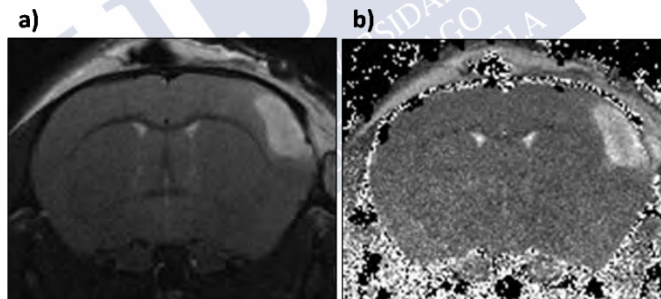


Figure 43. Example of a a) T2-weighted image and b) T2-map to measure the infarct volume with the ImageJ.

### 7.9.2. T2\*-weighted sequence

T2\*-weighted images were acquired using a multi-gradient-echo sequence (MGE) with a 5 ms TE, 1.2 s TR, 8 echoes with 4.5 ms

echo spacing, 100 KHz spectral bandwidth, FA of 20°, 16 slices of 0.55 mm, 2 averages, 19.2 × 19.2 mm<sup>2</sup> FOV with saturation bands to suppress signal outside this FOV, a matrix size of 256 × 256 (isotropic in-plane resolution of 75 μm/pixel × 75 μm/pixel) and implemented with fat suppression option. The acquisition time was 10 min. An example of T2\*-weighted image is represented in Figure 44.

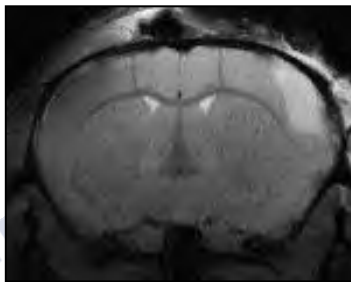


Figure 44. Example of T2\*-weighted image.

### 7.9.3. Quantification of hypo-signals in T2\*-weighted images

The hypo-signals in T2\*-weighted images were quantified by two different methods. We used ImageJ to quantify these signals. In both methods, we perform the quantification in all the groups treated with NCs, in which the hypo-signals appeared, in five animals treated with saline and in five animals treated with rtPA. We used only the MRI performed 24 h after the treatment administration.

On one hand, we selected a small hypo-signal area in the ischemic region using the T2\* maps. Mean grey value is the average gray value within the selection (Figure 45-a). This is the sum of the gray values of all the pixels in the selection divided by the number of pixels. The quantification was performed in a selected area of the ipsilateral hemisphere.

On the other hand, we measured hypo-signals through the area fraction of T2\*-weighted images (Figure 45-b). Using this method we calculate the percentage of pixels in the image or selection that have been highlighted in the ischemic region.

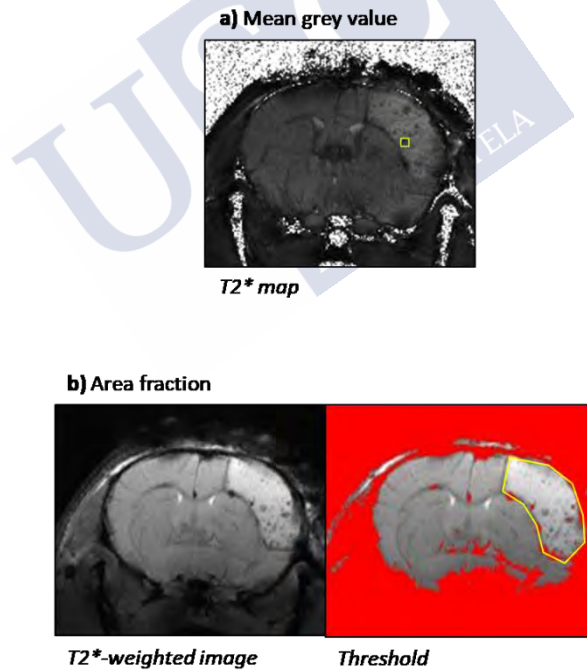


Figure 45. Methods to quantify the hypo-signals in T2\*-weighted images. a) Mean grey value. b) Area fraction.

#### 7.9.4. Data analysis

MRI post-processing was performed using ImageJ software (W. Rasband, NIH, USA) on independent workstation.

#### 7.10. Statistical analysis

All data are presented as the mean and SD of the mean (mean  $\pm$  SD). Data was first examined to assess distribution using the D'Agostino-Pearson omnibus normality test. **Student's** *t*-test was used to test the differences between two groups. One-way or two-way analysis of variance (ANOVA) followed by post-hoc Bonferroni evaluation were used to detect significant differences between groups. Statistical significance was set at  $P < 0.05$ . The statistical analysis was conducted using GraphPad Prism 5.01.

Treatments were specifically assigned to each animal due to experimental limitations in synthesizing the NCs.



Results

---





## 8. Preliminary study

### 8.1. *In vitro* rtPA activity

Initially, we performed the synthesis of rtPA complexed with gelatin and Zn acetate, and later the thrombolytic activity was determined using a commercial kit (amidolytic activity) and by its ability to reduce the weight of clots (fibrinolytic activity) as it is indicated in Material and Methods.

#### 8.1.1. Amidolytic activity

Figure 46 represents the amidolytic activity of the different groups of treatment. The group treated with rtPA is considered as 100 %. Vehicle and vehicle + US did not have activity. There are no differences between rtPA (1.5 mg/mL) and rtPA (1.5 mg/mL) + US. When the activity of the encapsulated rtPA (1.5 mg/mL) was measured, a significant decrease was found compared to rtPA ( $P < 0.001$ ), while the application of the US to the sample results almost complete the recovering of the activity.

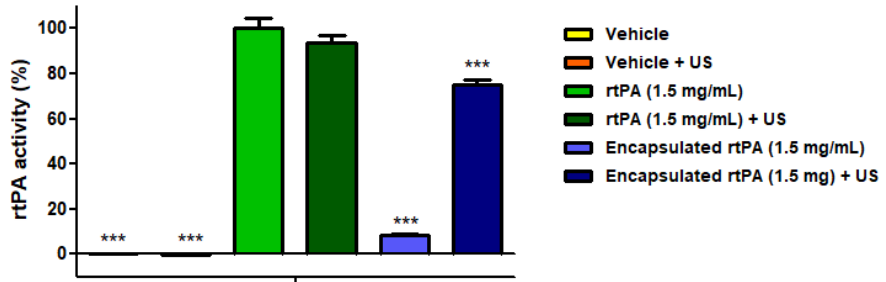


Figure 46. Amidolytic activity determined by Sensolyte<sup>®</sup>. All data represent mean  $\pm$  SD (three independent measurements). In all data statistical significance was assessed by the *t*-test: each sample was compared with Alteplase (\*\*\*) $P$ <0.001).

### 8.1.2. Fibrinolytic activity

In the Figure 47 is showed the percentage of the reduction of the clots *in vitro* assays. The incubation of the clots with the vehicle (saline) or vehicle + US, results in a  $10.7 \pm 6.7$  % and  $13.8 \pm 7.4$  % of reduction of weight respect to the original weight.

However, when rtPA (1.5 mg/mL) or rtPA (1.5 mg/mL) + US were added to the clots, the reduction is much higher ( $42.1 \pm 11.1$  % and  $42.2 \pm 9.9$  % respectively).

The addition of encapsulated rtPA (1.5 mg/mL) to the blood clots caused a reduction of  $21.5 \pm 10.2$  %, similar to the groups treated with the vehicle. In the case of the encapsulated rtPA + US the fibrinolytic activity was recovered, achieving a weight reduction of  $38.9 \pm 12.8$  %.

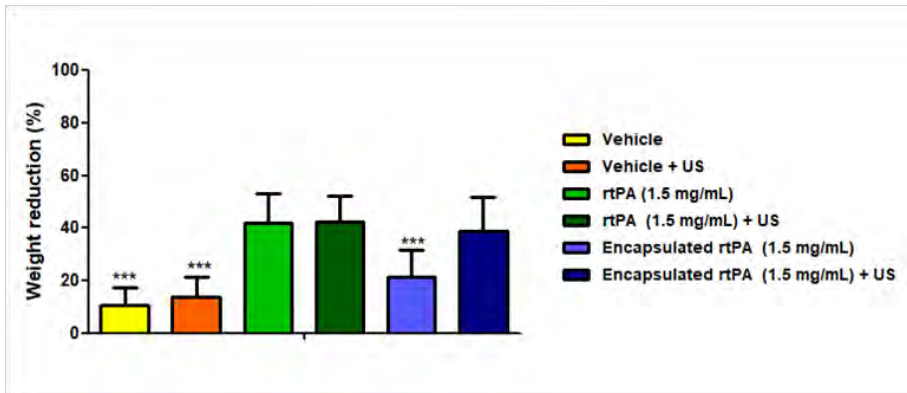


Figure 47. Fibrinolytic activity determined by a reduction in blood clot weight. All data represent mean  $\pm$  SD (fourteen independent measurements). In all data statistical significance was assessed by the *t*-test: each sample was compared with Alteplase (\* $P < 0.05$ ; \*\* $P < 0.01$ ; \*\*\* $P < 0.001$ ).

## 8.2. *In vivo* release

Blood rtPA activity was determined in the four *in vivo* groups tested ( $n = 4$ ), before treatment administration (basal), and 5, 15 and 40 min later. A total of thirty-two animals were used to this study. Thirteen of them were discarded due to problems during the surgery (Figure 48).

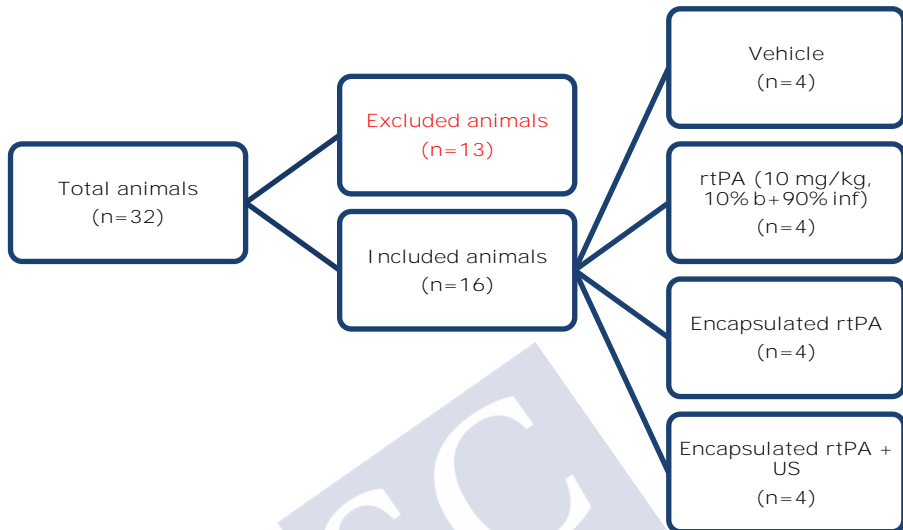


Figure 48. Animals included in the study.

The rtPA activity in the group treated with rtPA (10 mg/kg, 10 % bolus + 90 % infusion) showed an increase in the first minutes followed by a decline in activity over the 40 min. Groups treated with encapsulated rtPA showed that differences between applying or not the US because in both groups an increase of the activity was observed, which reflects that the stability of the rtPA encapsulation observed *in vitro* assays could not be reproduced *in vivo* models (Figure 49).

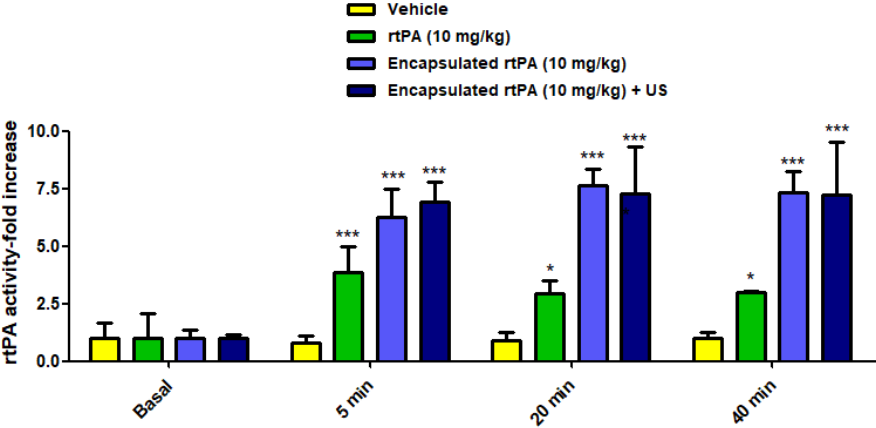
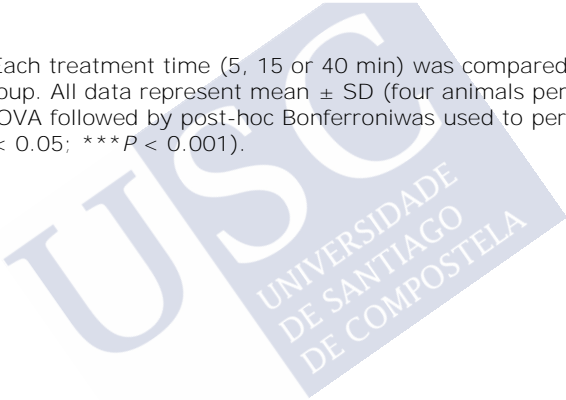


Figure 49. Each treatment time (5, 15 or 40 min) was compared with rtPA levels in the saline group. All data represent mean  $\pm$  SD (four animals per treatment gorup). Two-way ANOVA followed by post-hoc Bonferroniwas used to perform the statistical analysis(\* $P < 0.05$ ; \*\*\* $P < 0.001$ ).



## 9. Section 1: *In vitro* optimization of rtPA nanocapsules.

Previous studies showed that **rtPA** encapsulation done **with gelatin and Zn acetate** complex was estable. Thrombolytic activity of rtPA could be trigger by the use of US. Unfortunately, the successfull encapsulation observed *in vitro* assays, could no be reproduced once administrated these nanocomplexs of rtPA in *in vivo* models. Therefore a new encapsulation protocol for rtPA based on sonosensitive LbL capsule system coated with and without gelatin was tested.

### 9.1. Synthesis and characterization

#### 9.1.1. Protein labeling

Before characterize the LBL encapsulation, dye-labeled protein was performed. Figure 50 illustrates the quantification method used for dye-labeled protein quantification, which is the correlation between the concentration of the protein and its fluorescence. Once the protein is labeled, we perform the Bradford assay to quantify the amount of protein. Although the ratio dye-to-protein was kept constant, 25 dyes/protein, the labeling efficiency is different. In case of BSA-FITC the slope is 5.8, while in case of rtPA-FITC is 1.5. This is due to the difference between the lysine residues in the BSA and rtPA to which fluorophore binds (60 vs 22 respectively).

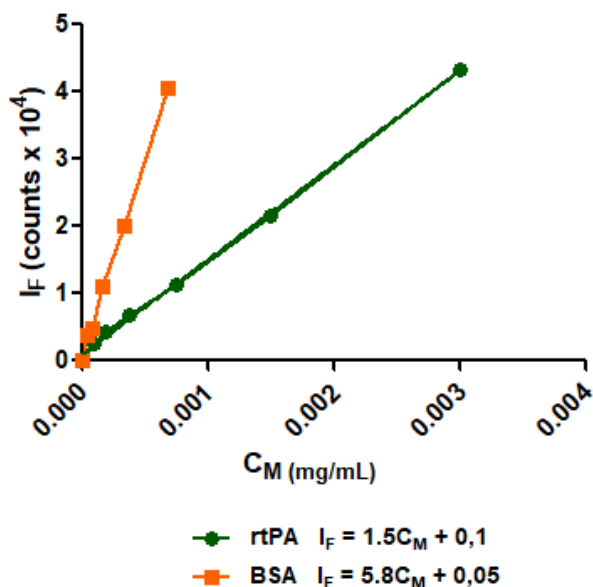


Figure 50. Examples of correlation between concentration  $C_M$  (as determined by the Bradford assay) and fluorescence counts  $I$  ( $\times 10^4$ ). Linear fits in each case were used to calculate unknown concentrations  $C_M$  of rtPA-FITC and BSA-FITC.

### 9.1.2. Structural characterization of iron oxide nanoparticles

As it was indicated in Section 6.1.2 these NCs were also labeled with magnetite ( $\text{Fe}_3\text{O}_4$ ) for subsequently MRI tracking. After the synthesis of the ioNPs (iron oxide nanoparticles), they were characterized through TEM images. The average of the ioNPs core diameter ( $d_{\text{NP}}$ ) was measured with Image J software resulting in  $d_{\text{NP}} = 13.03 \pm 1.08$  nm (Figure 51).

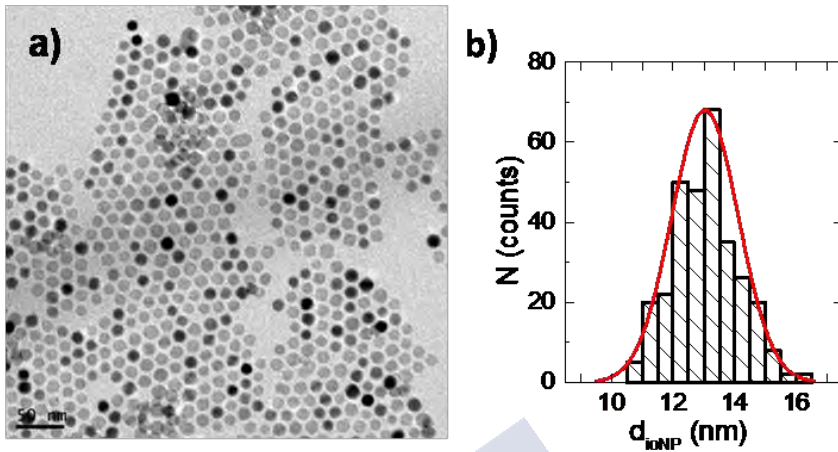


Figure 51. a) TEM micrograph of ioNPs (scale bar is 50 nm). b) Size histogram obtained with ImageJ software after measuring the core diameter of 300 ioNPs.

ICP-MS was used to know the different metal concentrations. The results revealed the following metal concentration: Zn: 0.07  $\mu\text{g/L}$ , Mn: 0.13  $\mu\text{g/L}$  and Fe: 1.21  $\mu\text{g/L}$ . The stoichiometry found was  $\text{Zn}_{0.1}\text{Mn}_{0.2}\text{Fe}_{2.7}\text{O}_4$  and the inorganic concentration (including the oxygen content) was 0.9 g/L.

The ioNPs molar concentration ( $C_{\text{NP}}$ ) was calculated as followed (the organic contribution is not considered). The mass of a single NP ( $m_{\text{NP}}$ ) was determined as the product of the core material density ( $\rho$ ) and the core volume ( $V_{\text{NP}}$ ). Therefore, the molar mass of the ioNPs  $M_{\text{NP}}$  can be calculated by multiplying the  $m_{\text{NP}}$  by the Avogadro's number. Since Fe is the most predominant metal in the core ferrite, the magnetite ( $\text{Fe}_3\text{O}_4$ ) density value ( $5.18 \text{ g/cm}^{-3}$ ) was used for these calculations.



$$m_{NP} = \rho \cdot V_{NP}$$

$M_{NP}$  was  $3.61 \times 10^6$  g/mol.

The volumen of a single ioNP  $V_{NP}$  was calculated using the following expression. The  $d_{NP}$  value used was determined via TEM. The  $V_{NP}$  is equal to  $1.15 \times 10^{-18}$  cm<sup>3</sup>.

$$V_{NP} = \frac{4}{3} \cdot \pi \cdot \left(\frac{d_{NP}}{2}\right)^3$$

Then, the molar  $C_{NP}$  was determined using the following equation resulting in a concentration of  $2.50 \times 10^{-7}$  M (0.25  $\mu$ M).

$$C_{NP} = \frac{M_{NP}}{V}$$

The results showed a hydrodynamic diameter (in number) of  $22.3 \pm 1.7$  nm (polydispersity index, PDI=0.24) and zeta potential value of  $-55.2 \pm 1.7$  mV

### 9.1.3. Nanocapsules as contrast agents

To evaluate whether NCs particles are an appropriate contrast agent, relaxivity was assessed by magnetic resonance in an agar phantom template with increasing concentrations of iron coupled to NCs.

When we represent the iron concentration against the relaxation rate ( $1/T_2$ ), the ioNPs showed a relaxivity  $r_2 = 409.1 \text{ mM}^{-1}\text{s}^{-1}$  (Figure 52).

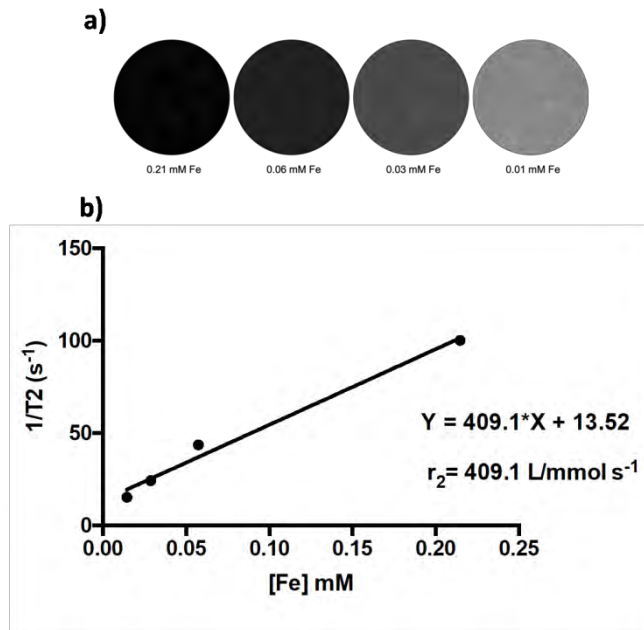


Figure 52. T2-weighted images of an agar phantom template, with crescent concentrations of ioNPs. b) Relaxivity values obtained with T2-weighted image.

Furthermore, we performed an intracerebral injection of the NC@rtPA in the brain to evaluate the contrast provided by these NCs compared to the injection of saline in the tissue.

For this purpose, we injected  $2\mu\text{L}$  of NC@rtPA ( $4.2 \times 10^7$  NCs/mL) in the right hemisphere, and the same volume in the left hemisphere (Figure 53-a). Figure 53-b shows that T2-weighted

signal decreased 64 %, generating a hypointensity area with increased contrast compared to a tissue with the saline injection. Regarding T2\*-weighted signal intensity is decreased by 78 %. NPs concentrated in the injection spot enhance the contrast with the normal brain tissue in both, T2-weighted and T2\*-weighted sequences.

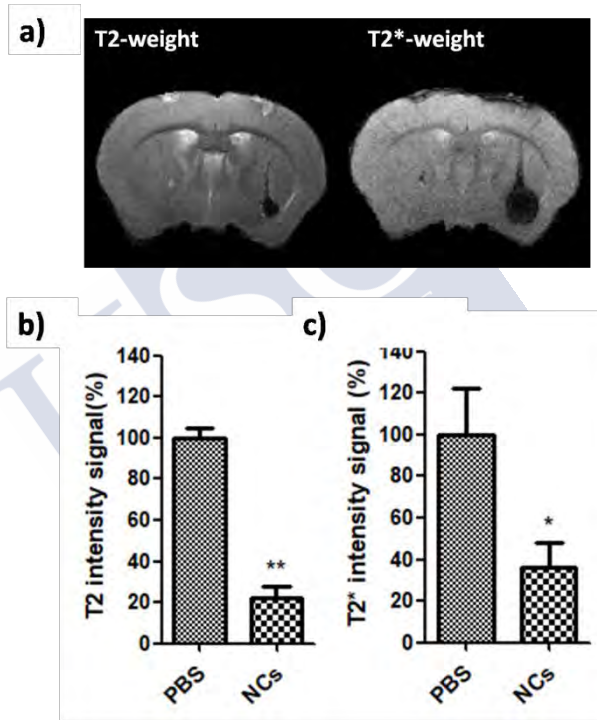


Figure 53. Contrast of NPs in the brain parenchyma. a) T2-weighted image. b) T2\*-weighted image.

#### 9.1.4. Structural characterization of nanocores and nanocapsules

The morphology and mean diameter ( $d_c$ ) of macromolecule-loaded (BSA or rtPA) nanocores were analyzed by SEM after drop casting on silice substrates. Selected examples are shown in Figure 54.

After measuring the diameter of 300 core@BSA using ImageJ the  $d_{c@BSA}$  is  $617 \pm 80$  nm. In the case of core@rtPA the  $d_{c@rtPA}$  is  $651 \pm 76$  nm.

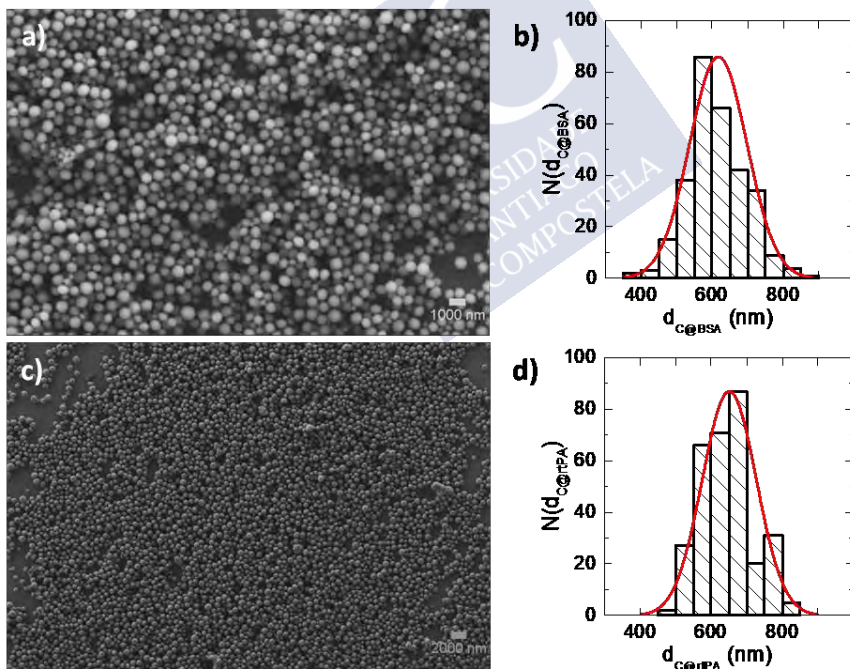


Figure 54. a) Low magnification SEM micrograph of core@BSA (scale bar is 1000 nm). b) Size histogram of core@BSA. c) Low magnification SEM micrograph of core@rtPA (scale bar is 2000 nm). d) Size histogram of core@rtPA. Cores with BSA (core@BSA), cores with rtPA (core@rtPA).

After LbL, the morphology of NC@BSA or NC@rtPA was also analyzed by SEM after drop casting on silice substrates. After measuring the diameter 300 NC@BSA we performed the size histogram that is represented in Figure 55-b, the diameter is  $735 \pm 130$  nm. In the case of NC@rtPA without gelatin, the diameter determined measuring 150 NC was  $549 \pm 88$  nm.

Moreover, Figure 55-e,f shows the SEM images of NC@rtPA with gelatin. Also, in Figure 55-f ioNPs are distinguishable as bright dots in the polymer shell of collapsed NCs.



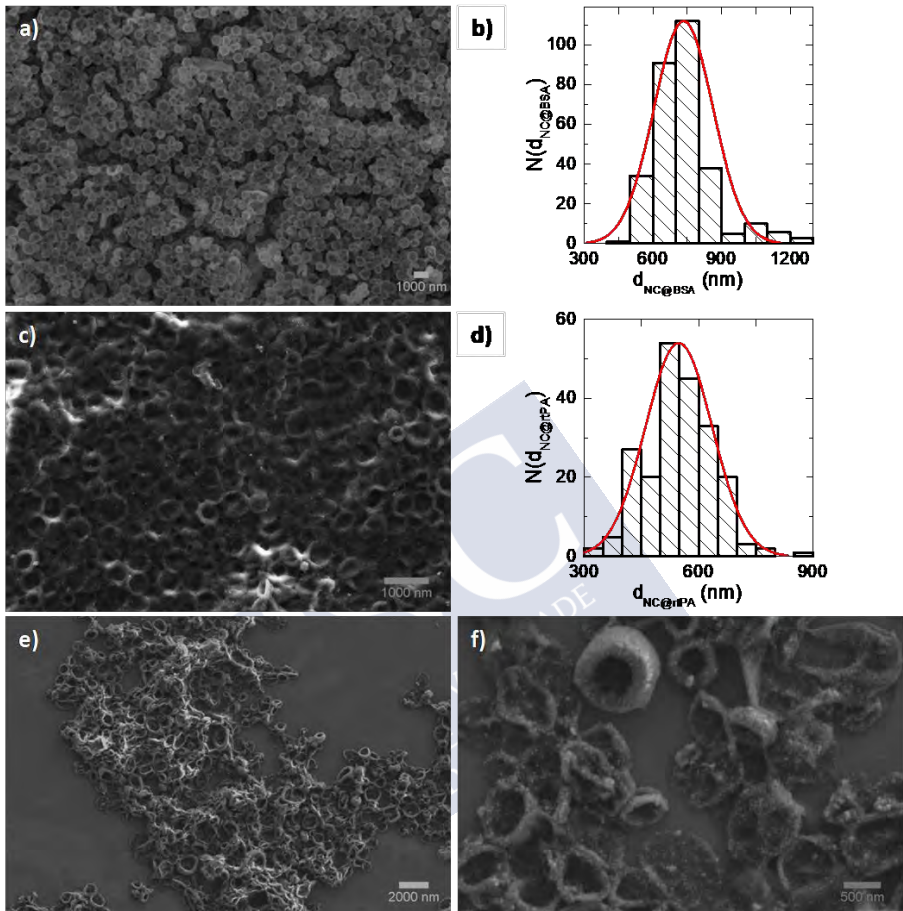


Figure 55. a) Low magnification SEM micrograph of NC@BSA (scale bar is 1000 nm). b) Size histogram of NC@BSA. c) Low magnification SEM micrograph of NC@rtPA without gelatin (scale bar is 1000 nm). d) Size histogram of NC@rtPA without gelatin. e,f) Low and high magnification SEM micrographs of NC@rtPA with gelatin (scale bar is 2000 nm and 500 nm).

DLS was used to determine the hydrodynamic sizes and the zeta potential values of nanocores and NCs. Table 8 and Figure 56

shows the mean average values (three independent measurements) of selected samples.

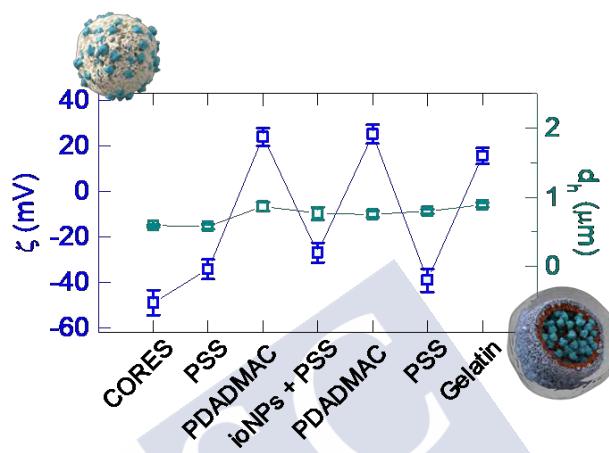


Figure 56. Mean values of zeta-potential (blue colored square symbols) and hydrodynamic diameter (green colored square symbols) evolution after each layer.

Table 8. Hydrodynamic diameter from the intensity ( $d_{H,I}$ ) and number ( $d_H$ ) DLS distributions, and PDI. SD values were calculated from three independent measurements.

Sample	LbL-step	$d_{H,I}$ (nm)	$d_H$ (nm)	PDI	Zeta potential (mV)
NC@rtPA	core-rtPA	648 ± 26	592 ± 17	0.09	-48.9 ± 5.5
	1 <sup>st</sup> PSS	638 ± 34	577 ± 35	0.13	-34.3 ± 4.3
	1 <sup>st</sup> PDADMAC	909 ± 73	869 ± 61	0.30	23.9 ± 3.8
	1 <sup>st</sup> ioNPs/PSS	796 ± 11	765 ± 91	0.28	-26.9 ± 4.4
	2 <sup>nd</sup> PDADMAC	821 ± 77	755 ± 44	0.30	25.2 ± 4.1
	2 <sup>nd</sup> PSS	834 ± 36	799 ± 32	0.18	-39.1 ± 5.1
	gelatin+EDTA	890 ± 34	890 ± 33	0.62	15.6 ± 3.6
NC@BSA	core-BSA	664 ± 9	623 ± 19	0.14	-41.7 ± 2.6
	PSS - 6×(PDADMAC/PSS)	864 ± 38	851 ± 38	0.09	17.3 ± 0.90
	PSS - 6×(PDADMAC/PSS) + EDTA	1119 ± 80	1080 ± 64	0.08	-16.8 ± 0.7

### 9.1.5. Stability of the encapsulation

To establish the robustness of NCs for protein encapsulation and to determine the minimum suitable number of polyelectrolyte bL, we



performed a leaking assay. The potential leaking of model dye-labeled BSA from NCs (NCs@BSA) with 2bL, 4bL and 6bL (shell composition: PSS/PDADMAC - ioNPs/PSS - (PDADMAC/PSS)  $\times 1, \times 3$ , or  $\times 5$ ) was investigated, quantifying the leaking of encapsulated dye-labeled cargo after LbL, both without or after **“dissolving” the CaCO<sub>3</sub>** matrix. The NCs were precipitated and the cargo was quantified in the PT and the SN. As Figure 57 shows the encapsulation was stable unless during one week.



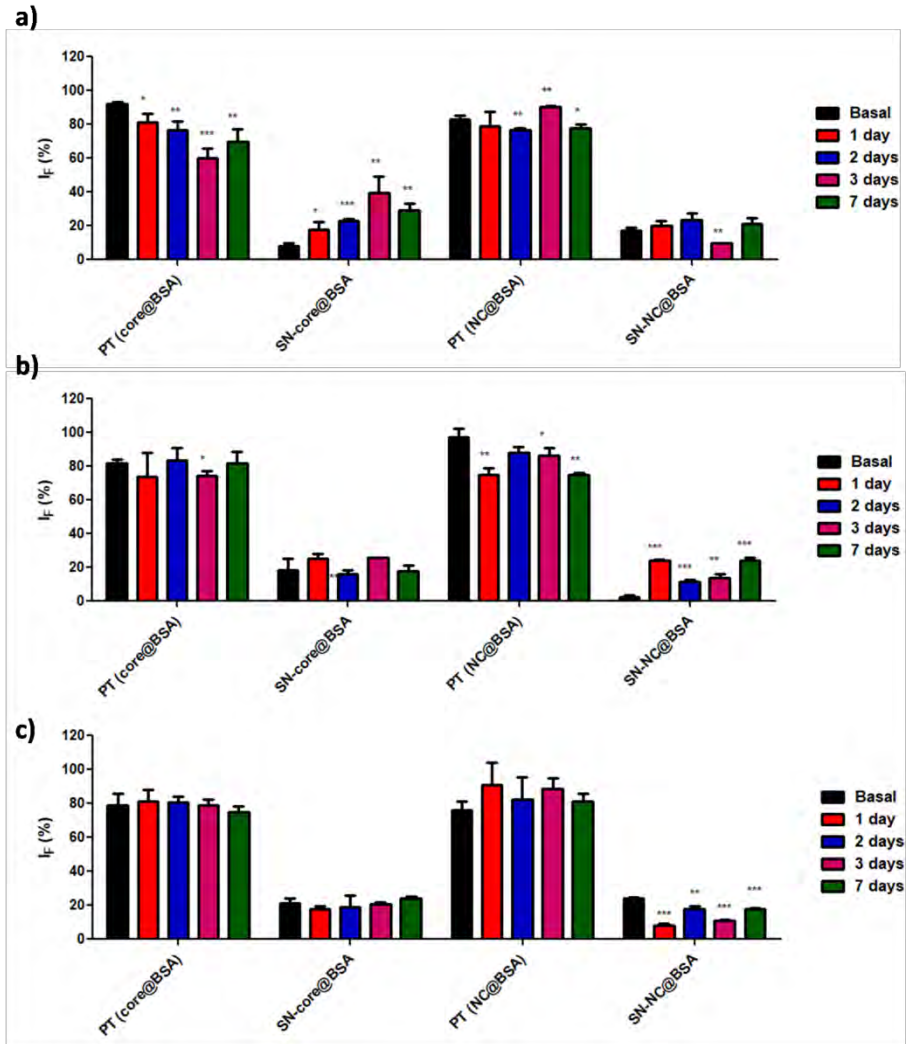


Figure 57. BSA encapsulation stability after LbL in cores (without “dissolving” the  $\text{CaCO}_3$  matrix) or NCs, both systems with increasing bL configurations: a) 2bL, b) 4bL and c) 6bL for one week in PBS. The statistical significance was assessed by the *t*-test. Each time point (1, 2, 3 and 7 days) was compared with the  $I_F$  of the corresponding control (basal) (ns, not significant; \* $P < 0.05$ ; \*\* $P < 0.01$ ; \*\*\* $P < 0.001$ ).

After checking the encapsulation stability in the NC@BSA, we performed the same experiment in NC@rtPA (shell composition: PSS/PDADMAC - ioNPs/PSS - (PDADMAC/PSS) - gelatin). Likewise, 2bL NC@rtPA without and with gelatin only showed residual rtPA leaking after one week, both in cases of dissolving the CaCO<sub>3</sub> matrix. We demonstrated here that two polymer bL (with or without an outermost gelatin layer) were robust enough to prevent cargo leaking from NCs (Figure 58).

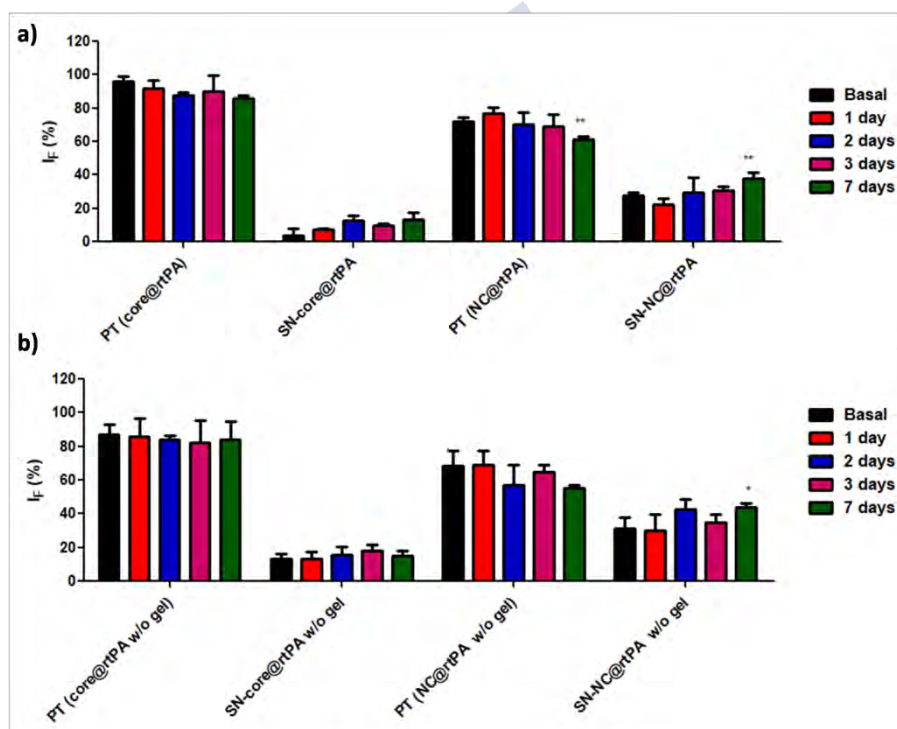


Figure 58. rtPA encapsulation stability after LbL in cores (without “dissolving” the CaCO<sub>3</sub> matrix) or NCs, both systems with and without gelatin: a) 2bL with gelatin, b) 2bL without gelatin for one week in PBS with arginine. Each time point (1, 2, 3 and 7 days) was compared with the  $I_F$  of the corresponding control (basal) (ns, not significant; \* $P < 0.05$ ; \*\* $P < 0.01$ ).

9.1.1. Nanocapsule stability

Nanocapsule stability was also tested by flow cytometry. Results of the NC@rtPA and NC@rtPA without gelatin are shown in Figure 59, confirmed that the stability for at least 8 h after synthesis.

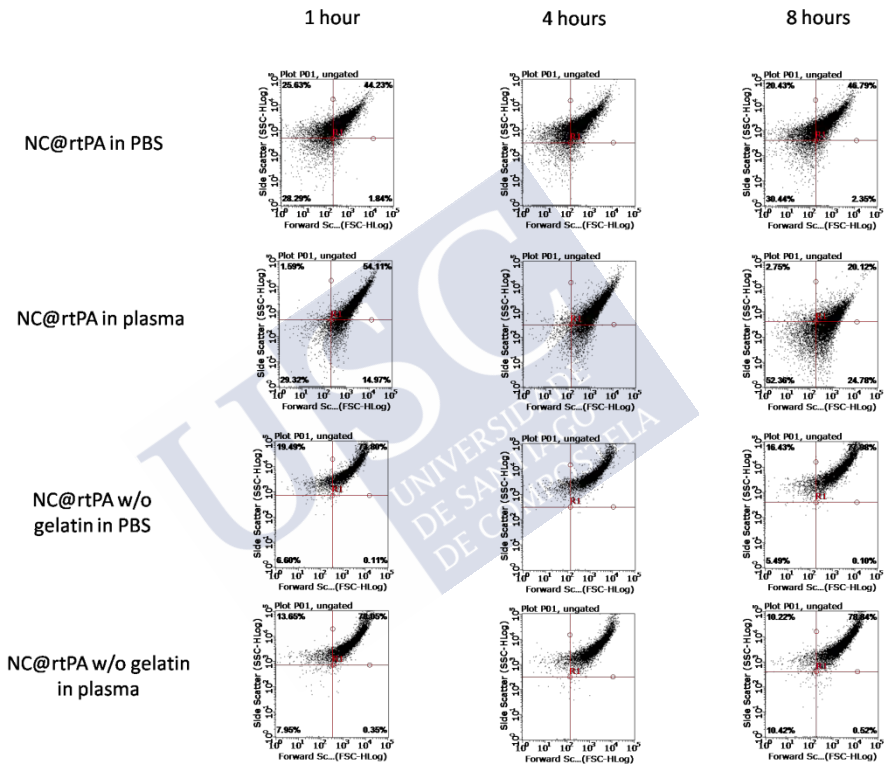


Figure 59. Citometry analysis of the NC@rtPA and NC@rtPA without gelatin in plasma and in PBS at 1, 4 and 8 hours.

### 9.1.2. Protein loading into the nanocapsules

The amount of protein per NCs was calculated using the calibration curve of fluorescence and the cytometer. Using the calibration curve we could know the concentration of the protein, and with the flow cytometer analysis the number of NCs/mL.

Figure 60 shows the variation of the flow cytometer SS signal and the FS in relation to the fluorescently labeled encapsulated molecule (rtPA and BSA). Dispersions of 800 nm NCs were analyzed, generating a distinctive SS signal from the background (PBS buffer). Concentrations between 100 to 1000 NCs/ $\mu$ L for 800 nm NCs were analyzed. The number of events measured in the corresponding NC gate divided by the acquired volume gives the final NC concentration (Table 9).

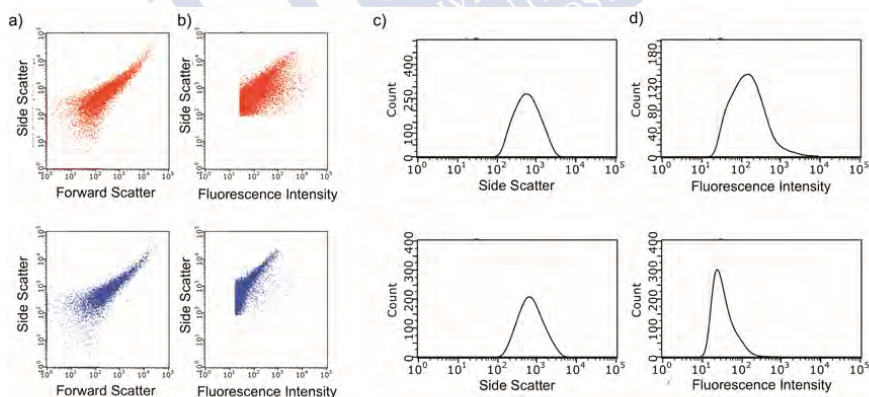


Figure 60. NCs dispersion analysis by flow cytometry. a) Scatter density plots of FS signal versus SS signal for different NCs with diverse cargoes: rTPA (red) and BSA (blue). b) Scatter density plots of SS signal versus FS or NCs with the different cargoes: rTPA (red) and BSA (blue). c) Representative histograms of SS distribution of different NCs samples (rTPA and BSA). d) Representative histograms of MFI from the different channels associated with the encapsulated cargo.

Table 9. Number of macromolecules encapsulated per NCs for different batches of NCs.

Sample	NC/mL	$\mu\text{g rtPA/mL}$	$\text{pgrtPA / NC}$	No. protein/NC
NC@rtPA	$4.71 \times 10^8$	12.9	0.03	$2.09 \times 10^5$
	$4.38 \times 10^8$	14.7	0.03	$2.56 \times 10^5$
	$4.54 \times 10^8$	15.3	0.03	$2.58 \times 10^5$
	$4.95 \times 10^8$	10.5	0.02	$1.61 \times 10^5$
	$4.04 \times 10^8$	18.7	0.05	$3.53 \times 10^5$
	$4.60 \times 10^8$	11.4	0.02	$1.89 \times 10^5$
	$4.72 \times 10^8$	13.2	0.03	$2.13 \times 10^5$
	$4.64 \times 10^8$	16.1	0.03	$2.65 \times 10^5$

### 9.1.3. Theoretical protein loading in the nanocapsules

The theoretical calculation of the maximum load, for a protein of 70 kDa (such as the rtPA) per NC is explained below. The volume of an 800 nm NC ( $V_{\text{NC}}$ ) is calculated from the radius ( $r$ ).

$$V = \frac{4}{3} \times \pi \times r^3$$

$$V_{\text{NC}} = \frac{4}{3} \cdot \pi \cdot 400^3 = 2.68 \cdot 10^8 \text{ nm}^3$$

The theoretical radius of the rtPA was calculated from the following formula described in previous studies<sup>253</sup>:

$$R_{\min} = \left( \frac{3V}{4\pi} \right)^{1/3} = 0.066M^{1/3}$$

$$R_{\text{rtPA}} = 0.066 \times 70000^{1/3} = 2.72 \text{ nm}$$

In which R is the radius of the molecule in nm and M is the molecular weight in Da. And its volume ( $V_{\text{rtPA}}$ ) is calculated as above.

$$V_{\text{rtPA}} = \frac{4}{3} \cdot \pi \cdot 2.72^3 = 84.29 \text{ nm}^3$$

The maximum loading of protein per NC is calculated as follows:

$$\text{Maximum loading} = \frac{V_{\text{rtPA}}}{V_{\text{NC}}} = \frac{84.292}{2.68 \cdot 10^8} = 3.18 \times 10^6 \text{ rtPA molecules/NC}$$

$$\text{rtPA molarity} = 3.18 \times 10^6 \frac{\text{rtPA molecules}}{6.022 \cdot 10^{23}} = 5.28 \cdot 10^{-18} \text{ M}$$

$$5.28 \cdot 10^{-18} = \frac{\text{rtPA grams} / 70000}{1}$$

$$\text{rtPA grams} = 3.70 \cdot 10^{-13} \text{ grams} = 0.37 \text{ pg}$$

Theoretically, the maximum loading of rtPA per NC is 0.37 pg.

Our data showed a loading of 0.02-0.05 pg/NCs. Therefore, a 5.4-13.5 % of the theoretical load was achieved.

## 9.1.4. Quantification of protein/mg of sample

To calculate the mg of protein per mg of sample, NC@rtPA and NC@rtPA without gelatin were freeze dried. The results are shown in Table 10. The amount of and rtPA per mg of sample resulted in 1.44  $\mu\text{g}/\text{mg}$  and 1.67  $\mu\text{g}/\text{mg}$  in the NC without and with gelatin respectively.

Table 10. Amount of protein per NC in mg.

Sample	Protein concentration (mg/mL)	Volume simple (mL)	Protein (mg)	NC (mg)	$\mu\text{g}$ protein/mg NC
NC@rtPA	0.013	0.1	0.0013	0.9	1.44
NC@rtPA w/o gelatin	0.015	0.1	0.0015	0.9	1.67



### 9.1.5. Minimum information reported in bio-nano experimental literature

Following the checklist of Faria et al, we performed the next table (Table 11) to summarize the material characterization, biological characterization and details of experimental protocols of the developed NCs.

Table 11. Miribel checklist.

Component	Representative Units	Reported when...	
		Test tube	In vivo
Material Characterization			
Synthesis and composition	-	✓	
Size	nm	✓	
Size dispersity and aggregation	dispersity index	✓	
Zeta potential	mV	✓	
Drug loading	pg rtPA/NC, number protein/NC, µg rtPA/mg sample	✓	
Drug release	%	✓	
Targeting	µg gelatin/NCs	✓	
Labeling	pg Fe/NC	✓	
Drug leaking	%	✓	
Biological Activity			
Amidolytic activity	% activity compared to "free" rtPA	✓	

Stability against inhibitors	% activity compared to "free" rtPA	✓	
Fibrinolytic activity	absorbance 520nm	✓	
US sensitivity	%	✓	✓
Toxicity	Non-altered levels of creatinine, GOT and GPT.		✓
Justification of biological model	-		✓
Experimental protocol details			
Administered dose	mass		✓
Method of administration			✓
Method of blood extraction			✓
US application	MHz, W/cm <sup>2</sup>	✓	✓
Imaging details			✓
Biodistribution	% ID (Fe), $\mu\text{g Fe/g organ}$		✓
Details of data analysis		✓	✓

## 9.2. *In vitro* rtPA activity

### 9.2.1. Amidolytic activity

An rtPA chromogenic peptide substrate was used to quantify the activity of FITC-labeled rtPA in solution, inside de nanocores, and in the cavity of NCs. The low MW (MW = 659 Da) of the peptide results in its capability to cross the polymeric shell of NCs. As controls, rtPA amidolytic activity of NCs without the outmost gelatin layer, loaded either with rtPA or with BSA, was quantified.

Figure 61 shows that compared with Alteplase (taken as reference), we found the same rtPA amidolytic activity among all samples.

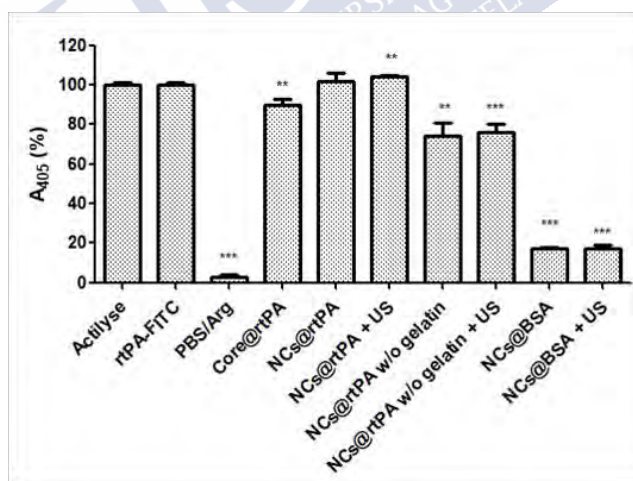


Figure 61. Chromogenic assay for determination of the enzymatic activity of rtPA encapsulated in cores and NCs. All data represent mean  $\pm$  SD (three independent measurement). In all data statistical significance was assessed by the t-test: each sample was compared with Alteplase (100 % taken as reference) ( $P^{**}<0.01$ ;  $P^{***}<0.001$ ).

### 9.2.2. rtPA protection against plasminogen activator inhibitor

Additionally, in order to dissect whether the encapsulated rtPA was protected from its natural inhibitor, that is, the PAI-1 (MW = 43 kDa), "free"rtPA-FITC, NC@rtPA with and without gelatin (NC@rtPA w/o gel) and NC@BSA were mixed with PAI-1 and rtPA chromogenic peptide substrate.

Results (Figure 62) showed that the PAI-1 inhibited the activity of non-encapsulated rtPA. In contrast, encapsulated rtPA had the same activity with the PAI-1 incubation and without it, in both NC@rtPA and NC@rtPA without gelatin.

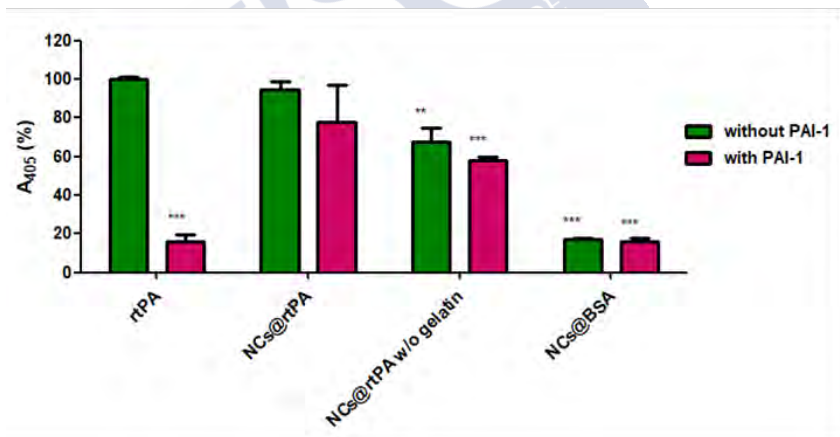


Figure 62. Chromogenic assay in the presence of PAI-1 for determination of the enzymatic activity of rtPA encapsulated in nanocores and NCs. In all data statistical significance was assessed by the *t*-test; each sample was compared with Alteplase (100 % taken as reference) (P\*\*<0.01; \*\*\*P<0.001).

### 9.3. *In vitro* release

#### 9.3.1. Analysis of changes in the fluorescence

The quantification of US-triggered release of proteins (BSA and rtPA) from the cavity of NCs was first indirectly estimated from fluorescence measurements: relative fluorescence of the SN with respect to the fluorescence of the precipitated product (cargo non-released).

First, to demonstrate US-triggered protein release from the cavity of NCs, we applied US to 2, 4 and 6 bL NC@BSA during 15 or 120 min. The frequency and intensity of the US did not change: 0.72 W/cm<sup>2</sup>, 2 MHz. With the 15 min US application, fluorescence analysis showed that only the 2bL NCs showed substantial BSA release (50 %) in the SN (release of the dye-labeled BSA), after precipitation of NCs (Figure 63-a). After 120 min US application, again, only in the 2bL system, we found more than 60 % BSA release.

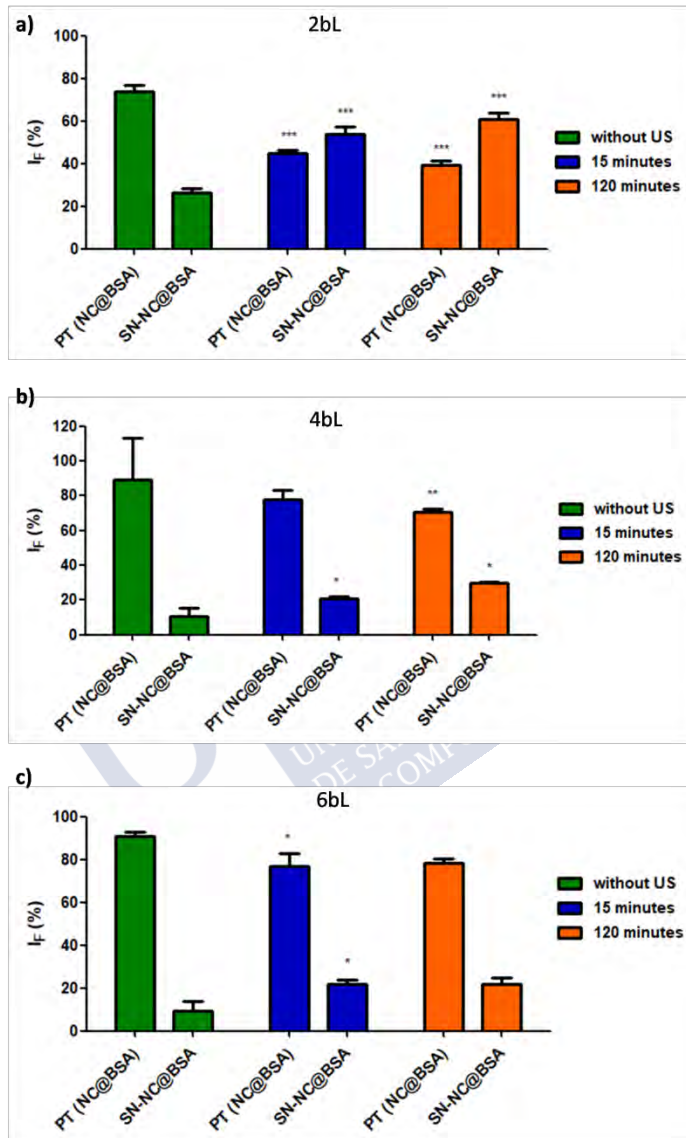


Figure 63. Fluorescence-quantified US-triggered delivery of BSA from 2, 4 and 6 bL NC@BSA after 15 and 120 min US application. In all data statistical significance was assessed by the *t*-test: each SN was compared with its control without US, and each PT (NC@BSA 2, 4, or 6bL) was compared with its control without US (\* $P < 0.05$ ; \*\* $P < 0.01$ ; \*\*\* $P < 0.001$ ).

Once, we knew that 2bL and 15 min was enough to release the drug from the cavity, we performed similar experiments with NC@rtPA (2bL and gelatin), and confirmed that after 15-min US application 50 % of the encapsulated rtPA was found in the SN (Figure 64). Due to these results, we used the NC@rtPA 2bL for following experiments.

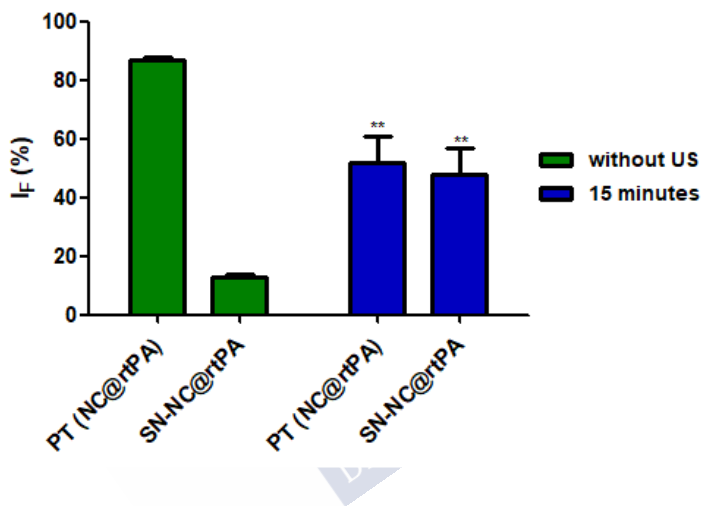


Figure 64. Fluorescence-quantified US-triggered delivery of rtPA from 2bL NC@rtPA after 15 min US application. In all data statistical significance was assessed by the *t*-test: SN after US application was compared with its control without US, and PT (NC@rtPA) was compared with its control without US ( $P^{**} < 0.01$ ).

### 9.3.2. Analysis of changes in flow cytometry

The SS and FS measurements were performed in the SN and PT with and without US. Fluorescence and SS signals were recorded to gather information of the fluorescently labeled encapsulated cargo (rtPA).

Analysis revealed changes in the SN and PT after applying US to the NCs, showing an increase in the fluorescence and in number of events in the SN, and a decrease in the PT after the US application. This assay confirmed US-triggered release of rtPA (Figure 65).

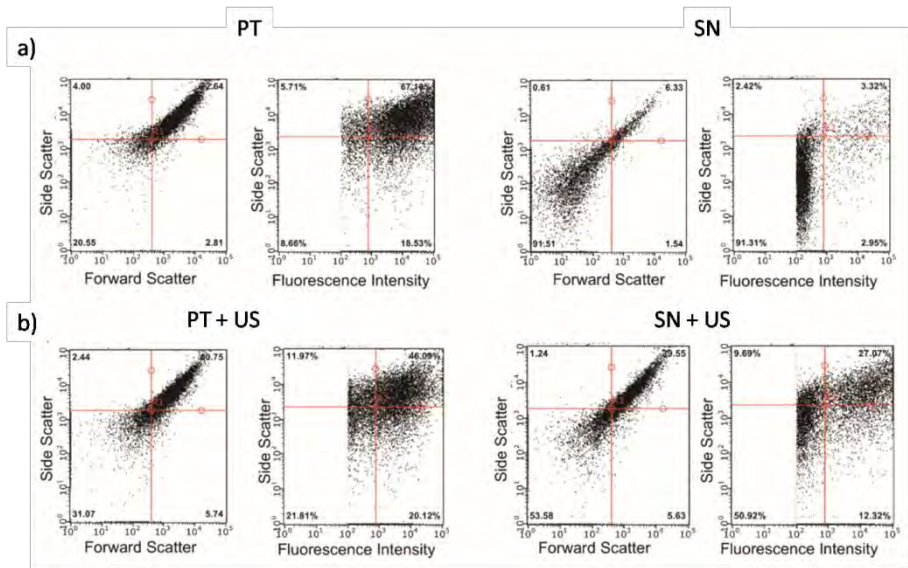


Figure 65. NCs dispersion analysis after US treatment by flow cytometry. The variation of the flow cytometry SS and the FS of the NC and SN in relation to the US application are shown. a) Scatter density plots of FS signal versus SS signal, and SS signal versus fluorescence signal (corresponding to the 512/18 nm channel for control PT and SN. b) Scatter density plots of FS signal versus SS signal, and SS signal versus fluorescence signal (corresponding to the 512/18 nm channel for control PT and SN after US treatment).



### 9.3.3. Structural changes in the morphology

Figure 66 shows examples of SEM images, before and after the US application. There were morphological changes in the NCs when US was applied.

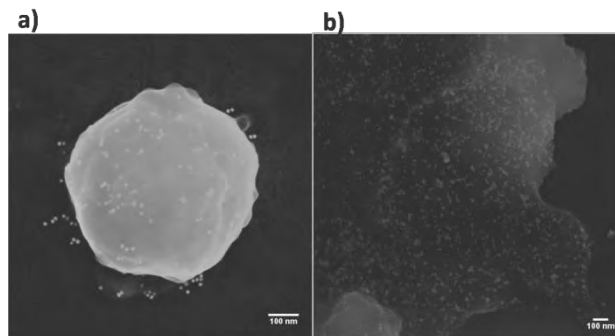


Figure 66. SEM images of NCs a) before applying US, and b) after applying it.

### 9.3.4. rtPA activity

Once US-triggered rtPA release was confirmed by fluorescence and flow cytometry measurements, the enzymatic activity of the released rtPA was quantified by a fluorogenic assay (Sensolyte® AMC tPA activity assay). This assay relies on the ability of rtPA to process a fluorogenic substrate, leading to a fluorescence increase. The reason to use a second assay, fluorogenic instead of chromogenic, was because it allows reliable rtPA amidolytic activity quantification in physiological media such as blood and plasma.

The results are shown in Figure 67. After applying US the activity in the SN (SN-NC@rtPA) was significantly higher ( $P < 0.001$ ) compared with the SN without US. This assay confirmed that the released rtPA is fully bioactive and in agreement with fluorescence and flow cytometry assays of the SN.

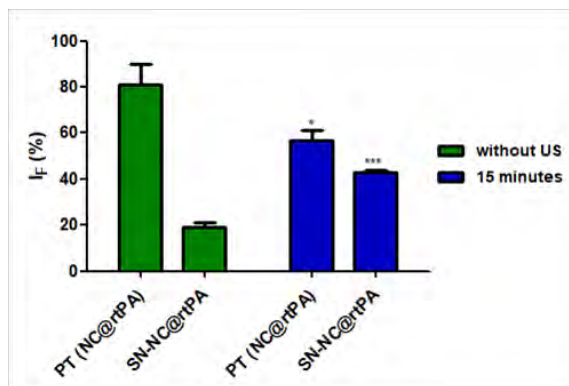


Figure 67. Enzymatic activity of the released rtPA quantified by the fluorogenic assay SensoLyte®. All data mean  $\pm$  SD (three independent measurements). In all statistical significance was assessed by the *t*-test: each sample was compared with the corresponding system without US (\*\*\*)  $P < 0.001$ ).

### 9.3.5. Fibrinolytic activity: clot assay

Then, a clot assay was performed largely following previous reports<sup>254</sup>, in which the efficiency (bioactivity) of the US-released rtPA to reduce the size of clots (artificially pre-formed in microwell plates) was evaluated indirectly, that is, by measuring the **absorbance at 520 nm (red) that increases as the clots “dissolve”** (Figure 68-a). Initially, as calibration, we added solutions of rtPA of increasing concentrations (0-100  $\mu\text{g}/\text{mL}$ ). Then, also as control, NC@BSA ( $4.2 \times 10^7$  NCs/mL) was added, showing no effect (no

significant increased absorbance reading with or without US application).

In case of NC@rtPA ( $4.2 \times 10^7$  NCs/mL, 1  $\mu\text{g/mL}$  rtPA encapsulated) was added; without US application, clots were only partially dissolved, which we ascribed to residual rtPA leaking. In case of US application, clots were dissolved in the same way as the group treated with "free" 1 mg/kg rtPA, showing a similar activity.

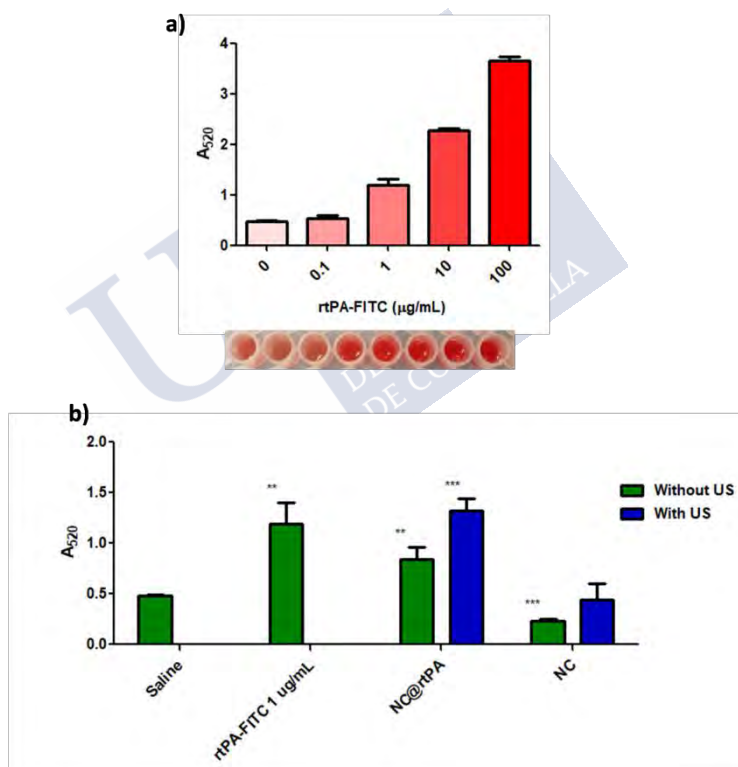


Figure 68. Absorption at 520 nm ( $A_{520}$ ) after adding to the clots: a) "free" rtPA or b) 1 mg/mL rtPA encapsulated (w/o US) in NC or rtPA released after US, and control samples. All data mean  $\pm$  SD (three independent measurements). In all statistical significance was assessed by the *t*-test: each sample was compared with the saline group (\* $P < 0.05$ ; \*\* $P < 0.01$ ; \*\*\* $P < 0.001$ ).

## 10. Section II: *In vivo* studies of rtPA nanocapsules

### 10.1. Ultrasound safety in the brain

In this Section, we investigated if the application of US in the brain can damage the BBB. To perform this assay we used the EB technique. This compound binds to the albumin, which could be detected in the brain parenchyma when the BBB is damaged.

A total of 18 animals were used to determine if US damage the BBB (Figure 69). Two animals were discarded, because they died after the ischemia. Four animals were used for each study group (see Section 7.2).

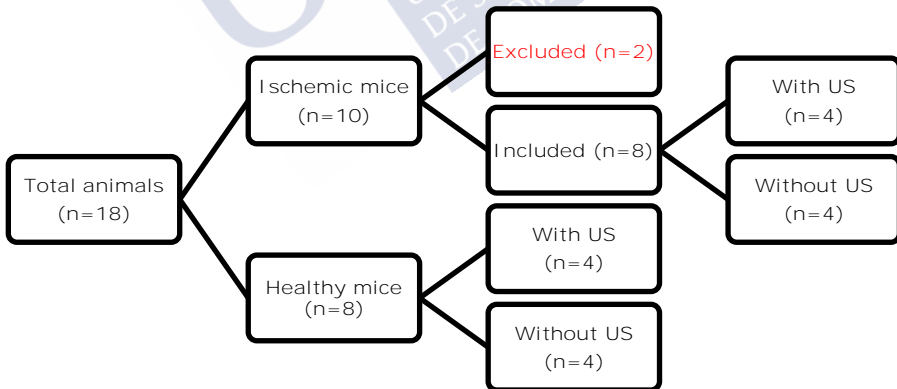


Figure 69. Included animals in the study of the BBB damage.

We administered the EB to healthy and ischemic animals just before the application of US in the brain. In addition, we had two control groups (healthy and ischemic animals) to which no ultrasound was applied.

Before analyzing the amount of EB in the brains, we performed a calibration curve (0-64  $\mu\text{g}/\text{mL}$ ) to correlate the absorbance (630 nm) with the amount of EB in the brains (Figure 70-a).

Figure 70-b shows that there were no differences between US application or not in healthy animals. An increase in the ipsilateral hemisphere of the ischemic groups can be observed, due to the ischemic injury itself, in which the BBB is damaged. However, there were no differences between the ischemic animals treated with US compared with the ischemic group without US. The US application did not show differences in the BBB integrity.

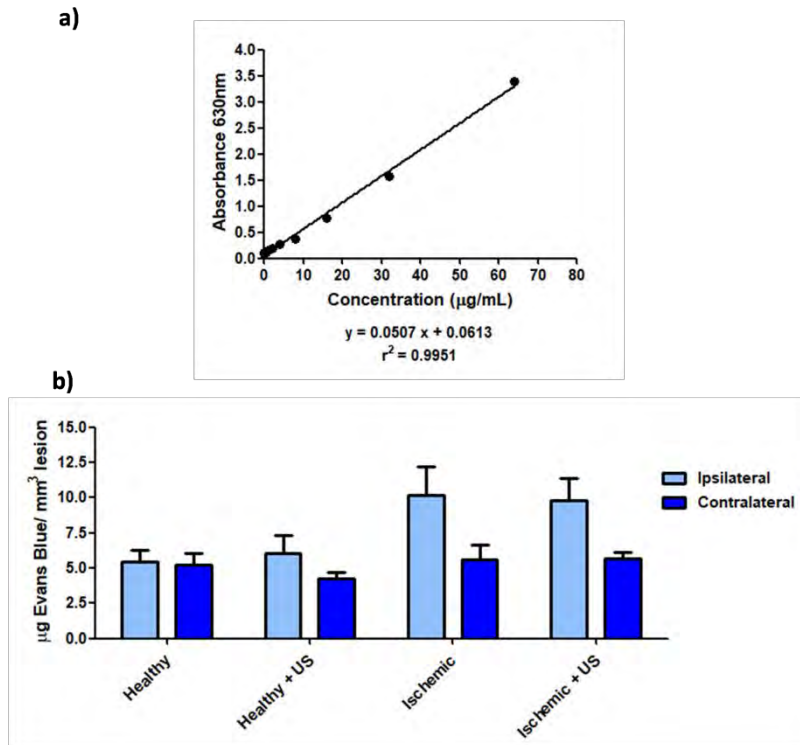
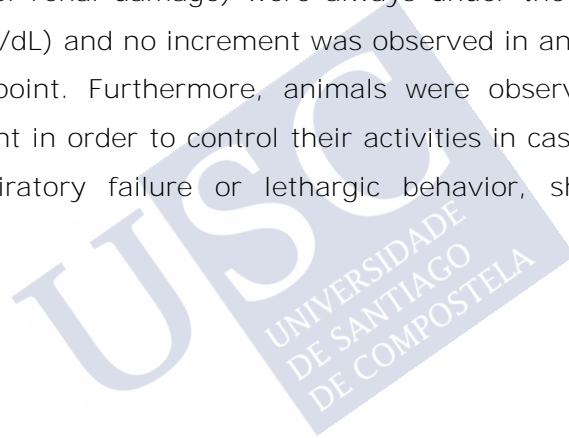


Figure 70. a) Examples of correlation between concentration and absorbance of EB. b) Amount ( $\mu\text{g}$ ) of EB corrected by the weight (g) of the brains, in healthy and ischemic animals in which EB was administered and US was applied later. All data mean  $\pm$  SD (four animals per treatment group). In all data statistical significance was assessed by the  $t$ -test: each ipsilateral hemisphere was compared with its control without US, and each contralateral hemisphere was compared with its control without US.

## 10.2. Nanocapsules safety *in vivo*

In this study, three healthy animals were used to analyze the security of the NC@rtPA administration by MRI analysis of the brain and measuring the GOT, GPT and creatinine levels in blood.

A dose of 1 mg/kg rtPA was used for the *in vivo* experiments. Mice were followed by MRI for 7 days to evaluate the possible associated damage in the brain. No ischemic or hemorrhagic damage was observed with the MRI in any group (Figure 71-a); there was also no evidence of NC in the brain, which suggested no apparent BBB disruption. There was no increment in GOT and GPT activity (markers of hepatic damage) in any of the groups compared to the baseline levels (Figure 71-b). Creatinine levels (marker of renal damage) were always under the detection limit ( $<0.5$  mg/dL) and no increment was observed in any of the groups or time point. Furthermore, animals were observed during the experiment in order to control their activities in case of presenting any respiratory failure or lethargic behavior, showing normal activity.



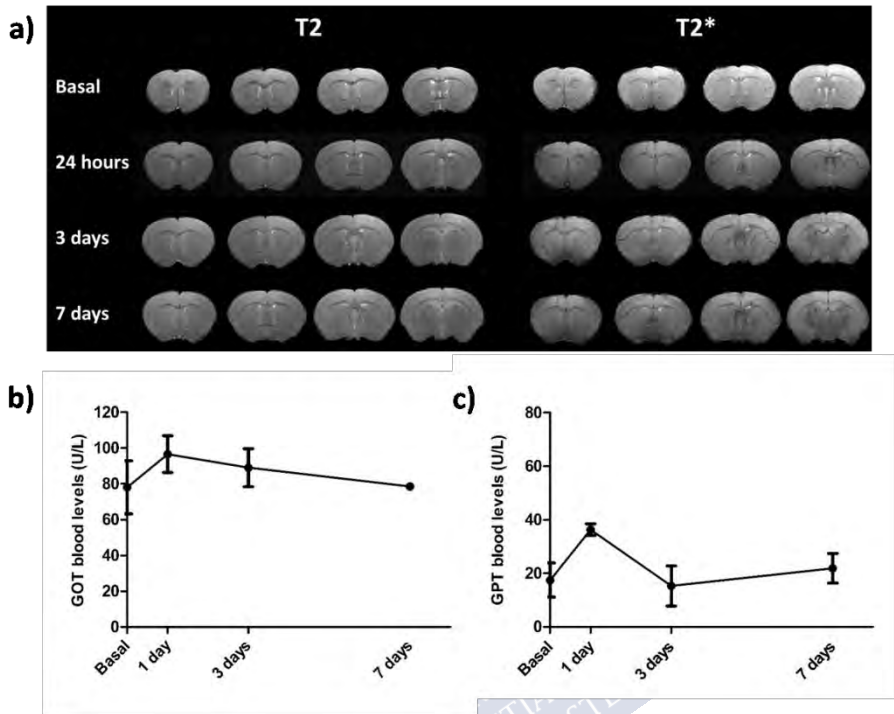


Figure 71. a) T2 and T2\* weighted images after IV administration of 1 mg/kg rtPA in NC@rtPA with ioNPs in one of the bL. b) GOT levels at basal, one, three, and 7 days after IV administration. c) GPT levels at basal, one, three, and 7 days after IV administration.

### 10.3. *In vivo* release

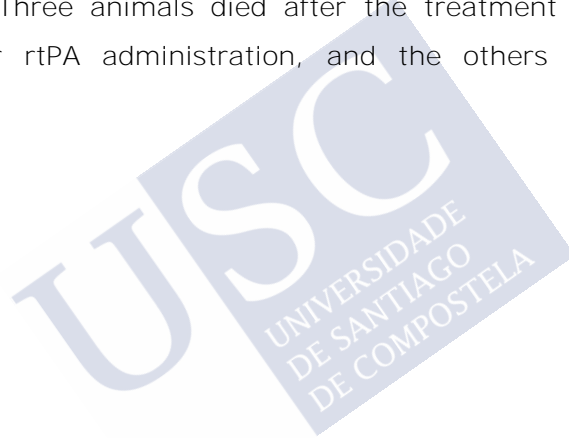
In this Section, rtPA release from the cavity of NCs was studied in Swiss mice. For this purpose, rtPA enzymatic activity was quantified with the SensoLyte assay kit in extracted plasma samples.



10.3.1. Blood extraction Basal, 5, 15, 40 min

Blood rtPA activity was determined in the five groups tested (n=3), before treatment administration (blood rtPA basal levels), and 5, 15 and 40 min after treatment administration.

A total of 36 animals were used in this study, of which eight were excluded (Figure 72). Five animals were excluded before the treatment administration due to damage in the CCA during the surgery. Three animals died after the treatment administration, one after rtPA administration, and the others after NC@rtPA injection.



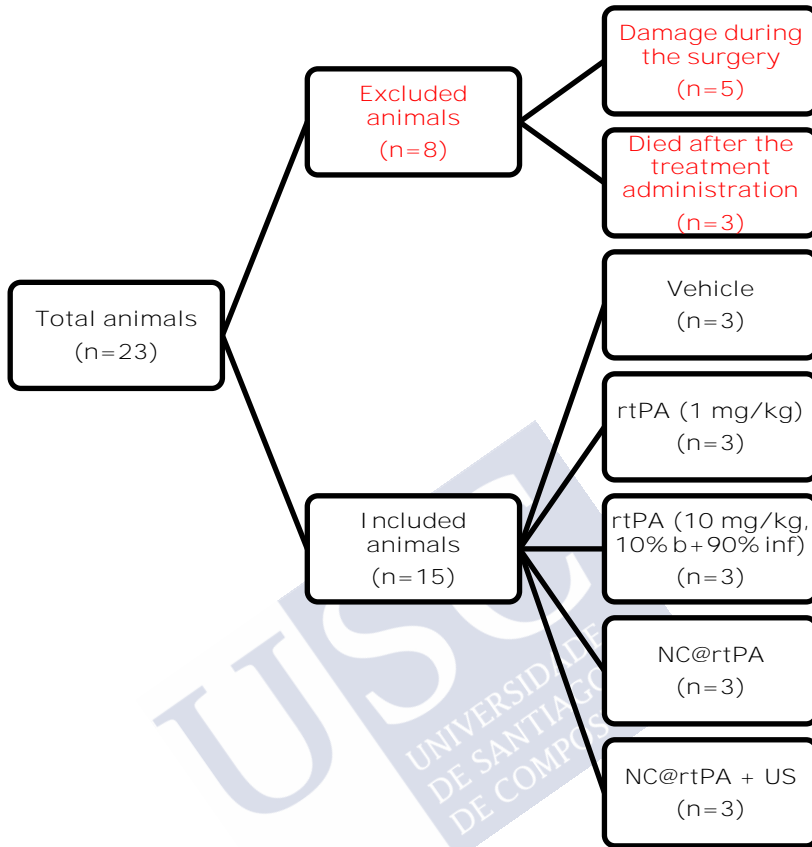


Figure 72. Animals included in the study. Nanocapsules with rtPA and gelatin (NC@rtPA).

In order to compare between US-released (from NC@rtPA) and non-encapsulated rtPA, i.v. administration of rtPA was used at 1 mg/kg dose (approximately 25-30  $\mu\text{g}$  rtPA per mouse). Additionally, a higher dose (10 mg/kg, approximately 250-300  $\mu\text{g}$  rtPA per mouse) of non-encapsulated rtPA was administrated.

Results are shown in Figure 73. In case of non-encapsulated rtPA (1 or 10 mg/kg), as expected, rtPA activity rapidly decreased due to the low half-life of rtPA (5 min). Such decay was less pronounced in the 10 mg/kg case due to the administration protocol (10 % bolus + 90 % infusion over 40 min). After 40 min of administration of non-encapsulated rtPA, its activity is in either case about 3-fold with respect to basal levels. In case of NC@rtPA (1 mg/kg), rtPA activity was initially reduced compared to the non-encapsulated rtPA samples. This reduced activity may be due to some rtPA leaking *in vivo*, which after 40 min, however, dropped to basal levels. In case of US-application (40 min) after administration of NC@rtPA (1 mg/kg), a completely new trend arose: rtPA activity increased over time, reaching about 3.5-fold or 2.5-fold increase compared with 1 mg/kg or 10 mg/kg free rtPA, respectively, after 40 min. This result was particularly important as it demonstrated that the half-life of rtPA can be greatly enhanced by encapsulation in our sonosensitive NCs and US is able to revert the rtPA activity.

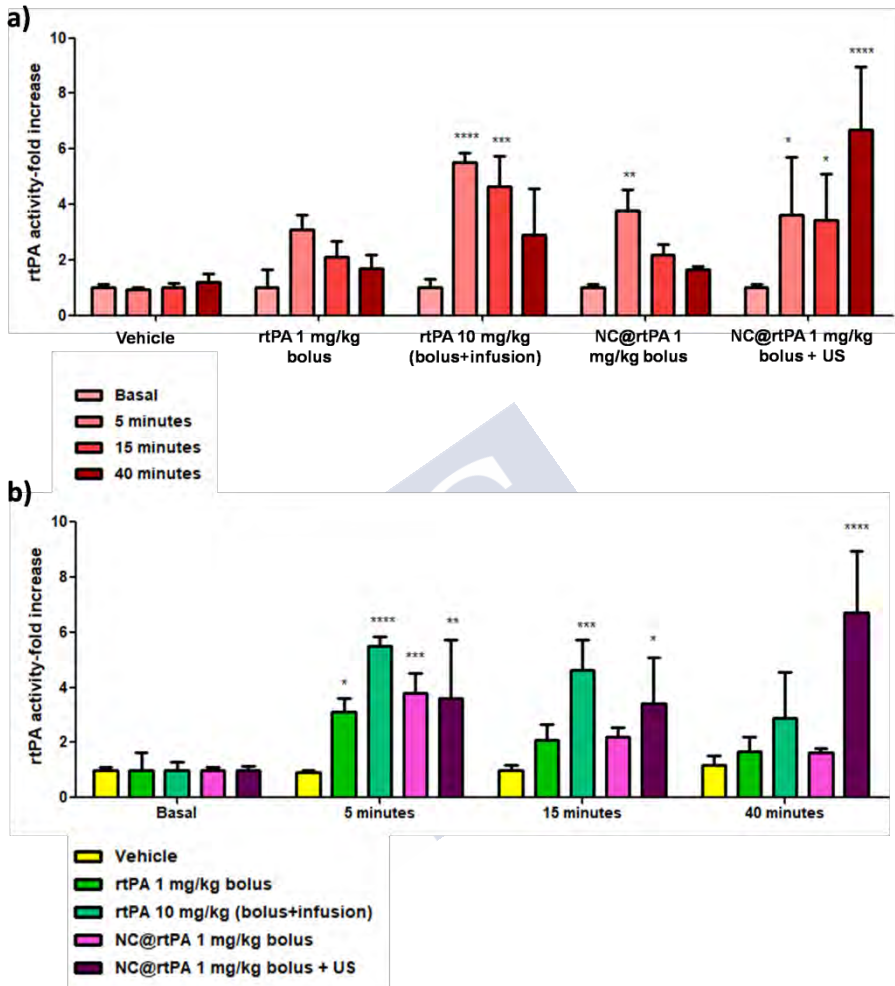


Figure 73. rtPA activity in plasma. All data mean  $\pm$  SD (three animals per group of treatment). Two-way ANOVA followed by post-hoc Bonferroni was used to perform the statistical analysis. a) Each treatment time (5, 15 or 40 min) was compared with rtPA levels in the saline group. b) Each treatment was compared with the corresponding rtPA basal levels ( $*P < 0.05$ ;  $**P < 0.01$ ;  $***P < 0.001$ ). Nanocapsules with rtPA and gelatin (NC@rtPA).

### 10.3.2. Blood extraction Basal, 1, 5, 15, 40 min

In the previous study, blood sampling started 5 min after treatment administration, however taking into account that rtPA has a short half-life (less than 5 min) maybe some changes in the first minutes occurred. For this reason, we performed the same experiment adding the 1 min blood extraction.

Blood rtPA activity was determined in the 8 groups tested (n=3), before treatment administration (blood rtPA basal levels), and 1, 5, 15 and 40 min later.

A total of 30 animals were used in this study, of which 6 were excluded (Figure 74). Three animals were excluded before the treatment administration due to damage in the CCA during the surgery. Three animals died after NC@rtPA administration

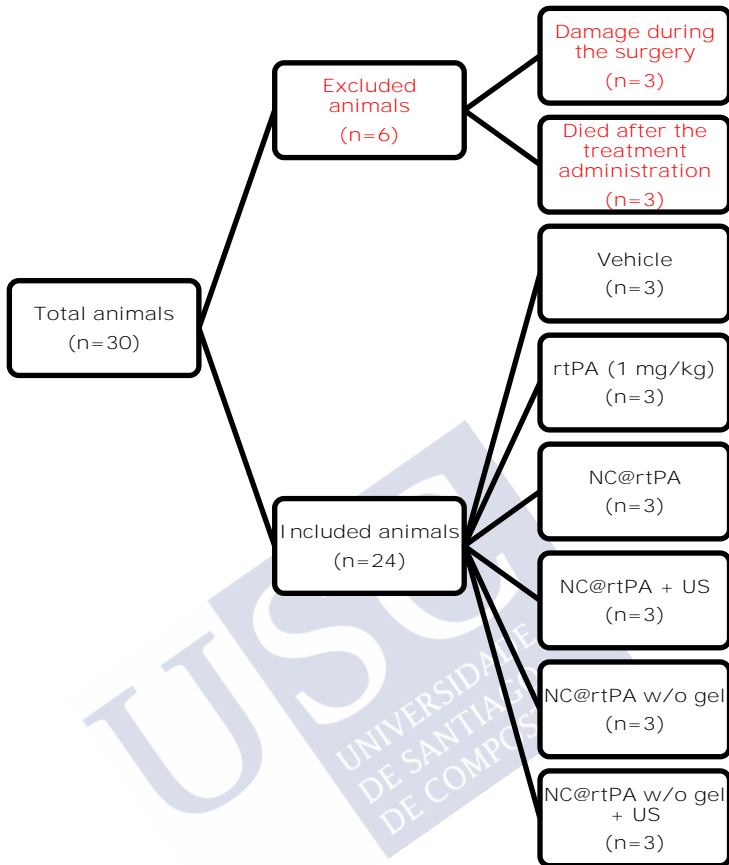


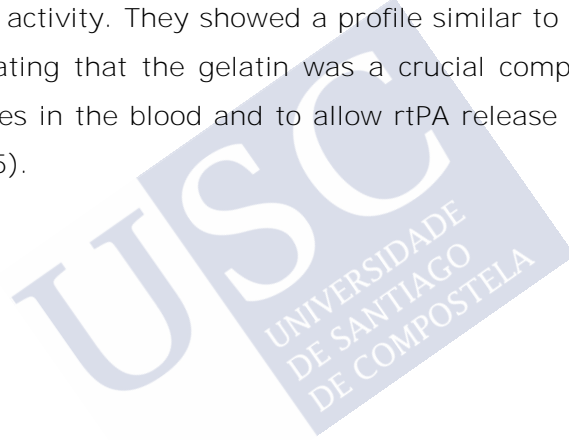
Figure 74. Included animals in the study. Nanocapsules with rtPA and gelatin (NC@rtPA), nanocapsules with rtPA and without gelatin (NC@rtPA w/o gel).

As in the previous experiment, rtPA plasmatic activity was increased in rtPAcontrol groups, showing a decrease after 1 min.

The group treated with NC@rtPA, according to our previous results, showed an increment in the first 5 min. Thus, its plasmatic activity was almost similar to the vehicle group after 40 min. However, in the group treated with NC@rtPA + US rtPA activity

increased significantly over 40 min ( $P < 0.001$ ), exhibiting more activity than the group treated with rtPA.

Interestingly, the administration of NC@rtPA without gelatin showed a plasmatic kinetic quite different from the NC@rtPA that were synthesized with gelatin. In this case, the application of US was independent from rtPA plasmatic activity. Since the first blood extraction after the treatment administration, both NC@rtPA without gelatin or NC@rtPA without gelatin + US increases the plasmatic activity. They showed a profile similar to the NC@rtPA + US, indicating that the gelatin was a crucial component to make NCs stables in the blood and to allow rtPA release by applying US (Figure 75).



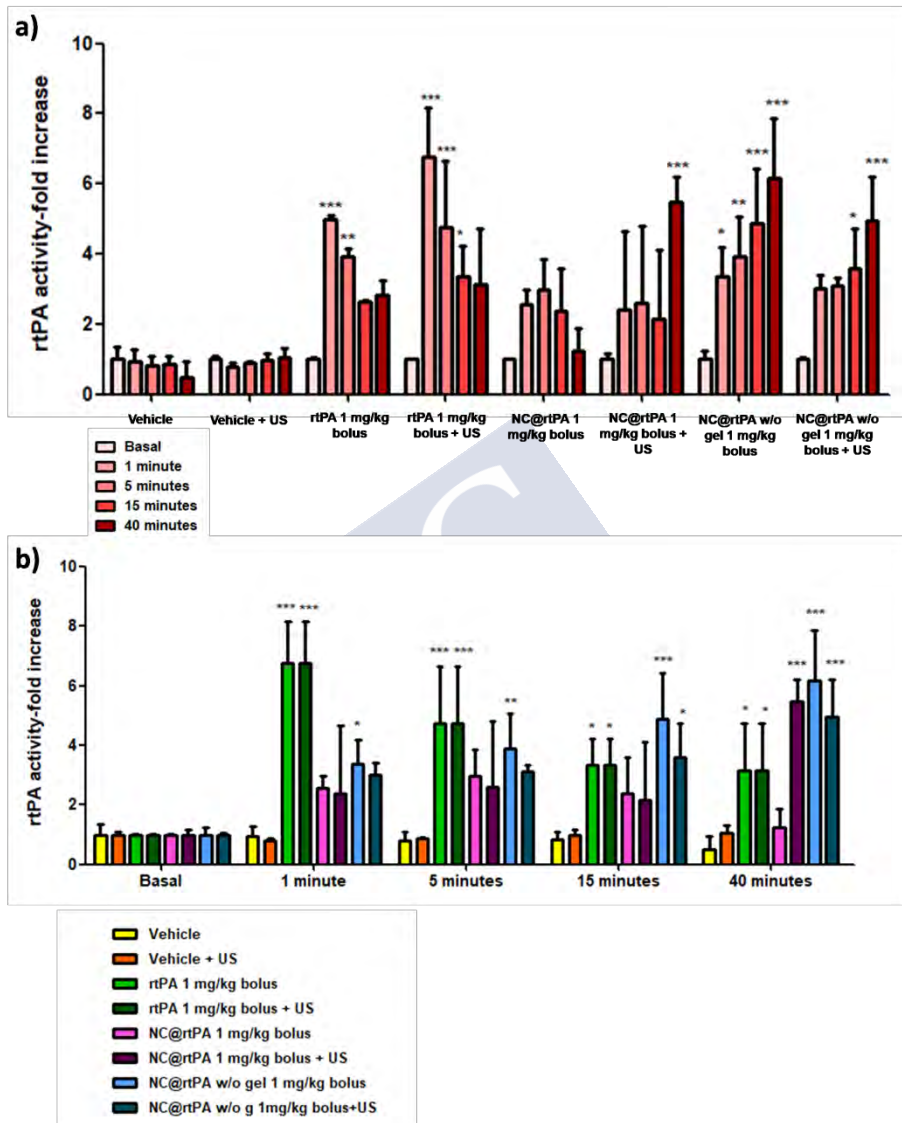


Figure 75. rtPA activity in plasma. All data mean  $\pm$  SD (three animals per group of treatment). Two-way ANOVA followed by post-hoc Bonferroni was used to perform the statistical analysis. a) Each treatment time (1, 5, 15 or 40 min) was compared with rtPA levels in the saline group. b) Each treatment was compared with the corresponding rtPA basal levels ( $*P < 0.05$ ;  $**P < 0.01$ ;  $***P < 0.001$ ). Nanocapsules with rtPA and gelatin (NC@rtPA), nanocapsules with rtPA and without gelatin (NC@rtPA w/o gel).



#### 10.4. Therapeutic effect

In this Section, the therapeutic effect of the NC@rtPA (with and without gelatin, and with and without US) was investigated in an ischemic animals model induced by *in situ* thrombus formation in the MCA. The reperfusion rate, infarct volume, and HT were studied in nine groups tested (n=5-9).

A total of 140 animals were included in the study. Seventy-four of them were excluded due to damage in the MCA during the surgery (n=13), problems with the monitoring of the CBF (n=9) or reperfusion (n=39) before the treatment administration. Thirteen of them died after the treatment administration, four after rtPA, two after saline, and seven after NC@rtPA (Figure 76).

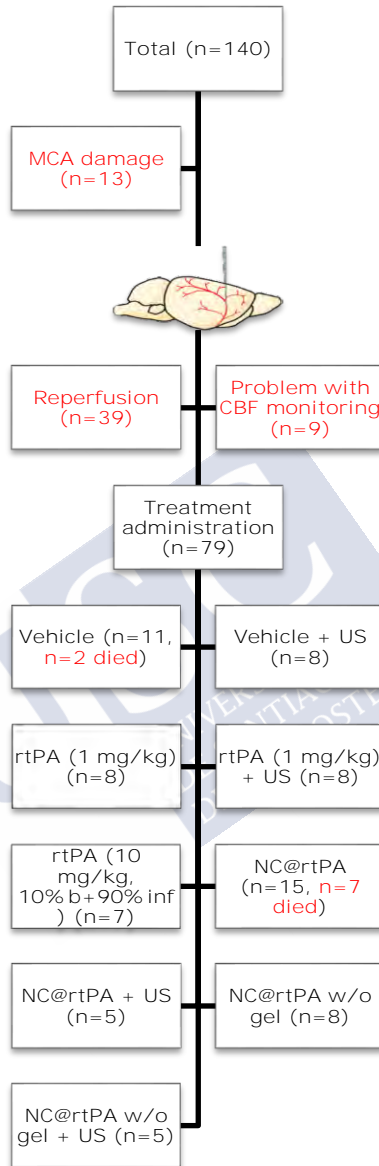


Figure 76. Included animals in the study of the therapeutic effect. Nanocapsules with rtPA and gelatin (NC@rtPA), nanocapsules with rtPA and without gelatin (NC@rtPA w/o gel).

### 10.4.1. Effect of nanocapsules on cerebral blood flow

CBF was stable in all groups after the thrombin injection. In all groups, local injection of thrombin in the MCA caused an immediate drop (to ~20 % of baseline) of CBF. Animals treated only with the vehicle (saline), had a permanent occlusion that was stable throughout the registration of CBF (80 min).

Reperfusion was considered when the CBF reached 40 % of baseline. The percentages of animals that reperfused during the monitoring of CBF after the treatment administration are represented in Figure 77.

As well as none of the animals treated with the vehicle reperfused, 20 % of the animals treated only with US exhibited reperfusion.

Treatment with 1 mg/kg rtPA 30 min after the thrombin injection induced higher reperfusion rate (87.5 % of mice) than the control group. Sixty-seven per cent of mice showed reperfusion after the 1 mg/kg rtPA and the US application. The group treated with 10 mg/kg rtPA (10 % bolus + 90 % infusion over 40 min) showed less reperfusion than the group treated with 1 mg/kg rtPA (bolus), in which only 40 % of all animals reperfused.

In the groups treated with NCs, the only group in which reperfusion occurred was in the NC@rtPA + US, in which the 60 % of all animals treated reperfused.

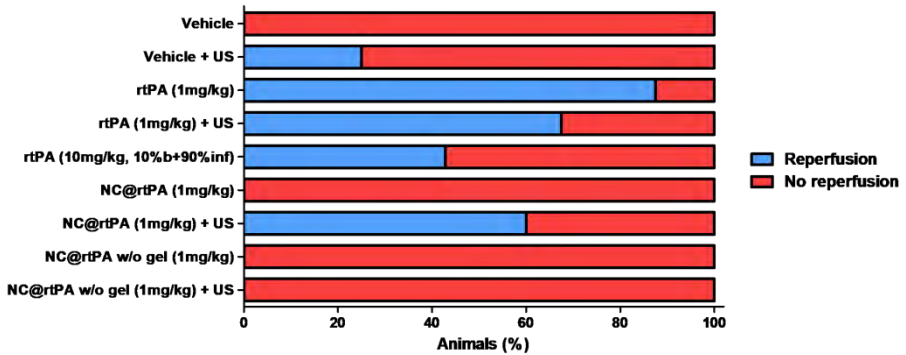


Figure 77. Reperfusion rates of the different groups of treatment. Nanocapsules with rtPA and gelatin (NC@rtPA), nanocapsules with rtPA and without gelatin (NC@rtPA w/o gel).

#### 10.4.2. Effect of nanocapsules on infarct volume

The results in reperfusion rates were related with the infarct volumes. The volumes were analyzed by MRI, measuring the infarct area in T2-map. Figure 78 shows a selected MRI from each group at 24 h and Figure 79 the same animals at 3 days.

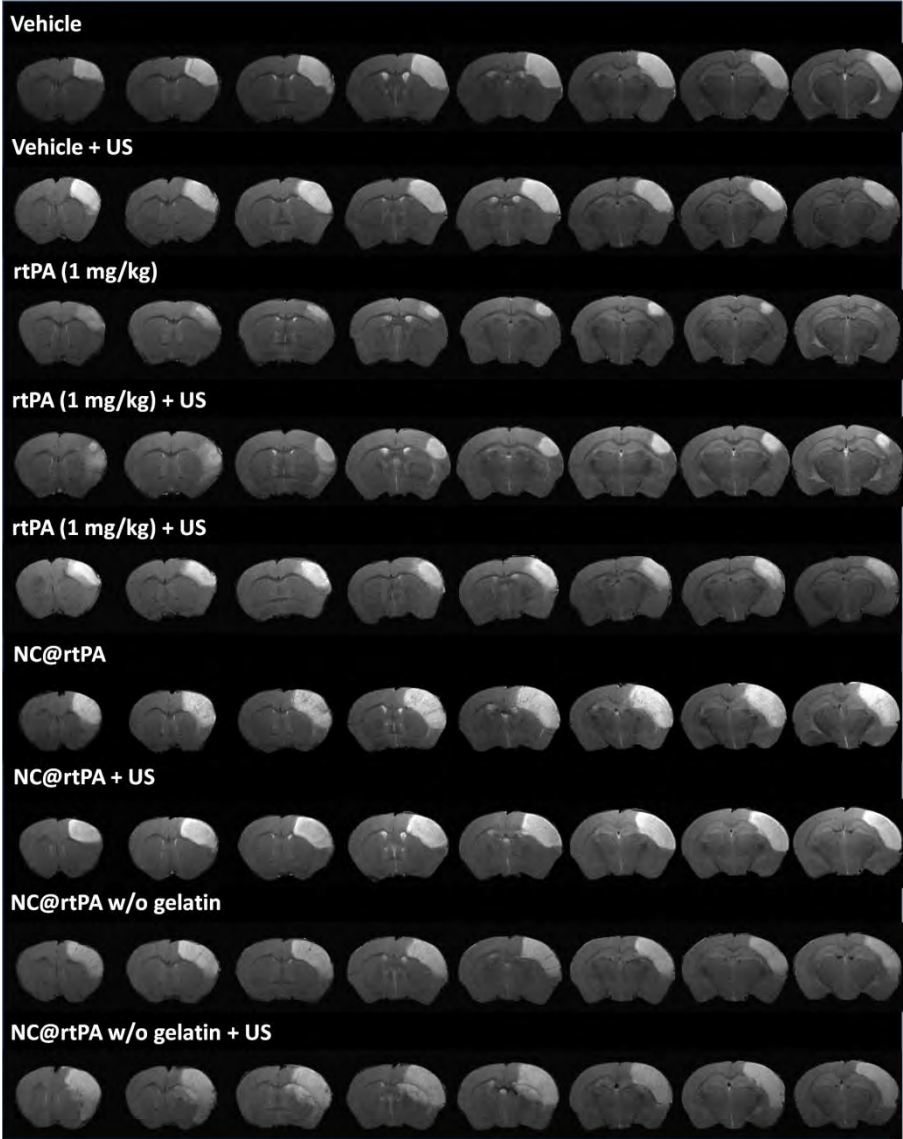


Figure 78. T2-weighted images of each treatment group at 24 hours after the treatment administration. Nanocapsules with rtPA and gelatin (NC@rtPA), nanocapsules with rtPA and without gelatin (NC@rtPA w/o gel).

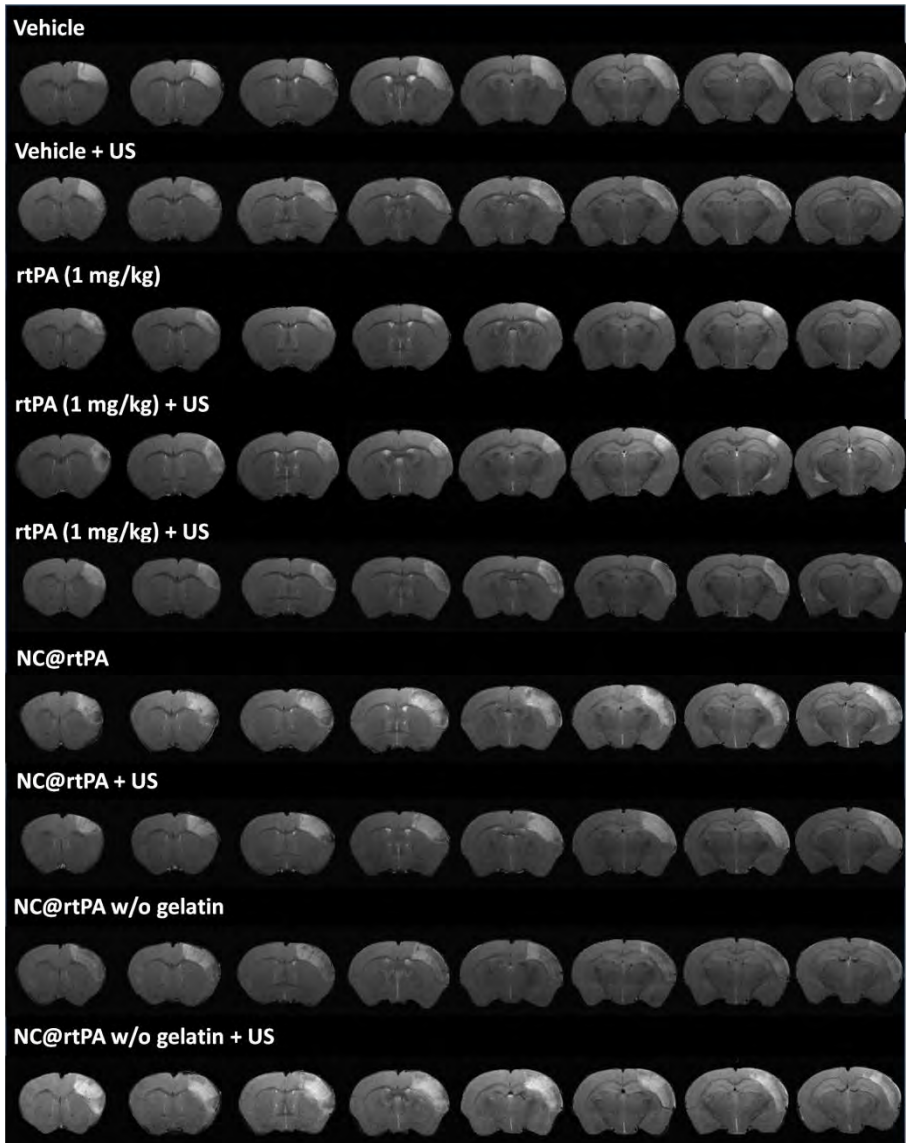


Figure 79. T2-weighted images of each treatment group at 3 days after the treatment administration. Nanocapsules with rtPA and gelatin (NC@rtPA), nanocapsules with rtPA and without gelatin (NC@rtPA w/o gel).

Infarct volumes at 24 h and 3 days are represented in Figure 80 and in Table 12. Permanent occlusions caused a cortical infarct of  $30.0 \pm 10.3 \text{ mm}^3$  after 24 hours. The application of US showed a tendency to increase the infarct area ( $39.0 \pm 9.9 \text{ mm}^3$ ).

The administration of rtPA caused a significant reduction of the infarct volume both without US ( $16.1 \pm 9.1 \text{ mm}^3$ ,  $P < 0.05$ ) and with US ( $15.3 \pm 10.6 \text{ mm}^3$ ,  $P < 0.01$ ) compared with the vehicle group. Furthermore, the administration of 10 mg/kg rtPA (10 % bolus + 90 % infusion over 40 min) exhibited a non-significant reduction of the infarct volume ( $18.7 \pm 16.5 \text{ mm}^3$ ).

On the other hand, the group treated with the NCs, showed an increase of the infarct area, specially the groups treated with NC@rtPA ( $53.1 \pm 19.8 \text{ mm}^3$ ) and NC@rtPA without gelatin ( $50.3 \pm 14.8 \text{ mm}^3$ ), whose increase was significantly higher ( $P < 0.01$ ) than the control group in both cases. In groups treated with NC@rtPA + US ( $30.6 \pm 13.0 \text{ mm}^3$ ) and NC@rtPA w/o gelatin + US ( $42.9 \pm 15.5 \text{ mm}^3$ ), the infarct had a tendency to increase, especially the group treated without gelatin. Moreover, the application of US in the group treated with NC@rtPA showed an infarct volume lower than the NC@rtPA without US.

Infarct volumes at 3 days have a similar profile as the results at 24 h.

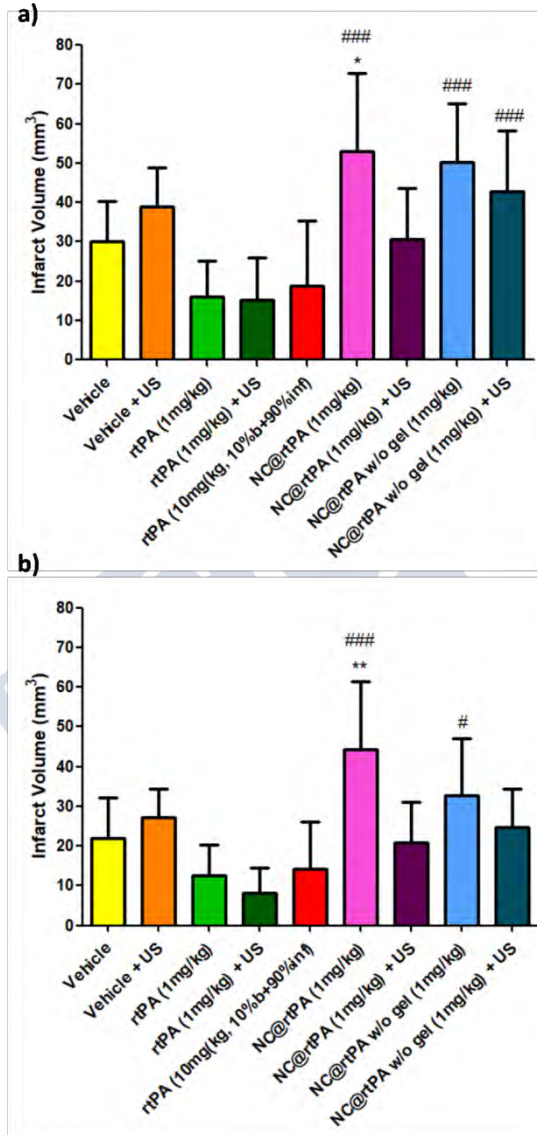


Figure 80. Infarct volume at a) 24 h and b) 3 days. One-way ANOVA followed by post-hoc Bonferroni was used to perform the statistical analysis. (\* $P < 0.05$ ; \*\* $P < 0.01$  compared with the vehicle group; # $P < 0.05$ ; ### $P < 0.001$  compared with the rPA group). Nanocapsules with rtPA and gelatin (NC@rtPA), nanocapsules with rtPA and without gelatin (NC@rtPA w/o gel).



Table 12. Infarct volume at 24 h and 3 days of each treatment group. Nanocapsules with rtPA and gelatin (NC@rtPA), nanocapsules with rtPA and without gelatin (NC@rtPA w/o gel).

Treatment group	Infarct volume (mm <sup>3</sup> )					
	24 hours			3 days		
Vehicle	30.0	±	10.3	22.0	±	10.1
Vehicle + US	39.0	±	9.9	27.1	±	7.2
rtPA (1 mg/kg)	16.1	±	9.1	12.7	±	7.5
rtPA (1 mg/kg) + US	15.3	±	10.6	8.1	±	6.5
rtPA (10 mg/kg, 10 % b+90 % inf)	18.7	±	16.5	12.0	±	4.3
NC@rtPA	53.1	±	19.8	44.4	±	17.1
NC@rtPA + US	30.6	±	13.0	21.0	±	10.1
NC@rtPA w/o gel	50.3	±	14.8	32.8	±	14.2
NC@rtPA w/o gel + US	42.9	±	15.5	24.7	±	9.6

#### 10.4.3. T2\*-weighted sequences

Figure 81 and Figure 82 showed selected images of T2\*-weighted images at 24 h and 3 days after the surgery, respectively.

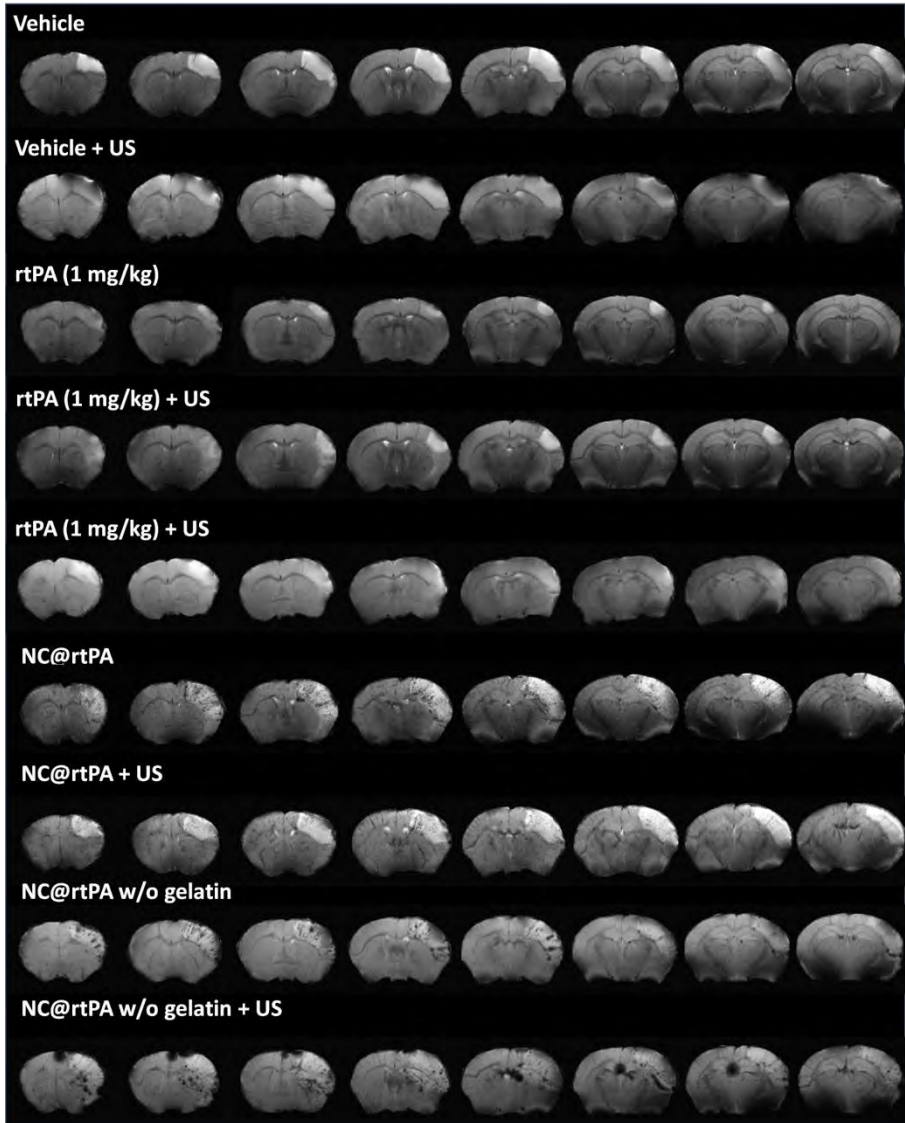


Figure 81. T2\*-weighted images of each treatment group 24 hours after the treatment administration. Nanocapsules with rtPA and gelatin (NC@rtPA), nanocapsules with rtPA and without gelatin (NC@rtPA w/o gel).

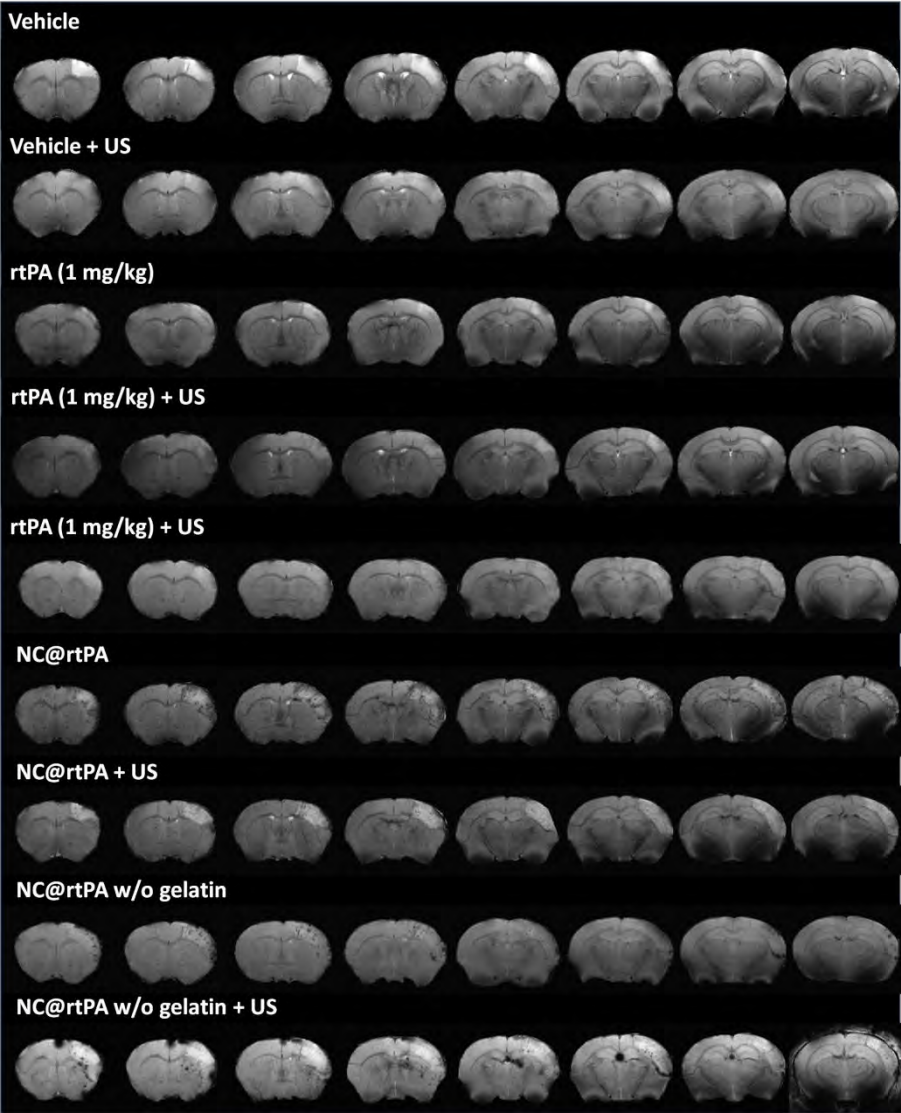


Figure 82. T2\*-weighted images of each treatment group 3 days after the treatment administration. Nanocapsules with rtPA and gelatin (NC@rtPA), nanocapsules with rtPA and without gelatin (NC@rtPA w/o gel).

In T2\*-weighted images some hypo-signals in the ischemic region were found, especially in the groups treated with NCs. The percentage of animals treated with these NCs that presented hypo-signal are represented in the Figure 83.

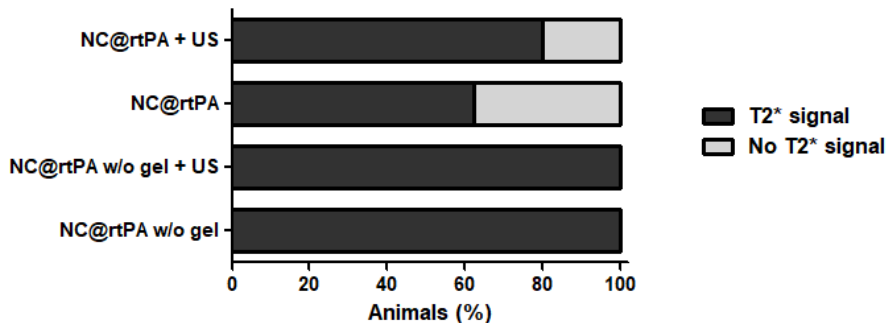


Figure 83. Percentage of animals treated with NCs that presented signals in T2\*-weighted images. Nanocapsules with rtPA and gelatin (NC@rtPA), nanocapsules with rtPA and without gelatin (NC@rtPA w/o gel).

To evaluate the aggregation of NCs in the brain region, we calculated the mean grey value in T2\* maps. The quantification was performed in the ipsilateral hemisphere 24 h after the treatment administration. Using this method, we found that the signal decreased between 64-80 % respects to the vehicle group (Figure 84). However, no differences were found between the groups treated with NCs, demonstrating that there were no differences in the target with or without gelatin.

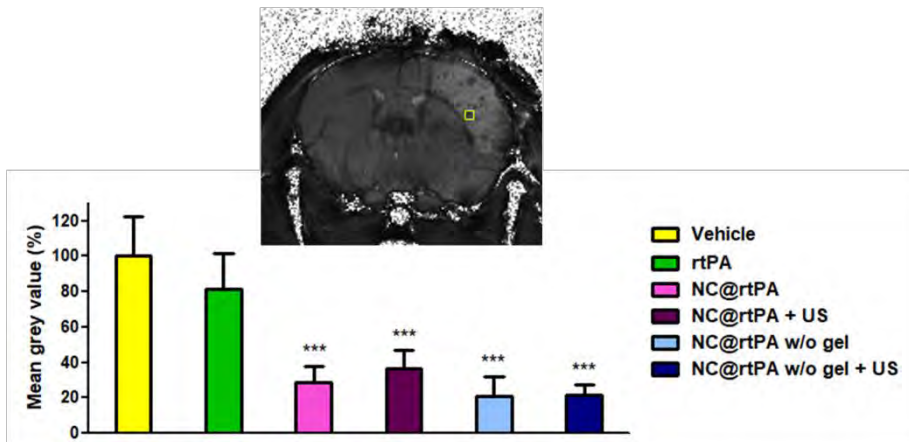


Figure 84. Quantification of mean grey value. All data mean  $\pm$  SD. In all statistical significance was assessed by the *t*-test: each sample was compared with the vehicle group ( $P^{***} < 0.001$ ). Nanocapsules with rtPA and gelatin (NC@rtPA), nanocapsules with rtPA and without gelatin (NC@rtPA w/o gel).

We also measured hypo-signals through the area fraction of T2\*-weighted images. The area highlighted in red in the ischemic region was significantly increased in the group treated with NCs respect to the vehicle group ( $P < 0.05$ ) in the NC@rtPA, NC@rtPA without gelatin and NC@rtPA without gelatin + US groups (Figure 85). However, as in the method using the mean grey value, no differences were found in the groups treated with NCs, establishing that both methods did not showed differences in the target with gelatin.

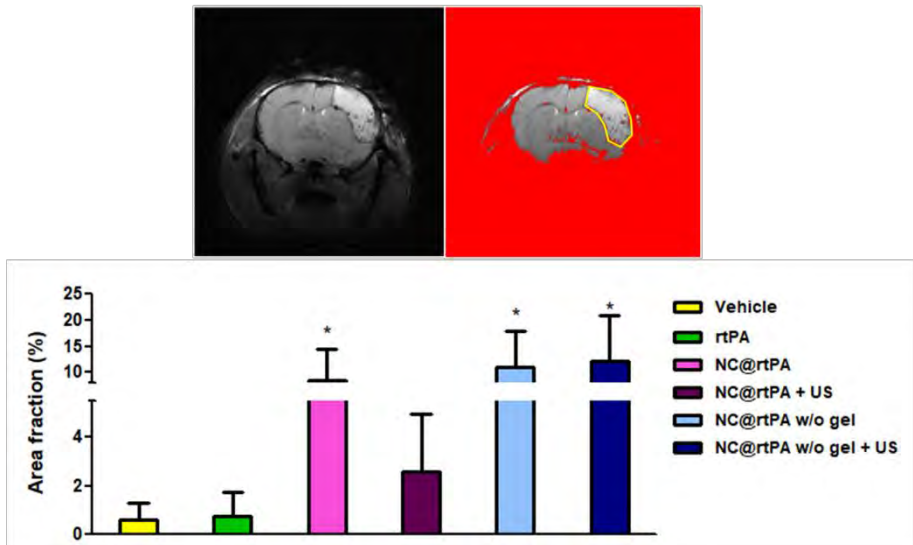


Figure 85. Quantification of mean area fraction. All data mean  $\pm$  SD. In all statistical significance was assessed by the *t*-test; each sample was compared with the vehicle group ( $P^* < 0.05$ ). Nanocapsules with rtPA and gelatin (NC@rtPA), nanocapsules with rtPA and without gelatin (NC@rtPA w/o gel).

#### 10.4.4. Histology

Hematoxylin and eosin staining was performed in ischemic mice treated with NC@rtPA and NC@rtPA without gelatin to study if the hypo-signals found in the MRI analysis was hemorrhages or the iONPs contrast.

Stains showed small microhemorrhages in the ischemic region that are not fully localized with MRI signals. Also the microhemorrhages do not appear to be large enough to be detectable by MRI (Figure 86).

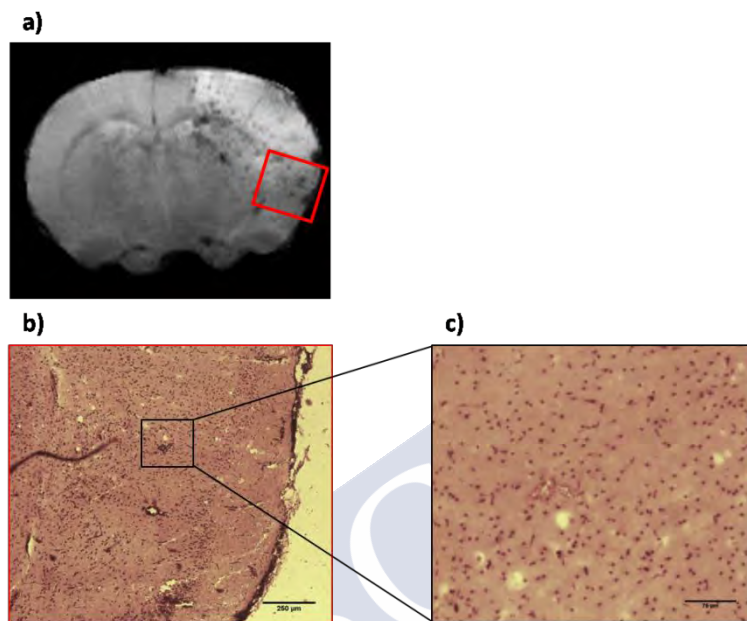


Figure 86. Hematoxylin and eosin staining. a) MRI slice corresponding to the staining. b) Hematoxylin and eosin staining (scale bar is 250  $\mu\text{m}$ ). c) Hematoxylin and eosin staining (scale bar is 75  $\mu\text{m}$ ).

## 10.5. Biodistribution

Finally, taking advantage of the composition of the ioNPs, we decided to analyze the amount of Fe of all the organs of animals to study the biodistribution of the NCs. This was carried out using the ICP-MS analysis, and quantifying the amount of Fe in each organ. The mice used to study the release *in vivo* (Section 10.3) and the therapeutic effect (Section 10.4) were sacrificed at the end of the procedure, and the organs were analyzed.

Figure 87 shows that there is no accumulation of Fe in any organ at 40 min (healthy mice to study the release *in vivo*) or 7 days (ischemic mice to study the therapeutic effect) after the treatment administration.

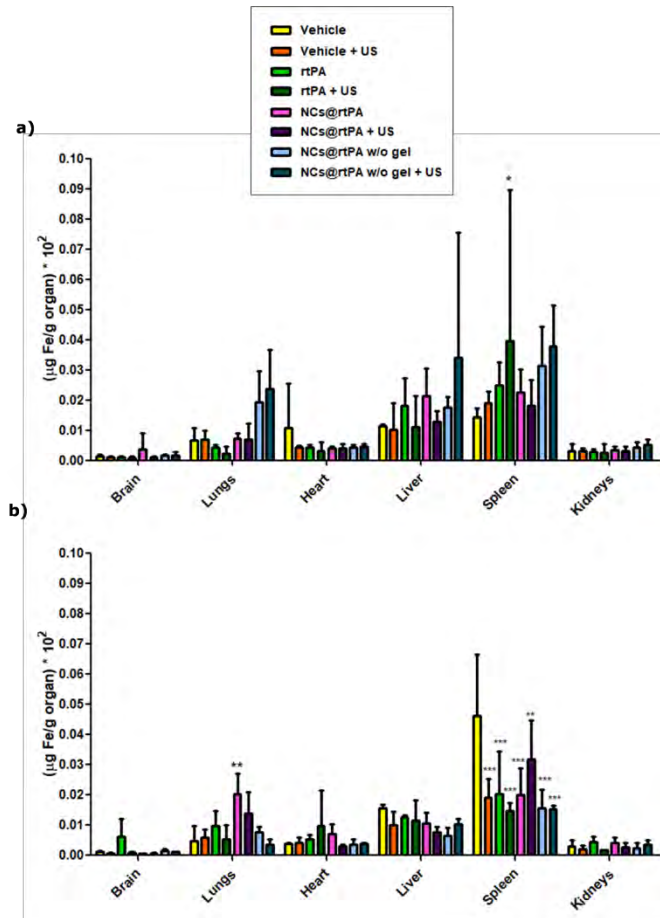


Figure 87. ICP results. a) Amount of Fe/organ 40 min after the administration (mice to study the release *in vivo*). b) Amount of Fe/organ 7 days after the treatment administration (mice to study the therapeutic effect). Nanocapsules with rtPA and gelatin (NC@rtPA), nanocapsules with rtPA and without gelatin (NC@rtPA w/o gel).





Discussion

---



## 11. Section I: *In vitro* optimization of rtPA nanocapsules

rtPA is considered the gold standard drug treatment of ischemic stroke. Nonetheless, not all the patients treated with rtPA achieve recanalization, and it is only applicable to less than 10-20 % of the patients due to its narrow therapeutic window, risk of sICH and neurotoxicity. Furthermore, rtPA has a short half-life in the bloodstream, less than 5 min, what makes its administration complex, requiring an initial bolus injection followed by continuous systemic perfusion to achieve and keep the therapeutic dose in blood<sup>255</sup>. Several strategies have been developed to increase both the circulation half-life of rtPA and the thrombolytic activity, such as its encapsulation in NPs. An innovative approach in that regard is the use of an external trigger to release the rtPA in the ischemic region, being US an effective trigger that is already approved for use in ischemic stroke<sup>163</sup>. Using gelatin to create NC would have the advantage of use it as a component to bind to the vWF of thrombi<sup>214</sup> and as an internal trigger release to be degraded by MMP<sup>176, 177</sup>. This approach was successfully tested in cardiology, supporting the use of this system in ischemic stroke, as discussed next.

Initially, we carried out a study following the publication of Kawata et al<sup>214</sup> and we reproduced the simple synthesis protocol, which consist in mixing rtPA, gelatin and Zn acetate. To study whether this system effectively prevented rtPA activity and recovered it

through the application of US, we performed two *in vitro* activity assays. On one hand, a commercial activity kit was carried out demonstrating that without the application of US there was not any rtPA activity, however, when the activity was measured in encapsulated rtPA with US, the activity was fully recovered. This formulation was even tested in *in vitro* clots, demonstrating that the fibrinolytic activity followed the same pattern that in the previous experiment. Clots treated with encapsulated rtPA only reduced its weight by 21 %, while with the application of US the clot weight was reduced by 39 %, a similar result as the treatment **with "free" rtPA**. This was in accordance with the publication of Kawata et al<sup>214</sup> in which rtPA activity was 50 % reduced and completely recovered by US application *in vitro*. The next step was to administer this system to healthy mice and extract blood to study the release of the rtPA *in vivo*. However, the results showed that the release of the rtPA was independent of US, and we observed the same rtPA activity in all the groups treated with rtPA (**"free" or** encapsulated with and without US) These results was in disagreement with the above publication, in which rtPA plasmatic activity in the group treated with encapsulated rtPA was 71 % lower than the rtPA treatment, and it was recovered by the US. Despite following an easy and simple protocol, and the similarity of the *in vitro* results with the original work, the *in vivo* assay showed that this formulation was no stable when it was administered in mice. Thus, these complexes of rtPA, gelatin and Zn acetate do not have the right standards for testing the therapeutic effect of encapsulated rtPA as they were not stable enough to carry out *in*

*in vivo* studies, and therefore this first formulation was discarded for further experiments.

Due to these preliminary results, we decided to perform a more stable system, consisting in encapsulate first the tPA inside  $\text{CaCO}_3$  cores and then coat those cores with several layers of polymers following a LbL technique, a versatile method which allows the encapsulation of proteins without expose them to severe conditions, and the use of different polyelectrolyte to recover these cores<sup>219</sup>. In our case, we used two proteins labeled with FITC to encapsulate; one was rtPA and the other BSA, which was used to perform the characterization of the NCs.

One of the most important aspects when encapsulating proteins is to know the amount of protein within the NCs. In terms of encapsulation efficiency, (amount of protein encapsulated in relation to the amount of protein added in the synthesis) our systems shown 1.5 % and 24.4 % for BSA and rtPA nanocores, respectively. The reported amount of rtPA encapsulated in other studies varies a lot, since 6 %<sup>256</sup> to 98 %<sup>257</sup>, depending on the experimental design. We ascribe the relatively high encapsulation efficiency of the rtPA due to the influence of proteins in the biomineralization of  $\text{CaCO}_3$ <sup>258</sup>. We performed a theoretical calculation of the maximum amount of rtPA that could be encapsulated per NC, obtaining a maximum of 0.37 pg of rtPA for a 800 nm NC. After the synthesis of the NC@rtPA we achieved between 0.02-0.05 pg rtPA/NC, which was calculated by fluorescence (rtPA concentration) and flow cytometry analysis (number of NCs), achieving 13 % of the maximum loading.

It is important to note that each new synthesis was characterized, using the corresponding rtPA calibration curve to know the amount of protein, and by cytometry to know the number of capsules and their profile. In this way, both for *in vitro* and *in vivo* experiments, the amount of rtPA was known accurately in order to be able to compare it with the appropriate controls.

We performed three types of NCs depending on the number of bL (2, 4 or 6). To accomplish the LbL we used PSS/PDACMAC as negative and positive polyelectrolytes, ioNPs and gelatin. PSS/PDACMAC LbL systems have been widely used *in vitro*, showing insignificant toxicity<sup>259, 260</sup>. There are other polyelectrolytes more biocompatible, such as chitosan, poly-L-arginine, poly-L-lysine<sup>219, 224</sup>, with which the same methodology could be carried out without important modifications. However, for our purpose, the robustness of the non-biodegradable PSS/PDADMAC system is well-suited to that end.

NC@BSA with 2bL, 4bL and 6bL were employed to evaluate the NCs strength and to determine the minimum number of suitable polyelectrolyte bL. Regardless of the number of bL, all these systems were stable during one week. Typically, macromolecules having relatively high molecular weights (~above 1-10 kDa) cannot diffuse in or out through the semipermeable LbL shell (pores size ~ 3-5 nm) as shown extensively with different encapsulated macromolecules in LbL microcapsules<sup>223, 231, 261</sup>. In the case of microcapsules (diameter around 5  $\mu\text{m}$ ) at least a 4bL structure is typically used to prevent cargo leaking<sup>262</sup>. In contrast with them, our 800 nm NCs are stable with only 2bL.

Next, in order to demonstrate US-triggered protein release from the cavity of NCs and to optimize our sonosensitive nanocarrier, we used the NC@BSA with increasing number of polyelectrolyte bL (2, 4 or 6), and we exposed them to US during 15 or 120 min. The US parameters (0.72 W/cm<sup>2</sup>, 2 MHz) were the same as in clinical transcranial Doppler sonography<sup>244</sup>. In the present work, with 15 min US application, fluorescence analysis showed that only the 2bL NCs showed substantial BSA release (50 %). After 120 min US application, again, only in the 2bL system showed BSA release (> 60 %). However, 4bL and 6bL did not response to US, with both 15 and 120 min of exposure. The response to the US depending on the number of bL is in concordance with other works, which described that the greater the number of layers, using the same ultrasound parameter, the smaller deformation of the LbL capsules<sup>234</sup>. In terms of the amount of protein released, these *in vitro* results are in agreement with other similar capsules, which obtained the same release using similar US parameters in doxorubicin LbL microcapsules<sup>230</sup>.

Furthermore, we analyzed the properties of our nanocapsules as contrast agents, which had a layer of doped ioNPs, widely used material, to confer MRI capabilities to our carrier. We measured a relaxivity of 409.1 mM<sup>-1</sup>s<sup>-1</sup> in T<sub>2</sub>, showing a promising performance as contrast agents compared with other commercial agents<sup>263</sup> and other studies in the field of drug delivery systems<sup>264</sup>. This contrast properties were tested *in vivo*, after intracerebral administration, and compared with a vehicle group showing a decrease of signal intensity around 64 % in T<sub>2</sub>-weighted image and 78 % in T<sub>2</sub>\*-

weighted image. This validates its use as contrast agent that together with the drug delivery properties make these nanostructures a useful tool in the stroke field.

Based on the stability and US-release study of NC@BSA, we chose 2bL to perform the NC@rtPA. Both leaking and US-release *in vitro* were performed with the encapsulated rtPA in 2bL NCs with and without gelatin, showing the same behavior as NC@BSA. In the leaking study, it only showed residual rtPA in the SN after one week. The behavior of NC@rtPA is similar to the NC@BSA, exhibiting 50 % of rtPA release from the NCs after the US application. This rtPA release by applying US is in agreement with other studies which obtained similar results<sup>204</sup>. Nevertheless, some works demonstrated a high protein release by applying similar parameters of US, the difference between this work and ours is that they used MB more sensible to US and they applied it during 1 h<sup>265</sup>.

Later, we carried out different assays to evaluate the rtPA bioactivity, both inside the NCs and once released from them by US. First, we used a chromogenic substrate widely used in similar studies<sup>170, 211, 266</sup>. It was used to quantify the rtPA-FITC activity in solution, inside the CaCO<sub>3</sub> cores, in the cavity of NCs and after the US application. Notice that due to the low MW of the chromogenic substrate (MW = 659 Da), it can pass through the pores of both the porous CaCO<sub>3</sub> and the semipermeable LbL shell, thereby allowing for quantifications rtPA activity in all the scenarios. In all the cases we found the same activity compared with the Alteplase, which confirms that the labeling with FITC, the nanocores



synthesis, the LbL technique, the dissolution of the core and the US application did not affect the rtPA activity. Additionally, in order to dissect whether the encapsulated rtPA is protected from its main inhibitor (PAI-1), **“free” and encapsulated rtPA were incubated with PAI-1** and the chromogenic substrate. Conversely to what happens with the substrate, PAI-1 (MW=43 kDa) cannot cross the semipermeable shell. As expected, PAI-1 inhibited the activity of non-encapsulated rtPA. In contrast, encapsulated rtPA kept its activity because PAI-1 cannot diffuse through the LbL porous shell due to its size. From our knowledge this is the first study in which the PAI-1 protection is tested, that is particularly relevant since PAI-1 is an rtPA inhibitor that is present in the bloodstream and therefore, as it anticipates the potential benefits of using *in vivo* the NC proposed; that is, rtPA half-life in blood may be greatly improved by encapsulation in NCs.

The main drawback of the substrates used in this work is that the measured activity is related to the amidolytic activity of the rtPA, rather than to the fibrinolytic activity. To demonstrate that the fibrinolytic activity was not affected, a clot assay in a microwell plate was performed. The fibrinolytic activity was evaluated indirectly, measuring the absorbance (520 nm) that increases as the clots dissolve. NC@rtPA without US partially dissolved the clots, which we ascribe to the residual rtPA leaking. In the case of NC@rtPA + US, clots were dissolved as in the group treated with **“free” rtPA, showing 1.6 times more thrombolysis** than the group treated with NC@rtPA. Despite just being able to release 50 % of all the rtPA encapsulated, as it was discussed previously, the

fibrinolytic activity achieved is the same than in the group treated with "free" rtPA. The fibrinolytic activity is particularly noteworthy because is one of the most important characteristics associated with the clinical applications, reason why it is tested in almost all the studies that encapsulate rtPA. For example, in the publication of Jin H. et al the fibrinolysis was increased after applying US to the nanosystem that encapsulates uPA, and they also found that some fibrinolysis occurs when the clot is incubated with the NCs without US<sup>265</sup>.

The NC@tPA developed here, with 2bL, and coated with and without gelatin, showed a remarkable stability, much higher than the first system developed with tPA, gelatin and Zn acetate, that showed negligible or residual tPA release under storage, and protection front tPA inhibitors. Also, this 2bL NC@tPA showed a US-triggered release and both amidolytic and fibrinolytic activity, making this systems ideal for the goal of this project. For all the mentioned reasons, we selected the NC@rtPA for the *in vivo* studies discussed next.

## 12. Section II: *In vivo* studies of rtPA nanocapsules

In this section the release of the NC@rtPA and its therapeutic effect were studied *in vivo*. First, we studied the US safety in the brain and the NC toxicity *in vivo*. The rationale for performing the security assay on the use of US is due to its relation with the BBB disruption. Several investigators have used frequencies of kHz to accelerate thrombolysis, which resulted in an increase in the risk of intracerebral hemorrhages and tissue injury<sup>267-269</sup>. Furthermore, the clinical trial TRUMBI, in which 300 kHz was used, had to be stopped prematurely due to augmented sICH events<sup>128</sup>. Mechanisms by which low frequencies are related to an increase of hemorrhages are due to abnormal permeability of the BBB caused by this frequency<sup>270</sup>. In contrast, 2 MHz US has shown to increase thrombolysis without risk both *in vivo* and in clinical trials, reason why we decided to use the same parameters<sup>126, 243</sup>. We demonstrated that 2 MHz US did not damage the BBB in healthy animals, even after 40 min exposure, and it did not increase the BBB disruption in ischemic animals. In our case, the study was carried out with EB, which binds to albumin and can only cross the BBB when it is damaged<sup>247</sup>. Regarding the NC toxicity, three standard toxicity markers were evaluated after i.v. administration of NC@rtPA (1 mg/kg rtPA dose, bolus): GOT and GPT as hepatotoxicity markers, and creatinine levels as nephrotoxicity marker. These markers are widely used to assess toxicity after

administration of nanomaterials in rodent models, since liver and kidneys are the most likely recipients of the nanoparticles after i.v. administration<sup>249</sup>. After 7 days monitoring the toxicity markers, the blood analysis showed normal enzymatic levels, demonstrating the low or even negligible toxicity profile of NC@tPA *in vivo*. Despite our initial concerns about the possible toxicity of the polymers used in the synthesis of NC, the NC did not show any toxicity *in vivo*, even after applying US.

Next, the *in vivo* enzymatic activity of US-released rtPA was quantified in extracted plasma samples before the treatment. All the treatments were administered i.v. as bolus and at final concentration of 1 mg/kg rtPA. Additionally, a higher dose (10 mg/kg, 10 % bolus + 90 % infusion) of non-encapsulated rtPA was administered as a control following the current administration protocol used in the clinic and in other preclinical studies. In preclinical mouse models, the 10-fold rtPA dose is motivated by the characteristics of the fibrinolytic system in rodents, which is known to be about 10 times less sensitive to rtPA than in humans<sup>271</sup>. In this study, NC@rtPA showed a similar activity profile as 1 mg/kg rtPA. However, when US was applied a completely new trend arose, rtPA activity increased over time, reaching about 3.5-fold and 2.5-fold increase compared with 1 mg/kg or 10 mg/kg free rtPA, respectively, after 40 min. These activity values are even higher than the rtPA activity observed in the group treated with rtPA perfusion. This result is particularly important as it demonstrates that the half-life of rtPA can be greatly enhanced by encapsulation in our sonosensitive NCs. This would be a great

advantage compared to the current rtPA formulation, because we could increase the profits of the i.v. administration that remains the routine treatment during the acute phase of ischemic stroke and can be easily managed in the stroke units. Despite the many studies performed on nanocarriers with rtPA, only a few investigated the circulation time in blood. The main approaches to increase the half-life of the rtPA *in vivo* have been the used of PEG, as a molecule to camouflage the protein or for coupling to the liposomes membrane<sup>185, 186, 196, 198</sup>. In recent years, a new strategy has emerged in the field of the drug delivery systems, which is the use of cell membranes to increase the circulation time of nanosystems. In this context, platelets and red blood cells have been used to attach rtPA on the NPs surface<sup>216-218</sup>. Both PEG and biomimetic systems have resulted in the increase of rtPA half-life to about 2 hours. In this study, despite knowing that after 40 min rtPA plasmatic activity is higher than in the group which received the regular administration of rtPA, we are not able to quantify the half-life due to experimental limitations on blood collection. Ideally, blood samples should be obtained for a longer period of time, but the volume needed for each measurement is too large (200  $\mu$ L) for the total amount of blood a mouse has (~3 mL).

Another point to emphasize is the profile found in the NC@rtPA without gelatin and NC@rtPA without gelatin + US groups. In both cases rtPA activity increased over time, probably due to rtPA release from the NC, and US was not necessary to release the rtPA when the gelatin is not added to the NCs, a behavior that was not observed *in vitro*. This could be partially explained by the surficial

properties of the NC. Surface charge of NC is one of the remarkable parameters that determine its fate *in vivo*. It has been demonstrated that highly cationic or anionic NPs are rapidly cleared from circulation by the RES (reticuloendothelial system), which could explain the performance of our two different NCs. The fact that NC@rtPA without gelatin had a highly negative zeta potential (-40 mV) could cause increased uptake by the liver and the immediate release of the rtPA without the US application, while NC@rtPA (with gelatin) that had a slightly positive zeta potential (+15 mV) could be maintained stable in circulation for longer time<sup>272</sup>. Additionally, it is widely studied that gelatin can improve the pharmacokinetic profile due to the presence in its structure the RGD sequence, what makes it have low antigenicity, prolong its circulatory time and evade the RES<sup>273, 274</sup>. Overall, everything indicates that the gelatin is a crucial component to maintain the stability and response to US of the NCs *in vivo*.

Then, all NCs (with and without gelatin) were tested in a thromboembolic model of ischemia in mice, in which the beneficial effect rtPA-induced reperfusion is similar to those occurring in humans<sup>74</sup>. In agreement with the clinical data that suggest that early rtPA administration is the optimal strategy<sup>275</sup>, we administered the different treatment 30 min after the ischemia. In order to analyze the therapeutic effect, three aspects were analyzed: reperfusion, infarct volume and HT.

As it was stated before, there are inherent differences in the fibrinolytic system between animal and human studies, being 10-fold less sensitive the murine system. This has meant that most of

the studies have been carried out using a rtPA high-dose (10 mg/kg)<sup>271</sup>. In our study, we used 10 mg/kg rtPA (bolus + perfusion) and 1 mg/kg rtPA (bolus), and we found that there were no differences between the two doses, what is in accordance with other studies that suggest that the correct dose in murine models is 1 mg/kg<sup>276</sup>. On the other hand, also related to the reperfusion rates, it is interesting to note that conversely what happens in other studies we did not find a high improvement in the recanalization rate or infarct volume when we applied US or rtPA+US compared with rtPA alone. However, in the literature it is described higher thrombolysis rates *in vivo* that could be explained because the majority of studies used MB, which increase the thrombolytic efficacy of US<sup>277-279</sup>.

An interesting point was that among all groups treated with NCs, the experimental group treated with NC@rtPA (with gelatin) + US was the only that showed therapeutic effect, respect to the rest of the groups treated with NCs (without gelatin, without gelatin + US, with gelatin without US). This can be explained by: i) the stability of NC@rtPA in the bloodstream; ii) they can reach the thrombus; and iii) they can release the rtPA from the cavity of the NC by the US application. Contrary to what we had hypothesized, MMP are not able to work as an internal trigger release by degrading the gelatin. If this had happened the group treated with NC@rtPA would have shown a reduction in the infarct volume. This demonstrates that US is crucial to release the rtPA in the occluded region. Comparing our results with other studies, we found higher recanalization rates using NC@rtPA, but it is difficult to compare

because the differences in the target, for example the thrombin<sup>211</sup>, or in the triggering using a magnetic field instead of US<sup>191</sup>. Also the different models of ischemia and the artery occluded difficult the comparison between different systems and the time to administered the treatments.

It is important to remark that despite observing a small reduction in the volume of infarction, the NC@rtPA + US treatment is not better than the administration of "free" rtPA.

All the groups that received NCs increased the infarct volume compared with controls, what appears to be an accumulation effect of them in the ischemic region that cause a microvascular occlusion. This increase in the infarct volume is also associated with the thrombus, because when the NCs were administered in healthy animals no hemorrhages or ischemia were found in the brain. This effect is one of the main drawbacks of the LbL capsules due to its size and its lack of elasticity to pass through small and occluded capillaries<sup>228, 280</sup>. Another aspect to consider when analyzing the MRI data is the hypo-signals found in T2\*-weighted images, that also only appeared in the groups treated with NCs. Two considerations make us believe that these signals are the NCs, which have ioNPs between the layers. One is associated to the MRI signal in the brain, in relation to the TE in T2\*-weighted images, which are similar to previous studies in which mesenchymal cells labeled with magnetite NPs were injected through the ICA, that is directly into the brain<sup>281, 282</sup>. On the other hand, and discarding the possibility of NC to cause hemorrhages, the signal of the hemorrhages changes along the days, becoming



hyper-signals due to the high amount of Fe<sup>283</sup>, <sup>284</sup>. As it was showed in the 3 days MRI, these signals are disappearing or becoming fainter. Moreover, the histological analysis using hematoxylin-eosin carried out afterwards discarded the presence of hemorrhage detectable by MRI in the brain. Furthermore, we tried to quantify the hypo-signals in the ischemic region to study if the target was most successful with the NC@rtPA with or without gelatin, but the results showed that there were not differences. The MRI study confirmed the presence of the NC in the brain, mostly localized in the ischemic region, and proving that these systems could be use as a targeted delivery system of rtPA to thrombi, although some modification should be made to improve the therapeutic efficacy, such as smaller particle size and higher release rate.

We have demonstrated that these systems were stable and protected the rtPA activity *in vitro*. Furthermore, they only released the protein when the US was applied, showing sensitivity to US. The administration of NC *in vivo* in healthy animals showed two important findings: gelatin was necessary to maintain the NC@rtPA stability once administered, and we could reach higher activity of rtPA in plasma administering NC@rtPA (1 mg/kg) as bolus than rtPA at a dose 10 times higher as bolus and perfusion. The study in ischemic animals to prove the therapeutic effect showed that the i.v. administration in the tail vein allowed the NC to reach the ischemic region. A point to remark is that animals treated with NC@rtPA and US manifested higher recanalization rates than the rest of the groups treated with the NCs. However,

the infarct volume in this group was larger than the groups treated with “free” rtPA, so that improvements in the formulation of NCs should be taken into account for increase the therapeutic effect.

Overall, we have proved that LbL NCs are promising nanocarriers for the triggered release of rtPA in the brain with potential application in ischemic stroke.





Conclusions

---



### 13. Section I: *In vitro* optimization of rtPA nanocapsules

- NC@rtPA with a diameter of 800 nm were successfully synthesized by the LbL technique, using PSS, PDACMAC, ioNPs and gelatin, in CaCO<sub>3</sub> templates.
- rtPA was successfully encapsulated in the nanostructures, achieving rtPA loadings between 0.02-0.05 pg rtPA/NCs, what corresponds to 5-13 % of the maximum theoretical loading capacity of the system.
- 2, 4 and 6bL NCs were shown to maintain the stability of the rtPA encapsulation upon storage, at least for one week.
- The formulation process did not affect the activity of rtPA. Encapsulated rtPA inside the NCs maintained its activity after the nanocores synthesis, the LbL process, the dissolution of the CaCO<sub>3</sub> and after the US application.
- Encapsulated rtPA was protected from its inactivation by its main endogenous inhibitor PAI-1.
- 2bL NCs showed the best response to US, showing a 50 % release after 15 min of US exposition. The released rtPA maintains its amidolytic and fibrinolytic activity.
- The developed NC@rtPA were also visualized by MRI. When the NCs were injected in the brain parenchyma they

showed a decrease in the signal of 64 % in T2-weighted image and 78 % in T2\*-weighted image.

#### 14. Section II: *In vivo* studies of rtPA nanocapsules

- The application of US in healthy and ischemic brains did not show disruption of the BBB, validating the security of the US in animal models.
- The i.v. administration of the NC did not show ischemic or hemorrhagic damage. Furthermore, the analysis of hepatotoxic and nephrotoxic makers did not vary along the days, demonstrating the safety of the NC@rtPA.
- rtPA plasmatic activity after the NC@rtPA administration and US application was maintained elevated during at least 40 min, which demonstrates an increase in half-life of rtPA by encapsulating in NC.
- The activity of the released rtPA from the NCs was ~ 3.5-fold-higher compared to the same amount of non-encapsulated rtPA (1 mg/kg).
- In addition, NC@rtPA without gelatin showed an augment in the rtPA plasmatic activity during the same time, independent on the US application, demonstrating that the

gelatin was a crucial component for maintaining the stability *in vivo* and the response to US.

- The administration of NC@rtPA with US application showed an increase in the number of reperfused animals and a decrease in the infarct volume, compared to the rest of the groups treated with NCs.
- The therapeutic effect of the NC@rtPA is not better than the **treatment with "free" rtPA**, although increase the *in vivo* half-life of the treatment.
- T2\*-weighted images illustrated the appearance of hypo-signals in the ischemic region in all the groups treated with NCs (with and without gelatin and US). This demonstrated the targeted delivery of the NC to the ischemic region.
- Hematoxylin-eosin staining confirmed that the hypo-signals detected in the MRI studies were not hemorrhages.







Conclusiones

---



## 15. Sección I: Optimización *in vitro* de las nanocápsulas con rtPA

- Se sintetizaron nanocápsulas que encapsulan rtPA con un diámetro de 800 nm. Para ello se utilizó la técnica del **“layer-by-layer”, utilizando PSS; PDACMAC, nanopartículas de óxido de hierro y gelatina para recubrir núcleos de CaCO<sub>3</sub>.**
- El rtPA ha sido encapsulado en las nanoestructuras logrando cargas de entre 0.02-0.05 pg rtPA/NC, lo que corresponde a un 5-13 % de la máxima carga teórica que podría tener el nanosistema.
- Nanocápsulas de 2, 4 y 6 bicapas han demostrado mantener la estabilidad del rtPA durante el almacenamiento, al menos durante una semana.
- El proceso de formulación no afectó a la actividad del rtPA. El rtPA encapsulado dentro de las nanocápsulas mantuvo su actividad tras las síntesis de los núcleos, el proceso de **“layer-by-layer”, la disolución de los núcleos de CaCO<sub>3</sub>** y tras aplicar ultrasonidos.
- El rtPA encapsulado fue protegido de su inactivación por su principal inhibidor endógeno, el PAI-1.

- Nanocápsulas de 2 bicapas mostraron ser las más óptimas para responder a los ultrasonidos, mostrando un 50 % de liberación tras la aplicación de estos durante 15 minutos. La liberación de rtPA mantuvo su actividad amidolítica y fibrinolítica.
- El desarrollo de las nanocápsulas de rtPA fueron estudiadas mediante resonancia magnética. Cuando las nanocápsulas fueron inyectadas en el parénquima cerebral mostraron una disminución de la señal de T2 de un 64 % y de un 78 % de la señal de T2\*.

## 16. Sección II: Estudio *in vivo* de las nanocápsulas con rtPA

- La aplicación de ultrasonidos en animales sanos e isquémicos no mostró disrupción de la barrera hematoencefálica, validando la seguridad de los ultrasonidos en modelos animales.
- La administración intravenosa de las nanocápsulas no mostró daño isquémico ni hemorrágico. Además, el análisis de marcadores de nefrotoxicidad y hepatotoxicidad no varió a lo largo de los días, demostrando la seguridad de las nanocápsulas con rtPA.

- La actividad plasmática del rtPA tras la administración de las nanocápsulas (con gelatina) y la aplicación de ultrasonidos se mantuvo elevada al menos durante 40 minutos, lo que demostró un aumento en la vida media del rtPA mediante su encapsulación.
- La actividad del rtPA liberado de las nanocápsulas fue 3.5 veces mayor, comparado con la misma cantidad de rtPA no encapsulado (1 mg/kg).
- A mayores, las nanocápsulas sin gelatina mostraron un aumento de la actividad plasmática del rtPA durante el mismo tiempo, independientemente de la aplicación de ultrasonidos, demostrando que la gelatina era un componente crucial para mantener la estabilidad *in vivo* y la respuesta a ultrasonidos.
- La administración de nanocápsulas con rtPA y la aplicación de ultrasonidos mostró un aumento en el número de animales que reperfundieron y que disminuyeron el volumen de infarto, comparado con el resto de los grupos tratados con nanocápsulas.
- El efecto terapéutico de las nanocápsulas con rtPA y ultrasonidos no es mejor que el tratamiento con rtPA sin encapsular, a pesar de aumentar la vida media *in vivo* del tratamiento.
- Las imágenes de resonancia magnética en secuencia T2\* mostraron la aparición de hipo-señales en la región

isquémica en todos los grupos tratados con nanocápsulas (con y sin gelatina, y con y sin ultrasonidos). Esto demostró la liberación dirigida de las nanocápsulas a la región isquémica

- La tinción con hematoxilina-eosina confirmó que las hiposignales detectadas en la resonancia magnética no eran hemorragias.





## Bibliography

---





1. Investigators WMPP. The world health organization monica project (monitoring trends and determinants in cardiovascular disease): A major international collaboration. *Journal of clinical epidemiology*. 1988;41:105-114
2. Rodríguez-Yáñez M FMC, Pérez-, Concha T CJ, Zarranz J. Enfermedades vasculares cerebrales. *Neurología*. 2008;Cuarta Edición ed. Madrid, España: Elsevier España: 337-411
3. Bonita R. Epidemiology of stroke. *The lancet neurology*. 1992;339:342-344
4. Feigin VL, Lawes CM, Bennett DA, Anderson CS. Stroke epidemiology: A review of population-based studies of incidence, prevalence, and case-fatality in the late 20th century. *The lancet neurology*. 2003;2:43-53
5. Díaz-Guzmán J, Egido-Herrero J, Fuentes B, Fernández-Pérez C, Gabriel-Sánchez R, Barberà G, Abilleira S. Incidence of strokes in spain: The iberictus study. Data from the pilot study. *Revista de neurología*. 2009;48:61-65
6. Feigin VL, Lawes CM, Bennett DA, Barker-Collo SL, Parag V. Worldwide stroke incidence and early case fatality reported in 56 population-based studies: A systematic review. *The Lancet Neurology*. 2009;8:355-369
7. Arboix A DJ, Pérez-Sempere A, Álvarez-Sabín J. Ictus: Tipos etiológicos y criterios diagnósticos. *Revista de neurología*. 2002;17:3-12
8. Calandre L, Arnal C, Ortega JF, Bermejo F, Felgeroso B, Del Ser T, Vallejo A. Risk factors for spontaneous cerebral hematomas. Case-control study. *Stroke*. 1986;17:1126-1128
9. Arboix A. Cardiovascular risk factors for acute stroke: Risk profiles in the different subtypes of ischemic stroke. *World journal of clinical cases*. 2015;3:418-429
10. Adams Jr HP, Bendixen BH, Kappelle LJ, Biller J, Love BB, Gordon DL, Marsh 3rd E. Classification of subtype of acute ischemic stroke. Definitions for use in a multicenter clinical trial. Toast. Trial of org 10172 in acute stroke treatment. *Stroke*. 1993;24:35-41
11. Collaborators GLRoS. Global, regional, and country-specific lifetime risks of stroke, 1990 and 2016. *New England Journal of Medicine*. 2018;379:2429-2437
12. Bushnell CD, Chaturvedi S, Gage KR, Herson PS, Hurn PD, Jimenez MC, Kittner SJ, Madsen TE, McCullough LD, McDermott M. Sex differences in stroke: Challenges and opportunities. *Journal of Cerebral Blood Flow & Metabolism*. 2018;38:2179-2191
13. O'Donnell MJ, Chin SL, Rangarajan S, Xavier D, Liu L, Zhang H, Rao-Melacini P, Zhang X, Pais P, Agapay S. Global and regional effects of potentially modifiable risk factors associated with acute stroke in 32 countries (interstroke): A case-control study. *The Lancet Neurology*. 2016;388:761-775

14. Arboix A, García-Eroles L, Oliveres M, Massons JB, Targa C. Clinical predictors of early embolic recurrence in presumed cardioembolic stroke. *Cerebrovascular Diseases*. 1998;8:345-353
15. Stassen JM, Arnout J, Deckmyn H. The hemostatic system. *Current medicinal chemistry*. 2004;11:2245-2260
16. Okafor ON, Gorog DA. Endogenous fibrinolysis: An important mediator of thrombus formation and cardiovascular risk. *Journal of the American College of Cardiology*. 2015;65:1683-1699
17. Pryzdial EL, Lee FM, Lin BH, Carter RL, Tegegn TZ, Belletrutti MJ. Blood coagulation dissected. *Transfusion and Apheresis Science*. 2018
18. Gale AJ. Continuing education course# 2: Current understanding of hemostasis. *Toxicologic pathology*. 2011;39:273-280
19. Furie B, Furie BC. Mechanisms of thrombus formation. *New England Journal of Medicine*. 2008;359:938-949
20. Chapin JC, Hajjar KA. Fibrinolysis and the control of blood coagulation. *Blood Reviews*. 2015;29:17-24
21. De Meyer SF, Andersson T, Baxter B, Bendszus M, Brouwer P, Brinjikji W, Campbell BC, Costalat V, Davalos A, Demchuk A, Dippel D, Fiehler J, Fischer U, Gilvarry M, Gounis MJ, Gralla J, Jansen O, Jovin T, Kallmes D, Khatri P, Lees KR, Lopez-Cancio E, Majoie C, Marquering H, Narata AP, Nogueira R, Ringleb P, Siddiqui A, Szikora I, Vale D, von Kummer R, Yoo AJ, Hacke W, Liebeskind DS. Analyses of thrombi in acute ischemic stroke: A consensus statement on current knowledge and future directions. *International journal of stroke*. 2017;12:606-614
22. Henderson SJ, Weitz JI, Kim PY. Fibrinolysis: Strategies to enhance the treatment of acute ischemic stroke. *Journal of thrombosis and haemostasis : JTH*. 2018;16:1932-1940
23. Castillo J. Fisiopatología de la isquemia cerebral. *Revista de Neurología*. 2000;30:459-464
24. Back T. Pathophysiology of the ischemic penumbra—revision of a concept. *Cellular and molecular neurobiology*. 1998;18:621-638
25. Astrup J, Symon L, Branston N, Lassen N. Cortical evoked potential and extracellular  $K^+$  and  $H^+$  at critical levels of brain ischemia. *Stroke*. 1977;8:51-57
26. Hansen AJ. Effect of anoxia on ion distribution in the brain. *Physiological reviews*. 1985;65:101-148
27. Blank Jr W, Kirshner H. The kinetics of extracellular potassium changes during hypoxia and anoxia in the cat cerebral cortex. *Brain research*. 1977;123:113-124
28. Choi DW. Ionic dependence of glutamate neurotoxicity. *Journal of Neuroscience*. 1987;7:369-379
29. Choi DW, Rothman SM. The role of glutamate neurotoxicity in hypoxic-ischemic neuronal death. *Annual Review of Neuroscience*. 1990;13:171-182

30. White BC, Sullivan JM, DeGracia DJ, O'Neil BJ, Neumar RW, Grossman LI, Rafols JA, Krause GS. Brain ischemia and reperfusion: Molecular mechanisms of neuronal injury. *Journal of the neurological sciences*. 2000;179:1-33
31. Choi DW. Excitotoxic cell death. *Journal of neurobiology*. 1992;23:1261-1276
32. Schiene K, Bruehl C, Zilles K, Qu M, Hagemann G, Kraemer M, Witte OW. Neuronal hyperexcitability and reduction of gabaa-receptor expression in the surround of cerebral photothrombosis. *Journal of Cerebral Blood Flow & Metabolism*. 1996;16:906-914
33. Banasiak KJ, Xia Y, Haddad GG. Mechanisms underlying hypoxia-induced neuronal apoptosis. *Progress in neurobiology*. 2000;62:215-249
34. Grandati M, Verrecchia C, Revaud M, Allix M, Boulu R, Plotkine M. Calcium-independent no-synthase activity and nitrites/nitrates production in transient focal cerebral ischaemia in mice. *British journal of pharmacology*. 1997;122:625-630
35. Nogawa S, Zhang F, Ross ME, Iadecola C. Cyclo-oxygenase-2 gene expression in neurons contributes to ischemic brain damage. *Journal of Neuroscience*. 1997;17:2746-2755
36. McDonald ES, Windebank AJ. Mechanisms of neurotoxic injury and cell death. *Neurologic clinics*. 2000;18:525-540
37. Jander S, Kraemer M, Schroeter M, Witte OW, Stoll G. Lymphocytic infiltration and expression of intercellular adhesion molecule-1 in photochemically induced ischemia of the rat cortex. *Journal of Cerebral Blood Flow & Metabolism*. 1995;15:42-51
38. **Rami A, Agarwal R, Botez G, Winckler J.** M-calpain activation, DNA fragmentation, and synergistic effects of caspase and calpain inhibitors in protecting hippocampal neurons from ischemic damage. *Brain research*. 2000;866:299-312
39. Hebert M, Lesept F, Vivien D, Macrez R. The story of an exceptional serine protease, tissue-type plasminogen activator (tpa). *Revue neurologique*. 2016;172:186-197
40. Mendez AA, Samaniego EA, Sheth SA, Dandapat S, Hasan DM, Limaye KS, Hindman BJ, Derdeyn CP, Ortega-Gutierrez S. Update in the early management and reperfusion strategies of patients with acute ischemic stroke. *Critical care research and practice*. 2018;2018
41. Chamorro A, Dirnagl U, Urra X, Planas AM. Neuroprotection in acute stroke: Targeting excitotoxicity, oxidative and nitrosative stress, and inflammation. *The Lancet. Neurology*. 2016;15:869-881
42. Castillo J, Dávalos A, Marrugat J, Noya M. Timing for fever-related brain damage in acute ischemic stroke. *Stroke*. 1998;29:2455-2460

43. Campos F, Blanco M, Barral D, Agulla J, Ramos-Cabrer P, Castillo J. Influence of temperature on ischemic brain: Basic and clinical principles. *Neurochemistry international*. 2012;60:495-505
44. Vieites-Prado A, Iglesias-Rey R, Fernandez-Susavila H, da Silva-Candal A, Rodriguez-Castro E, Grohn OH, Wellmann S, Sobrino T, Castillo J, Campos F. Protective effects and magnetic resonance imaging temperature mapping of systemic and focal hypothermia in cerebral ischemia. *Stroke*. 2016;47:2386-2396
45. Kaur H, Prakash A, Medhi B. Drug therapy in stroke: From preclinical to clinical studies. *Pharmacology*. 2013;92:324-334
46. Chamorro Á, Amaro S, Castellanos M, Segura T, Arenillas J, Martí-Fàbregas J, Gállego J, Krupinski J, Gomis M, Cánovas D. Safety and efficacy of uric acid in patients with acute stroke (urico-ictus): A randomised, double-blind phase 2b/3 trial. *The Lancet Neurology*. 2014;13:453-460
47. Hurtado O, Moro MA, Cárdenas A, Sánchez V, Fernández-Tomé P, Leza JC, Lorenzo P, Secades JJ, Lozano R, Dávalos A. Neuroprotection afforded by prior citicoline administration in experimental brain ischemia: Effects on glutamate transport. *Neurobiology of disease*. 2005;18:336-345
48. Secades JJ, Frontera G. Cdp-choline: Pharmacological and clinical review. *Methods and findings in experimental and clinical pharmacology*. 1995;17 Suppl B:1-54
49. Hurtado O, Cardenas A, Pradillo J, Morales J, Ortego F, Sobrino T, Castillo J, Moro M, Lizasoain I. A chronic treatment with cdp-choline improves functional recovery and increases neuronal plasticity after experimental stroke. *Neurobiology of disease*. 2007;26:105-111
50. Dávalos A, Alvarez-Sabin J, Castillo J, Diez-Tejedor E, Ferro J, Martínez-Vila E, Serena J, Segura T, Cruz V, Masjuan J. International citicoline trial on acute stroke trial i, 2012. Citicoline in the treatment of acute ischaemic stroke: An international, randomised, multicentre, placebo-controlled study (ictus trial). *The Lancet Neurology*. 2012;11:349-357
51. Castillo J, Dávalos A, Naveiro J, Noya M. Neuroexcitatory amino acids and their relation to infarct size and neurological deficit in ischemic stroke. *Stroke*. 1996;27:1060-1065
52. Castillo J, Dávalos A, Noya M. Progression of ischaemic stroke and excitotoxic aminoacids. *The Lancet Neurology*. 1997;349:79-82
53. Castillo J, Dávalos A, Noya M. Aggravation of acute ischemic stroke by hyperthermia is related to an excitotoxic mechanism. *Cerebrovascular Diseases*. 1999;9:22-27
54. Castillo M, Babson J. Ca<sup>2+</sup>-dependent mechanisms of cell injury in cultured cortical neurons. *Neuroscience*. 1998;86:1133-1144
55. Ginsberg MD. Current status of neuroprotection for cerebral ischemia: Synoptic overview. *Stroke*. 2009;40:S111-S114

56. Jia M, Njapo SAN, Rastogi V, Hedna VS. Taming glutamate excitotoxicity: Strategic pathway modulation for neuroprotection. *CNS drugs*. 2015;29:153-162
57. Campos F, Sobrino T, Ramos-Cabrer P, Argibay B, Agulla J, Perez-Mato M, Rodriguez-Gonzalez R, Brea D, Castillo J. Neuroprotection by glutamate oxaloacetate transaminase in ischemic stroke: An experimental study. *Journal of cerebral blood flow and metabolism*. 2011;31:1378-1386
58. Campos F, Sobrino T, Ramos-Cabrer P, Castillo J. Oxaloacetate: A novel neuroprotective for acute ischemic stroke. *The international journal of biochemistry & cell biology*. 2012;44:262-265
59. Perez-Mato M, Iglesias-Rey R, Vieites-Prado A, Dopico-Lopez A, Argibay B, Fernandez-Susavila H, da Silva-Candal A, Perez-Diaz A, Correa-Paz C, Gunther A, Avila-Gomez P, Isabel Loza M, Baumann A, Castillo J, Sobrino T, Campos F. Blood glutamate eeat2-cell grabbing therapy in cerebral ischemia. *EBioMedicine*. 2019;39:118-131
60. da Silva-Candal A, Perez-Diaz A, Santamaria M, Correa-Paz C, Rodriguez-Yanez M, Arda A, Perez-Mato M, Iglesias-Rey R, Brea J, Azuaje J, Sotelo E, Sobrino T, Loza MI, Castillo J, Campos F. Clinical validation of blood/brain glutamate grabbing in acute ischemic stroke. *Annals of Neurology*. 2018;84:260-273
61. O'Collins VE, Macleod MR, Donnan GA, Horky LL, van der Worp BH, Howells DW. 1,026 experimental treatments in acute stroke. *Annals of Neurology*. 2006;59:467-477
62. Shi L, Rocha M, Leak RK, Zhao J, Bhatia TN, Mu H, Wei Z, Yu F, Weiner SL, Ma F, Jovin TG, Chen J. A new era for stroke therapy: Integrating neurovascular protection with optimal reperfusion. *Journal of cerebral blood flow and metabolism*. 2018;38:2073-2091
63. Hayashi T, Deguchi K, Nagotani S, Zhang H, Sehara Y, Tsuchiya A, Abe K. Cerebral ischemia and angiogenesis. *Current neurovascular research*. 2006;3:119-129
64. Le Belle JE, Orozco NM, Paucar AA, Saxe JP, Mottahedeh J, Pyle AD, Wu H, Kornblum HI. Proliferative neural stem cells have high endogenous ros levels that regulate self-renewal and neurogenesis in a pi3k/akt-dependant manner. *Cell stem cell*. 2011;8:59-71
65. Arenillas JF, Sobrino T, Castillo J, Davalos A. The role of angiogenesis in damage and recovery from ischemic stroke. *Current treatment options in cardiovascular medicine*. 2007;9:205-212
66. Brea D, Sobrino T, Ramos-Cabrer P, Castillo J. [reorganisation of the cerebral vasculature following ischaemia]. *Revista de Neurología*. 2009;49:645-654
67. Sobrino T, Hurtado O, Moro MA, Rodriguez-Yanez M, Castellanos M, Brea D, Moldes O, Blanco M, Arenillas JF, Leira R, Davalos A,

- Lizasoain I, Castillo J. The increase of circulating endothelial progenitor cells after acute ischemic stroke is associated with good outcome. *Stroke*. 2007;38:2759-2764
68. Becerra-Calixto A, Cardona-Gómez GP. The role of astrocytes in neuroprotection after brain stroke: Potential in cell therapy. *Frontiers in molecular neuroscience*. 2017;10:88
69. Longa EZ, Weinstein PR, Carlson S, Cummins R. Reversible middle cerebral artery occlusion without craniectomy in rats. *Stroke*. 1989;20:84-91
70. Kudo M, Aoyama A, Ichimori S, Fukunaga N. An animal model of cerebral infarction. Homologous blood clot emboli in rats. *Stroke*. 1982;13:505-508
71. Busch E, Kruger K, Hossmann KA. Improved model of thromboembolic stroke and rt-pa induced reperfusion in the rat. *Brain Research*. 1997;778:16-24
72. Tamura A, Graham DI, McCulloch J, Teasdale GM. Focal cerebral ischaemia in the rat: 1. Description of technique and early neuropathological consequences following middle cerebral artery occlusion. *Journal of cerebral blood flow and metabolism*. 1981;1:53-60
73. Chen ST, Hsu CY, Hogan EL, Maricq H, Balentine JD. A model of focal ischemic stroke in the rat: Reproducible extensive cortical infarction. *Stroke*. 1986;17:738-743
74. Orset C, Macrez R, Young AR, Panthou D, Angles-Cano E, Maubert E, Agin V, Vivien D. Mouse model of in situ thromboembolic stroke and reperfusion. *Stroke*. 2007;38:2771-2778
75. Sharkey J, Ritchie IM, Kelly PA. Perivascular microapplication of endothelin-1: A new model of focal cerebral ischaemia in the rat. *Journal of cerebral blood flow and metabolism*. 1993;13:865-871
76. Zivin JA, DeGirolami U, Kochhar A, Lyden PD, Mazzarella V, Hemenway CC, Henry ME. A model for quantitative evaluation of embolic stroke therapy. *Brain Research*. 1987;435:305-309
77. Macrae IM. Preclinical stroke research--advantages and disadvantages of the most common rodent models of focal ischaemia. *British Journal of Pharmacology*. 2011;164:1062-1078
78. Garcia-Bonilla L, Rosell A, Torregrosa G, Salom JB, Alborch E, Gutierrez M, Diez-Tejedor E, Martinez-Murillo R, Agulla J, Ramos-Cabrer P, Castillo J, Gasull T, Montaner J. Recommendations guide for experimental animal models in stroke research. *Neurologia*. 2011;26:105-110
79. Kagitani H, Tagawa M, Hatanaka K, Ikari T, Saito A, Bando H, Okada K, Matsuo O. Expression in e. Coli of finger-domain lacking tissue-type plasminogen activator with high fibrin affinity. *FEBS letters*. 1985;189:145-149
80. Bu G, Williams S, Strickland DK, Schwartz AL. Low density lipoprotein receptor-related protein/alpha 2-macroglobulin

- receptor is an hepatic receptor for tissue-type plasminogen activator. *Proceedings of the National Academy of Sciences of the United States of America*. 1992;89:7427-7431
81. Hajjar KA, Jacovina AT, Chacko J. An endothelial cell receptor for plasminogen/tissue plasminogen activator. I. Identity with annexin ii. *The Journal of biological chemistry*. 1994;269:21191-21197
  82. Correa F, Gauberti M, Parcq J, Macrez R, Hommet Y, Obiang P, Hernangómez M, Montagne A, Liot G, Guaza C. Tissue plasminogen activator prevents white matter damage following stroke. *Journal of Experimental Medicine*. 2011;208:1229-1242
  83. Kuiper J, Otter M, Rijken D, Van Berkel T. Characterization of the interaction in vivo of tissue-type plasminogen activator with liver cells. *Journal of Biological Chemistry*. 1988;263:18220-18224
  84. Fredriksson L, Li H, Fieber C, Li X, Eriksson U. Tissue plasminogen activator is a potent activator of pdgf-cc. *The EMBO journal*. 2004;23:3793-3802
  85. Lopez-Atalaya JP, Roussel BD, Levrat D, Parcq J, Nicole O, Hommet Y, Benchenane K, Castel H, Leprince J, To Van D. Toward safer thrombolytic agents in stroke: Molecular requirements for nmda receptor-mediated neurotoxicity. *Journal of Cerebral Blood Flow & Metabolism*. 2008;28:1212-1221
  86. Docagne F, Parcq J, Lijnen R, Ali C, Vivien D. Understanding the functions of endogenous and exogenous tissue-type plasminogen activator during stroke. *Stroke*. 2015;46:314-320
  87. Casse F, Bardou I, Danglot L, Briens A, Montagne A, Parcq J, Alahari A, Galli T, Vivien D, Docagne F. Glutamate controls tpa recycling by astrocytes, which in turn influences glutamatergic signals. *The Journal of neuroscience*. 2012;32:5186-5199
  88. Zlokovic BV, Wang L, Sun N, Haffke S, Verrall S, Seeds NW, Fisher MJ, Schreiber SS. Expression of tissue plasminogen activator in cerebral capillaries: Possible fibrinolytic function of the blood-brain barrier. *Neurosurgery*. 1995;37:955-961
  89. Rijken DC, Lijnen HR. New insights into the molecular mechanisms of the fibrinolytic system. *Journal of thrombosis and haemostasis : JTH*. 2009;7:4-13
  90. Yepes M, Roussel BD, Ali C, Vivien D. Tissue-type plasminogen activator in the ischemic brain: More than a thrombolytic. *Trends in neurosciences*. 2009;32:48-55
  91. Thiebaut AM, Gauberti M, Ali C, De Lizarrondo SM, Vivien D, Yepes M, Roussel BD. The role of plasminogen activators in stroke treatment: Fibrinolysis and beyond. *The Lancet Neurology*. 2018;17:1121-1132
  92. Parcq J, Bertrand T, Montagne A, Baron A, Macrez R, Billard J, Briens A, Hommet Y, Wu J, Yepes M. Unveiling an exceptional zymogen: The single-chain form of tpa is a selective activator of

- nmda receptor-dependent signaling and neurotoxicity. *Cell death and differentiation*. 2012;19:1983
93. Donnan GA, Davis SM, Parsons MW, Ma H, Dewey HM, Howells DW. How to make better use of thrombolytic therapy in acute ischemic stroke. *Nature Reviews Neurology*. 2011;7:400
  94. Tissue plasminogen activator for acute ischemic stroke. *The New England journal of medicine*. 1995;333:1581-1587
  95. Brott TG, Haley EC, Jr., Levy DE, Barsan W, Broderick J, Sheppard GL, Spilker J, Kongable GL, Massey S, Reed R, et al. Urgent therapy for stroke. Part i. Pilot study of tissue plasminogen activator administered within 90 minutes. *Stroke*. 1992;23:632-640
  96. Haley EC, Jr., Levy DE, Brott TG, Sheppard GL, Wong MC, Kongable GL, Torner JC, Marler JR. Urgent therapy for stroke. Part ii. Pilot study of tissue plasminogen activator administered 91-180 minutes from onset. *Stroke*. 1992;23:641-645
  97. Wahlgren N, Ahmed N, Davalos A, Ford GA, Grond M, Hacke W, Hennerici MG, Kaste M, Kuelkens S, Larrue V, Lees KR, Roine RO, Soenne L, Toni D, Vanhooren G. Thrombolysis with alteplase for acute ischaemic stroke in the safe implementation of thrombolysis in stroke-monitoring study (sits-most): An observational study. *The Lancet Neurology*. 2007;369:275-282
  98. Hacke W, Donnan G, Fieschi C, Kaste M, von Kummer R, Broderick JP, Brott T, Frankel M, Grotta JC, Haley EC, Jr., Kwiatkowski T, Levine SR, Lewandowski C, Lu M, Lyden P, Marler JR, Patel S, Tilley BC, Albers G, Bluhmki E, Wilhelm M, Hamilton S. Association of outcome with early stroke treatment: Pooled analysis of atlantis, ecass, and ninds rt-pa stroke trials. *The Lancet Neurology*. 2004;363:768-774
  99. Hacke W, Kaste M, Bluhmki E, Brozman M, Davalos A, Guidetti D, Larrue V, Lees KR, Medeghri Z, Machnig T, Schneider D, von Kummer R, Wahlgren N, Toni D. Thrombolysis with alteplase 3 to 4.5 hours after acute ischemic stroke. *The New England journal of medicine*. 2008;359:1317-1329
  100. Ma H, Campbell BC, Parsons MW, Churilov L, Levi CR, Hsu C, Kleinig TJ, Wijeratne T, Curtze S, Dewey HM. Thrombolysis guided by perfusion imaging up to 9 hours after onset of stroke. *The New England Journal of Medicine*. 2019;380:1795-1803
  101. Campbell BC, Ma H, Ringleb PA, Parsons MW, Churilov L, Bendzus M, Levi CR, Hsu C, Kleinig TJ, Fatar M. Extending thrombolysis to 4- 5-9 h and wake-up stroke using perfusion imaging: A systematic review and meta-analysis of individual patient data. *The Lancet Neurology*. 2019
  102. Sandercock P, Wardlaw JM, Lindley RI, Dennis M, Cohen G, Murray G, Innes K, Venables G, Czlonkowska A, Kobayashi A, Ricci S, Murray V, Berge E, Slot KB, Hankey GJ, Correia M, Peeters A, Matz



- K, Lyrer P, Gubitz G, Phillips SJ, Arauz A. The benefits and harms of intravenous thrombolysis with recombinant tissue plasminogen activator within 6 h of acute ischaemic stroke (the third international stroke trial [ist-3]): A randomised controlled trial. *The Lancet Neurology*. 2012;379:2352-2363
103. Hill MD, Goyal M, Demchuk AM, Fisher M. Ischemic stroke tissue-window in the new era of endovascular treatment. *Stroke*. 2015;46:2332-2334
104. Dorado L, Millan M, Davalos A. Reperfusion therapies for acute ischemic stroke: An update. *Current cardiology reviews*. 2014;10:327-335
105. Deguchi I, Tanahashi N, Takao M. Clinical study of intravenous, low-dose recombinant tissue plasminogen activator for acute cerebral infarction: Comparison of treatment within 3 hours versus 3-4.5 hours. *Journal of stroke and cerebrovascular diseases*. 2018;27:1033-1040
106. Hacke W, Kaste M, Fieschi C, Toni D, Lesaffre E, von Kummer R, Boysen G, Bluhmki E, Hoxter G, Mahagne MH, et al. Intravenous thrombolysis with recombinant tissue plasminogen activator for acute hemispheric stroke. The european cooperative acute stroke study (ecass). *Journal of the American Medical Association*. 1995;274:1017-1025
107. Yaghi S, Willey JZ, Cucchiara B, Goldstein JN, Gonzales NR, Khatri P, Kim LJ, Mayer SA, Sheth KN, Schwamm LH. Treatment and outcome of hemorrhagic transformation after intravenous alteplase in acute ischemic stroke: A scientific statement for healthcare professionals from the american heart association/american stroke association. *Stroke*. 2017;48:e343-e361
108. Yaghi S, Eisenberger A, Willey JZ. Symptomatic intracerebral hemorrhage in acute ischemic stroke after thrombolysis with intravenous recombinant tissue plasminogen activator: A review of natural history and treatment. *Journal of the American Medical Association*. 2014;71:1181-1185
109. Hacke W, Kaste M, Fieschi C, von Kummer R, Davalos A, Meier D, Larrue V, Bluhmki E, Davis S, Donnan G, Schneider D, Diez-Tejedor E, Trouillas P. Randomised double-blind placebo-controlled trial of thrombolytic therapy with intravenous alteplase in acute ischaemic stroke (ecass ii). Second european-australasian acute stroke study investigators. *The Lancet Neurology*. 1998;352:1245-1251
110. Whiteley WN, Slot KB, Fernandes P, Sandercock P, Wardlaw J. Risk factors for intracranial hemorrhage in acute ischemic stroke patients treated with recombinant tissue plasminogen activator: A systematic review and meta-analysis of 55 studies. *Stroke*. 2012;43:2904-2909

111. Jickling GC, Liu D, Stamova B, Ander BP, Zhan X, Lu A, Sharp FR. Hemorrhagic transformation after ischemic stroke in animals and humans. *Journal of cerebral blood flow and metabolism*. 2014;34:185-199
112. Kharitonova TV, Melo TP, Andersen G, Egado JA, Castillo J, Wahlgren N. Importance of cerebral artery recanalization in patients with stroke with and without neurological improvement after intravenous thrombolysis. *Stroke*. 2013;44:2513-2518
113. Menon BK, Al-Ajlan FS, Najm M, Puig J, Castellanos M, Dowlatshahi D, Calleja A, Sohn SI, Ahn SH, Poppe A, Mikulik R, Asdaghi N, Field TS, Jin A, Asil T, Boulanger JM, Smith EE, Coutts SB, Barber PA, Bal S, Subramanian S, Mishra S, Trivedi A, Dey S, Eesa M, Sajobi T, Goyal M, Hill MD, Demchuk AM. Association of clinical, imaging, and thrombus characteristics with recanalization of visible intracranial occlusion in patients with acute ischemic stroke. *Journal of the American Medical Association*. 2018;320:1017-1026
114. Kharitonova T, Thoren M, Ahmed N, Wardlaw J, von Kummer R, Thomassen L, Wahlgren N, investigators S. Disappearing hyperdense middle cerebral artery sign in ischaemic stroke patients treated with intravenous thrombolysis: Clinical course and prognostic significance. *Journal of Neurology, Neurosurgery & Psychiatry*. 2009;80:273-278
115. Iglesias-Rey R, Rodríguez-Yáñez M, Rodríguez-Castro E, Pumar JM, Arias S, Santamaría M, López-Dequidt I, Hervella P, Correa-Paz C, Sobrino T. Worse outcome in stroke patients treated with rt-pa without early reperfusion: Associated factors. *Translational stroke research*. 2018;9:347-355
116. Seners P, Turc G, Maier B, Mas J-L, Oppenheim C, Baron J-C. Incidence and predictors of early recanalization after intravenous thrombolysis: A systematic review and meta-analysis. *Stroke*. 2016;47:2409-2412
117. Yoo J, Baek JH, Park H, Song D, Kim K, Hwang IG, Kim YD, Kim SH, Lee HS, Ahn SH, Cho HJ, Kim GS, Kim J, Lee KY, Song TJ, Choi HY, Nam HS, Heo JH. Thrombus volume as a predictor of nonrecanalization after intravenous thrombolysis in acute stroke. *Stroke*. 2018;49:2108-2115
118. Molina CA, Montaner J, Arenillas JF, Ribo M, Rubiera M, Alvarez-Sabín J. Differential pattern of tissue plasminogen activator-induced proximal middle cerebral artery recanalization among stroke subtypes. *Stroke*. 2004;35:486-490
119. Shuaib A, Butcher K, Mohammad AA, Saqqur M, Liebeskind DS. Collateral blood vessels in acute ischaemic stroke: A potential therapeutic target. *The Lancet. Neurology*. 2011;10:909-921
120. Miteff F, Levi CR, Bateman GA, Spratt N, McElduff P, Parsons MW. The independent predictive utility of computed tomography

- angiographic collateral status in acute ischaemic stroke. *Brain*. 2009;132:2231-2238
121. Bang OY, Saver JL, Kim SJ, Kim GM, Chung CS, Ovbiagele B, Lee KH, Liebeskind DS. Collateral flow averts hemorrhagic transformation after endovascular therapy for acute ischemic stroke. *Stroke*. 2011;42:2235-2239
  122. Fugate JE, Rabinstein AA. Absolute and relative contraindications to iv rt-pa for acute ischemic stroke. *The Neurohospitalist*. 2015;5:110-121
  123. Barros P. Neurovascular ultrasound in emergency settings: Diagnostic and therapeutic aspects. *Journal of Neurological Disorders & Stroke*. 2015;3:1100
  124. Bader KB, Bouchoux G, Holland CK. Sonothrombolysis. *Therapeutic ultrasound*. Springer; 2016:339-362.
  125. Meairs S. Sonothrombolysis. *Translational neurosonology*. Karger Publishers; 2015:83-93.
  126. Alexandrov AV, Molina CA, Grotta JC, Garami Z, Ford SR, Alvarez-Sabin J, Montaner J, Saqqur M, Demchuk AM, Moye LA, Hill MD, Wojner AW. Ultrasound-enhanced systemic thrombolysis for acute ischemic stroke. *The New England journal of medicine*. 2004;351:2170-2178
  127. Schellinger PD, Alexandrov AV, Barreto AD, Demchuk AM, Tsvigoulis G, Kohrmann M, Alleman J, Howard V, Howard G, Alexandrov AW, Brandt G, Molina CA. Combined lysis of thrombus with ultrasound and systemic tissue plasminogen activator for emergent revascularization in acute ischemic stroke (clotbust-er): Design and methodology of a multinational phase 3 trial. *International journal of stroke*. 2015;10:1141-1148
  128. Daffertshofer M, Gass A, Ringleb P, Sitzer M, Sliwka U, Els T, Sedlaczek O, Koroshetz WJ, Hennerici MG. Transcranial low-frequency ultrasound-mediated thrombolysis in brain ischemia: Increased risk of hemorrhage with combined ultrasound and tissue plasminogen activator: Results of a phase ii clinical trial. *Stroke*. 2005;36:1441-1446
  129. Wright C, Hynynen K, Goertz D. In vitro and in vivo high-intensity focused ultrasound thrombolysis. *Investigative radiology*. 2012;47:217-225
  130. Shaw GJ, Dhamija A, Bavani N, Wagner KR, Holland CK. Arrhenius temperature dependence of in vitro tissue plasminogen activator thrombolysis. *Physics in medicine and biology*. 2007;52:2953-2967
  131. Yenari MA, Palmer JT, Bracci PM, Steinberg GK. Thrombolysis with tissue plasminogen activator (tpa) is temperature dependent. *Thrombosis research*. 1995;77:475-481
  132. Schwarzenberg H, Muller-Hulsbeck S, Brossman J, Gluer CC, Bruhn HD, Heller M. Hyperthermic fibrinolysis with rt-pa: In vitro

- results. *Cardiovascular and interventional radiology*. 1998;21:142-145
133. Chernysh IN, Everbach CE, Purohit PK, Weisel JW. Molecular mechanisms of the effect of ultrasound on the fibrinolysis of clots. *Journal of thrombosis and haemostasis : JTH*. 2015;13:601-609
134. Meunier JM, Holland CK, Lindsell CJ, Shaw GJ. Duty cycle dependence of ultrasound enhanced thrombolysis in a human clot model. *Ultrasound in medicine & biology*. 2007;33:576-583
135. Pitt WG, Hussein GA, Staples BJ. Ultrasonic drug delivery--a general review. *Expert opinion on drug delivery*. 2004;1:37-56
136. Izadifar Z, Babyn P, Chapman D. Mechanical and biological effects of ultrasound: A review of present knowledge. *Ultrasound in medicine & biology*. 2017;43:1085-1104
137. Chen C-J, Ding D, Starke RM, Mehndiratta P, Crowley RW, Liu KC, Southerland AM, Worrall BB. Endovascular vs medical management of acute ischemic stroke. *Neurology*. 2015;85:1980-1990
138. Rodrigues FB, Neves JB, Caldeira D, Ferro JM, Ferreira JJ, Costa J. Endovascular treatment versus medical care alone for ischaemic stroke: Systematic review and meta-analysis. *bmj*. 2016;353:i1754
139. Reddrop C, Moldrich RX, Beart PM, Farso M, Liberatore GT, Howells DW, Petersen K-U, Schleuning W-D, Medcalf RL. Vampire bat salivary plasminogen activator (desmoteplase) inhibits tissue-type plasminogen activator-induced potentiation of excitotoxic injury. *Stroke*. 2005;36:1241-1246
140. Hacke W, Albers G, Al-Rawi Y, Bogousslavsky J, Davalos A, Eliasziw M, Fischer M, Furlan A, Kaste M, Lees KR. The desmoteplase in acute ischemic stroke trial (dias) a phase ii mri-based 9-hour window acute stroke thrombolysis trial with intravenous desmoteplase. *Stroke*. 2005;36:66-73
141. Furlan AJ, Eyding D, Albers GW, Al-Rawi Y, Lees KR, Rowley HA, Sachara C, Soehngen M, Warach S, Hacke W. Dose escalation of desmoteplase for acute ischemic stroke (dedas) evidence of safety and efficacy 3 to 9 hours after stroke onset. *Stroke*. 2006;37:1227-1231
142. Benedict CR, Refino CJ, Keyt BA, Pakala R, Paoni NF, Thomas GR, Bennett WF. New variant of human tissue plasminogen activator (tpa) with enhanced efficacy and lower incidence of bleeding compared with recombinant human tpa. *Circulation*. 1995;92:3032-3040
143. Tanswell P, Modi N, Combs D, Danays T. Pharmacokinetics and pharmacodynamics of tenecteplase in fibrinolytic therapy of acute myocardial infarction. *Clinical pharmacokinetics*. 2002;41:1229-1245

144. Barreto AD. Intravenous thrombolytics for ischemic stroke. *Neurotherapeutics : the journal of the American Society for Experimental NeuroTherapeutics*. 2011;8:388-399
145. Donnan GA, Davis SM, Chambers BR, Gates PC, Hankey GJ, McNeil JJ, Rosen D, Stewart-Wynne EG, Tuck RR. Streptokinase for acute ischemic stroke with relationship to time of administration: Australian streptokinase (ask) trial study group. *Journal of the American Medical Association*. 1996;276:961-966
146. Hommel M, Cornu C, Boutitie F, Boissel JP. Thrombolytic therapy with streptokinase in acute ischemic stroke. *The New England journal of medicine*. 1996;335:145-150
147. Furlan A, Higashida R, Wechsler L, Gent M, Rowley H, Kase C, Pessin M, Ahuja A, Callahan F, Clark WM, Silver F, Rivera F. Intra-arterial prourokinase for acute ischemic stroke. The proact ii study: A randomized controlled trial. Prolyse in acute cerebral thromboembolism. *Journal of the American Medical Association*. 1999;282:2003-2011
148. Kase CS, Furlan AJ, Wechsler LR, Higashida RT, Rowley HA, Hart RG, Molinari GF, Frederick LS, Roberts HC, Gebel JM, Sila CA, Schulz GA, Roberts RS, Gent M. Cerebral hemorrhage after intra-arterial thrombolysis for ischemic stroke: The proact ii trial. *Neurology*. 2001;57:1603-1610
149. Mitchell PJ, Yan B, Brozman M, Ribo M, Marder V, Courtney KL, Saver JL. Plasmin (human) administration in acute middle cerebral artery ischemic stroke: Phase 1/2a, open-label, dose-escalation, safety study. *Journal of stroke and cerebrovascular diseases*. 2017;26:308-320
150. Thijs VN, Peeters A, Vosko M, Aichner F, Schellinger PD, Schneider D, Neumann-Haefelin T, Rother J, Davalos A, Wahlgren N, Verhamme P. Randomized, placebo-controlled, dose-ranging clinical trial of intravenous microplasmin in patients with acute ischemic stroke. *Stroke*. 2009;40:3789-3795
151. Gravanis I, Tsirka SE. Tissue-type plasminogen activator as a therapeutic target in stroke. *Expert Opinion on Therapeutic Targets*. 2008;12:159-170
152. Berekashvili K, Soomro J, Shen L, Misra V, Chen PR, Blackburn S, Dannenbaum M, Grotta JC, Barreto AD. Safety and feasibility of argatroban, recombinant tissue plasminogen activator, and intra-arterial therapy in stroke (artss-ia study). *Journal of stroke and cerebrovascular diseases*. 2018;27:3647-3651
153. Knecht T, Borlongan C, Dela Pena I. Combination therapy for ischemic stroke: Novel approaches to lengthen therapeutic window of tissue plasminogen activator. *Brain Circulation*. 2018;4:99-108
154. Sun YY, Morozov YM, Yang D, Li Y, Dunn RS, Rakic P, Chan PH, Abe K, Lindquist DM, Kuan CY. Synergy of combined tpa-

- edaravone therapy in experimental thrombotic stroke. *PloS one*. 2014;9:e98807
155. Campos F, Qin T, Castillo J, Seo JH, Arai K, Lo EH, Waeber C. Fingolimod reduces hemorrhagic transformation associated with delayed tissue plasminogen activator treatment in a mouse thromboembolic model. *Stroke*. 2013;44:505-511
156. Macrez R, Obiang P, Gauberti M, Roussel B, Baron A, Parcq J, Casse F, Hommet Y, Orset C, Agin V, Bezin L, Berrocso TG, Petersen KU, Montaner J, Maubert E, Vivien D, Ali C. Antibodies preventing the interaction of tissue-type plasminogen activator with n-methyl-d-aspartate receptors reduce stroke damages and extend the therapeutic window of thrombolysis. *Stroke*. 2011;42:2315-2322
157. Wyseure T, Rubio M, Denorme F, Martinez de Lizarrondo S, Peeters M, Gils A, De Meyer SF, Vivien D, Declerck PJ. Innovative thrombolytic strategy using a heterodimer diabody against tafi and pai-1 in mouse models of thrombosis and stroke. *Blood*. 2015;125:1325-1332
158. Lapchak PA, Doyan S, Fan X, Woods CM. Synergistic effect of ajw200, a von willebrand factor neutralizing antibody with low dose (0.9 mg/mg) thrombolytic therapy following embolic stroke in rabbits. *Journal of Neurology and Neurophysiology*. 2013;4
159. Roncal C, Martinez de Lizarrondo S, Salicio A, Chevilley A, Rodriguez JA, Rosell A, Couraud PO, Weksler B, Montaner J, Vivien D, Paramo JA, Orbe J. New thrombolytic strategy providing neuroprotection in experimental ischemic stroke: Mmp10 alone or in combination with tissue-type plasminogen activator. *Cardiovascular Research*. 2017;113:1219-1229
160. Zhang L, Zhang ZG, Zhang RL, Lu M, Krams M, Chopp M. Effects of a selective cd11b/cd18 antagonist and recombinant human tissue plasminogen activator treatment alone and in combination in a rat embolic model of stroke. *Stroke*. 2003;34:1790-1795
161. Dilnawaz F, Acharya S, Sahoo SK. Recent trends of nanomedicinal approaches in clinics. *International journal of pharmaceutics*. 2018;538:263-278
162. Chan WCW. Nanomedicine 2.0. *Acc Chem Res*. 2017;50:627-632
163. Liu S, Feng X, Jin R, Li G. Tissue plasminogen activator-based nanothrombolysis for ischemic stroke. *Expert opinion on drug delivery*. 2018;15:173-184
164. Huang T, Li N, Gao J. Recent strategies on targeted delivery of thrombolytics. *Asian Journal of Pharmaceutics*. 2019
165. Bonnard T, Gauberti M, Martinez de Lizarrondo S, Campos F, Vivien D. Recent advances in nanomedicine for ischemic and hemorrhagic stroke. *Stroke*. 2019;50:1318-1324
166. Gunawan ST, Kempe K, Bonnard T, Cui J, Alt K, Law LS, Wang X, Westein E, Such GK, Peter K, Hagemeyer CE, Caruso F.

- Multifunctional thrombin-activatable polymer capsules for specific targeting to activated platelets. *Advance Materials*. 2015;27:5153-5157
167. Vaidya B, Agrawal GP, Vyas SP. Functionalized carriers for the improved delivery of plasminogen activators. *International journal of pharmaceutics*. 2012;424:1-11
168. Hua X, Liu P, Gao YH, Tan KB, Zhou LN, Liu Z, Li X, Zhou SW, Gao YJ. Construction of thrombus-targeted microbubbles carrying tissue plasminogen activator and their in vitro thrombolysis efficacy: A primary research. *Journal of Thrombosis and Thrombolysis*. 2010;30:29-35
169. Hua X, Zhou L, Liu P, He Y, Tan K, Chen Q, Gao Y, Gao Y. In vivo thrombolysis with targeted microbubbles loading tissue plasminogen activator in a rabbit femoral artery thrombus model. *Journal of Thrombosis and Thrombolysis*. 2014;38:57-64
170. Juenet M, Aid-Launais R, Li B, Berger A, Aerts J, Ollivier V, Nicoletti A, Letourneur D, Chauvierre C. Thrombolytic therapy based on fucoidan-functionalized polymer nanoparticles targeting p-selectin. *Biomaterials*. 2018;156:204-216
171. Pawlowski CL, Li W, Sun M, Ravichandran K, Hickman D, Kos C, Kaur G, Sen Gupta A. Platelet microparticle-inspired clot-responsive nanomedicine for targeted fibrinolysis. *Biomaterials*. 2017;128:94-108
172. Kang C, Gwon S, Song C, Kang PM, Park SC, Jeon J, Hwang DW, Lee D. Fibrin-targeted and h<sub>2</sub>o<sub>2</sub>-responsive nanoparticles as a theranostics for thrombosed vessels. *ACS nano*. 2017;11:6194-6203
173. Molloy CP, Yao Y, Kammoun H, Bonnard T, Hoefler T, Alt K, Tovar-Lopez F, Rosengarten G, Ramsland PA, van der Meer AD, van den Berg A, Murphy AJ, Hagemeyer CE, Peter K, Westein E. Shear-sensitive nanocapsule drug release for site-specific inhibition of occlusive thrombus formation. *Journal of thrombosis and haemostasis : JTH*. 2017;15:972-982
174. Holme MN, Fedotenko IA, Abegg D, Althaus J, Babel L, Favarger F, Reiter R, Tanasescu R, Zaffalon PL, Ziegler A, Muller B, Saxer T, Zumbuehl A. Shear-stress sensitive lenticular vesicles for targeted drug delivery. *Nature nanotechnology*. 2012;7:536-543
175. Korin N, Kanapathipillai M, Matthews BD, Crescente M, Brill A, Mammoto T, Ghosh K, Jurek S, Bencherif SA, Bhatta D, Coskun AU, Feldman CL, Wagner DD, Ingber DE. Shear-activated nanotherapeutics for drug targeting to obstructed blood vessels. *Science*. 2012;337:738-742
176. Sumii T, Lo EH. Involvement of matrix metalloproteinase in thrombolysis-associated hemorrhagic transformation after embolic focal ischemia in rats. *Stroke*. 2002;33:831-836

177. Shargh VH, Hondermarck H, Liang M. Gelatin-albumin hybrid nanoparticles as matrix metalloproteinases-degradable delivery systems for breast cancer therapy. *Nanomedicine*. 2017;12:977-989
178. Xu Y, Zhang J, Liu X, Huo P, Zhang Y, Chen H, Tian Q, Zhang N. Mmp-2-responsive gelatin nanoparticles for synergistic tumor therapy. *Pharmaceutical development and technology*. 2019:1-26
179. Fleige E, Quadir MA, Haag R. Stimuli-responsive polymeric nanocarriers for the controlled transport of active compounds: Concepts and applications. *Advance Drug Delivery Reviews*. 2012;64:866-884
180. Hsu H-L, Chen J-P. Preparation of thermosensitive magnetic liposome encapsulated recombinant tissue plasminogen activator for targeted thrombolysis. *Journal of Magnetism and Magnetic Materials*. 2017;427:188-194
181. Xu F, Liao K, Wu Y, Pan Q, Wu L, Jiao H, Guo D, Li B, Liu B. Optimization, characterization, sulfation and antitumor activity of neutral polysaccharides from the fruit of *borjoa sorbilis* cuter. *Carbohydrate Polymers*. 2016;151:364-372
182. Voros E, Cho M, Ramirez M, Palange AL, De Rosa E, Key J, Garami Z, Lumsden AB, Decuzzi P. Tpa immobilization on iron oxide nanocubes and localized magnetic hyperthermia accelerate blood clot lysis. *Advanced Functional Materials*. 2015;25:1709-1718
183. Cheng R, Huang W, Huang L, Yang B, Mao L, Jin K, ZhuGe Q, Zhao Y. Acceleration of tissue plasminogen activator-mediated thrombolysis by magnetically powered nanomotors. *ACS nano*. 2014;8:7746-7754
184. Rapoport N. Drug-loaded perfluorocarbon nanodroplets for ultrasound-mediated drug delivery. *Therapeutic ultrasound*. Springer; 2016:221-241.
185. Berger H, Jr., Pizzo SV. Preparation of polyethylene glycol-tissue plasminogen activator adducts that retain functional activity: Characteristics and behavior in three animal species. *Blood*. 1988;71:1641-1647
186. Absar S, Choi S, Yang VC, Kwon YM. Heparin-triggered release of camouflaged tissue plasminogen activator for targeted thrombolysis. *Journal of controlled release*. 2012;157:46-54
187. Absar S, Choi S, Ahsan F, Cobos E, Yang VC, Kwon YM. Preparation and characterization of anionic oligopeptide-modified tissue plasminogen activator for triggered delivery: An approach for localized thrombolysis. *Thrombosis research*. 2013;131:e91-e99
188. Absar S, Kwon YM, Ahsan F. Bio-responsive delivery of tissue plasminogen activator for localized thrombolysis. *Journal of controlled release*. 2014;177:42-50



189. Zhou J, Guo D, Zhang Y, Wu W, Ran H, Wang Z. Construction and evaluation of fe<sub>3</sub>o<sub>4</sub>-based plga nanoparticles carrying rtpa used in the detection of thrombosis and in targeted thrombolysis. *ACS Applied Materials & Interfaces*. 2014;6:5566-5576
190. Decuzzi P, Ferrari M. The adhesive strength of non-spherical particles mediated by specific interactions. *Biomaterials*. 2006;27:5307-5314
191. Hu J, Huang S, Zhu L, Huang W, Zhao Y, Jin K, ZhuGe Q. Tissue plasminogen activator-porous magnetic microrods for targeted thrombolytic therapy after ischemic stroke. *ACS Applied Materials & Interfaces*. 2018;10:32988-32997
192. El-Sherbiny IM, Elkholi IE, Yacoub MH. Tissue plasminogen activator-based clot busting: Controlled delivery approaches. *Global Cardiology Science and Practice*. 2014;2014:336-349
193. Heeremans JL, Gerritsen HR, Meusen SP, Mijnheer FW, Gangaram Panday RS, Prevost R, Klufft C, Crommelin DJ. The preparation of tissue-type plasminogen activator (t-pa) containing liposomes: Entrapment efficiency and ultracentrifugation damage. *Journal of Drug Targeting*. 1995;3:301-310
194. Heeremans JL, Prevost R, Bekkers ME, Los P, Emeis JJ, Klufft C, Crommelin DJ. Thrombolytic treatment with tissue-type plasminogen activator (t-pa) containing liposomes in rabbits: A comparison with free t-pa. *Journal of Thrombosis and Haemostasis*. 1995;73:488-494
195. Harris JM, Chess RB. Effect of pegylation on pharmaceuticals. *Nature Reviews Drug Discovery*. 2003;2:214-221
196. Kim JY, Kim JK, Park JS, Byun Y, Kim CK. The use of pegylated liposomes to prolong circulation lifetimes of tissue plasminogen activator. *Biomaterials*. 2009;30:5751-5756
197. Absar S, Nahar K, Kwon YM, Ahsan F. Thrombus-targeted nanocarrier attenuates bleeding complications associated with conventional thrombolytic therapy. *Pharmaceutical Research*. 2013;30:1663-1676
198. Huang Y, Yu L, Ren J, Gu B, Longstaff C, Hughes AD, Thom SA, Xu XY, Chen R. An activated-platelet-sensitive nanocarrier enables targeted delivery of tissue plasminogen activator for effective thrombolytic therapy. *Journal of controlled release*. 2019;300:1-12
199. Everbach EC, Francis CW. Cavitational mechanisms in ultrasound-accelerated thrombolysis at 1 mhz. *Ultrasound in medicine & biology*. 2000;26:1153-1160
200. Molina CA, Ribo M, Rubiera M, Montaner J, Santamarina E, Delgado-Mederos R, Arenillas JF, Huertas R, Purroy F, Delgado P, Alvarez-Sabin J. Microbubble administration accelerates clot lysis during continuous 2-mhz ultrasound monitoring in stroke patients

- treated with intravenous tissue plasminogen activator. *Stroke*. 2006;37:425-429
201. Yan WC, Chua QW, Ong XJ, Sharma VK, Tong YW, Wang CH. Fabrication of ultrasound-responsive microbubbles via coaxial electrohydrodynamic atomization for triggered release of tpa. *Journal of Colloid and Interface Science*. 2017;501:282-293
202. Yan W-C, Ong XJ, Pun KT, Tan DY, Sharma VK, Tong YW, Wang C-H. Preparation of tpa-loaded microbubbles as potential theranostic agents: A novel one-step method via coaxial electrohydrodynamic atomization technique. *Chemical Engineering Journal*. 2017;307:168-180
203. Tiukinhoy-Laing SD, Huang S, Klegerman M, Holland CK, McPherson DD. Ultrasound-facilitated thrombolysis using tissue-plasminogen activator-loaded echogenic liposomes. *Thrombosis research*. 2007;119:777-784
204. Smith DA, Vaidya SS, Kopechek JA, Huang SL, Klegerman ME, McPherson DD, Holland CK. Ultrasound-triggered release of recombinant tissue-type plasminogen activator from echogenic liposomes. *Ultrasound in medicine & biology*. 2010;36:145-157
205. Laing ST, Moody MR, Kim H, Smulevitz B, Huang SL, Holland CK, McPherson DD, Klegerman ME. Thrombolytic efficacy of tissue plasminogen activator-loaded echogenic liposomes in a rabbit thrombus model. *Thrombosis research*. 2012;130:629-635
206. Tiukinhoy-Laing SD, Buchanan K, Parikh D, Huang S, MacDonald RC, McPherson DD, Klegerman ME. Fibrin targeting of tissue plasminogen activator-loaded echogenic liposomes. *Journal of Drug Targeting*. 2007;15:109-114
207. Shaw GJ, Meunier JM, Huang SL, Lindsell CJ, McPherson DD, Holland CK. Ultrasound-enhanced thrombolysis with tpa-loaded echogenic liposomes. *Thrombosis research*. 2009;124:306-310
208. Park Y, Liang J, Yang Z, Yang VC. Controlled release of clot-dissolving tissue-type plasminogen activator from a poly(l-glutamic acid) semi-interpenetrating polymer network hydrogel. *Journal of controlled release*. 2001;75:37-44
209. Chung TW, Wang SS, Tsai WJ. Accelerating thrombolysis with chitosan-coated plasminogen activators encapsulated in poly-(lactide-co-glycolide) (plga) nanoparticles. *Biomaterials*. 2008;29:228-237
210. Wang SS, Chou NK, Chung TW. The t-pa-encapsulated plga nanoparticles shelled with cs or cs-grgd alter both permeation through and dissolving patterns of blood clots compared with t-pa solution: An in vitro thrombolysis study. *Journal of Biomedical Materials Research Part A*. 2009;91:753-761
211. Li C, Du H, Yang A, Jiang S, Li Z, Li D, Brash JL, Chen H. Thrombosis-responsive thrombolytic coating based on

- thrombin-degradable tissue plasminogen activator (t-pa) nanocapsules. *Advanced Functional Materials*. 2017;27:1703934
212. Mihalko E, Huang K, Sproul E, Cheng K, Brown AC. Targeted treatment of ischemic and fibrotic complications of myocardial infarction using a dual-delivery microgel therapeutic. *ACS nano*. 2018;12:7826-7837
213. Uesugi Y, Kawata H, Jo J, Saito Y, Tabata Y. An ultrasound-responsive nano delivery system of tissue-type plasminogen activator for thrombolytic therapy. *Journal of controlled release*. 2010;147:269-277
214. Kawata H, Uesugi Y, Soeda T, Takemoto Y, Sung JH, Umaki K, Kato K, Ogiwara K, Nogami K, Ishigami K, Horii M, Uemura S, Shima M, Tabata Y, Saito Y. A new drug delivery system for intravenous coronary thrombolysis with thrombus targeting and stealth activity recoverable by ultrasound. *Journal of the American College of Cardiology*. 2012;60:2550-2557
215. Kroll AV, Fang RH, Zhang L. Biointerfacing and applications of cell membrane-coated nanoparticles. *Bioconjugate Chemistry*. 2017;28:23-32
216. Murciano JC, Medinilla S, Eslin D, Atochina E, Cines DB, Muzykantov VR. Prophylactic fibrinolysis through selective dissolution of nascent clots by tpa-carrying erythrocytes. *Nature biotechnology*. 2003;21:891-896
217. Vankayala R, Corber SR, Mac JT, Rao MP, Shafie M, Anvari B. Erythrocyte-derived nanoparticles as a theranostic agent for near-infrared fluorescence imaging and thrombolysis of blood clots. *Macromolecular bioscience*. 2018;18:e1700379
218. Hu Q, Qian C, Sun W, Wang J, Chen Z, Bomba HN, Xin H, Shen Q, Gu Z. Engineered nanoplatelets for enhanced treatment of multiple myeloma and thrombus. *Advanced Materials*. 2016;28:9573-9580
219. Becker AL, Johnston AP, Caruso F. Layer-by-layer-assembled capsules and films for therapeutic delivery. *Small*. 2010;6:1836-1852
220. Horcajada P, Chalati T, Serre C, Gillet B, Sebrie C, Baati T, Eubank JF, Heurtaux D, Clayette P, Kreuz C, Chang JS, Hwang YK, Marsaud V, Bories PN, Cynober L, Gil S, Ferey G, Couvreur P, Gref R. Porous metal-organic-framework nanoscale carriers as a potential platform for drug delivery and imaging. *Nature materials*. 2010;9:172-178
221. Karimi M, Ghasemi A, Sahandi Zangabad P, Rahighi R, Moosavi Basri SM, Mirshekari H, Amiri M, Shafaei Pishabad Z, Aslani A, Bozorgomid M, Ghosh D, Beyzavi A, Vaseghi A, Aref AR, Haghani L, Bahrami S, Hamblin MR. Smart micro/nanoparticles in stimulus-responsive drug/gene delivery systems. *Chemical Society Reviews*. 2016;45:1457-1501

222. De Temmerman ML, Demeester J, De Smedt SC, Rejman J. Tailoring layer-by-layer capsules for biomedical applications. *Nanomedicine*. 2012; 7: 771-788
223. Ochs M, Carregal-Romero S, Rejman J, Braeckmans K, De Smedt SC, Parak WJ. Light-addressable capsules as caged compound matrix for controlled triggering of cytosolic reactions. *Angewandte Chemie International Edition in English*. 2013; 52: 695-699
224. Oliveira MB, Hatami J, Mano JF. Coating strategies using layer-by-layer deposition for cell encapsulation. *Chemistry, an Asian journal*. 2016; 11: 1753-1764
225. Gil PR, Loretta L, Muñoz\_Javier A, Parak WJ. Nanoparticle-modified polyelectrolyte capsules. *Nano Today*. 2008; 3: 12-21
226. De Cock LJ, De Koker S, De Geest BG, Grooten J, Vervaet C, Remon JP, Sukhorukov GB, Antipina MN. Polymeric multilayer capsules in drug delivery. *Angewandte Chemie International Edition*. 2010; 49: 6954-6973
227. Larrañaga A, Lomora M, Sarasua J-R, Palivan CG, Pandit A. Polymer capsules as micro-/nanoreactors for therapeutic applications: Current strategies to control membrane permeability. *Progress in Materials Science*. 2017; 90: 325-357
228. Hayashi K, Yamada S, Hayashi H, Sakamoto W, Yogo T. Red blood cell-like particles with the ability to avoid lung and spleen accumulation for the treatment of liver fibrosis. *Biomaterials*. 2018; 156: 45-55
229. Muñoz Javier A, Del Pino P, Bedard M, Ho D, Skirtach A, Sukhorukov G, Plank C, Parak W. Photoactivated release of cargo from the cavity of polyelectrolyte capsules to the cytosol of cells. *Langmuir*. 2008; 24: 12517-12520
230. Chen J, Ratnayaka S, Alford A, Kozlovskaya V, Liu F, Xue B, Hoyt K, Kharlampieva E. Theranostic multilayer capsules for ultrasound imaging and guided drug delivery. *ACS nano*. 2017; 11: 3135-3146
231. Song W, He Q, Möhwald H, Yang Y, Li J. Smart polyelectrolyte microcapsules as carriers for water-soluble small molecular drug. *Journal of Controlled Release*. 2009; 139: 160-166
232. Alford A, Rich M, Kozlovskaya V, Chen J, Sherwood J, Bolding M, Warram J, Bao Y, Kharlampieva E. Ultrasound-triggered delivery of anticancer therapeutics from mri-visible multilayer microcapsules. *Advances in Therapy*. 2018; 1: 1800051
233. Shchukin DG, Gorin DA, Möhwald H. Ultrasonically induced opening of polyelectrolyte microcontainers. *Langmuir*. 2006; 22: 7400-7404
234. Korolovych VF, Grishina OA, Inozemtseva OA, Selifonov AV, Bratashov DN, Suchkov SG, Bulavin LA, Glukhova OE, Sukhorukov GB, Gorin DA. Impact of high-frequency ultrasound on nanocomposite microcapsules: In silico and in situ visualization. *Physical chemistry chemical physics : PCCP*. 2016; 18: 2389-2397

235. Skirtach AG, De Geest BG, Mamedov A, Antipov AA, Kotov NA, Sukhorukov GB. Ultrasound stimulated release and catalysis using polyelectrolyte multilayer capsules. *Journal of materials chemistry*. 2007;17:1050-1054
236. De Geest BG, Skirtach AG, Mamedov AA, Antipov AA, Kotov NA, De Smedt SC, Sukhorukov GB. Ultrasound-triggered release from multilayered capsules. *Small*. 2007;3:804-808
237. Kolesnikova TA, Gorin DA, Fernandes P, Kessel S, Khomutov GB, Fery A, Shchukin DG, Möhwald H. Nanocomposite microcontainers with high ultrasound sensitivity. *Advanced Functional Materials*. 2010;20:1189-1195
238. Campos F, Qin T, Castillo J, Seo JH, Arai K, Lo EH, Waeber C. Fingolimod reduces hemorrhagic transformation associated with delayed tissue plasminogen activator treatment in a mouse thromboembolic model. *Stroke*. 2013;44:505-511
239. Jang Jt, Nah H, Lee JH, Moon SH, Kim MG, Cheon J. Critical enhancements of mri contrast and hyperthermic effects by dopant-controlled magnetic nanoparticles. *Angewandte Chemie International Edition*. 2009;121:1260-1264
240. Hu hn J, Carrillo-Carrion C, Soliman MG, Pfeiffer C, Valdeperez D, Masood A, Chakraborty I, Zhu L, Gallego M, Yue Z. Selected standard protocols for the synthesis, phase transfer, and characterization of inorganic colloidal nanoparticles. *Chemistry of Materials*. 2016;29:399-461
241. Faria M, Bjornmalm M, Thurecht KJ, Kent SJ, Parton RG, Kavallaris M, Johnston APR, Gooding JJ, Corrie SR, Boyd BJ, Thordarson P, Whittaker AK, Stevens MM, Prestidge CA, Porter CJH, Parak WJ, Davis TP, Crampin EJ, Caruso F. Minimum information reporting in bio-nano experimental literature. *Nature nanotechnology*. 2018;13:777-785
242. Rouch A, Vanucci-Bacque C, Bedos-Belval F, Baltas M. Small molecules inhibitors of plasminogen activator inhibitor-1—an overview. *European journal of medicinal chemistry*. 2015;92:619-636
243. Choi JJ, Selert K, Gao Z, Samiotaki G, Baseri B, Konofagou EE. Noninvasive and localized blood-brain barrier disruption using focused ultrasound can be achieved at short pulse lengths and low pulse repetition frequencies. *Journal of cerebral blood flow and metabolism*. 2011;31:725-737
244. Kaczynski J, Home R, Shields K, Walters M, Whiteley W, Wardlaw J, Newby DE. Reproducibility of transcranial doppler ultrasound in the middle cerebral artery. *Cardiovascular ultrasound*. 2018;16:15
245. Cleveland RO, Averkiou MA, Crum LA, McAteer JA. Measurements of the effect of polypropylene vials on ultrasound propagation. *The Journal of the Acoustical Society of America*. 1996;99:2478-2500

246. Wang H-L, Lai TW. Optimization of evans blue quantitation in limited rat tissue samples. *Scientific reports*. 2014; 4: 6588
247. Wang Z, Leng Y, Tsai LK, Leeds P, Chuang DM. Valproic acid attenuates blood-brain barrier disruption in a rat model of transient focal cerebral ischemia: The roles of hdac and mmp-9 inhibition. *Journal of cerebral blood flow and metabolism*. 2011; 31: 52-57
248. Etame AB, Diaz RJ, Smith CA, Mainprize TG, Hynynen K, Rutka JT. Focused ultrasound disruption of the blood-brain barrier: A new frontier for therapeutic delivery in molecular neurooncology. *Neurosurgical focus*. 2012; 32: E3
249. Gustafson HH, Holt-Casper D, Grainger DW, Ghandehari H. Nanoparticle uptake: The phagocyte problem. *Nano today*. 2015; 10: 487-510
250. Espinosa A, Di Corato R, Kolosnjaj-Tabi J, Flaud P, Pellegrino T, Wilhelm C. Duality of iron oxide nanoparticles in cancer therapy: Amplification of heating efficiency by magnetic hyperthermia and photothermal bimodal treatment. *ACS nano*. 2016; 10: 2436-2446
251. Kolosnjaj-Tabi J, Di Corato R, Lartigue L, Marangon I, Guardia P, Silva AK, Luciani N, Clement O, Flaud P, Singh JV, Decuzzi P, Pellegrino T, Wilhelm C, Gazeau F. Heat-generating iron oxide nanocubes: Subtle "destructorators" of the tumoral microenvironment. *ACS nano*. 2014; 8: 4268-4283
252. Talamini L, Violatto MB, Cai Q, Monopoli MP, Kantner K, Krpetić Ze, Perez-Potti A, Cookman J, Garry D, Silveira CP. Influence of size and shape on the anatomical distribution of endotoxin-free gold nanoparticles. *ACS nano*. 2017; 11: 5519-5529
253. Erickson HP. Size and shape of protein molecules at the nanometer level determined by sedimentation, gel filtration, and electron microscopy. *Biological procedures online*. 2009; 11: 32-51
254. Hansen CE, Myers DR, Baldwin WH, Sakurai Y, Meeks SL, Lyon LA, Lam WA. Platelet-microcapsule hybrids leverage contractile force for targeted delivery of hemostatic agents. *ACS nano*. 2017; 11: 5579-5589
255. Katzan IL, Hammer MD, Hixson ED, Furlan AJ, Abou-Chebl A, Nadzam DM. Utilization of intravenous tissue plasminogen activator for acute ischemic stroke. *Archives of neurology*. 2004; 61: 346-350
256. Hu J, Huang W, Huang S, ZhuGe Q, Jin K, Zhao Y. Magnetically active fe<sub>3</sub>o<sub>4</sub> nanorods loaded with tissue plasminogen activator for enhanced thrombolysis. *Nano Research*. 2016; 9: 2652-2661
257. Heid S, Unterweger H, Tietze R, Friedrich RP, Weigel B, Cicha I, Eberbeck D, Boccaccini AR, Alexiou C, Lye S. Synthesis and characterization of tissue plasminogen activator-functionalized superparamagnetic iron oxide nanoparticles for targeted fibrin clot dissolution. *International journal of molecular sciences*. 2017; 18

258. Sommerdijk NA, de With G. Biomimetic caco3 mineralization using designer molecules and interfaces. *Chemical reviews*. 2008;108:4499-4550
259. Hauck TS, Ghazani AA, Chan WC. Assessing the effect of surface chemistry on gold nanorod uptake, toxicity, and gene expression in mammalian cells. *Small*. 2008;4:153-159
260. Szczepanowicz K, Bazylińska U, Pietkiewicz J, Szyk-Warszyska L, Wilk KA, Warszynski P. Biocompatible long-sustained release oil-core polyelectrolyte nanocarriers: From controlling physical state and stability to biological impact. *Advances in Colloid and Interface Science*. 2015;222:678-691
261. Carregal-Romero S, Ochs M, Rivera-Gil P, Ganas C, Pavlov AM, Sukhorukov GB, Parak WJ. Nir-light triggered delivery of macromolecules into the cytosol. *Journal of controlled release*. 2012;159:120-127
262. Palankar R, Pinchasik B-E, Schmidt S, De Geest BG, Fery A, Möhwald H, Skirtach AG, Delcea M. Mechanical strength and intracellular uptake of caco 3-templated lbl capsules composed of biodegradable polyelectrolytes: The influence of the number of layers. *Journal of Materials Chemistry B*. 2013;1:1175-1181
263. Wang YX. Superparamagnetic iron oxide based mri contrast agents: Current status of clinical application. *Quantitative imaging in medicine and surgery*. 2011;1:35-40
264. Vargas-Osorio Z, Da Silva-Candal A, Pineiro Y, Iglesias-Rey R, Sobrino T, Campos F, Castillo J, Rivas J. Multifunctional superparamagnetic stiff nanoreservoirs for blood brain barrier applications. *Nanomaterials*. 2019;9
265. Jin H, Tan H, Zhao L, Sun W, Zhu L, Sun Y, Hao H, Xing H, Liu L, Qu X, Huang Y, Yang Z. Ultrasound-triggered thrombolysis using urokinase-loaded nanogels. *International journal of pharmaceutics*. 2012;434:384-390
266. Smith ER, Hewitson TD, Cai MMX, Aghagolzadeh P, Bachtler M, Pasch A, Holt SG. A novel fluorescent probe-based flow cytometric assay for mineral-containing nanoparticles in serum. *Scientific Reports*. 2017;7:5686
267. Daffertshofer M, Hennerici M. Ultrasound in the treatment of ischaemic stroke. *The Lancet. Neurology*. 2003;2:283-290
268. Siegel RJ, Atar S, Fishbein MC, Brasch AV, Peterson TM, Nagai T, Pal D, Nishioka T, Chae JS, Birnbaum Y, Zanelli C, Luo H. Noninvasive, transthoracic, low-frequency ultrasound augments thrombolysis in a canine model of acute myocardial infarction. *Circulation*. 2000;101:2026-2029
269. Akiyama M, Ishibashi T, Yamada T, Furuhashi H. Low-frequency ultrasound penetrates the cranium and enhances thrombolysis in vitro. *Neurosurgery*. 1998;43:828-832; discussion 832-823

270. Reinhard M, Hetzel A, Kru"ger S, Kretzer S, Talazko J, Ziyeh S, Weber J, Els T. Blood-brain barrier disruption by low-frequency ultrasound. *Stroke*. 2006;37:1546-1548
271. Orset C, Haelewyn B, Allan SM, Ansar S, Campos F, Cho TH, Durand A, El Amki M, Fatar M, Garcia-Yebenes I, Gauberti M, Grudzenski S, Lizasoain I, Lo E, Macrez R, Margail I, Maysami S, Meairs S, Nighoghossian N, Orbe J, Paramo JA, Parienti JJ, Rothwell NJ, Rubio M, Waeber C, Young AR, Touze E, Vivien D. Efficacy of alteplase in a mouse model of acute ischemic stroke: A retrospective pooled analysis. *Stroke*. 2016;47:1312-1318
272. Sadat SM, Jahan ST, Haddadi A. Effects of size and surface charge of polymeric nanoparticles on in vitro and in vivo applications. *Journal of Biomaterials and Nanobiotechnology*. 2016;7:91
273. Santoro M, Tatara AM, Mikos AG. Gelatin carriers for drug and cell delivery in tissue engineering. *Journal of controlled release*. 2014;190:210-218
274. Elzoghby AO. Gelatin-based nanoparticles as drug and gene delivery systems: Reviewing three decades of research. *Journal of controlled release*. 2013;172:1075-1091
275. Jansen O, Schellinger P, Fiebich J, Hacke W, Sartor K. Early recanalisation in acute ischaemic stroke saves tissue at risk defined by mri. *The Lancet Neurology*. 1999;353:2036-2037
276. Haelewyn B, Rizzo JJ, Abbraini JH. Human recombinant tissue-plasminogen activator (alteplase): Why not use the 'human' dose for stroke studies in rats? *Journal of cerebral blood flow and metabolism*. 2010;30:900-903
277. Saguchi T, Onoue H, Urashima M, Ishibashi T, Abe T, Furuhashi H. Effective and safe conditions of low-frequency transcranial ultrasonic thrombolysis for acute ischemic stroke: Neurologic and histologic evaluation in a rat middle cerebral artery stroke model. *Stroke*. 2008;39:1007-1011
278. Flores R, Hennings LJ, Lowery JD, Brown AT, Culp WC. Microbubble-augmented ultrasound sonothrombolysis decreases intracranial hemorrhage in a rabbit model of acute ischemic stroke. *Investigative radiology*. 2011;46:419-424
279. Auvoire L, Sennoga CA, Hyvelin JM, Ossant F, Escoffre JM, Tranquart F, Bouakaz A. Microbubbles combined with ultrasound therapy in ischemic stroke: A systematic review of in-vivo preclinical studies. *PLoS one*. 2018;13:e0191788
280. Blanco E, Shen H, Ferrari M. Principles of nanoparticle design for overcoming biological barriers to drug delivery. *Nature biotechnology*. 2015;33:941-951
281. Argibay B, Trekker J, Himmelreich U, Beiras A, Topete A, Taboada P, Perez-Mato M, Vieites-Prado A, Iglesias-Rey R, Rivas J, Planas AM, Sobrino T, Castillo J, Campos F. Intraarterial route increases



- the risk of cerebral lesions after mesenchymal cell administration in animal model of ischemia. *Scientific Reports*. 2017; 7: 40758
282. Guldris N, Argibay B, Gallo J, Iglesias-Rey R, Carbo-Argibay E, Kolen'ko YV, Campos F, Sobrino T, Salonen LM, Banobre-Lopez M, Castillo J, Rivas J. Magnetite nanoparticles for stem cell labeling with high efficiency and long-term in vivo tracking. *Bioconjugate Chemistry*. 2017; 28: 362-370
283. Rodriguez JA, Sobrino T, Lopez-Arias E, Ugarte A, Sanchez-Arias JA, Vieites-Prado A, de Miguel I, Oyarzabal J, Paramo JA, Campos F, Orbe J, Castillo J. Cm352 reduces brain damage and improves functional recovery in a rat model of intracerebral hemorrhage. *Journal of the American Heart Association*. 2017; 6
284. da Silva-Candal A, Vieites-Prado A, Gutierrez-Fernandez M, Rey RI, Argibay B, Mirelman D, Sobrino T, Rodriguez-Frutos B, Castillo J, Campos F. Blood glutamate grabbing does not reduce the hematoma in an intracerebral hemorrhage model but it is a safe excitotoxic treatment modality. *Journal of cerebral blood flow and metabolism*. 2015; 35: 1206-1212







## Annexes

---





## RESOLUCIÓN DE AUTORIZACIÓN DE PROXECTOS DE EXPERIMENTACIÓN ANIMAL

**Expediente núm.:** 15010/2019/004

**Data de inicio:** 05.02.2019

**Persoa interesada:** Francisco Campos Pérez

**Procedemento:** resolución de autorización

**Forma de inicio:** solicitude da persoa interesada

### ANTECEDENTES

A persoa interesada, como representante do centro CIMUS (Universidade de Santiago de Compostela), presentou con data 05.02.2019 unha solicitude para a realización do proxecto de experimentación animal (entrada no Rexistro Electrónico da Xunta de Galicia 2019/246024), cuxos datos se detallan a continuación:

**Denominación do proxecto:** *Nanopartículas biomiméticas para a administración dirixida de nanomedicinas*

**Nome do centro usuario:** Animalario do CIMUS

**Persoa responsable do proxecto:** Francisco Campos Pérez

**Establecemento onde se realizarán os procedementos do proxecto (ou lugar xeográfico no caso de traballos de campo):** Animalario do CIMUS

**Clasificación do proxecto :** Tipo I  Tipo II  Tipo III

### CONSIDERACIÓNS LEGAIS E TÉCNICAS

1 O Real decreto 53/2013, de 1 de febreiro (BOE 34, do 8 de febreiro), polo que se establecen as normas básicas aplicables para a protección dos animais utilizados en experimentación e outros fins científicos, incluíndo a docencia, establece no seu artigo 33 as condicións de autorizacións dos proxectos con animais de experimentación.

2 O artigo 88 da Lei 39/2015, de 1 de outubro, do procedemento administrativo común das administracións públicas (BOE 236, do 2 de outubro de 2015) establece que a resolución que poña fin o procedemento decidirá todas as cuestións expostas polos interesados e aquelas outras derivadas deste.

3 O Servizo de Gandaría da Coruña revisou a documentación achegada na solicitude e o resultado favorable da avaliación do proxecto, realizada polo órgano habilitado da Sección de Experimentación Animal do Comité de Bioética da Universidade de Santiago de Compostela.

Esta xefatura territorial é competente para ditar unha resolución, de conformidade co Decreto 149/2018, do 5 de decembro, polo que se establece a estrutura orgánica da





Consellería do Medio Rural e se modifica parcialmente o Decreto 177/2016, do 15 de decembro, polo que se fixa a estrutura orgánica da Vicepresidencia e das consellerías da Xunta de Galicia (DOG 235, do 11 de novembro).

De acordo con todo o indicado, RESOLVO:

- 1 Autorizar o proxecto solicitado.
- 2 O mencionado proxecto precisa someterse a unha avaliación retrospectiva tras finalizar a súa autorización.
- 3 A autorización deste proxecto terá unha duración de dous anos e unha vez transcorrido este tempo deberá ser autorizado de novo.

A citada autorización é unicamente válida nas condicións que figuran no expediente. Ante calquera cambio significativo no proxecto que poida ter efectos negativos sobre o benestar dos animais, deberá solicitar a confirmación da autorización ao Servizo Provincial de Gandaría.

Esta autorización poderá ser suspendida, no caso de que o proxecto non se leve a cabo de acordo coas condicións de autorización e retirada, previo expediente tramitado ao que se lle dará audiencia.

Contra a presente resolución, que non lle pon fin á vía administrativa, poderá interpoñer un recurso de alzada ante o conselleiro de Medio Rural. O prazo comezará a contar dende o día seguinte ao da recepción desta resolución. Todo isto, segundo o disposto nos artigos 121 e 122 da citada Lei 39/2015.

Mediante este escrito notifícaselle ao CIMUS da USC esta resolución segundo o esixido no artigo 40.1 da antedita Lei 39/2015.



**JOSÉ MANUEL CIFUENTES MARTÍNEZ, PRESIDENTE DEL COMITÉ DE BIOÉTICA DE LA UNIVERSIDAD DE SANTIAGO DE COMPOSTELA**, cuya Sección de Experimentación animal ha sido designada como Órgano Habilitado para la evaluación de proyectos de experimentación animal por resolución de la Xunta de Galicia, con fecha 11 de noviembre de 2013, de acuerdo con lo exigido por el RD 53/2013 de 1 de febrero, por el que se establecen las normas básicas aplicables para la protección de los animales utilizados en experimentación y otros fines científicos, incluyendo la docencia,

#### INFORMA:

Que el proyecto de investigación titulado: **“Nanopartículas biomiméticas para la administración dirigida de nanomedicinas”** del que es investigador responsable **D. Francisco Campos Pérez**, ha sido examinado por el Comité de Bioética de esta Universidad, Sección de Experimentación Animal, llegando a las siguientes conclusiones:

Con respecto a su finalidad, se trata de un proyecto de investigación traslacional o aplicada cuyo objetivo fundamente el desarrollo de nanosistemas biomiméticos basados en cubiertas celulares (extraídas de células madre mesenquimales y/o plaquetas) para dirigir nanomedicinas a su lugar de acción (diana).

- Con respecto a los requisitos de las 3Rs,
  - No cabe la posibilidad de reemplazo ya que no se han encontrado otros métodos o estrategias de ensayo que permitan llevar a cabo los experimentos propuestos en este trabajo.
  - La experimentación se realizará en un centro registrado como usuario de animales de experimentación por lo que la manipulación, manejo y supervisión de los animales durante todo el proyecto será llevada a cabo por personas capacitadas. El grupo investigador lo componen personas con capacitaciones A, B y C, lo que asegura su preparación para garantizar el bienestar animales durante todos los procedimientos (requisito de refinamiento).
  - Finalmente, con respecto al requisito de reducción, se considera que el número de animales a utilizar es el mínimo imprescindible para la obtención de los resultados.
- La clasificación de los procedimientos en función de su grado de severidad es de “leve pa ra los procedimientos 1, 3 y “severo” para los procedimiento 2 y 4.
- Con respecto al balance de los daños y los beneficios, los procedimientos se efectúan bajo analgesia y anestesia previa a la administración de sustancias e intervenciones quirúrgicas por lo que se minimiza el dolor, angustia y sufrimiento. Los métodos de sacrificio descritos (sobredosis de anestesia) se encuentran entre los indicados por el propio RD 53/2013.
- Se han examinado las situaciones y excepciones previstas en el punto e) del artículo 34. 2 encontrando que ninguna de ellas es aplicable en este proyecto.
- El el proyecto se clasifica como tipo III y por tanto debe ser sometido a evaluación retrospectiva. Este Comité considera que dicha evaluación debería efectuarse a los dos años de la concesión de la autorización.

Por todas estas razones, este Comité acordó emitir un **INFORME FAVORABLE**.

En la evaluación de este proyecto NO HA EXISTIDO CONFLICTO DE INTERESES.

Lugo, 17 de abril de 2018







**Certificado de reconocimiento de la capacitación para manejar animales utilizados, criados o suministrados con fines de experimentación y otros fines científicos, incluyendo la docencia. Orden ECC/566/2015, de 20 de marzo**

<p>D./Dña. CLARA CORREA PAZ, con DNI/NIE 32702585N ha obtenido el reconocimiento de la capacitación para realizar las funciones de:</p> <p>CUIDADO DE LOS ANIMALES</p> <p>EUTANASIA DE LOS ANIMALES</p> <p>REALIZACIÓN DE LOS PROCEDIMIENTOS</p>	
<p>en los siguientes grupos de especies animales:</p> <p>ROEDORES</p>	
<p>Nº de certificado: CAP-0938-17</p>	
<p><b>ORGANISMO QUE EXPIDE EL CERTIFICADO</b></p> <p>Dirección General de Agricultura y Ganadería. Consejería de Medio Ambiente, Administración Local y Ordenación del Territorio. Comunidad de Madrid</p>	
<p>El reconocimiento de la capacitación para la realización de las funciones relacionadas en este certificado surtirá efecto en todo el territorio nacional.</p>	
	<p><b>Sello</b></p>
<p>EL DIRECTOR GENERAL DE AGRICULTURA Y GANADERÍA</p> <p>(P.D.F Resolución de 2 de noviembre de 2015)</p> <p>EL SUBDIRECTOR GENERAL DE RECURSOS AGRARIOS</p> <p>Firmado digitalmente por JESUS CARPINTERO HERVAS Organización: COMUNIDAD DE MADRID Fecha: 2017.11.24 14:44:36 CET Huella dig.: 6ba19ffaa6f160ac712c047e468e5c3797d00543</p> <p>Fdo: Jesús Carpintero Hervás</p>	



RESOLUCIÓN DE RECONOCIMIENTO DE LA CAPACITACIÓN E INCLUSIÓN EN EL REGISTRO DE PERSONAL QUE MANEJA ANIMALES UTILIZADOS, CRIADOS O SUMINISTRADOS CON FINES DE EXPERIMENTACIÓN Y OTROS FINES CIENTÍFICOS, INCLUYENDO LA DOCENCIA (Orden ECC/566/2015, de 20 de marzo)

Vista la solicitud formulada por D./DÑA. CLARA CORREA PAZ, con DNI/NIE 32702585N, para obtener el reconocimiento de la capacitación para realizar las funciones de CUIDADO DE LOS ANIMALES, EUTANASIA DE LOS ANIMALES, REALIZACIÓN DE LOS PROCEDIMIENTOS en ROEDORES.

Visto el informe favorable del Área de Protección Animal.

Considerando que el solicitante cumple los requisitos para estimar su solicitud, por lo dispuesto en la Orden ECC/566/2015, de 20 de marzo, por la que se establecen los requisitos de capacitación que debe cumplir el personal que maneje animales utilizados, criados o suministrados con fines de experimentación y otros fines científicos, incluyendo la docencia.

Esta Dirección General ha resuelto: reconocer la capacitación a D./ DÑA. CLARA CORREA PAZ, con DNI/NIE 32702585N, para realizar las funciones de CUIDADO DE LOS ANIMALES, EUTANASIA DE LOS ANIMALES, REALIZACIÓN DE LOS PROCEDIMIENTOS en ROEDORES .

El mantenimiento de esta capacitación se debe demostrar al menos cada ocho años, en los términos que establece el artículo 20 de la Orden ECC/566/2015, de 20 de marzo, a partir de la fecha de esta Resolución.

Contra esta Resolución, que no agota la vía administrativa, cabe interponer recurso de alzada en el plazo de un mes, contado desde el día siguiente a la recepción de esta notificación, ante el Viceconsejero de Medio Ambiente, Administración Local y Ordenación del Territorio, conforme a lo establecido en el artículo 121 y siguientes de la Ley 39/2015, de 1 de octubre, del Procedimiento Administrativo Común de las Administraciones Públicas.

EL DIRECTOR GENERAL DE AGRICULTURA Y GANADERÍA

(P.D.F Resolución de 2 de noviembre de 2015)

EL SUBDIRECTOR GENERAL DE RECURSOS AGRARIOS

Firmado digitalmente por JESUS CARPINTERO HERVAS  
Organización: COMUNIDAD DE MADRID  
Fecha: 2017.11.24 14:37:10 CET  
Huella díg.: 6ba19ffaa6f160ac712c047e468c5c3797d00543

Fdo.: Jesús Carpintero Hervás



# Errata sheet

Doctoral Thesis

“Optimization of thrombolytic therapy in brain pathology”

Following the CIEDUS recommendations and after the Thesis Director’s agreement, the following changes have been performed in order to get the final approval for the Thesis dissertation.

- **Pag. 121-122. Review and rewrite of Objective 2.**

**Because of its incomplete description, the modifications are as follows:**

**2. *In vivo* studies of rtPA nanocapsules to test their potential applicability against cerebral ischemic damage:**

- To validate the *in vivo* safety of ultrasound parameters applying through the Doppler.
- To demonstrate the *in vivo* safety of nanocapsules administration.
- To demonstrate the *in vivo* release of rtPA from the nanocapsules by applying ultrasounds.
- To investigate the therapeutic effect of the nanocapsules in a thromboembolic model in mice.

- To analyze the biodistribution of the nanocapsules in the different organs.

- **Pag. 121-122. Change of abbreviations in Objectives.**

**In order to facilitate the reading of the Objectives, the modifications are as follows:**

The main goal of this project was to design, to synthesize and to test a sono-sensitive nanocapsules for the delivery of rtPA. In order to achieve the main goal, two specific aims were proposed in this Thesis:

**1. *In vitro* optimization of rtPA nanocapsules:**

- To design a suitable sono-sensitive nanocapsules for the delivery of rtPA.
- To synthesize and characterize the rtPA encapsulation in nanocapsules.
- To validate the rtPA activity in nanocapsules.
- To study the *in vitro* release by the application of ultrasounds.

**2. *In vivo* studies of rtPA nanocapsules to test their potential applicability against cerebral ischemic damage:**

- To validate the *in vivo* safety of ultrasound parameters applying through the Doppler.

- To demonstrate the *in vivo* safety of nanocapsules administration.
- To demonstrate the *in vivo* release of rtPA from the nanocapsules by applying ultrasounds.
- To investigate the therapeutic effect of the nanocapsules in a thromboembolic model in mice.
- To analyze the biodistribution of the nanocapsules in the different organs.

- **Pag. 259-261. Change of abbreviations in Conclusions.**

**In order to facilitate the reading of the Conclusions, the modifications are as follows:**

**Section I: *In vitro* optimization of rtPA nanocapsules**

- rtPA nanocapsules with a diameter of 800 nm were successfully synthesized by the layer-by-layer technique, using PSS, PDACMAC, iron oxide nanoparticles and gelatin, in calcium carbonate templates.
- rtPA was successfully encapsulated in the nanostructures, achieving rtPA loadings between 0.02-0.05 pg rtPA/NCs, what corresponds to 5-13 % of the maximum theoretical loading capacity of the system.
- Two, four and six bilayers nanocapsules were shown to maintain the stability of the rtPA encapsulation upon storage, at least for one week.

- The formulation process did not affect the activity of rtPA. Encapsulated rtPA inside the nanocapsules maintained its activity after the nanocores synthesis, the layer-by-layer process, the dissolution of the calcium carbonate and after the ultrasounds application.
- Encapsulated rtPA was protected from its inactivation by its main endogenous inhibitor plasminogen activator inhibitor 1.
- Two bilayers nanocapsules showed the best response to ultrasounds, showing a 50 % release after 15 minutes of ultrasounds exposition. The released rtPA maintains its amidolytic and fibrinolytic activity.
- The developed rtPA nanocapsules were also visualized by magnetic resonance imaging. When the nanocapsules were injected in the brain parenchyma they showed a decrease in the signal of 64 % in T2-weighted image and 78 % in T2\*-weighted image.

## **Section II: *In vivo* studies of rtPA nanocapsules**

- The application of ultrasounds in healthy and ischemic brains did not show disruption of the blood brain barrier, validating the security of the ultrasounds in animal models.
- The intravenous administration of the nanocapsules did not show ischemic or hemorrhagic damage. Furthermore, the analysis of hepatotoxic and nephrotoxic makers did not vary along the days, demonstrating the safety of the rtPA nanocapsules.

- rtPA plasmatic activity after the rtPA nanocapsules administration and ultrasounds application was maintained elevated during at least 40 minutes, which demonstrates an increase in half-life of rtPA by encapsulating in nanocapsules.
- The activity of the released rtPA from the nanocapsules was ~ 3.5-fold-higher compared to the same amount of non-encapsulated rtPA (1 mg/kg).
- In addition, rtPA nanocapsules without gelatin showed an augment in the rtPA plasmatic activity during the same time, independent on the ultrasounds application, demonstrating that the gelatin was a crucial component for maintaining the stability *in vivo* and the response to ultrasounds.
- The administration of rtPA nanocapsules with ultrasounds application showed an increase in the number of reperfused animals and a decrease in the infarct volume, compared to the rest of the groups treated with nanocapsules.
- The therapeutic effect of the rtPA nanocapsules is not better than the treatment with "free" rtPA, although increase the *in vivo* half-life of the treatment.
- T2\*-weighted images illustrated the appearance of hypo-signals in the ischemic region in all the groups treated with nanocapsules (with and without gelatin and ultrasounds). This demonstrated the targeted delivery of the nanocapsules to the ischemic region.

- Hematoxylin-eosin staining confirmed that the hypo-signals detected in the magnetic resonance imaging studies were not hemorrhages.

